

Topics in Geobiology 38

Neal S. Gupta

Biopolymers

A molecular paleontology approach

 Springer

Biopolymers

Aims and Scope Topics in Geobiology Book Series

Topics in Geobiology series treats geobiology – the broad discipline that covers the history of life on Earth. The series aims for high quality, scholarly volumes of original research as well as broad reviews. Recent volumes have showcased a variety of organisms including cephalopods, corals, and rodents. They discuss the biology of these organisms—their ecology, phylogeny, and mode of life – and in addition, their fossil record – their distribution in time and space.

Other volumes are more theme based such as predator-prey relationships, skeletal mineralization, paleobiogeography, and approaches to high resolution stratigraphy, that cover a broad range of organisms. One theme that is at the heart of the series is the interplay between the history of life and the changing environment. This is treated in skeletal mineralization and how such skeletons record environmental signals and animal-sediment relationships in the marine environment.

The series editors also welcome any comments or suggestions for future volumes.

Series Editors

Neil Landman, landman@amnh.org

P.J. Harries, harries@shell.cas.usf.edu

For further volumes:

<http://www.springer.com/series/6623>

Neal S. Gupta

Biopolymers

A molecular paleontology approach

 Springer

Neal S. Gupta
Department of Science and Technology
Laboratory for Terrestrial Environments
Bryant University
Smithfield, RI, USA

ISSN 0275-0120

ISBN 978-94-007-7935-8

ISBN 978-94-007-7936-5 (eBook)

DOI 10.1007/978-94-007-7936-5

Springer Dordrecht Heidelberg New York London

Library of Congress Control Number: 2014947516

© Springer Science+Business Media Dordrecht 2014

This work is subject to copyright. All rights are reserved by the Publisher, whether the whole or part of the material is concerned, specifically the rights of translation, reprinting, reuse of illustrations, recitation, broadcasting, reproduction on microfilms or in any other physical way, and transmission or information storage and retrieval, electronic adaptation, computer software, or by similar or dissimilar methodology now known or hereafter developed. Exempted from this legal reservation are brief excerpts in connection with reviews or scholarly analysis or material supplied specifically for the purpose of being entered and executed on a computer system, for exclusive use by the purchaser of the work. Duplication of this publication or parts thereof is permitted only under the provisions of the Copyright Law of the Publisher's location, in its current version, and permission for use must always be obtained from Springer. Permissions for use may be obtained through RightsLink at the Copyright Clearance Center. Violations are liable to prosecution under the respective Copyright Law.

The use of general descriptive names, registered names, trademarks, service marks, etc. in this publication does not imply, even in the absence of a specific statement, that such names are exempt from the relevant protective laws and regulations and therefore free for general use.

While the advice and information in this book are believed to be true and accurate at the date of publication, neither the authors nor the editors nor the publisher can accept any legal responsibility for any errors or omissions that may be made. The publisher makes no warranty, express or implied, with respect to the material contained herein.

Printed on acid-free paper

Springer is part of Springer Science+Business Media (www.springer.com)

Foreword

‘A good, approachable (i.e., accessible to people other than organic geochemists) book on molecular paleontology is welcome’

Harvard University, Cambridge, MA
August 2013

Andrew H. Knoll

Preface

The primary usefulness of this book is for organic geochemists, molecular palaeontologists, and molecular archeologists. Researchers interested in astrobiology from a paleontological perspective may also find this to be valuable. This provides an overview and an introduction to the science, including literature overview for non-geochemists. Analytical methods employed are included as a part of each chapter.

Kerogen and Sedimentary Organic Matter

Primary producers on Earth that contribute to large quantities of organic matter, of which about 0.1–1 % enters the geosphere as sedimentary organic matter. This sedimentary organic matter is broadly divided in two fractions: (1) bitumen (ca. 5 %) that is extractable using organic solvents and (2) kerogen that is insoluble in organic solvents.

Kerogen occurs in sedimentary rocks as finely dispersed organic macerals and is the most abundant form of organic carbon in the Earth's crust. With increasing burial and heating, hydrocarbons are produced from kerogen, but kerogen itself is a three-dimensional polymeric macromolecule cross-linked by aliphatic chains (containing O or S functional groups) in which clusters of aromatic sheets form an important part (N, S and O functional groups). In typical kerogen, for every 1,000 C atoms there are *c.*500–1,800 H, *c.*25–300 O, *c.*5–30 S and *c.*10–35 N atoms. The oxygen-containing functional groups include carboxylic acids, alcohols, carbonyls, esters, ethers and amides.

Kerogen Types

Kerogen is classified as type I, II or III.

Type I Kerogen

Type I kerogen is relatively rare and is associated with lacustrine and open marine deposits. It has a high H/C ratio (about 1.5) and a low O/C ratio (<0.1) due to significant contributions from lipid material, especially long-chain aliphatic components. These aliphatic components, especially in lacustrine kerogens, are thought to predominantly derive from algaenan, with contributions from amorphous bacterial material. Compared with the other kerogen types it contains proportionally lower amounts of aromatic units and heteroatoms. Oxygen is present in the carbon skeleton mainly as ester and ether groups. The freshwater alga *Botryococcusbraunii* is a major contributor to type I kerogens (e.g. torbanites of Scottish oil shales). The kerogen in the Eocene Green River oil shale of Colorado, Utah and Wyoming is another example of type I kerogen.

Type II Kerogen

Type II kerogen is more common than type I and can potentially be formed in a variety of environments. It has relatively high H/C and low O/C ratios. Aliphatic structures are important and comprise chains (chain length up to *c.* C₂₅) associated with polyaromatic units, which often form the nucleus of the kerogen structure. Ketone and carboxylic acid groups are more important than in type I kerogen and ester bonds are also abundant. In marine settings, a major source for Type II kerogen is the mixture of autochthonous organic matter from phytoplankton (and possibly also zooplankton and bacteria) and an allochthonous contribution of higher plant material.

Type III Kerogen

Type III kerogen is commonly found in terrestrial depositional environments and has low H/C (<1.0) and high O/C (up to 0.3) ratios, reflecting major contributions from vascular plant tissues. As with Type II kerogen, ketone and carboxylic acid groups are important with relatively minor contributions from ester groups. A significant proportion of oxygen in the carbon skeleton is in non-carbonyl groups (possibly heterocycles, ethers and methoxy groups). Aliphatic groups are present in relatively minor amounts, dominated by methyl and other short chain alkyl groups. Long chain alkyl compounds are also present in low amounts and probably originate from cuticular coatings (cutan and suberan) or from polymerisation of waxes.

Type IV Kerogen

Type IV kerogen primarily comprises black opaque debris which has no hydrocarbon generating potential. It is likely formed from higher plant matter that has been severely

oxidized or subjected to thermal stress (e.g. combustion) and then transported to its deposition site following reworking.

Kerogen Formation

The origin of kerogen has traditionally been attributed to random recombination reactions of biological components (neogenesis) or the survival of decay-resistant organic macromolecules (selective preservation). Earlier research has revealed an alternative process for kerogen formation by conversion of free aliphatic molecules into a resistant aliphatic macromolecule via *in situ polymerization*

Neogenesis

In the classical theory of geopolymer formation, kerogen is believed to derive from humic substances similar to the humic and fulvic acids found in soils. During early diagenesis in aquatic environments, the organic material deposited from primary producers is broken down by microbial action into smaller constituents, which then undergo condensation reactions, giving rise to humic substances. Microbial degradation and condensation follow in immediate succession, leading to a zone in the top few metres of sediment (and possibly also in the water immediately overlying it) where both processes are active at the same time. With increasing time and burial depth, most of this humic material becomes progressively insoluble due to increasing polycondensation, associated with the loss of superficial hydrophilic functional groups (e.g. OH and COOH). Insolubilization can begin quite early and apparently continues to significant depths, as suggested by the occurrence of humic acids at several hundred metres depth in sediments that contain abundant terrestrial detrital material. The humin-like material that is formed continues to undergo condensation and defunctionalization, resulting in kerogen. With increasing time and burial depth, kerogen is formed, e.g. by incorporation of low molecular weight lipids via ether and ester bonds.

Selective Preservation

The selective preservation of resistant biomacromolecules (with the possibility of minor microbial alteration) is also thought to be an important process in the formation of kerogens, and particularly those formed at very early stages of diagenesis. Highly aliphatic, insoluble and non-hydrolysable biopolymers that resist biodegradation have been detected in the protective outer layers of some extant higher plants and algae as well as in the corresponding fossil remains. These materials are termed cutan and suberan in terrestrial plant cuticles, and are believed to make significant

contributions to kerogen. Equivalent materials, termed algaenans, are found in the cell walls of eustigmatophytes (an order of the Xanthophyceae) and many chlorophytes, but have yet to be detected in diatoms and haptophytes, and may be rare in dinoflagellates. Highly aliphatic macromolecules have also been identified in the cell walls of cyanobacteria and may make a contribution to amorphous kerogen. The algaenans from most algae contain high molecular weight, long *n*-alkyl chains (e.g. from the chlorophyte *Tetraedron*, which is a major contributor to the Messel oil shale). Initial studies suggested that these algaenans were polyesters with *n*-alkyl chains of up to C₃₃. Algae can also contribute aromatic material to kerogen in the form of polyalkylphenolic macromolecules.

These resistant biomacromolecular structures discussed above are likely to become concentrated as more abundant and readily hydrolysable biopolymers, such as proteins and carbohydrates, are degraded. There is also the possibility for less resistant material to be protected against biodegradation within coatings of resistant material (e.g. polysaccharides within higher plant cuticular membranes and lipids within microbial cell walls). Selective preservation is also consistent with the preservation of certain parts of organisms such as ultralaminar walls, cuticles, spores and pollen, often recognized in both coal and kerogen. Consequently, this model has gained increasing popularity over the last two decades.

Thus, classical and selective preservation models can be considered end-member models of the scale of alteration that may be undergone by the biomacromolecular precursors of kerogen.

Sulphur Incorporation

Conditions favoring the activity of sulphate-reducing bacteria result in the production of sulfide, which usually reacts with iron (II) ions especially in some types of clastic and argillaceous sediments. Where there is a limited supply of iron (II), free hydrogen sulphide and polysulphides are produced during early diagenesis, and these compounds can react with certain functional groups in organic compounds, fostering incorporation of both sulfur and organic compounds into kerogen. Additionally, reaction of organic matter with inorganic sulphur species may render OM resistant against bacterial degradation and remineralisation leading to formation of kerogen. In fact, normally labile compounds such as carbohydrates can be preserved in kerogen via early diagenetic reactions with sulphides.

In Situ Polymerisation of Labile Components in Extant Organisms

The cuticle of the great majority of pre-Tertiary arthropod and plant fossils comprises a macromolecule with a significant aliphatic component. The convergence in composition with type I and/or II kerogens suggests that polymerisation of free aliphatic

components may be important in the preservation of these fossils. Fossils provide a key to understanding the process because they allow the end product of diagenetic maturation to be related directly to starting composition.

Evidence from Transformation of Arthropod Cuticle

Large numbers of invertebrates are protected by an outer layer known as the integument or cuticle. This provides protection against predators, a barrier to the environment and prevents desiccation. In arthropods, the cuticle consists of three major layers, the epicuticle, exocuticle and endocuticle. The epicuticle consists of waxes composed of straight-chain and branched hydrocarbons, wax esters, fatty acids, alcohols, ketones and sterols and prevents dehydration. The rest of the cuticle is composed of mainly two biopolymers, chitin and protein which form a complex structure cross-linked by catechol, aspartic and/or histidyl moieties. Chitin, a nitrogen containing polysaccharide provides the structural strength which is reinforced by the protein matrix. Additionally, CaCO_3 may provide biomineralisation and further strengthen the cuticle. The proportion of chitin to protein varies between taxa ranging from just traces in protozoa to up to 85 % in some crustacean cuticles. The preservation potential of chitin is higher than that of associated proteins. However, almost all of the estimated (around 10^{11} t) of chitin produced annually in the biosphere is consumed by decay, and only mineralised or sclerotized cuticles are normally preserved. Organically preserved animal cuticles are known from rocks as old as Cambrian (in the Burgess shale, where they provide template for the precipitation of clay minerals) and are relatively common throughout the Palaeozoic (scorpions and eurypterids). Decay experiments have shown that the chitin component of the cuticle degrades even in anoxic conditions, but still at a slower rate than that of protein. Pliocene asphalt deposits (e.g. Rancho La Brea in California) and organic rich glacial deposits preserve abundant insect cuticles. The proportion of the chitin that survives reflects the nature of sediment. A lower proportion of chitin is preserved in peat deposits than in clastic sediments. The lithological control is also evident in the preservation of insect cuticles and shrimps from Pliocene sediments of Willershausen, Germany. Cuticles deposited in oxygen-depleted waters of lake bottom yield a higher proportion of chitin, than that near the lake margins. The oldest deposited chitin survives in Oligocene (24.7 Ma) beetle cuticles, which also preserve traces of protein from maar type lake deposits at Enspel, Germany. In each case where the fossil cuticles reveal little chemical alteration, their morphological details are also remarkably preserved. Cuticles preserved in Pleistocene amber do show good chemical preservation and those extracted from 25 Ma Dominican amber are chemically changed. Curiously, analyses of a diversity of cuticles from Tertiary marine crustaceans reveal no compelling evidence that the original chemistry is even partially preserved. Paleozoic and Mesozoic arthropod cuticles often show well-preserved surface detail but lack any chitin protein component of the original cuticle. The chemical composition of the

cuticles reveals the presence of an *n*-alkyl component. This aliphatic composition does not reflect the original chitin-protein composition. Thus, the fossilisation of arthropod cuticles cannot be attributed to selective preservation of decay resistant components, but this long-term preservation relies on the diagenetic polymerisation of lipid constituents of the cuticle to an aliphatic composition. Thus, cuticular analysis can provide an important key to understanding preservation of organic matter in ancient sediments.

Evidence from Confined Pyrolysis Experiments/Experimental Heating

Preservation of organic fossils and fossil cuticles cannot be explained fully by either the neogenesis or selective preservation models. Recent analyses reveal that, while younger fossil arthropods may preserve traces of the more resistant elements of the chitin-protein complex that constitutes the cuticle, older fossils are dramatically altered and often yield an aliphatic signature similar to that of many plant fossils and kerogen. Selective preservation does not provide an adequate explanation, as the aliphatic components occurring in the cuticle of modern arthropods are not decay-resistant and differ in structure from those present in fossils. Thus, the convergence in the macromolecular composition of plant cuticles, animal cuticles, and kerogen cannot be explained simply on the basis of the known biochemical compositions of the living organisms.

Polymerization may be responsible for the aliphatic character of organic fossil remains, i.e. the chitin/protein complex has been transformed into a predominantly aliphatic macromolecule. The process does not involve random incorporation of external components (neogenesis model), and presumably results from degradation and *in situ* polymerization of components in the cuticle. As discussed below, artificial maturation experiments using confined pyrolysis in gold tubes confirmed that the cuticles of living arthropods alone can source an aliphatic macromolecule similar to that observed in fossil arthropods, i.e. free cuticular lipids or hydrolysable lipids may be transformed *in situ*. Since such lipid components occur in all organisms it is reasonable to suggest that a comparable process may operate in both arthropod and plant cuticles. Moreover, a comparable process could occur during the diagenesis of phytoplankton and other microorganisms and thus account for the large quantities of organic material represented by some kerogens. Evidence for the *in situ* polymerization model was illustrated by confined pyrolysis of arthropod cuticles in gold tubes. Initial experiments performed on degraded scorpion cuticles (*Pandinus imperator*) showed a proportional increase in the aliphatic component of the cuticle with increasing temperature. During pyrolysis for 24 h at 700 bars and 260 °C, the macromolecular composition of the cuticle was significantly altered. Characteristic protein and chitin moieties were absent in the residue (as analysed by py-GC/MS) and both phenols and C₅₋₂₀ *n*-alkanes and *n*-alk-1-enes were more abundant. At 350 °C, changes in the

cuticle composition were much more extensive: alkenes and alkanes were the predominant compounds released during pyrolysis, phenols were barely detected, and chitin and protein moieties were absent. Moreover, the pyrolysate of the cuticle that matured at 350 °C was very similar to that of a Carboniferous scorpion, suggesting that the experiments replicated at least aspects of geological. However, experiments were conducted only on modern scorpion cuticle.

Despite the limitations of artificial maturation experiments, these results showed that an aliphatic macromolecule was generated by thermal alteration of the original cuticular material. It was this that led to the formulation of the *in situ* polymerization model: that during thermal maturation, labile components such as chitin and protein are altered or lost while free and ester-bound aliphatic compounds are altered and recombine forming an aliphatic macromolecule. However, analyses were limited to the scorpion *Pandinus* and it is unclear how widely applicable these results were to cuticles with different chemical structures.

Contribution of Plants to Organic Matter

Terrestrial plants and marine phytoplankton in the oceans are primary photosynthesizers providing a source of food and energy for secondary organisms to utilise for the process of biosynthesising compounds needed for their own growth, survival and lifecycle. Ultimately, all living organisms, both primary and secondary photosynthesizers die and many are deposited in some kind of aquatic environment. The nature of the depositional environment plays a very important role in determining the amount of organic matter eventually preserved. Organic matter deposited in a highly anoxic environment, accompanied by rapid sedimentation/burial, is preserved in far greater concentration than in the oxic situation. Tissot and Welte have estimated that around 0.1 % of the organic carbon from photosynthetic cycle escaped and was fixed in the geological record. Differences in preservation relate to the efficiency of microbial reworking of organic matter. In addition, environment with very high productivity is more likely to produce organic-rich sediment. Thus productivity and preservation are the two main driving forces dictating survival of organic matter over geologic timescales.

Study of Leaves and Cuticles

Leaves, whether broad leaf foliage or coniferous needles, are the most dominant aboveground inputs to most soils. Other aerial inputs such as branches, bark and fruits account for only 20 % in temperate deciduous forests and 20–40 % in coniferous forests of total litter fall. Coarse woody debris may contribute 40–60 % of the total detrital biomass.

Compound class	Deciduous leaf	Conifer needle	Deciduous wood
Lipid	8	24	2–6
Carbohydrate (storage)	22	7	1–2
Cell wall polysaccharide	13	19	19–24
Cellulose	16	16	45–48
Lignin	21	23	17–26
Protein	9	2	?

Preservation of Plant Fossils

Fossil plants are generally preserved as impressions, permineralisations and organically preserved structures. Most modern plants lack biomineralised tissues; hence their survival relies heavily on preservation of organic remains. These include wood remains, pollen, spores, algae, leaves and propagules. Except for wood, they are rarely preserved as complete plant organs but just as resistant outer coverings (i.e. pollen and spore walls, algal cell walls, cuticle, seed coats and fruit walls). The chemical and physical composition of the plant structures vary, resulting in differences in their susceptibility to decay. Thus, structures that are most resistant, either physically and/or chemically, have the highest organic fossilisation potential.

Transformation of Plant Cuticles

The cuticle is the external covering on leaf and green stem surfaces and serves to (1) reduce water loss, (2) control gaseous exchange and (3) provides a barrier to fungal pathogens. The cuticle in modern plants is composed of a solvent soluble wax fraction and insoluble matrix. This matrix makes up the framework of the cuticle and is composed of biopolyestercutin and/or an insoluble non-hydrolysable macromolecule cutan. The chemical structure of cutin is well understood; based primarily on C₁₆ and C₁₈alkanoic acids. All three cuticular components (waxes, cutin, and cutan) are important to the decay-resistant nature of leaves and stems. In addition, the cuticle may also incorporate parts of the outer cell walls of the epidermis, which further contributes to its resistant nature.

The physical and chemical resistance of the cuticle helps preservation in the fossil record. However, in some cases, physically resistant outer coverings fail to survive, even though it is clear from other evidence that the species was present in the past, revealing that physical resistance does not necessarily guarantee fossilisation. Plant structures composed of both lignin and an aliphatic macromolecule are the most likely to be represented in the fossil record. However, the preservation potential of the aliphatic component itself is higher than that of lignin. In the case of the seed coat of *Typha*, cuticular layers containing the aliphatic macromolecule are selectively preserved, whereas thin walled lignified layers are lost upon fossilisation.

Conversely, plant remains lacking both lignin and an aliphatic macromolecule are unlikely to be preserved as organic fossils. Preservation of fossil leaves and cuticles is discussed at greater length later in the chapter as well.

The occurrence of plant cuticles in the fossil record has raised questions about the factors responsible for their preservation and their role in the formation of kerogen. Studies, investigating the chemical composition of cuticles, have concentrated on the resistant part of modern plant cuticles 'cutan', which yielded exclusively an aliphatic signature upon pyrolysis, thus being similar to that obtained by analyses of fossil specimens. More recent studies suggest the involvement of aromatic and/or fatty acid components in the overall chemical composition of the resistant part of the modern plant cuticle. Most modern plants whose cuticles have been shown to yield a residue of a non-saponifiable, chemically resistant macromolecule (e.g., *Agave americana* and *Clivia*) lack a fossil record, making investigation of the role of the resistant macromolecule in preservation processes especially difficult.

Fossil plant cuticles occur as minor constituents in coals and coaly shales and as major organic constituents in some organic-rich deposits of lacustrine or deltaic environments. Amongst other techniques, fossil cuticles have been studied using infrared (IR) spectroscopy in combination with pyrolysis–gas chromatography–mass spectrometry (Py–GC/MS). IR spectroscopy is a non-destructive technique for identifying functional groups in chemical structures, and pyrolysis yields chemical compounds formed by thermal degradation of the materials analysed. Both techniques enable analysis of very small samples such as fossil cuticles that are typically available only in milligram amounts. The combination of both methods allows detailed insight into the molecular structure of insoluble macromolecular material.

Möslé et al. (1998) and others at Royal Holloway England used recent and Mesozoic (Cretaceous) *Ginkgo* and conifer cuticles to study the chemical and structural changes during fossilisation and the significance of factors such as systematic affinity, original chemical composition and enclosing lithology that influence the preservation of the fossils, by using samples of similar thermal maturity and geological age. Samples of Recent *Ginkgo biloba*, Cretaceous *Ginkgo* and Cretaceous conifer cuticles (*Frenelopsis* and *Abietites*) from different enclosing lithologies and similar thermal maturity of the fossils were analysed by scanning and transmission electron microscopy, Fourier transform–infrared spectroscopy, and pyrolysis–gas chromatography/mass spectrometry. Recent and fossil *Ginkgo* cuticles under SEM revealed sheets, similar in appearance, varying in the abundance and texture of the cuticular papillae. TEM of the Recent *Ginkgo* showed an outer amorphous cuticle layer, a structured middle layer and an inner laminated layer of cell wall. The Cretaceous *Ginkgo* cuticles retained the amorphous layer and a modified structured layer. SEM of Cretaceous *Abietites* and *Frenelopsis* also show preservation of cuticle sheets, but each has distinctive morphology. These conifer cuticles are very thick (TEM), *Frenelopsis* cuticle has remarkable multi-laminar ultrastructure whilst *Abietites* is amorphous. *G. biloba* cuticle consists mainly of the natural polyester, cutin, as revealed by FT–IR and pyrolysis, indicated by an abundance of saturated, unsaturated and hydroxy fatty acids. IR spectra

of fossil cuticles, like modern cuticles, showed aliphatic C–H, hydroxyl and carbonyl functions. However, in fossils, the carbonyl ester was transformed to carboxylic acid or ketone groups. Pyrolysates of fossils showed phenolic constituents like modern cuticles but loss of cutin fatty acid monomers and an increased prominence of a homologous series of *n*-alkene and *n*-alkane fragments up to *n*-C₃₀. Since most recent cuticles, including those of conifers and *Ginkgo biloba*, do not yield a non-saponifiable highly resistant residue, they proposed that organic preservation of fossil species investigated involves the diagenetic stabilisation of chemically-labile aliphatic cutin constituents along with incorporation of waxes. These general chemical modifications characterise all fossil *Ginkgo* and conifer cuticles, irrespective of their enclosing lithology, systematic affinity, external morphology or internal ultrastructural preservation. However, there were clear chemical differences between the fossil samples that may be related to their systematic affinity.

Mösle et al. (1998) investigated material from four North American Carboniferous localities, which have yielded conifer, cordaite and pteridosperm cuticles in co-occurrence. The emphasis was to establish if chemosystematic signatures survive in spite of chemical alteration and, if so, if these are indicative of evolutionary relationships. The cuticles of different Late Carboniferous plants—Cordaitales from Lone Star Lake, Kansas, USA; Cordaitales, and pteridosperms (*Neuralethopteris* and *Eusphenopteris*) from Joggins, NS, Canada; and conifers of the genus *Walchia* from Garnett and Hamilton, both in Kansas, USA. Cuticles were preserved as sheets from larger leaves or as entire cuticle envelopes from smaller, scale-like leaves. Each cuticle has morphology diagnostic of the parent plant group reflected in external appendages and/or external/internal patterns indicative of the arrangement of underlying epidermal cells. Cuticle pyrolysates revealed a highly aliphatic character; however there were differences in the distribution and relative abundance of aliphatic hydrocarbons between the different genera. The pyrograms of the two *Cordaites* and the two *Walchia* were similar to one another but distinct from pyrograms of other seed plant cuticles, including those from the same localities. Hence, cuticles retain some chemosystematic signature.

Comparison amongst the pyrolysis profiles fossil samples showed that *Walchia* and *Cordaites*, both of the conifer/cordaite clade, are as different from each other as either is from *Eusphenopteris* or *Neuralethopteris* (pteridosperms). Indeed the *Cordaites* were more similar to *Neuralethopteris* whilst the *Walchia* are more similar to the *Eusphenopteris*. Thus, although the samples retained a genus-specific chemical signature it did not provide evidence of chemosystematic relationships at higher rank and does not reflect a sister group relationship between cordaites and conifers.

The model of selective preservation of plant cuticles stresses the contribution of the chemically resistant material termed cutan, which was proposed to produce the aliphatic homologous series observed in pyrograms of fossil specimens. These studies of cuticles from Recent conifers and *Ginkgo* showed the rarity of cutan as a significant cuticular constituent as determined by pyrolysis and showed the absence of cutan as chemically resistant material in the tested cuticles. Therefore, additional processes need to be invoked to account for the observed “aliphatic” signatures of

fossil plant cuticles. Possible explanations include: (1) the incorporation of cutin monomers via linkages more stable than carboxylic acid ester and (2) the formation of ether linkages by intermolecular reaction of alcohol and epoxy groups was proposed by Schmidt and Schönherr (1982) and elaborated by Tegelaar et al. (1991). This would certainly engender cutin monomers resistant to acid- or base-catalysed degradation, and capable of yielding hydrocarbon fragments of chain length less than the original (typically 16 or 18 C atom) upon pyrolysis. The generation of fragments of chain length greater than C₃₀ could be explained as a result of the di- or polymerisation of cutin constituents via carbon-carbon linkages along with the chemically stable incorporation of pre-existing chains of extra-cuticular material (in waxes up to 37 C atoms).

Research articles that have appeared before and are presented here in this volume as modifications, adaptations, reproductions with permission from publishers:

Gupta NS, Briggs DEG, Pancost RD (2006a) Molecular taphonomy of graptolites. Special paper. *J Geol Soc Lond* 163:897–900

Gupta NS, Briggs DEG, Collinson ME, Evershed RP, Pancost RD (2006b) Re-investigation of the occurrence of cutan in plants: implications for the leaf fossil record. *Paleobiology* 32:432–449

Gupta NS, Michels R, Briggs DEG, Evershed RP, Pancost RD (2006c) Organic preservation of fossil arthropods: an experimental study. *Proc R Soc Lond B* 273:1471–2954

Gupta NS, Tetlie OE, Briggs DEG, Pancost RD (2007a) Fossilization of Eurypterids: a product of molecular transformation. *Palaios* 22:399–407

Gupta NS, Briggs DEG, Collinson ME, Evershed RP, Michels R, Pancost RD (2007b) Reply to de Leeuw comment ‘on the origin of sedimentary aliphatic macromolecules’. *Org Geochem* 38:1585–1588

Gupta NS, Briggs DEG, Collinson ME, Evershed RP, Michels R, Pancost RD (2007c) Molecular preservation of plant and insect cuticles from the Oligocene Enspel Formation, Germany: evidence against derivation of aliphatic polymer from sediment. *Org Geochem* 38:404–418

Gupta NS, Briggs DEG, Collinson ME, Evershed RP, Michels R, Jack KS, Pancost RD (2007d) Evidence for the *in situ* polymerisation of labile aliphatic organic compounds during the preservation of fossil leaves: implications for organic matter preservation. *Org Geochem* 38:499–522

Gupta NS, Michels R, Briggs DEG, Collinson ME, Evershed RP, Pancost RD (2007e) Experimental evidence for formation of geomacromolecules from plant leaf lipids. *Org Geochem* 38:28–36

Gupta NS, Landman NH, Briggs DEG, Summons RE (2008a) Molecular structure of organic components in cephalopods: evidence for oxidative cross linking in fossil marine invertebrates. *Org Geochem* 39:1405–1414

Gupta NS, Love GD, Moo OC, Summons RE, Briggs DEG (2008b) Molecular taphonomy of macrofossils at the Cretaceous Las Hoyas formation, Spain. *Cretac Res* 29:1–8

Gupta NS, Yang H, Leng Q, Briggs DEG, Cody GD, Summons RE (2009a) Diagenesis of plant polymers: a study of decay and macromolecular preservation of *Metasequoia*. *Org Geochem* 40:802–809

Gupta NS, Cody G, Tetlie EO, Briggs DEG, Summons RE (2009b) Rapid association of lipids into macromolecules during experimental decay of invertebrates: initiation of geopolymer formation. *Org Geochem* 40:589–594

Gupta et al. (2014) Experimental formation of geomacromolecules from microbial lipids. *Org Geochem* 67:35–50

This book presents the results of a multi-disciplinary biogeochemical research/effort involving palaeontology, organic geochemistry, taphonomy, and sedimentology.

Smithfield, RI, USA
July 2013

Neal S. Gupta

References

Mösle B, Collinson ME, Finch P, Stankiewicz BA, Scott AC, Wilson R (1998) Factors influencing the preservation of plant cuticles: a comparison of morphology and chemical composition of modern and fossil examples. *Org Geochem* 29:1369–1380

Schmidt HW, Schönherr J (1982) Development of plant cuticles: occurrence and role of non-esterbonds in cutin of *Cliviaminiata* Reg. leaves. *Planta* 156:380–384

Tegelaar EW, Kerp H, Visscher H, Schenk PA, de Leeuw JW (1991) Bias of the paleobotanical record as a consequence of variations in the chemical composition of higher vascular plantcuticles. *Paleobiology* 17:133–144

Acknowledgements

This volume is a collection of papers and chapters that I have worked on in the field of molecular paleontology through my graduate dissertation at the University of Bristol (UK), as a postdoc at Yale University, (USA), MIT (USA) and the Geophysical Laboratory, Carnegie Institution of Washington (USA). Most of the research was carried out under the research supervision of Prof. Derek Briggs FRS, Prof. Roger Summons FRS, Prof. Richard D. Pancost, and Dr. George Cody. Professor Richard Evershed FRS provided valuable insights as well. Dr. B. Artur Stankiewicz was instrumental in very interesting research in this direction before 2001. The various funding agencies that have funded me over the last 10 years are the University of Bristol PhD studentship, American Chemical Society and a NASA Astrobiology fellowship. I spent close to a year at IISER-Mohali in India where I worked on this as well, funded through the Ramanujan Fellowship, as an Assistant Professor in 2010. Since I have been a postdoc, my wife Mary Elizabeth has patiently endured my long postdoctoral stint, also my family in India and also in Indiana have been very supportive.

The chapter on high P-T transformation of bacterial biopolymers was funded by an NAI fellowship and research was conducted in Dr. George Cody's lab at the Geophysical lab. All microbiology work was carried out in Dr. Andrew Steele's lab at the Geophysical lab as a part of my postdoc there. The NAI fellowship was awarded to me through the MIT NAI team, in conjunction with the Geophysical Lab. Dr. Marilyn Fogel has provided very helpful comments and advise constantly on several occasions. Since my postdoctoral years, Dr. Hong Yang (Bryant University) has been very supportive and also in organizing a Research Scientist position for me at Bryant University after my return from India. Dr. Julio Mercader (University of Calgary) has redirected some of my research interest in the direction of archeology where these research principles can actively be applied. Professor Andrew Knoll (Harvard University) has provided very constructive comments on my research and on grant and fellowship applications. Dr. George Cody has very encouragingly supported a visiting

investigator position for me at the Geophysical Lab since 2011, and also provided access to the organic spectroscopy facility there, and at the Lawrence Berkeley National Lab in CA at the X-Ray synchrotron.

Acknowledgements for chapters, in specific:

Organic Preservation of Biopolymers in Fossil Leaves

The project was funded through a research grant awarded to Richard D. Pancost (RDP), Derek E. G. Briggs (DEGP), and Raymond Michels (RM) by the Petroleum Research Fund, American Chemical Society. Field work was funded by awards to Neal from the Geological Society of London, the Palaeontological Association and the Bob Savage Trust of the University of Bristol. T. Cosgrove is thanked for access to the Bristol NMR facility. We are grateful to I. D. Bull and R. Berstan for their technical assistance and the NERC for funding the Bristol node of the Life Sciences Mass Spectrometry Facility. We are also grateful to R. Brooker for analytical assistance, to A. Brain for specialist assistance with TEM studies, to J.-F. Euvrard and F. Baudin of CECA for allowing us to collect at St. Bazile, and to B. Riou for acting as our guide at the site. A. W. Stott carried out preliminary py-GC-MS analyses of fossil leaves collected in a previous field trip. P. F. van Bergen, P. D. Hatcher, G. A. Logan and J. W. de Leeuw are thanked for reviewing and discussions earlier.

Migration of Organic Molecules from Sediment to Fossils

Michael Wuttke and Marcus Poschmann allowed for access and assistance at the Enspel site, and for additional material. Dr. Ian Bull and the NERC Life Sciences Mass Spectrometry Facility are thanked for analytical assistance and access to equipment. Tony Brain is thanked for his specialist help with transmission electron microscopy and Richard Hodges (Natural Resources Institute) for providing modern weevils. The Geological Society of London and the Paleontological Society provided travel funds that allowed Neal to visit the site, and the ACS-PRF provided funds for consumables and analyses.

Transformation of Arthropod Biopolymers in High P-T Conditions

Research presented in this chapter was funded in part through a research grant awarded to R.D.P., D.E.G.B. and R.M. by the Petroleum Research Fund, American Chemical Society. I. Bull and R. Berstan are thanked for their analytical support. The mass spectrometry facilities used in this study at the Bristol Biogeochemistry

Research Centre were supported in part by a grant from the UK Joint Higher Education Research Investment Fund and the University of Bristol. M. E. Collinson provided advice and discussion.

Distribution of Cutan in Modern Leaves

This project was funded in part through a research grant awarded to R.D.P., D.E.G.B., and Raymond Michels by the Petroleum Research Fund, American Chemical Society. I. Bull, R. Berstan, and the Bristol Node of the NERC Life Sciences Mass Spectrometry Facility are thanked for analytical support. S. Derenne, P. Finch, and R. Michels provided useful discussion during the course of this project. P. F. van Bergen, T. T. Nguyen Tu, and H. Yang are thanked for their critical comments on this research.

Molecular Preservation of Graptolites

C. Underwood, A. Scott and D. McIlroy are thanked for useful comments on a previous version of the paper. The Bristol node of the NERC mass spectrometric facility is thanked for analytical help.

C. Glasstris is thanked for supplying the Rhabdopleura samples.

Molecular Preservation of Eurypterids

Apart from modern *Limulus*, analyses were carried out at the Natural Environment Research Council mass-spectrometry facility at the School of Chemistry, University of Bristol. *Limulus* analysis was carried out at the Geobiology Laboratory at the Massachusetts Institute of Technology, courtesy of Roger Summons. O.E.T. is funded by Norges Forskningsråd, grant 166647/V30. Samuel J. Cieurca, Jr., collected the specimens and retained the flaking cuticle. Mark Brandon and Elizabeth Wong helped with the Raman study, and Andrew Scott provided samples from Joggins and Lone Star Lake and vitrinite reflectance values for these localities.

The research has additionally benefited from comments by Jochen Brocks and Graham Logan.

Molecular Decay of Plant Biopolymers

C. Brown at the Stonerose Interpretive Center in Republic permitted collection of specimens of fossil *Metasequoia* and B.A. Le-Page at the PECO Energy Company provided *Metasequoia* from Axel Heiberg. C. Colonero is thanked for analytical

assistance at MIT, E. Champion for editing and two anonymous reviewers for constructive comments on the research. Embedding and thin sectioning of leaves were carried out in the Center for Brain Research, Medical University of Vienna with the help of U. Juszczak. Staff members of the center and Miss Juszczak are sincerely thanked. Acknowledgment is made to the donors of the American Chemical Society Petroleum Research Fund for support of this research through a grant awarded to D.E.G.B and a Summer Research Fellowship fund for Prof. Hong Yang (Bryant University).

Molecular Decay of Arthropod Biopolymers

E. Lazo-Wasem and D. Drew identified the penaeid shrimp. Research grant from the American Chemical Society Petroleum Research Fund provided research support. J. de Leeuw and A. Stankiewicz have provided constructive and helpful reviews.

Contents

1	Molecular Decay of Plant Biopolymers	1
	Introduction.....	2
	Natural Decay	2
	Experimental Heating (Maturation).....	3
	Fossils	3
	Analysis	3
	Chemistry of Modern Plant Tissue and Decay Series Samples.....	4
	Microscopy of Modern and Fossil Material	7
	Chemistry of Fossil Tissue.....	9
	Experimental Heating	10
	References.....	14
2	Distribution of Cutan in Modern Leaves	17
	Introduction.....	17
	Samples and Preparation.....	19
	Analytical Results	22
	The Occurrence of Cutan in Modern Leaves	27
	Cutan and the Leaf Fossil Record.....	33
	Explanations for the Aliphatic Component in Fossils	34
	The Ecology and Physiology of Plants with Cutan-Containing Leaves	36
	References.....	37
3	Organic Preservation of Biopolymers in Fossil Leaves	43
	Introduction.....	43
	Samples.....	45
	Microscopic Analyses	46
	Organic Geochemical Analyses	46
	Microscopic Investigations	48
	Gross Morphology	48
	Internal Organisation.....	48
	Surface Structures	52

Chemistry of Modern Leaves	54
Chemistry of the Diatomite	56
Chemistry of Fossil Leaves.....	57
Spectroscopic Studies	62
Saponification	64
Aliphatic Composition of Modern Plants.....	64
Composition of the Ardèche Fossil Leaves	67
Possible Origin of the Aliphatic Macromolecule in the Ardèche Fossil Leaves.....	69
Implications	70
References.....	71
4 Migration of Organic Molecules from Sediment to Fossils.....	75
Introduction.....	76
Materials and Method	76
Analytical Protocol	78
Analytical Results	79
Ultrastructural Preservation of Fossils	79
Molecular Preservation of Fossils and Associated Sediment.....	81
Structural and Molecular Preservation	88
Comparison Between Sediment and Fossil	90
References.....	91
5 Molecular Transformation of Plant Biopolymers in High P-T Conditions.....	95
Introduction.....	95
Materials and Methods	96
Preparing the Gold Cell	97
Autoclave Experiment	97
Implications	98
References.....	105
6 Lipid Incorporation During Experimental Decay of Arthropods	107
Introduction.....	107
Materials and Methods	108
Chemical Analysis	109
¹³ C NMR Analysis	109
Changes in Gross Morphology During Decay.....	110
Changes in Ultrastructure During Decay.....	110
Changes in Macromolecular Chemistry During Decay.....	111
References.....	116
7 Molecular Preservation of Eurypterids	119
Introduction.....	119
Material	121

Methods	123
Results	125
Discussion.....	127
References.....	132
8 Transformation of Arthropod Biopolymers in High P-T Conditions	135
Introduction.....	135
Material and Methods.....	136
Composition of Samples Used in Experiments	137
Composition of the Cuticle and Lipid Compounds Matured Without Chemical Treatment	139
Composition of Cuticle Matured After Chemical Treatment	139
Discussion.....	141
References.....	144
9 Molecular Preservation in Graptolites.....	147
Methods	149
Results	149
Discussion.....	152
References.....	154
10 Molecular Transformation of Bacteria at High P-T Conditions	157
Introduction.....	157
Materials and Methods	158
Results and Discussion	159
References.....	162
11 Preservation of Organic Fossils at the Las Hoyas Formation, Spain.....	165
Introduction.....	165
Geological Setting and Fossil Material.....	166
Analytical Protocol	167
Results	168
Discussion and Conclusion.....	173
References.....	174

Chapter 1

Molecular Decay of Plant Biopolymers

Abstract Analysis of modern *Metasequoia* leaves revealed the presence of structural polyester cutin, guaiacyl lignin units and polysaccharides. Analysis of environmentally decayed *Metasequoia* leaves revealed that guaiacyl lignin units and cellulose were degraded more relative to vinyl phenol (the last being the primary pyrolysis product of cutin and plant cuticles) suggesting that cutin is likely more stable than lignin and cellulose during early diagenesis contrary to some previous studies. This is supported by electron microscopy of changes in the cellular structure and cuticle of the modern, decayed, and fossil *Metasequoia* leaves. Analysis of *Metasequoia* fossils from the Eocene of Republic (Washington State) showed a significant aliphatic component without detection of biopolymeric lignin and polysaccharides. Fossils from the Eocene of Axel Heiberg revealed the presence of lignin and an aliphatic polymer up to C₂₉ with cellulose and fossils from the Miocene Clarkia deposit in Idaho of USA revealed lignin and an aliphatic polymer up to C₂₇ without any polysaccharides. Modern *Metasequoia* needle was heated experimentally in confined conditions that generated a macromolecular composition with an aliphatic polymer up to C₃₂ and additional phenolic compounds similar to those present in the fossils. Experimental heating of cutin is known to generate an aliphatic polymer with carbon chain length <C₂₀ demonstrating that the *n*-alkyl component with carbon chain length >C₂₀ in the heated *Metasequoia* needle is a product of incorporation of longer chain plant waxes indicated by the odd over even predominance of the >C₂₇ *n*-alkanes. The resistant nature of cutin compared to lignin and polysaccharides explains the ubiquitous presence of an *n*-alkyl component (<C₂₀) in fossil leaves even when polysaccharides are absent and lignin has decayed.

Keywords Lignin • Cellulose • Cutin • Mass spectrometry • Fossil • Preservation

Introduction

Metasequoia Miki ex Hu and Cheng (dawn redwood) was first described as a fossil (Miki 1941) before its endangered living species *M. glyptostroboides* Hu and Cheng was discovered in central-southwest China (Hu and Cheng 1948; Fulling 1976). It has a long and well documented fossil record, displaying remarkable anatomical and morphological stasis since the Cretaceous (Chaney 1951; Liu et al. 1999; Yang and Jin 2000; LePage et al. 2005). Some *Metasequoia* fossil remains are among the best preserved plant fossil material (Yang et al. 2005, 2007) and its molecular diagenesis and preservation can be used to explore the relative preservation potential of cutin, lignin and cellulose.

Hedges and Weliky (1989) physically isolated intact needles of fir, hemlock and cedar from different horizons of a recent sediment core from a coastal marine bay, and from nearby trees and forest litter; they demonstrated a greater preservation potential of lignin than polysaccharides, as observed in other studies (Hedges et al. 1985; Kelleher et al. 2006). While observing a rapid degradation of carbohydrates during initial decay, Kelleher et al. (2006) also noted the stability of aliphatic components from leaf cuticle. Some studies have shown, however, that cutin, an important aliphatic component of cuticle, has a lower preservation potential than lignin (Goñi and Hedges 1990; Opsahl and Benner 1995), in which case fossil leaves should primarily reveal an aromatic signal (derived from lignin, polysaccharides and their diagenetically altered components) and not an aliphatic one (cuticular components). However, leaf fossils invariably reveal a composition with a significant aliphatic component, with or without the presence of biopolymeric lignin and/or polysaccharides.

In order to understand the preservation of the primary structural biopolymers (lignin, cutin, and cellulose), *Metasequoia* leaf samples which had decayed in the natural environment over a year or more were analysed chemically and microscopically to evaluate the preserved biomolecules and their relative preservation potential (Bland et al. 1998; Clifford et al. 1995; Eglinton and Hamilton 1967; Goñi and Hedges 1992; Haddad et al. 1992; Kolattukudy 1980; Landais et al. 1989; Nip et al. 1986) and then compared to the chemistry of fossils from the Miocene of Clarkia (Idaho State, USA), and Eocene of Republic (Washington State, USA) and Axel Heiberg (Canadian Arctic Archipelago). Heating experiments were conducted on modern *Metasequoia* in gold capsules to evaluate the transformation of these biopolymers for comparison with the composition of fossils and sedimentary organic matter.

Natural Decay

A series of leaf samples of *Metasequoia glyptostroboides* representing a sequence of various stages of tissue development and decay (referred to hereafter as “decay series samples”) was collected from the Mt. Auburn Cemetery (42.6 N, 71.2 E), MA, U.S.A. during fall through winter of 2004. This tree, Mt. Auburn Cemetery Accession #19510001, was planted at the northern bank of the Willow Pond in 1951

with seed stock from the Arnold Arboretum of Harvard University, which was obtained from China in 1947. Samples 1–3 were picked directly from the south side of the tree to represent samples that were green (sample 1) through those showing the onset of a change of colour (sample 2) to those turned red (sample 3) during stages of senescence on the tree. Sample 4 was collected from the ground directly under the same tree following leaf fall. Samples 5 and 6 were obtained from the lake under the tree using an environmental dredge. Sample 5 was collected from the water-sediment interface, whereas sample 6 was obtained from sediments representing deposition of the previous years. The leaves of sample 5 were lighter in colour than those of sample 6. Following collection, all samples were divided into two sets; one was air dried and kept in paper envelopes for morphological investigation and the other was frozen immediately for chemical analysis. C and N concentrations were obtained for sample 1 and 6, the two end members.

Experimental Heating (Maturation)

Modern *Metasequoia* needles were crushed in liquid N₂, powdered and heated in sealed gold cells at 350 °C without any chemical pre-treatment under a confinement pressure of 700 bar for 24 h in the absence of water (see Michels et al. 1995; Hautevelle et al. 2006; Gupta et al. 2007a). This technique generates a chemical composition similar to that of organic fossils, particularly the aliphatic component. Hence, it can be used to explore how different structural components and biopolymers in plants contribute to the formation of a geopolymer. The temperature chosen was that at which the most dramatic change in chemical composition was observed during a previous investigation of arthropod cuticle (Stankiewicz et al. 2000; Gupta et al. 2007a). These experiments were conducted at the hydrothermal lab of the Geophysical Lab, Carnegie Institution.

Fossils

Fossil leaves of *Metasequoia* were collected from sediments of Republic (Eocene, Washington State, USA), Clarkia (Miocene, Idaho, USA), and Axel Heiberg (Eocene, Canada).

Analysis

Pyrolysis-gas chromatography-mass spectrometry (Py-GC-MS) reveals bulk macromolecular information that has been used extensively for the characterization of insoluble fossil organic matter (Larter and Horsfield 1993; Logan et al. 1993; Gupta

et al. 2007b, c). Compounds generated were identified by comparing their spectra with those reported in the literature (Gupta et al. 2006; Gupta and Pancost 2004; Ralph and Hatfield 1991; van Bergen et al. 1997) as well as those obtained from model reference compounds lignin and cellulose commercially obtained from Sigma-Aldrich. Modern and fossil samples were pyrolysed using a CDS 5150 Pyroprobe by heating at 650 °C for 20 s. Compound detection and identification were performed with on line GC-MS in full scan mode using a Hewlett Packard HP6890 gas chromatograph interfaced to a Micromass AutoSpec Ultima magnetic sector mass spectrometer. GC was performed with a J&W Scientific DB-1MS column (60 m × 0.25 mm I.D., 0.25 µm film thickness) using He as carrier gas. The oven was programmed from 50 °C (held 1 min) to 300 °C (held 28 min) at 8 °C min⁻¹. The source was operated in the electron ionization (EI) mode at 70 eV ionization energy at 250 °C. The AutoSpec full scan rate was 0.80 s/decade over a mass range of 50–700 Da with an inter-scan delay of 0.20 s.

For analysis of experimentally matured samples, samples were subjected to thermodesorption of weakly bound or non-covalently bound components (at 310 °C, Gupta et al. 2007a) and then subjected to pyrolysis at 650 °C in order to analyze the macromolecular component. Fresh, decayed, and fossil leaves were extracted 15 min × 3 times with 2:1 Dichloromethane: Methanol to remove soluble lipids.

Leaves of decay series samples were air dried. They were softened in water before they were prepared for embedding and thin sectioning. Conventional embedding and thin sectioning (2 µm) methods were applied with Toluidine Blue as the stain. Mounted thin slides were observed with a Nikon light microscope and photographed using an integral Nikon digital camera. For scanning electron microscopy (SEM), the leaves were softened and cut transversely in their middle portion. One piece of each leaf of about 1 mm long was mounted on a SEM stub with one of its cut sides facing upwards. Leaf pieces on stubs were air dried and sputter coated with approximately 20 nm of gold and examined with a JSM-6400 Scanning Microscope at 15 kV. The fossil leaf of *Metasequoia* from Miocene Clarkia was macerated in a 30 % HF solution overnight to dissolve the adhering matrix before cutting, and then treated similarly for SEM observation.

Chemistry of Modern Plant Tissue and Decay Series Samples

Figure 1.1 shows the Py-GC-MS total ion trace of fresh leaves (sample 1) of *Metasequoia glyptostroboides* from which the lipids have been extracted together with traces of leaves subjected to environmental decay (samples 4–6). Lignin (guaiacyl units), polysaccharides (e.g., levoglucosan from cellulose), C16 saturated and unsaturated fatty acyl moieties (derived from internal lipids and cutin), benzenes, vinyl phenol and alkyl phenols are abundant, as expected for a modern gymnosperm leaf (van Bergen et al. 1997), whereas *n*-alkanes and *n*-alk-1-enes were detected in trace amounts (as also noted in *Metasequoia* by Yang et al. 2005, Fig. 3).

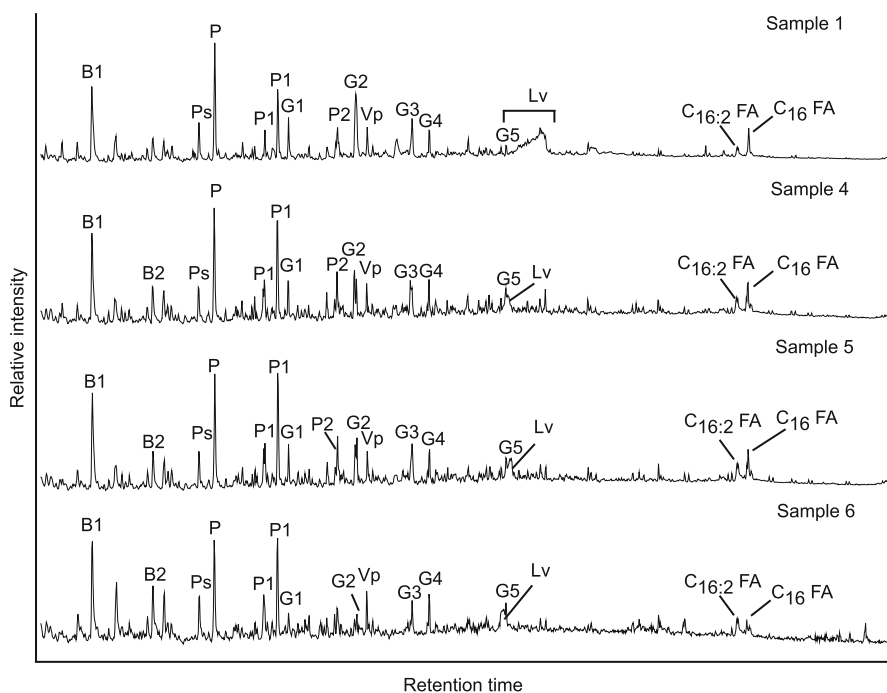


Fig. 1.1 Total ion chromatogram from Py-GC-MS of modern *Metasequoia glyptostroboides* after lipid extraction (sample 1), and at various stages of natural decay (samples 4–6). Ps: polysaccharide derivative; P: phenol; Bn: alkyl phenol; Pn: alkyl phenols, where n denotes number of carbons in the alkyl component; Vp: vinyl phenol, G denotes guaiacyl lignin units (G1 2-methoxy phenol, G2 2-methoxy-4-methyl phenol, G3 4-ethenyl-2-methoxyphenol; G5 3-allyl-6-methoxyphenol); Lv Levoglucosan; C_{16:2}FA C₁₆ diunsaturated fatty acid, C₁₆FA saturated fatty acid

Figure 1.2 highlights the molecular species of interest in this study: the mass chromatograms showing the distribution of the pyrolysis products of vinyl phenol vs. lignin (Fig. 1.2a) and vinyl phenol vs. cellulose (Fig. 1.2b), respectively. Clearly, the guaiacyl lignin units in sample 1 (undecayed) decrease progressively in abundance to vinyl phenol (through sample 4–6, Fig. 1.2a); a trend observed in levoglucosan derived from cellulose when compared to vinyl phenol (Fig. 1.2b). Vinyl phenol may be produced by thermal breakdown of the *p*-hydroxyphenol unit in certain types of lignin as a part of woody tissue, but in leaves it is mainly related to *p*-coumaric acid. It is present both as ester- and ether-linked units in woody tissues (as part of lignin), and also as part of decay-resistant cuticle (Tegelaar et al. 1989). Vinyl phenol (4-ethenyl phenol) is produced, along with C₁₆ unsaturated fatty acids as the primary thermal breakdown product during pyrolysis of cutin (Tegelaar et al. 1989) and isolated cuticles (Mösle et al. 1998) and is derived from *p*-coumaric acid as part of decay-resistant cuticle (Tegelaar et al. 1989). For these reasons, changes in the chemical composition of the leaves have been determined by the abundance of specific moieties relative to that of vinyl phenol. Vinyl phenol has been used as a marker for cutin and cuticle in

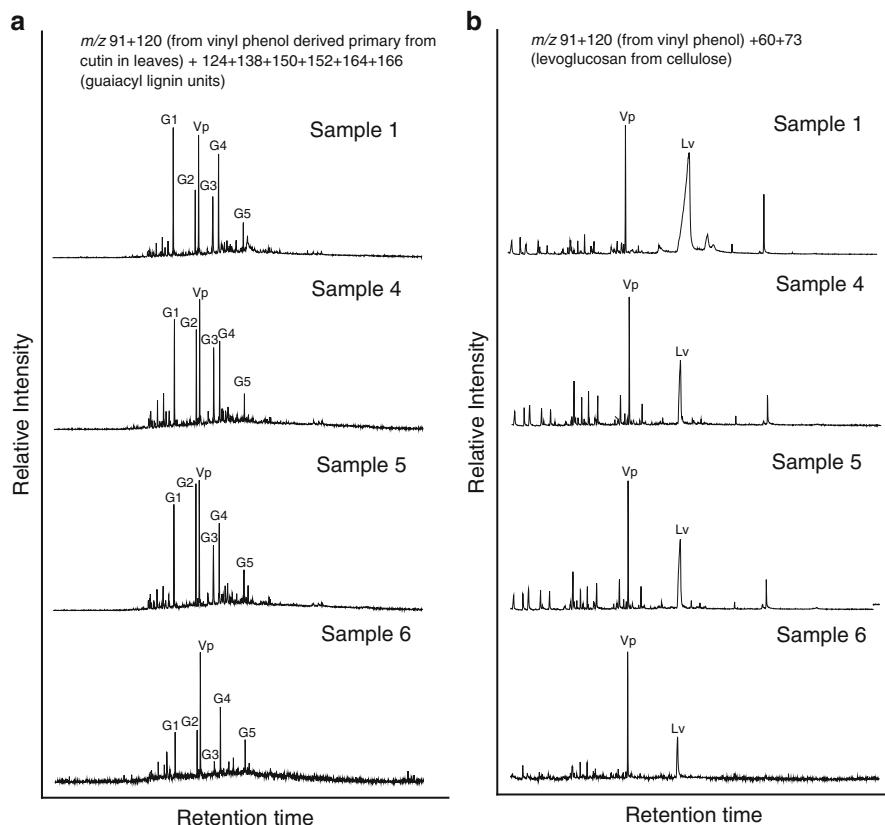


Fig. 1.2 Partial ion chromatogram from Py-GC-MS analysis of modern *Metasequoia* after lipid extraction at different stages of decay. (a) m/z 91 + 120 (from vinyl phenol derived primary from cutin in leaves) + 124 + 138 + 150 + 152 + 164 + 166 (guaiaacyl lignin units) and (b) 91 + 120 (from vinyl phenol) + 60 + 73 (levoglucosan from cellulose) showing the distribution of vinyl phenol vs. lignin pyrolysis products and vinyl phenol vs. cellulose pyrolysis products, respectively. Samples 2 and 3 remained largely unaltered, as demonstrated by microscopy and macromolecular analysis and are not figured. Symbols same as those used in Fig. 1.1

monitoring the decay of biopolymeric constituents of leaves (Gupta and Pancost 2004) and changes in the chemical composition of leaves have been monitored on the basis of the abundance of specific moieties relative to that of vinyl phenol (4-ethenyl phenol) as a characteristic product of cutin (Tegelaar et al. 1989; Möslé et al. 1998). Samples 1, 2, and 3 represent stages of a senescence progression while still attached to the tree and were chemically similar. Both lignin and cellulose were degraded relative to cutin during the year long period (Fig. 1.2). This is further supported by the observation that in Fig. 1.1 $C_{16:2}$ fatty acid produced from the thermal breakdown of cutin is largely undiminished in relative abundance in sample 6 when compared to sample 1. Measurement of bulk C and N concentrations revealed a 10 wt.% loss in C and 0.15 wt.% loss in N in sample 6 when compared to sample 1.

Microscopy of Modern and Fossil Material

Examination of the decay series samples using light microscopy (Fig. 1.3) and SEM (Fig. 1.4) revealed no evident change in the leaves of samples 1–4. Morphological changes were evident in samples 5 and 6, with extensive loss of internal tissue in sample 6, which had decayed for at least a year. The modern leaf (Fig. 1.3a) has a thin epidermal cell layer covered by a cuticular membrane on both the adaxial (upper) and the abaxial (lower) sides. Below the adaxial epidermis there are 1–2 layers of palisade cells (also called “arm palisade” cells: see Sterling 1949), under which a large amount of sponge parenchyma (more or less collapsed, probably due to air drying and water softening) occupies the largest portion of the mesophyll. The abaxial epidermis is covered by a thinner cuticular membrane. The epidermis is interrupted by stomata. At the midvein, the vascular bundle is surrounded by 1–2 layers of parenchymatous bundle sheath cells. Sclerenchymatous cells (fibres) are evident at both adaxial and abaxial sides of the vascular bundle and probably represent a bundle “cap.” Within the bundle sheath and “cap” lies the adaxial xylem and the abaxial phloem. A central resin canal is located adaxial to the vascular bundle and a resin canal occurs at each leaf margin, giving a total of three. Following decay for at least a year (Fig. 1.3b, sample 6) there was no obvious change in the epidermis or its covering cuticular membrane, but changes were observed in the internal tissue. Arm palisade cells had largely collapsed, leaving only a layer of crushed cell

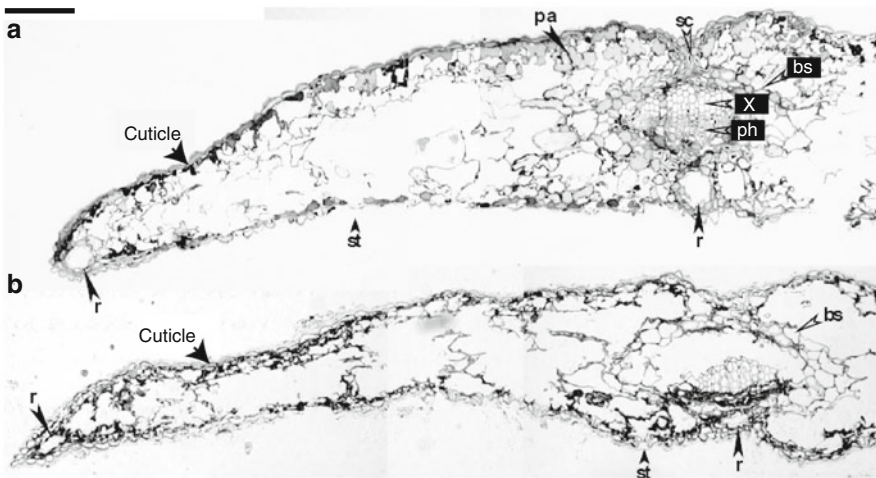


Fig. 1.3 Light microscopy photographs of transverse section of leaves of decay series of samples of *Metasequoia glyptostroboides*, showing only half of the leaf (left) and the midvein portion (right). (a) Sample 2. (b) Sample 6. In contrast to a, b shows extensive loss of internal tissue after at least 1 year of decay in water. Scale bar=0.1 mm. bs bundle sheath, pa palisade parenchyma, ph phloem, r resin canal (each leaf has a median resin canal adaxial to the single vascular bundle and two marginal resin canals), sc sclerenchyma, st stoma, x xylem

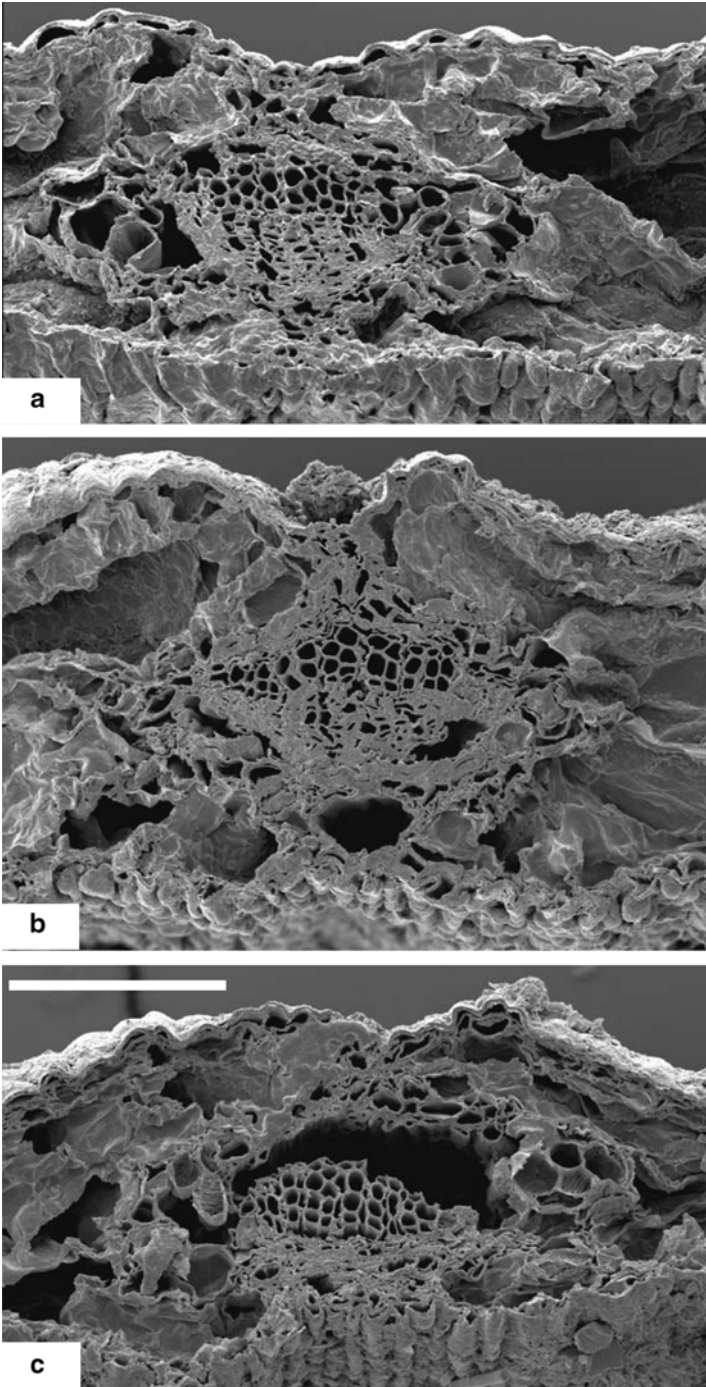


Fig. 1.4 SEM photographs of transverse section of leaves of decay series samples of *Metasequoia glyptostroboides*, showing only the midvein portion, with adaxial surface upwards. (a) Sample 1. (b) Sample 5. (c) Sample 6. Compared with Sample 1 (a), cells of Sample 5 (b) have not changed much but those of Sample 6 (c) largely collapsed. Scale bar 100 μm (for all three figures.)

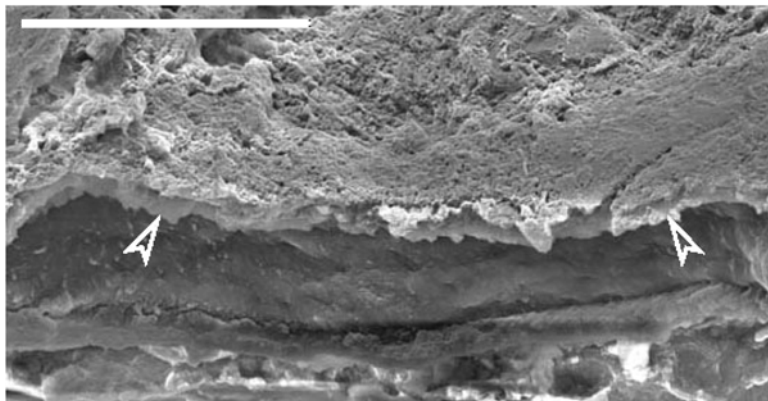


Fig. 1.5 SEM photograph of transverse section of a common compression fossil leaf of *Metasequoia* collected from the Clarkia Miocene deposit, showing the presence of external cuticular membrane (arrowheads) although all other internal tissue has decayed. Scale bar 6 μm

material beneath the adaxial epidermis. Sponge cells had also collapsed. The vascular bundle has largely decayed (see also Fig. 1.4c). The parenchymatous bundle sheath showed the least change: almost all the cells were preserved, but the cell wall had thinned (compare with Figs. 1.3a, 1.4a–b). Cells in the xylem had not collapsed much but the cell wall had thinned. Cells in the phloem had collapsed, causing the phloem to appear more compressed (see also Fig. 1.4b). Sclerenchymatous cells were not evident. The resin canals were more or less unaltered but the surrounding cells were crushed. A common compression fossil leaf of *Metasequoia* from the Miocene Clarkia locality was examined under SEM (Fig. 1.5) for comparison. It shows that the internal tissue, including the epidermis, has decayed, but the cuticular membrane is still clearly evident.

Chemistry of Fossil Tissue

The fossil *Metasequoia* from Clarkia (Fig. 1.6a) did not yield any polysaccharides including levoglucosan, but revealed the presence of lignin, alkyl phenols, vinyl phenol, benzene, pristene and an aliphatic component up to C_{27} . Analysis of fossil *Metasequoia* from the Eocene of Axel Heiberg (Fig. 1.6b) detected the presence of biopolymeric lignin, levoglucosan from cellulose and vinyl phenol, benzene, pristene, alkyl phenol derivatives and an aliphatic component up to C_{29} . Pyrolysis of fossil *Metasequoia* from the Middle Eocene of Republic (Fig. 1.6c) revealed no trace of biopolymeric lignin or polysaccharides, but yielded benzene derivatives, alkyl phenols and an *n*-alkyl component consisting of alkane and alkene homologues up to C_{23} . Thus, *n*-alkyl components indicate the occurrence of a significant long chain aliphatic geopolymer in the fossil leaves that is not evident in the modern sample, indicating that it is a product of diagenesis.

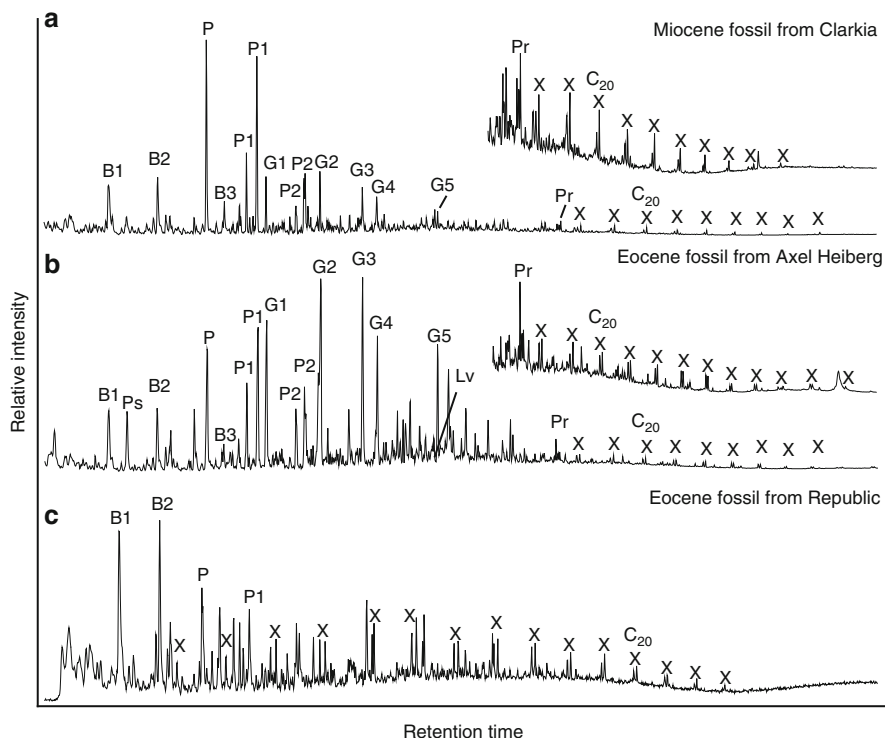


Fig. 1.6 Total ion chromatogram from Py-GC-MS analysis of fossil *Metasequoia* from (a) Miocene of Clarkia, (b) Eocene of Axel Heiberg (Canada), (c) Eocene of Republic. Note the presence of long-chain *n*-alkane/alk-1-enes (X); carbon chain length is denoted by Cn. Other symbols as Fig. 1.1. Note lack of preserved biopolymers in fossil from Republic, presence of lignin from Clarkia and both lignin and cellulose from Axel Heiberg. All fossils have a macromolecular aliphatic content C_{27} and above (displayed inset for Clarkia and Axel Heiberg) that is absent in the modern leaf

Experimental Heating

Modern *Metasequoia* needles were experimentally heated in confined conditions at 350 °C, 700 bars, without any chemical treatment, to investigate the transformation of biological precursors at this elevated pressure and temperature. Thermodesorption (TD-GC-MS) at 310 °C yielded primarily *n*-alkanes from C_{15} – C_{29} , alkyl phenols and alkyl naphthalenes. Py-GC-MS analysis of the residue following thermodesorption yielded *n*-alkane/*n*-alk-1-ene homologues from C_{8} – C_{32} , indicating the presence of an *n*-alkyl macromolecular component (Fig. 1.7). The most abundant homologues were those from C_{10} – C_{18} . The longer chain length *n*-alkanes ($>C_{27}$) showed an odd over even predominance. Apart from the aliphatics, other important pyrolysis products included phenol and its alkyl derivatives and benzene and its alkyl derivatives. The guaiacyl-related lignin moieties, polysaccharides and vinyl phenol evident in

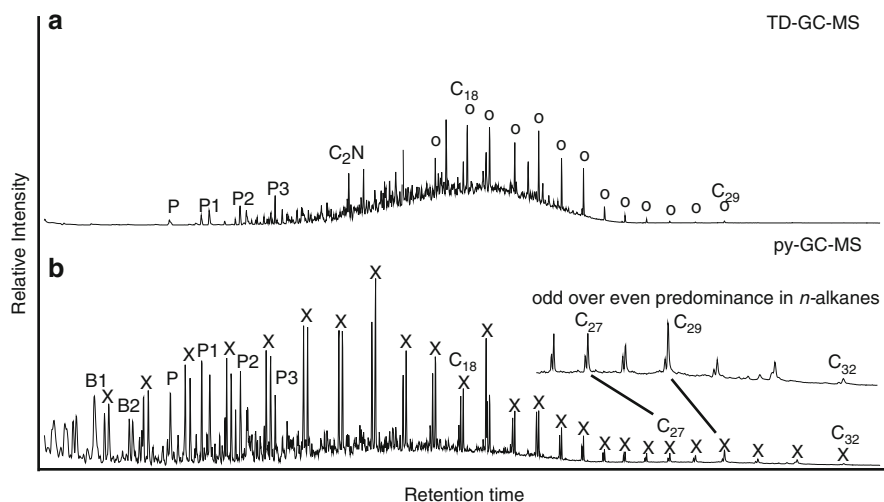


Fig. 1.7 Total ion chromatogram from (a) Thermodesorption (TD)-GC-MS analysis of experimentally heated Modern *Metasequoia* leaf (b) py-GC-MS analysis matured modern *Metasequoia* following thermodesorption of the same. C₂N C₂Naphthalene, O *n*-alkanes. Other same symbols as in Figs. 1.1 and 1.6

the fresh leaf tissue were not detected in the experimentally heated leaves, presumably due to thermal transformation of these biopolymers during the experiment.

Structural biopolymers have been documented in morphologically well-preserved *Metasequoia* leaves of Late Paleocene–Early Eocene age from the Ellesmere Island (Canadian Arctic Archipelago), where they revealed the preservation of polysaccharides and lignin and vinyl phenol (Yang 2005; Yang et al. 2005). Middle Eocene leaves from the Axel Heiberg Island (Canadian Arctic Archipelago) analysed here yielded lignin products similar to those identified from the Ellesmere Island fossils, with polysaccharide moieties (Yang et al. 2007; Jahren and Stenberg 2008). *Metasequoia* leaves from the Miocene Clarkia site in Idaho, USA, in contrast, are characterized by a dramatic reduction in polysaccharide moieties (Logan et al. 1993; Yang et al. 2005). The fossils from the Eocene of Republic do not show any lignin or polysaccharides but are composed of a macromolecular *n*-alkyl component. Such a macromolecular aliphatic component is absent in the modern *Metasequoia* and hence a product of diagenesis. Other important components of the fossil leaves released by pyrolysis are pristenes. These isoprenoids are most likely related to the pyrolysis of tocopherol (Goosens et al. 1984; Höld et al. 2001). Indeed, fossil leaves display a ubiquitous aliphatic composition, with little or no preservation of lignin and polysaccharides, especially in fossils older than Cenozoic (see Table 2 in Gupta et al. 2006). Cutan was not detected in the modern analogues of *Metasequoia* and cannot be the source of the macromolecular aliphatics (Gupta et al. 2006; de Leeuw et al. 2006).

This gradation in the nature of biomolecular preservation in *Metasequoia* leaves is paralleled by their morphological preservation as revealed by SEM (Yang et al. 2005).

Yang et al. (2005) argued that the final pyrolysis products of fossil material reflect both original molecular composition and tissue-specific degradation, suggesting that comparative studies of molecular preservation are best performed on an individual tissue (or organ) within an evolutionarily conserved taxonomic lineage. Indeed, SEM investigation of *Metasequoia* from the Miocene of Clarkia and from the decayed samples here showed that the progressive loss of internal tissue is paralleled by the biomolecular pattern observed using chemical analysis. However, some studies of fossil leaves of other taxa have shown that this is not always the case; in some instances morphological preservation may not be a good predictor of chemical preservation (Logan et al. 1993; Möslle et al. 1998; Collinson et al. 2000).

Investigations of the preservation of plant biopolymers have used high resolution solid state nuclear magnetic resonance (NMR) spectroscopy and microscopy (Hedges and Mann 1979; Cody and Sághi-Szabó 1999; Kelleher et al. 2006), and chemolytic methods based on the products of cutin and lignin following CuO oxidation (Goñi and Hedges 1990; Goñi et al. 1993; Opsahl and Benner 1995). Polysaccharides generally show a lower preservation potential than lignin (Hedges et al. 1988; Kelleher et al. 2006). Lignin has been detected in biopolymeric form in sediments of Pleistocene age (Hartog et al. 2004) and in 0.6 my old lake sediments (Ishiwatari and Uzaki 1987), possibly where fungal degradation is limited (Hedges and Mann 1979; Goñi et al. 1993; Benner et al. 1990a, b).

In a previous study evaluating the relative preservation potential of cutin and lignin, Goñi and Hedges (1990) collected whole green litter, fir, hemlock and cedar needles, from Dabob Bay (Washington State, USA) and found that cutin acids accounted for ~3 % of the tissue in green needles, ~4 % in needle litter, 0.5–1.5 % in sedimentary needles, and about 0.1 % of the organic carbon in bulk sediments. Analysis of 100 year old needles of the same taxa revealed that ca. 80 % of the original cutin acids in fresh green needles were lost. Goñi and Hedges (1990) concluded that cutin was more reactive than lignin and polysaccharides, this reactivity being facilitated by hydroxyl groups and the presence of double bonds in the cutin structure.

Opsahl and Benner (1995) investigated long term (4 year) subaqueous decomposition in five different vascular plant tissues, including mangrove leaves and wood (*Avicennia germinans* L.), cypress needles and wood (*Taxodium distichum* (L.) Rich.) and smooth cordgrass (*Spartina alterniflora* Loisel). All tissues were decomposed under identical conditions and final mass losses were 97, 68, 86, 39 and 93 %, respectively, indicating extensive degradation of both cutin and lignin. Analysis of the lignin component of herbaceous tissues, using alkaline CuO oxidation, indicated that change in the lignin content was strongly dependent on tissue type, ranging from 77 % enrichment for smooth cord grass to 6 % depletion for cypress needles. In contrast, depletion of cutin was extensive (65–99 %) for all herbaceous tissues.

In the present study, the total C content of *Metasequoia* leaves decreased by 10 % in the leaves buried in the lake sediment. Lignin and cellulose degraded faster than cutin as revealed through tracking the pyrolysis products of cuticular components vs. lignin and cellulose, and using microscopy to investigate tissue loss in

environmental samples 1 year old or more. This result differs from those discussed above (Opsahl and Benner 1995). A number of factors may account for this discrepancy, including both biotic and abiotic as well as environmental and preservation conditions. Additionally, earlier work used chemolysis rather than pyrolysis to analyse the samples. As cuticles constitute a multi-layered structure with a diverse chemistry, a chemical degradation approach targeted at specific bipolymeric moieties may not be adequate to rank the preservational potential of each category of biomolecules in a single chemolytic protocol. In addition to the different analytical techniques employed and different natural setting (i.e., marine vs. lacustrine), the discrepancy may reflect differences in the duration of decay. Using HR-MAS NMR (high resolution- magic angle spinning- nuclear magnetic spectroscopy) spectroscopy, Kelleher et al. (2006) documented an increase in the proportion of aliphatic cutin components of pine needles during the first 10 weeks of their natural decay when this concentration plateaued at a high level throughout the experiment. Thus, it appears that cutin of plant cuticles survive well at least during the early states of transformation as our new data indicate. If lignin were more robust than cutin, a fossil leaf should yield a primarily aromatic signal from biopolymeric and diagenetically altered lignin. An aliphatic signal should not dominate after the loss of cutin. However, as discussed above, most fossil leaves reveal a significant aliphatic content. The results of our study may explain why fossil cuticles are often preserved with a ubiquitous aliphatic composition, even where internal tissue has degraded. Even in examples where no cuticular material is evident under SEM, an aliphatic composition is still evident in fossil leaves due to lipid incorporation of internal tissue material from cellular membrane components (Gupta et al. 2007c). Moreover, Gupta and Pancost (2004) observed that internal tissues, despite being protected by the cuticle, are susceptible to decay as a result of microbial entry through stomata.

Analyses of modern *Metasequoia* leaves have revealed the presence of the structural polyester cutin, guaiacyl lignin units and polysaccharides as the primary biomolecules. *Metasequoia* leaves that have undergone natural decay at a lake-sediment setting to various degrees over a year long period revealed that guaiacyl lignin units and cellulose had degraded more relative to cutin. These data suggest that cutin and cuticular components (and their diagenetically altered products) are likely more stable than both lignin and cellulose during early diagenesis. Electron microscopy revealed changes in the cellular structure and cuticle of the modern and decayed leaves and confirmed there was no obvious change in the epidermis and covering cuticular membrane. In addition, arm palisade cells and sponge cells largely collapsed, the vascular bundle had largely decayed and the cell wall in the xylem had thinned after a year of decay. Fossil leaf of *Metasequoia* from the Miocene Clarkia locality revealed that the internal tissue, including the epidermis, has decayed, but the cuticular membrane was still clearly evident, supporting the preservation insights provided by the decay experiment.

Analysis of Tertiary *Metasequoia* fossils from the Eocene of Republic (Washington State) showed a significant aliphatic component without detection of biopolymeric lignin and polysaccharides. Fossils from the Eocene of Axel Heiberg

revealed the presence of lignin and aliphatic polymer up to C_{29} with minor amounts of cellulose. Fossils from the Miocene of *Clarkia* revealed lignin and an aliphatic polymer up to C_{27} without any polysaccharides. Thus, analysis of fossils revealed a significant macromolecular aliphatic component that was absent in the modern counterpart, attributing to its formation during diagenesis. The resistant nature of cutin compared to lignin and polysaccharides explains the ubiquitous presence of an *n*-alkyl component ($<C_{20}$) in fossil leaves and terrestrially derived organic matter even when the analysis reveals that polysaccharides are absent and lignin has decayed; cutin and its diagenetically altered products contribute significantly to the of aliphatic components in sedimentary organic matter.

References

- Benner R, Weliky K, Hedges JI (1990a) Early diagenesis of mangrove leaves in a tropical estuary: molecular-level analyses of neutral sugars and lignin-derived phenols. *Geochim Cosmochim Acta* 54:1991–2001
- Benner R, Hatcher PG, Hedges JI (1990b) Early diagenesis of mangrove leaves in a tropical estuary: bulk chemical characterization using solid-state ^{13}C NMR and elemental analyses. *Geochim Cosmochim Acta* 54:2003–2013
- Bland HA, van Bergen PF, Carter JF, Evershed RP (1998) Early diagenetic transformations of proteins and polysaccharides in archaeological plant remains. In: Stankiewicz BA, van Bergen PF (eds) Nitrogen-containing macromolecules in the bio- and geosphere, vol 707, ACS symposium series.
- Chaney RW (1951) A revision of fossil *Sequoia* and *Taxodium* in western North America based on the recent discovery of *Metasequoia*. *Trans Am Philos Soc New Ser* 40:171–239
- Clifford DJ, Carson DM, McKinney DE, Bortiatynski JM, Hatcher PG (1995) A new rapid technique for the characterization of lignin in vascular plants: thermochemolysis with tetramethylammonium hydroxide (TMAH). *Org Geochem* 23:169–175
- Cody GD, Sághi-Szabó G (1999) Calculation of the ^{13}C NMR chemical shift of ether linkages in lignin derived geopolymers: constraints on the preservation of lignin primary structure with diagenesis. *Geochim Cosmochim Acta* 63:193–205
- Collinson ME, Möslle B, Finch P, Wilson R, Scott AC (2000) Preservation of plant cuticles. *Acta Palaeobot Suppl* 2:629–632
- de Leeuw JW, Versteegh GJM, van Bergen PF (2006) Biomacromolecules of algae and plants and their fossil analogues. *Plant Ecol* 182:209–233
- Eglinton G, Hamilton RJ (1967) Leaf epicuticular waxes. *Science* 156:1322–1334
- Fulling EG (1976) *Metasequoia*—fossil and living. *Bot Rev* 42:215–315
- Goñi MA, Hedges JI (1990) The diagenetic behavior of cutin acids in buried conifer needles and sediments from a coastal marine environment. *Geochim Cosmochim Acta* 54:3083–3093
- Goñi MA, Hedges JI (1992) Lignin dimers: structures, distribution, and potential geochemical applications. *Geochim Cosmochim Acta* 56:4025–4043
- Goñi MA, Nelson B, Blanchette RA, Hedges JI (1993) Fungal degradation of wood lignins: geochemical perspectives from CuO-derived phenolic dimers and monomers. *Geochim Cosmochim Acta* 57:3985–4002
- Goosens H, de Leeuw JW, Schenck PA, Brassell SC (1984) Tocopherols as likely precursors of pristane in ancient sediments and crude oils. *Nature* 312:440–442
- Gupta NS, Pancost RD (2004) Biomolecular and physical taphonomy of angiosperm leaf during early decay: implications for fossilisation. *Palaios* 19:428–440

- Gupta NS, Collinson ME, Briggs DEG, Evershed RP, Pancost RD (2006) Reinvestigation of the occurrence of cutan in plants: implications for the leaf fossil record. *Paleobiology* 32:432–449
- Gupta NS, Michels R, Briggs DEG, Collinson ME, Evershed RP, Pancost RD (2007a) Experimental evidence for formation of geomacromolecules from plant leaf lipids. *Org Geochem* 38:28–36
- Gupta NS, Briggs DEG, Collinson ME, Evershed RP, Michels R, Pancost RD (2007b) Molecular preservation of plant and insect cuticles from the Oligocene Enspel Formation, Germany: evidence against derivation of aliphatic polymer from sediment. *Org Geochem* 38:404–418
- Gupta NS, Briggs DEG, Collinson ME, Evershed RP, Michels R, Jack KS, Pancost RD (2007c) Evidence for the in situ polymerisation of labile aliphatic organic compounds during the preservation of fossil leaves: implications for organic matter preservation. *Org Geochem* 38:499–522
- Haddad RI, Newell SY, Martens CS, Fallon RD (1992) Early diagenesis of lignin-associated phenolics in the salt marsh grass *Spartina alterniflora*. *Geochim Cosmochim Acta* 56:3751–3764
- Hartog N, van Bergen PF, de Leeuw JW, Griffioen J (2004) Reactivity of organic matter in aquifer sediments: geological and geochemical controls. *Geochim Cosmochim Acta* 68:1281–1292
- Hauteville Y, Michels R, Lannuzel F, Malartre F, Trouiller A (2006) Confined pyrolysis of extant land plants: a contribution to palaeochemotaxonomy. *Org Geochem* 37:1546–1561
- Hedges JI, Mann DC (1979) The characterization of plant tissues by their lignin oxidation products. *Geochim Cosmochim Acta* 43:1803–1807
- Hedges JI, Weliky K (1989) Diagenesis of conifer needles in a coastal marine environment. *Geochim Cosmochim Acta* 53:2659–2673
- Hedges JI, Cowie GL, Ertel JR, Barbour JR, Hatcher PG (1985) Degradation of carbohydrates and lignins in buried woods. *Geochim Cosmochim Acta* 49:701–711
- Hedges JI, Blanchette RA, Weliky K, Devol AH (1988) Effects of fungal degradation on the CuO oxidation products of lignin: a controlled laboratory study. *Geochim Cosmochim Acta* 52:2717–2726
- Höld IM, Schouten S, Van der Gaast SJ, Sinninghe Damsté JS (2001) Origin of prist-1-ene and prist-2-ene in kerogen pyrolysates. *Chem Geol* 172:201–212
- Hu HH, Cheng WC (1948) On the new family Metasequoiaceae and on *Metasequoia glyptostroboides*, a living species of the genus *Metasequoia* found in Szechuan and Hupeh. *Bull Fan Meml Inst Bot New Ser* 2:153–162
- Ishiwatari R, Uzaki M (1987) Diagenetic changes of lignin compounds in a more than 0.6 million-year-old lacustrine sediment (Lake Biwa, Japan). *Geochim Cosmochim Acta* 51:321–328
- Jahren AH, Stenberg LSL (2008) Annual patterns within tree rings of the Arctic middle Eocene (ca. 45 Ma): isotopic signatures of precipitation, relative humidity, and deciduousness. *Geology* 36:99–102
- Kelleher BP, Simpson MJ, Simpson AJ (2006) Assessing the fate and transformation of plant residues in the terrestrial environment using HR-MAS NMR spectroscopy. *Geochim Cosmochim Acta* 70:4080–4094
- Kolattukudy PE (1980) Biopolyester membranes of plants: cutin and suberin. *Science* 208:990–1000
- Landais P, Michels R, Poty B (1989) Pyrolysis of organic matter in cold-seal autoclaves. *J Anal Appl Pyrolysis* 16:103–115
- Larter SR, Horsfield B (1993) Determination of structural components of kerogens by the use of analytical pyrolysis methods. *Top Geobiol* 11:271–287
- LePage BA, Yang H, Matsumoto M (2005) The evolution and biogeographic history of *Metasequoia*. In: LePage BA, Williams CJ, Yang H (eds) *The geobiology and ecology of Metasequoia*. Springer, pp 3–114
- Liu Y, Li C, Wang Y (1999) Studies on fossil *Metasequoia* from north-east China and their taxonomic implications. *Bot J Linn Soc* 130:267–297
- Logan GA, Boon JJ, Eglinton G (1993) Structural biopolymer preservation in Miocene leaf fossils from the Clarkia site, Northern Idaho. *Proc Natl Acad Sci U S A* 90:2246–2250

- Michels R, Landais P, Torkelson BE, Philp RP (1995) Effects of confinement and water pressure on oil generation during confined pyrolysis, hydrous pyrolysis and high pressure hydrous pyrolysis. *Geochim Cosmochim Acta* 59:1589–1604
- Miki S (1941) On the change of flora in eastern Asia since Tertiary period: I. The clay or lignite beds flora in Japan with special reference to the *Pinus trifolia* bed in central Hondo. *Jpn J Bot* 11:237–303
- Mösle B, Collinson ME, Finch P, Stankiewicz BA, Scott AC, Wilson R (1998) Factors influencing the preservation of plant cuticles: a comparison of morphology and chemical comparison of modern and fossil examples. *Org Geochem* 29:1369–1380
- Nip M, Tegelaar EW, Brinkhuis H, de Leeuw JW, Schenk PA, Holloway PJ (1986) Analysis of modern and fossil plant cuticles by Curie point Py-GC and Curie point Py-GC-MS: recognition of a new, highly aliphatic and resistant biopolymer. *Org Geochem* 10:769–778
- Opsahl S, Benner R (1995) Early diagenesis of vascular plant tissues: lignin and cutin decomposition and biogeochemical implications. *Geochim Cosmochim Acta* 59:4889–4904
- Ralph J, Hatfield RD (1991) Pyrolysis-GC-MS characterization of forage materials. *J Agric Food Chem* 39:1426–1437
- Stankiewicz BA, Briggs DEG, Michels R, Collinson ME, Evershed RP (2000) Alternative origin of aliphatic polymer in kerogen. *Geology* 28:559–562
- Sterling C (1949) Some features in the morphology of *Metasequoia*. *Am J Bot* 36:461–471
- Tegelaar EW, de Leeuw JW, Holloway PJ (1989) Some mechanisms of flash pyrolysis of naturally occurring higher plant polyesters. *J Anal Appl Pyrolysis* 15:289–295
- van Bergen PF, Bull ID, Poulton PR, Evershed RP (1997) Organic geochemical studies of soils from the Rothamsted Classical Experiments—I. Total lipid extracts, solvent insoluble residues and humic acids from Broadbalk Wilderness. *Org Geochem* 26:117–135
- Yang H (2005) Biomolecules from living and fossil *Metasequoia*: biological and geological applications. In: LePage BA, Williams CJ, Yang H (eds) *The geobiology and ecology of Metasequoia*. Springer, pp 253–281
- Yang H, Jin J-H (2000) Phytogeographic history and evolutionary stasis of *Metasequoia*: geological and genetic information contrasted. *Acta Palaeontol Sin Suppl* 39:288–307
- Yang H, Huang Y, Leng Q, LePage BA, Williams CJ (2005) Biomolecular preservation of Tertiary *Metasequoia* fossil *lagerstätten* revealed by comparative pyrolysis analysis. *Rev Palaeobot Palynol* 134:237–256
- Yang H, Leng Q, LePage BA (2007) Labile biomolecules in three-dimensionally preserved early Tertiary *Metasequoia* leaves from Ellesmere Island, Canada. Biological and geological applications. *Bull Peabody Mus Nat Hist Yale Univ* 48:317–328

Chapter 2

Distribution of Cutan in Modern Leaves

Abstract Cutan, a resistant non hydrolysable aliphatic biopolymer, was first reported in the cuticle of *Agave americana* and has generally been considered ubiquitous in leaf cuticles along with the structural biopolyester cutin. Because leaves and cuticles in the fossil record almost always have an aliphatic composition, it was argued that selective preservation of cutan played an important role in leaf preservation. However, the analysis of leaves using chemical degradation techniques involving hydrolysis to test for the presence of cutan reveals that it is absent in 16 of 19 taxa (angiosperm and gymnosperm), including many previously reported to contain cutan on the basis of pyrolysis data. Cutan is clearly much less widespread in leaves than previously thought and its presence or absence does not exert any major bias on the preservation of leaves in the fossil record. In the absence of cutan, other constituents—cutin, plant waxes and internal plant lipids—are incorporated into the geomacromolecule and contribute to the formation of a resistant fossil geopolymer.

Keywords Aliphatic biopolymers • Algaenan • Aliphatic • Cuticle

Introduction

Leaf fossils (including both complete leaves and their isolated cuticles) are widely used in applied paleobotany. Jones and Rowe (1999) provide a useful summary of many examples. Applications include paleobiodiversity analysis (Burnham 1993), paleoclimate analysis to determine both temperature and precipitation (Wolfe 1995; Wilf 1997; Wiemann et al. 1998; Jacobs 2002; Kowalski 2002; Kowalski and Dilcher 2003; Sun et al. 2003; Wilf et al. 2003; Liang et al. 2003; Glasspool et al. 2004), understanding plant paleoecology (Burnham et al. 1999; Royer et al. 2005) and vegetational history (Mai 1995; Collinson and Hooker 2003; Hill 2004), documenting insect/plant interaction (Glasspool et al. 2003), determining vegetation response to key global change events (Wing et al. 2005) and reconstructing

paleoatmospheric carbon dioxide levels (Royer et al. 2001). Underpinning all of this research is the assumption that either (i) the fossil record of leaves is representative of ancient plants and vegetation or (ii) the biases in the leaf fossil record are understood. Some aspects of taphonomic bias that result from transport processes or growth environment are partly understood and can be taken into account through a detailed understanding of facies associations. For example, high proportions of stenophylls and non-entire margined leaves at streamsides may yield an anomalously cool climate signal compared to the surrounding vegetation (Liang et al. 2003).

The outer cuticle of leaves is made up of the structural biopolymer cutin (primarily C₁₆ and C₁₈ hydroxy fatty acids; Kolattukudy 1980), which is hydrolysable under basic conditions, surface waxes (soluble in organic solvents) and, in some cases, the resistant non hydrolysable aliphatic biopolymer cutan (Nip et al. 1986a, b). The outer cuticle protects the internal tissues composed of more labile biopolymers—polysaccharides, lignin, and proteins. Chemical analyses of fossil leaves and cuticles have shown that although relatively ‘younger’ fossil material may preserve carbohydrates and lignin (Briggs et al. 2000, and references therein) fossil leaves and cuticles older than the Tertiary very often yield a dominant aliphatic signal (Nip et al. 1986a, b; Tegelaar et al. 1991; Logan et al. 1993; van Bergen et al. 1994; Möhle et al. 1997, 1998; Collinson et al. 1998; Stankiewicz et al. 1998b; Gupta et al. 2007a, b).

Tegelaar et al. (1991) argued that the leaf fossil record is biased in favor of leaves containing the highly resistant, highly aliphatic, non-hydrolysable macromolecule cutan in their cuticles. Any bias due to the presence or absence of cutan must be understood if data from fossil leaves are to be applied reliably in multidisciplinary research.

Cutan is a long chain aliphatic biopolymer resistant to hydrolysis (i.e., an aliphatic residue is recovered after base and acid hydrolysis: Nip et al. 1986a, b; Tegelaar et al. 1989c; McKinney et al. 1996; Mosle et al. 1997, 1998; Schouten et al. 1998) and was therefore interpreted as a diagenetically stable polymer that can survive in the fossil record with little chemical change (Nip et al. 1986a, b; Tegelaar et al. 1989a). Its diagenetic stability is due to largely non-hydrolysable ether linkages and sterically protected ester functional groups (for structural details refer to McKinney et al. 1996; Schouten et al. 1998). Cutan was first described and documented by Nip et al. (1986a, b) from the leaf cuticle of modern *Agave americana*, a monocotyledon flowering plant. Nip et al. (1986a) reported that the leaf cuticle of another monocotyledon, *Clivia miniata*, gave similar results to *Agave* and also contained cutan. Tegelaar et al. (1991) reported a characteristic cutan signature (an aliphatic signal of an extended homologous series of *n*-alkanes, *n*-alk-1-enes and *n*-alkadienes) in chromatograms generated by Curie-point pyrolysis of isolated complete cuticles of 11 of 13 modern plants analysed. However, this result was based on analysis using solely pyrolysis GC-MS, and did not involve isolating the cutan biopolymer from the modern plants using hydrolytic techniques. Tegelaar et al. (1991) equated the aliphatic signal with the material defined as non-ester cutin in maturing *Clivia miniata* cuticles by Schmidt and Schönherr (1982) and interpreted it as cutan. The apparently widespread occurrence of an aliphatic signal in

modern plants, combined with the dominantly aliphatic composition of fossil leaves and cuticles, led Tegelaar et al. (1991) to infer that selective preservation of cutan accounts for the preservation of fossil leaves, thus biasing the fossil record in favor of leaves containing the biopolymer cutan.

Mösle et al. (1997, 1998) and Collinson et al. (1998) sought to demonstrate the presence or absence of cutan on the basis that it should be recoverable as a residue after acid and base hydrolysis as initially documented by Nip et al. (1986b). Collinson et al. (1998) analysed leaf cuticles of modern *Ginkgo biloba* (previously thought to contain cutan: Nip et al. 1986b; Tegelaar et al. 1991), as well as a wide variety of modern conifers (Collinson et al. 1998), but were unable to detect cutan in the living plant cuticles despite the presence of aliphatic components in their fossil equivalents. However, Boom et al. (2005) suggested that the use of oxidative conditions (hydrogen peroxide and acetic acid) to isolate the *Ginkgo* and conifer cuticles from the leaves could have broken down the cutan.

In order to investigate the importance of cutan in the taphonomy of plants, we tested for its presence (as a highly aliphatic polymer resistant to base and acid hydrolysis) in a variety of modern leaves (Table 2.1). Whole leaves were used as the starting point for the analyses to avoid any possibility of altering the cuticles by chemical isolation. The analyses included genera with an extensive leaf fossil record (e.g. *Acer*, *Quercus*), and with minimal or no known fossil record (e.g. *Gossypium*). Other taxa were included in the analyses to enable comparisons with previous work (e.g., Tegelaar et al. 1991): the monocotyledonous flowering plants *Agave americana* and *Clivia miniata* previously reported to contain cutan (including the ‘type’ example of cutan in *Agave*, the taxon in which it was originally defined), *Ginkgo* and the conifers *Metasequoia*, *Sciadopitys*, *Abies* and *Pinus*, previously reported to lack cutan.

Samples and Preparation

Samples of modern leaves (indicated on Table 2.1) were collected fresh from the University of Bristol and University of Nancy botanic gardens during November 2002 and April 2003, respectively. The selected leaves were well developed and mature. These gardens are situated several miles from the town center and hence the chemistry of the leaves is unlikely to be affected by urban pollution. The experimental protocol used for detecting the presence of cutan is outlined in Fig. 2.1. The modern leaves were crushed in liquid nitrogen using a mortar and pestle. They were transferred to glass vials and subjected to rigorous solvent extraction at room temperature for 8 h by adding 2:1-CH₂Cl₂ (dichloromethane): CH₃OH (methanol) in an ultrasonic bath, in order to remove the soluble lipids. The lipid extract was retained for later analysis. The insoluble residue (Residue 1) was dried in a flow of N₂ and subjected to base hydrolysis (saponification) to remove hydrolysable constituents, e.g. the biopolyester cutin. This involved preparing a solution of 1 M methanolic NaOH solution (in 95:5 v/v methanol: water) by dissolving two pellets (0.2 g each)

Table 2.1 Modern leaves and cuticles studied using chemical degradation techniques which reveal the presence (+) or absence (–) of cutan

Family	Genus	Species	Cutan
Gymnosperms			
Araucariaceae ^c	<i>Araucaria</i>		–
Cupressaceae ^c	<i>Cupressus</i>		–
Ginkgoaceae ^{a,d}	<i>Ginkgo</i>	<i>biloba</i>	–
Pinaceae ^a	<i>Abies</i>	<i>grandis</i>	–
Pinaceae ^c	<i>Abies</i>		–
Pinaceae ^c	<i>Cedrus</i>		–
Pinaceae ^c	<i>Picea</i>		–
Pinaceae ^a	<i>Pinus</i>	<i>sylvestris</i>	–
Pinaceae ^c	<i>Pinus</i>		–
Podocarpaceae ^b	<i>Podocarpus</i>		+
Podocarpaceae ^c	<i>Podocarpus</i>		–
Sciadopityaceae ^b	<i>Sciadopitys</i>	<i>verticillata</i>	–
Sciadopityaceae ^c	<i>Sciadopitys</i>		–
Taxodiaceae ^c	<i>Athrotaxis</i>		–
Taxodiaceae ^c	<i>Cunninghamia</i>		–
Taxodiaceae ^c	<i>Glyptostrobus</i>		–
Taxodiaceae ^c	<i>Metasequoia</i>		–
Taxodiaceae ^c	<i>Sequoia</i>		–
Taxodiaceae ^c	<i>Sequoiadendron</i>		–
Taxodiaceae ^c	<i>Taxodium</i>		–
Flowering plants			
Aceraceae ^a	<i>Acer</i>	<i>campestre</i>	–
Agavaceae ^{a,b,d,e}	<i>Agave</i>	<i>americana</i>	+
Betulaceae ^a	<i>Betula</i>	<i>alba</i>	–
Cactaceae ^b	<i>Cereus</i>		+
Clethraceae ^b	<i>Clethra</i>		–
Clusiaceae ^b	<i>Clusia</i>	<i>multiflora</i>	+
Clusiaceae ^b	<i>Clusia</i>	<i>rosea</i>	+
Ericaceae ^a	<i>Erica</i>	<i>herbaceae</i>	–
Fagaceae ^a	<i>Castanea</i>	<i>sativa</i>	–
Fagaceae ^a	<i>Quercus</i>	<i>robur</i>	–
Liliaceae ^{a,e}	<i>Clivia</i>	<i>miniata</i>	+
Malvaceae ^a	<i>Gossypium</i>	<i>hirsutum</i>	–
Myrsinaceae ^b	<i>Myrsine</i>	<i>guyanense</i>	–
Orchidaceae ^b	Unidentified epiphyte		+
Poaceae ^b	Unidentified		–
Rosaceae ^a	<i>Prunus</i>	<i>laurocerasus</i>	+ ^g
Rutaceae ^a	<i>Citrus</i>	<i>limon</i>	–
Salicaceae ^a	<i>Populus</i>	<i>hybrida</i>	–
Solanaceae ^{a,f}	<i>Lycopersicon</i>	<i>esculentum</i>	–
Vitaceae ^a	<i>Vitis</i>	<i>vinifera</i>	–

^aAnalysis of whole leaves, this investigation

^bEnzymatically isolated cuticles (Boom et al. 2005)

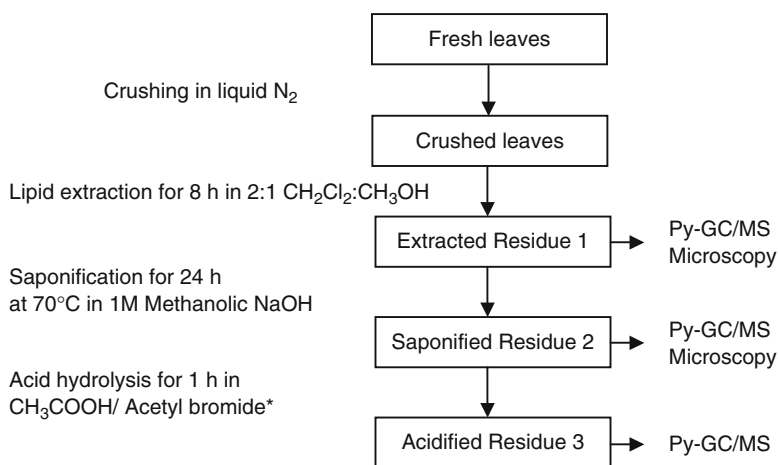
^cChemically isolated cuticle (Collinson et al. 1998)

^dChemically isolated cuticle (Mösle et al. 1998)

^eOther references: see text

^fFruit cuticle

^gResistance to acid hydrolysis not tested



*Applied to *Agave*, *Pinus*, and *Acer* to test the acid resistance of constituent biopolymers

Fig. 2.1 Analytical protocol used to detect the presence of cutan in leaves

of NaOH in 0.5 ml double distilled water and 9.5 ml methanol. This solution was added to Residue 1, which was then refluxed at 70 °C for 24 h in a reactitherm (Mösle et al. 1997). Thus, the resultant residue (Residue 2) is devoid of constituents that can be hydrolysed under basic conditions (e.g. cutin). Residue 2 from *Agave americana*, *Pinus sylvestris*, and *Acer campestre* was further subjected to acid hydrolysis (Mösle et al. 1997) as a control to test the acid resistance of *Agave*, one gymnosperm and one angiosperm, as cutan by definition should be resistant to acid treatment as well. The resultant residue (Residue 3) is devoid of constituents hydrolysable under basic and acidic conditions (e.g. lignin, cutan) and hence is resistant to both base and acid hydrolysis.

Untreated leaf, Residue 1 and Residue 2 of modern *Quercus robur* and *Pinus sylvestris* were studied using transmission electron microscopy (as described in Collinson et al. 1998) to determine the effects of base hydrolysis (saponification) on the leaf cuticle.

Flash pyrolysis-GC-MS was conducted on the residues of the extant leaves after lipid extraction (Residue 1), and after base hydrolysis (Residue 2) and, where present, after acid hydrolysis (Residue 3). Flash pyrolysis involves the thermal fragmentation of the chemical constituents of the sample at high temperatures in an inert gas stream. These fragments are then separated and identified by gas chromatography-mass spectrometry. Flash pyrolysis reveals bulk macromolecular information and it has been used extensively in the molecular characterisation of both modern and fossil plant tissues (see van Bergen 1999 for review). Samples were analysed with a Perkin Elmer GC/MS. A CDS (Chemical Data System) AS-2500 Pyroprobe pyrolysis unit was used with both the injector and interface temperature at 290 °C. 100–150 µg of tissue sample was introduced into quartz tubes and pyrolysed at 610 °C.

Pyrolysis products were separated using a DB-1 fused silica capillary column (30 m, 0.25 mm i.d., 0.1 μm film thickness) to evaluate the distribution of pyrolysis products of leaf tissue (Gupta and Pancost 2004), especially the *n*-alkyl component (for greater insight into the polar (non-aliphatic) compounds see Ralph and Hatfield 1991). The GC oven was programmed from 40 (held for 4 min) to 320 $^{\circ}\text{C}$ at 5 $^{\circ}\text{C min}^{-1}$ and held at that temperature for 15 min. Helium was the carrier gas. The MS was operated at 70 eV scanning over the range m/z 45–600 at 1 scan s^{-1} with an emission current of 300 μA (full scan mode). Two to three replicate samples were analysed to check the consistency of the runs. Compounds were identified using the NIST mass spectral library and from published spectra (Ralph and Hatfield 1991; Bland et al. 1998).

Analytical Results

The pyrolysis-GC/MS profile of *Agave americana* after solvent extraction (Residue 1) revealed a dominance of *n*-alkane and *n*-alk-1-ene homologues ranging in carbon number from C_8 to C_{35} and maximising at C_{28} (Fig. 2.2a), indicating the presence of a dominant *n*-alkyl component, which is characteristic of *Agave americana* (Tegelaar et al. 1991). Phenols and polysaccharide pyrolysis products are also present. Fatty acyl components were detected in relatively low abundance, as the *Agave* cuticle tissue was sampled from a fully developed, mature part of the plant where the ratio between cutin and cutan is relatively low; the proportion of cutin is greater in immature parts of the plant (Tegelaar et al. 1991). The pyrolysis-GC/MS profiles of Residue 2 (after saponification/base hydrolysis, Fig. 2.2b) and Residue 3 (after acid and base hydrolysis, Fig. 2.2c) show the persistence of *n*-alkane/alk-1-ene homologues including those with carbon chain length $>\text{C}_{20}$. These *n*-alkene/alkanes indicate the presence of cutan, consistent with results from a number of other studies (Nip et al. 1986a, b; Tegelaar et al. 1989c, 1991; McKinney et al. 1996; Möhle et al. 1997; Villena et al. 1999).

The pyrolysate of the angiosperm *Prunus laurocerasus* after extraction contains components related to polysaccharides, lignin and cutin, i.e., saturated and unsaturated C_{16} and C_{18} fatty acyl moieties (Fig. 2.3a: for details on the molecular structure and chemical formula of these compounds see Ralph and Hatfield 1991; van Bergen 1999). Also present is an *n*-alkyl component represented by *n*-alkane/alk-1-ene homologues ranging up to *n*- C_{32} ; *n*-alkane/alk-1-ene homologues from *n*- C_{26} to $_{31}$ are the most abundant. Inset Fig. 2.3a shows the distribution of the *n*-alkanes and *n*-alkenes separately to show more clearly the *n*-alkyl building components. As with *Agave*, the pyrolysate of Residue 2 from *Prunus laurocerasus* contains *n*-alkane/alk-1-ene homologues, including long chain homologues (Fig. 2.3b). The pyrolysate of post saponification Residue 2 of *Clivia miniata* also contains *n*-alkane/alk-1-ene homologues (data not shown) and a similar residue remains following acid hydrolysis (see also Villena et al. 1999).

In striking contrast, in all other leaves analysed, although *n*-alkane/alk-1-ene homologues are present in the pyrolysate of the extracted leaves (Residue 1), they

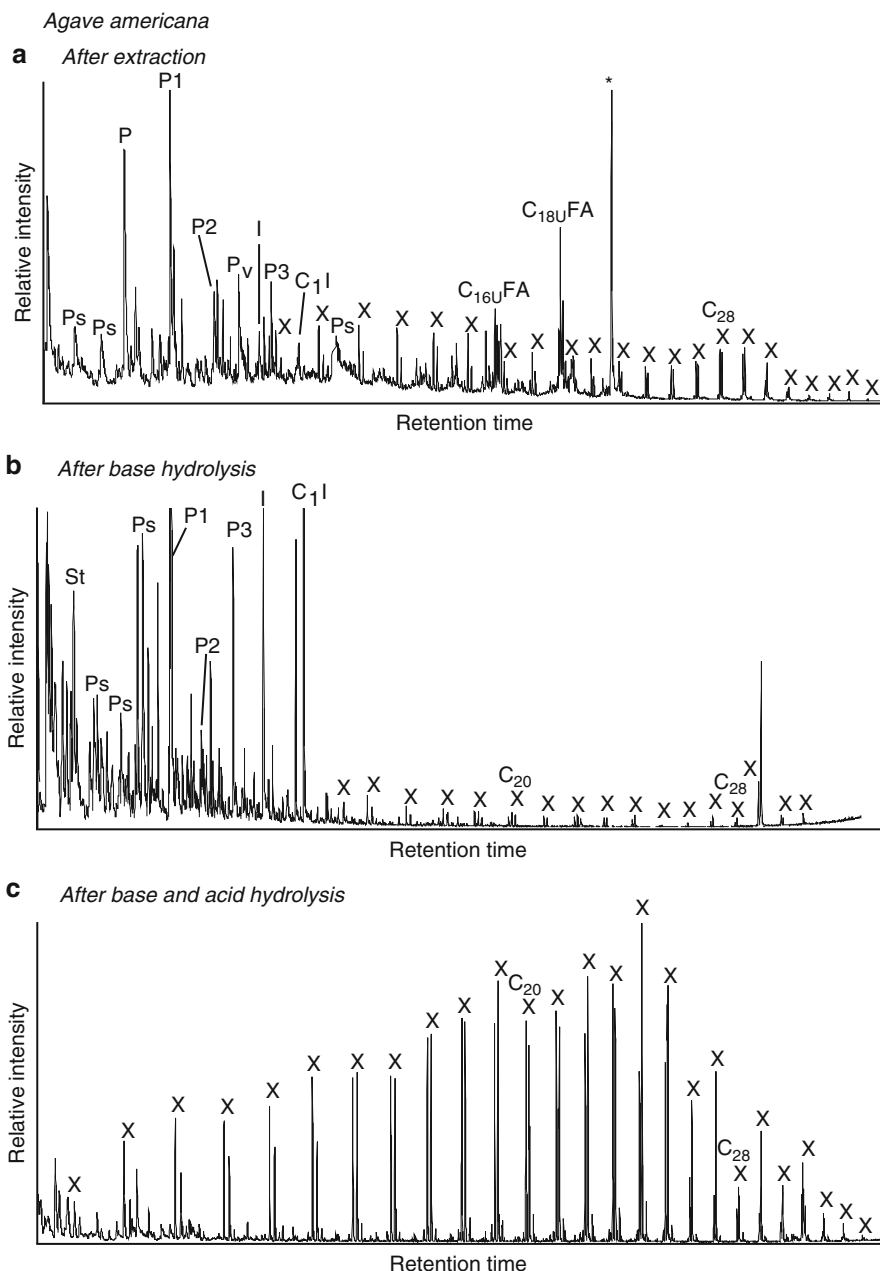


Fig. 2.2 Partial ion chromatogram showing py-GC/MS analyses of modern *Agave americana* cuticle and associated tissue (a) after lipid extraction (Residue 1); (b) after saponification (Residue 2); and (c) after saponification and acid hydrolysis (Residue 3). Note the presence of *n*-alkane/alk-1-ene homologues in all three fractions. Ps: polysaccharide pyrolysis products; P: phenol; Pn: alkyl phenols, where n denotes the number of carbon atoms in the alkyl component, Pv: vinyl phenol (derived from cutin), I: indole; C₁I: methyl indole; St: styrene; C₁₆FA: C₁₆ unsaturated fatty acid, and C₁₈FA: C₁₈ unsaturated fatty acid, X: *n*-alkane/alk-1-ene homologues (C_n refers to the carbon chain length). *contaminant. Peak at C₂₉-n-alkane is exaggerated due to co-elution with a contaminant

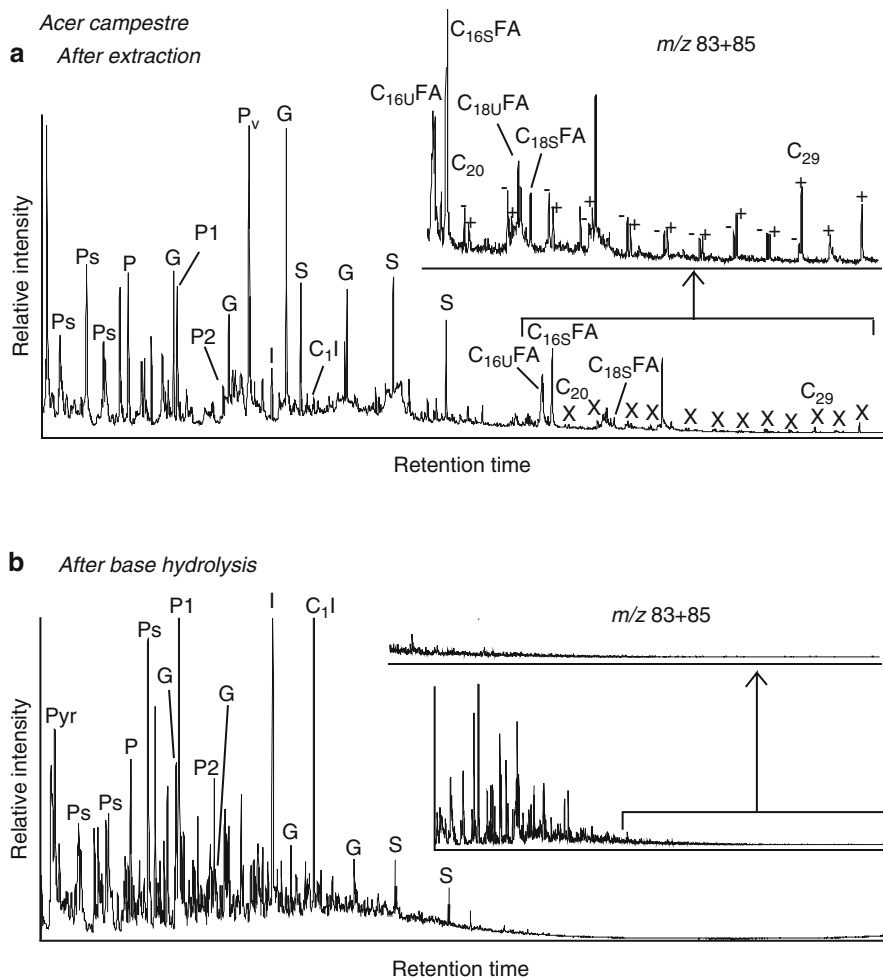


Fig. 2.4 Partial ion chromatogram showing the pyrolysis-GC/MS analysis of modern *Acer campestre* leaf (a) after lipid extraction (Residue 1); and (b) after lipid extraction followed by saponification (Residue 2). Note the presence of long-chain *n*-alkane/alk-1-ene homologues in trace amounts in the extracted plant tissue and its absence post saponification (as revealed by inset m/z 83+85 mass chromatograms). *Pyr* pyrrole derivative. Other legends same as in Figs. 2.2 and 2.3

in *Agave* or *Prunus*. The m/z 83+85 mass chromatogram (Fig. 2.4a inset) focuses on this homologous series of *n*-alkanes and *n*-alk-1-enes, which range in carbon number to C_{31} . The pyrolysate of Residue 2, following saponification, contain moieties related mainly to polysaccharides and lignin. Fatty acyl moieties and homologous series of *n*-alkanes and *n*-alk-1-enes are absent (Fig. 2.4b) in the pyrolysate. Saponification is expected to remove cutin, and the absence of fatty acyl moieties and vinyl phenol (Tegelaar et al. 1989b) in the pyrolysates of Residue 2 indicates that this has occurred.

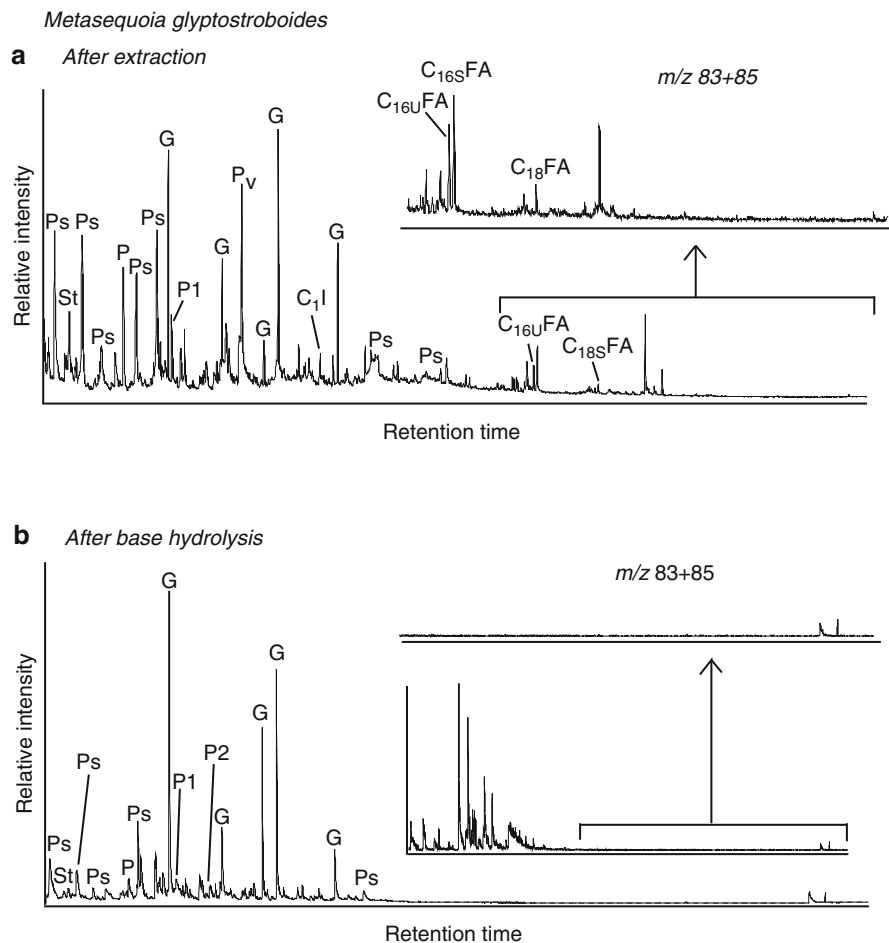


Fig. 2.5 Partial ion chromatogram showing the pyrolysis-GC/MS analysis of modern *Metasequoia glyptostroboides* leaf (**a**) after lipid extraction (Residue 1); and (**b**) after lipid extraction followed by saponification (Residue 2). Note the presence of long-chain *n*-alkane/alk-1-ene homologues in trace amounts in the extracted plant tissue and its absence post saponification (as revealed by inset m/z 83 + 85 mass chromatograms). Other legends same as in Figs. 2.2 and 2.3

Figure 2.5a shows the pyrolysis trace of the gymnosperm *Metasequoia glyptostroboides*. Lignin, polysaccharides and cutin moieties are abundant, whereas the *n*-alkanes and *n*-alk-1-enes are detected in extremely subordinate relative abundance (also see inset m/z 83 + 85 mass chromatogram; Yang et al. 2005, Fig. 3). The pyrolysate of Residue 2 post saponification (Fig. 2.5b) similarly contains polysaccharide and lignin moieties but no aliphatic component.

Data on all species investigated as part of this study are presented in Table 2.1. In all of these apart from *Agave*, *Prunus* and *Clivia* (see above), *n*-alkane/alk-1-ene homologues were present in the pyrolysate of Residue 1, albeit in low (but variable)

relative abundances that may be produced, for example, from secondary reactions in the pyroprobe or non extractable physically entrained waxes (e.g. wax esters; Sylvie Derenne, personal communication). However, none contained *n*-alkane/alk-1-ene homologues after saponification. In addition to *Agave*, two other examples (*Pinus* and *Acer*) of Residue 2 were subjected to acid hydrolysis. A small amount of Residue 3 was obtained and in both cases this yielded only lignin moieties upon pyrolysis and no aliphatic polymer, confirming the absence of cutan. This indicates that a single acid hydrolysis procedure does not remove lignin from a crushed leaf preparation but confirms the absence of any highly aliphatic resistant residue.

The Occurrence of Cutan in Modern Leaves

In this study, following solvent extraction, pyrolysis of all of the modern leaves (Residue 1) yielded predominantly carbohydrate, lignin, and protein moieties together with C₁₆ and C₁₈ fatty acids, reflecting the bulk composition of the leaf (Ralph and Hatfield 1991; Gupta and Pancost 2004). Residue 1 pyrolysates are also characterised by a series of *n*-alkane/*n*-alk-1-ene homologues. Because, the source of such an aliphatic signal from biological components other than cutan is unclear, this aliphatic signature was previously interpreted to result from the pyrolysis of cutan. The ubiquity of the signal prompted the hypothesis that cutan accounts for the aliphatic signal typically found in leaf fossils (Table 2.2; Tegelaar et al. 1991). However, in our study, pyrolysis of the residue after saponification (Residue 2) of 16 out of 19 leaves released products related solely to lignin and carbohydrates; no aliphatic components (neither fatty acids nor *n*-alkane/*n*-alk-1-ene homologues) were detected. Transmission electron microscopy of Residue 2 confirmed the absence of cuticle after hydrolysis (e.g., Möhle et al. 1997, 1998). However, cell walls were retained after the treatment, consistent with the presence of lignin and polysaccharide moieties in the pyrolysates post saponification. The absence of *n*-alkane/alk-1-ene homologues after saponification was also noted in modern *Quercus* leaf litter (van Bergen et al. 1998).

The absence of the aliphatic signal in the pyrolysates of Residue 2 reveals that the aliphatic components in the majority of leaves analysed are hydrolysable and thus, by definition, are not cutan. This means that cutan is absent in most of the flowering plant leaves previously interpreted as containing it (Tegelaar et al. 1991). The exceptions are *Agave americana*, *Clivia miniata* and *Prunus laurocerasus*, all of which yielded a residue diagnostic of cutan after saponification, a residue that was retained in *Agave* and *Clivia* (*Prunus* not tested in our study) in Residue 3 after acid hydrolysis. The presence of cutan in *Agave* and *Clivia* is concordant with many results from other laboratories (Nip et al. 1986a, b; Tegelaar et al. 1989c; McKinney et al. 1996; Möhle et al. 1997, 1998; Schouten et al. 1998; Villena et al. 1999) and proves that our protocol, using the whole leaf as a starting material, is able to detect cutan.

Cuticles isolated enzymatically in previous studies Boom et al. (2005) recorded cutan in the eudicots *Clusia rosea*, *C. multiflora* and *Cereus* sp., a cactus—presumably

Table 2.2 Molecular composition of leaves and cuticles in the fossil record revealing the presence of an ubiquitous *n*-alkyl component

Age	Fossil	Locality	Lithology	Pro	PS	P+	B+	Lig	Pr	F.A.	Aliphatic geopolymer	References
2-20 Ka	<i>Hymenaea</i>	Kenya	Amber	-	+	+	+	+	+	14, 16, 18:1	7-26 (even distrib.)	Stankiewicz et al. (1998a)
Miocene (Upper)	<i>Sciadopitys teritiaria</i>	Eschweiler, Germany		N.A.	N.A.	N.A.	+	N.A.	N.A.	16, 16:1, 16:2	6-31 (24-29)	Tegelaar et al. (1991)
Miocene (Upper)	<i>Pinus leitzii</i>	Gozdnica, Poland	Clay-silt	-	+	+	+	+	-	N.A.	N.A.	Stankiewicz et al. (1997)
Miocene (Upper)	<i>Sequoia langsdorffii</i>	Gozdnica, Poland	Clay-silt	-	+	+	+	+	-	N.A.	N.A.	Stankiewicz et al. (1997)
Miocene	<i>Glyptostrobus europaeus</i>	Orawa, Poland		-	-	+	+	+	-	14, 16, 18	13-27 (19-25)	Almendros et al. (1999a)
Miocene (Upper)	<i>Quercus</i>	Kreutzau, Germany		-	-	+	+	-	+	-	10-35 (even distrib.)	Nip et al. (1986a,b)
Miocene (Upper)	<i>Quercus palaecerris</i>	Ardèche, France	Diatomite	-	-	+	+	+	+	16, 18	10-31 (26-31)	Gupta et al. (2007a)
Miocene (Upper)	<i>Quercus suber</i>	Ardèche, France	Diatomite	-	-	+	+	+	+	16, 18	10-31 (26-31)	Gupta et al. (2007a)
Miocene (Upper)	<i>Quercus</i> sp.	Ardèche, France	Diatomite	-	-	+	+	+	+	-	10-31 (27-31)	Gupta et al. (2007a)
Miocene (Upper)	<i>Quercus hispanica</i>	Ardèche, France	Diatomite	-	-	+	+	+	+	16, 18	8-29 (26-29)	Gupta et al. (2007a)
Miocene (Upper)	<i>Pinus</i>	Ardèche, France	Diatomite	-	-	+	+	+	+	14, 16, 18	10-32 (26-31)	Gupta et al. (2007a)
Miocene (Upper)	<i>Populus alba</i>	Ardèche, France	Diatomite	-	-	-	+	-	+	-	9-30 (26-30)	Gupta et al. (2007a)
Miocene (Upper)	<i>Acer pseudocampestre</i>	Ardèche, France	Diatomite	-	-	+	+	+	+	16, 18	10-32 (26-31)	Gupta et al. (2007a)

Miocene (Upper)	<i>Vitis teutonica</i>	Ardèche, France	Diatomite	-	-	+	+	+	+	+	16	9-31 (26-31)	Gupta et al. (2007a)
Miocene (Upper)	<i>Castanea vesca</i>	Ardèche, France	Diatomite	-	-	+	+	+	+	+	16, 18	10-31 (26-31)	Gupta et al. (2007a)
Miocene (Upper)	<i>Tilia mastajana</i>	Ardèche, France	Diatomite	-	-	+	+	+	+	+	16	10-33 (26-31)	Gupta et al. (2007a)
Miocene (Upper)	<i>Robinia</i> sp.	Ardèche, France	Diatomite	-	-	+	+	+	+	+	16	10-31 (26-31)	Gupta et al. (2007a)
Miocene (Mid)	<i>Amentotaxus gladiifolia</i>	Salzhausen, Germany		N.A.	+	Tegelaar et al. (1991)							
Miocene (Mid)	<i>Magnolia</i>	Clarkia, USA	Clastic	-	-	+	+	+	+	+	-	+	Logan et al. (1993)
Miocene (Mid)	<i>Quercus</i>	Clarkia, USA	Clastic	-	-	+	+	+	+	+	-	+	Logan et al. (1993)
Miocene (Mid)	<i>Metasequoia</i>	Clarkia, USA	Clastic	-	+	+	+	+	+	-	-	+	Yang et al. (2005)
Oligocene	Conifer	Enspel, Germany	Clastic	-	-	+	+	+	+	+	6-30*	8-32 (11-15)	Gupta et al. (2007b)
Oligocene	Unidentified angiosperm	Enspel, Germany	Clastic	+	+	+	+	+	+	+	-	8-27 (12-20)	Gupta et al. (2007b)
Oligocene	<i>Hymenaea</i>	Dominica	Amber	-	-	+	+	+	-	+	16, 18:1, 18	7-26 (even distrib.)	Stankiewicz et al. (1998a)
Paleocene	<i>Ginkgo adiantoides</i>	Wyoming, USA	Mudrock	-	-	+	+	-	+	-	-	7-24 (even distrib.)	Collinson et al. (1998)
Paleocene/Eocene	<i>Metasequoia</i>	Ellesmere Island	Lignite	-	+	+	+	+	-	-	16	-	Yang et al. (2005)
Eocene	<i>Ocotea obtusifolia</i>	Tennessee, USA		N.A.	+	Tegelaar et al. (1991)							
Eocene	<i>Berryophyllum saffordii</i>	Kentucky, USA		N.A.	+	Tegelaar et al. (1991)							

(continued)

Table 2.2 (continued)

Age	Fossil	Locality	Lithology	Pro	PS	P+	B+	Lig	Pr	F.A.	Aliphatic geopolymer	References
Eocene (Mid)	<i>Rhodomyrtophyllum</i>	Geiseltal, Germany		N.A.	N.A.	N.A.	+	-	+		6-34 (27-32)	Tegelaar et al. (1991)
Eocene (Mid)	<i>Polyspora hallensis</i> ¹	Geiseltal, Germany		-	+	N.A.	+	+	+	16,18	6-34 (10-15 and 30-34)	Tegelaar et al. (1993)
Eocene (Mid)	<i>Metasequoia</i>	Axel Heiberg Island	Lignite	-	+	+	+	+	-	-	+	Yang et al. (2005)
Eocene (Lower)	cf. <i>Sapindus fructiferus</i>	Tennessee, USA		N.A.	N.A.	N.A.	+	N.A.	N.A.	+	+	Tegelaar et al. (1991)
Eocene	Unidentified	Messel, Germany		-	-	+	+	-	+	-	10-35 (even distrib.)	Nip et al. (1986a,b)
Cretaceous	<i>Squamastrobis tigrensis</i>	Patagonia, Argentina		-	-	+	+	-	-	6-18	9-29 (21 to 26)	Almendros et al. (1999b)
Cretaceous	<i>Ginkgo adiantoides</i>	North Dakota, USA	Mudrock	-	-	+	+	-	+	-	7-30 (8-13)	Mösle et al. (1998)
Cretaceous (Upper)	<i>Ginkgo covitacea</i>	China	Marl	-	-	+	+	-	+	-	7-28 (11-15)	Mösle et al. (1998)
Cretaceous (Upper)	<i>Protohedycarya ilicoides</i>	S.-Queedlinburg, Germany		N.A.	N.A.	N.A.	N.A.	N.A.	N.A.	+	+	Tegelaar et al. (1991)
Cretaceous (Lower)	<i>Frenelopsis</i>	Central Spain	Carbonate	-	-	+	+	-	-	-	7-27 (7-15)	Mösle et al. (1998)
Cretaceous (Lower)	<i>Abietites linkii</i>	NW Germany	Coal	-	-	+	+	-	-	-	6-30 (7-13)	Mösle et al. (1998)
Cretaceous	<i>Abietites</i>	Osterode, Germany		-	-	+	+	-	-	-	6-30 (6-15)	Nip et al. (1986a,b)
Cretaceous (Lower)	<i>Frenelopsis oligostomata</i>	Cerro de la Mesa (Spain)	Limestone	-	-	+	N.A.	-	-	14, 16, 18*	N.A.	Nip et al. (1986a,b)
Jurassic	<i>Ginkgo huttonii</i>	Scalby Ness, U.K.		-	-	+	+	-	-	-	7-23 (7-15)	Nip et al. (1986a,b)

Jurassic	<i>Ginkgo huttonii</i>	Yorkshire, UK	-	-	-	-	-	-	-	7-17 (9-14)	Mösle et al. (1997)
Jurassic (Mid)	<i>Pachypteris</i>	Scarborough, U.K.	Mudstone	-	-	-	-	-	-	10-28 (10-15)	Ewbank et al. (1996)
Permian	<i>Callipteris conferta</i>	Nahe, Germany	-	-	-	-	-	-	-	6-29 (7-14)	Nip et al. (1986a,b)
Carboniferous (Upper)	<i>Reticulopteris</i>	Indiana, USA	Coal ball	-	-	-	-	-	-	7-32 (10-16)	van Bergen et al. (1994)
Carboniferous (Upper)	<i>Neuropteris</i>	Indiana, USA	Coal ball	-	-	-	-	-	-	6-32 (10-20)	van Bergen et al. (1994)
Carboniferous (Upper)	<i>Karinopteris</i>	Indiana, USA	Paper coal	-	-	-	-	-	-	6-30 (6-13)	van Bergen et al. (1994)
Carboniferous (Upper)	<i>Alethopteris</i>	Kansas, USA	Coal ball	-	-	-	-	-	-	6-33 (9-17)	van Bergen et al. (1994)
Carboniferous (Step B)	Cordaite	Lone Star Lake, USA	Coal	-	-	-	-	-	-	6-30 (9-16)	Stankiewicz et al. (1998b)
Carboniferous (Step B)	<i>Walchia</i>	Garnett, USA	Limestone	-	-	-	-	-	-	7-30 (10-15)	Mösle et al. (2002)
Carboniferous (Step B)	<i>Walchia</i>	Hamilton, USA	Limestone	-	-	-	-	-	-	7-30 (10-15)	Mösle et al. (2002)
Carboniferous (Step B)	<i>Cordaites</i>	Lone Star Lake, USA	Coal	-	-	-	-	-	-	6-30 (10-15)	Mösle et al. (2002)
Carboniferous (Wes A)	Cordaite	Joggins, Canada	Clastic	-	-	-	-	-	-	6-30 (9-16)	Stankiewicz et al. (1998b)
Carboniferous (Wes A)	Pteridosperm	Joggins, Canada	Clastic	-	-	-	-	-	-	6-30 (9-14)	Stankiewicz et al. (1998b)
Carboniferous (Wes A)	<i>Cordaites</i>	Joggins, Canada	Clastic	-	-	-	-	-	-	6-30 (10-15)	Mösle et al. (2002)

(continued)

a stem not a leaf, one monocot (an epiphytic orchid) and one species of *Podocarpus* (a conifer). The cuticles were enzymatically isolated; the residue following acid and base hydrolysis yielded a highly aliphatic signal upon pyrolysis. There are two other recent reports of cutan: 1. in fruit cuticles of green pepper *Capsicum annuum* (Chefetz 2003), based on the presence of a residue from enzymatically isolated cuticles subjected to acid and base hydrolysis; 2. in stems of *Arabidopsis* (Xiao et al. 2004), based on a nonsaponifiable residue from enzymatically isolated cuticles. The materials were not analysed chemically. The *Capsicum* example meets the definition of cutan as yielding a non-saponifiable and non hydrolysable residue (although confirmation of the aliphatic signal would be preferable). It is not known, however, whether the *Arabidopsis* nonsaponifiable residue contained a highly aliphatic component or was composed entirely of lignin and polysaccharide moieties derived from the cell wall, which is clearly evident in the published TEM images of the cuticles (Xiao et al. 2004: Fig. 7).

Cutan and the Leaf Fossil Record

Cutan occurs in leaves of the living plants *Agave americana*, *Clivia miniata*, *Clusia rosea* and *C. multiflora*, an unnamed epiphytic orchid, *Cereus* (presumably stems), *Prunus laurocerasus* (resistance to acid hydrolysis not tested), and one *Podocarpus* species. There is no known fossil record of *Agave*, *Clivia*, epiphytic orchids, or cacti (e.g. Collinson et al. 1993; Herendeen and Crane 1995). Fossil Clusiaceae are represented in the late Cretaceous (Crepet and Nixon 1998) but by fossil flowers not leaves. There is one record of Clusiaceae leaves, preserved as impressions (i.e. organic material is absent) from the Tertiary of India (Ambwani 1991), but their identity is equivocal. *Prunus laurocerasus* has been reported from the Pliocene and Miocene of continental Europe (as *Laurocerasus*: Palamarev and Petkova 1987). However, *Prunus* leaf fossils are generally rare and the rosaceous subfamily Amygdaloideae (to which *P. laurocerasus* belongs: Lee and Wen 2001) is typically represented by fruit stones in Paleogene and younger strata (Mai 1984). *Podocarpus* leaves and pollen have been recorded from the Cretaceous, Paleogene, and Neogene of Australia (Hill 1994, 2004), although the leaves or phylloclades of many other Podocarpaceae are usually far more abundant and more diverse than *Podocarpus* leaves (e.g. Hill 1994, Table 12.1, p. 284). Although cutan has been reported in *Podocarpus* (Boom et al. 2005) it may not be present in all species (Collinson et al. 1998).

This study has shown that cutan is absent in the leaves of the living flowering plants *Acer campestre*, *Quercus robur*, *Castanea sativa*, *Citrus limon*, *Betula alba*, *Populus hybrida*, and *Gossypium hirsutum*, and the conifers *Pinus sylvestris*, *Metasequoia glyptostroboides* and *Abies grandis* (see Table 2.1 for complete list). We are not aware of a fossil record for *Citrus* or *Gossypium* leaves (e.g. Collinson et al. 1993). Fossil *Castanea* leaves are infrequent but are recorded in the late Neogene of Europe (Kvaček and Walther 1989) and the Oligocene and Neogene of Japan and China (Tanai 1995). Fossil *Betula* (Crane 1989; Walther 1999; Hably

et al. 2000) and *Populus* (Collinson 1992; Mai and Walther 1991) leaves are also infrequent but are known from the Paleogene onwards. Studies of fossil *Pinus* tend to focus on cones (Mai 1995) but leaves are also recorded in the Paleogene and Neogene (e.g. Kvaček and Rember 2000; Walther 1999). Leaves of *Acer*, *Quercus* and *Metasequoia* are abundant, diverse and widespread in the fossil record. *Acer* and *Quercus* are particularly well represented in North America, Asia and Europe from the Oligocene onwards (Prochazka and Buzek 1975; Daghljan and Crepet 1983; Wolfe and Tanai 1987; Kvaček and Walther 1989, 1998; Mai and Walther 1991; Mai 1995; Tanai 1995; Liu et al. 1996; Fotyanova 1997; Walther 1999; Kvaček and Rember 2000; Hably et al. 2000). *Metasequoia* is absent in the Cainozoic of Europe (Kvaček and Rember 2000; LePage et al. 2005) but has an extensive record from the Cretaceous onwards elsewhere in the Northern Hemisphere (LePage et al. 2005; Yang et al. 2005). It is important to note that these leaf fossils include both compressions and impressions. Impression fossils lack original organic material. If the presence of cutan in the cuticle were an important factor in leaf preservation leaves lacking cutan might be represented by a predominance of impression fossils over compression fossils but this is not the case.

The above data indicate that the presence of cutan in the leaf is not a strong predictor for a particularly abundant, widespread or diverse leaf fossil record of that taxon, nor is the presence of cutan a prerequisite for such a leaf fossil record. This does not mean that the presence of cutan in some leaves plays *no* role in the formation of fossils; cutan is resistant to a variety of diagenetic reactions and may influence leaf preservation. However, the lack of a correlation between the presence of cutan and a fossil record indicates that a variety of other factors, such as proximity to a depositional setting, redox conditions in the depositional setting and rates of burial, are far more important.

Explanations for the Aliphatic Component in Fossils

Most fossil leaves and cuticles are characterised by a strong aliphatic signal irrespective of plant type, enclosing lithology, depositional environment, locality and age (Table 2.2). The similarity between this aliphatic composition and that of cutan was one of the main reasons to invoke cutan as a primary control on fossil preservation (Tegelaar et al. 1991). It is now unclear if it was appropriate to place such an emphasis on the aliphatic composition of fossil organic matter, because the aliphatic content is generally overestimated when analysed by conventional pyrolysis and solid state ^{13}C NMR (e.g. forest soils investigated by Poirier et al. 2000). Nonetheless, it remains critical to identify the source of fossil aliphatic macromolecules in order to understand the chemical reactions that underpin fossil leaf taphonomy.

Selective preservation—The aliphatic composition of leaf fossils (Table 2.2) was interpreted previously as a direct consequence of decay resistance and selective preservation of the diagenetically stable aliphatic biopolymer cutan (Nip et al. 1986a, b; Tegelaar et al. 1991; de Leeuw and Largeau 1993). Cutan occurs in modern *Podocarpus*

and a similar aliphatic signal has been reported in a Neogene cuticle (Wijninga 1996) suggesting that cutan survived into the fossil record (Boom et al. 2005). However, the fossil sample was not identified as *Podocarpus*, but was one of five unidentified isolated dispersed cuticles (Wijninga 1996, Fig. 2.4), some of which were found in association with *Podocarpus* wood. There is no direct evidence for cutan preservation in fossils. Combined with the lack of cutan in many leaves with diverse fossil records, the above indicates that selective preservation of cutan is no longer tenable as an explanation for the highly aliphatic signal found in most leaf fossils.

Migration from sediment—Given the widespread occurrence of aliphatic components in sediments, insect, and plant fossils, the occurrence of aliphatic components in fossil leaves might be attributed to migration (Baas et al. 1995; van Bergen et al. 1995). This possibility, however, has been countered by several lines of evidence: (1) Aliphatic polymers are characteristically insoluble, and therefore relatively immobile (see Briggs 1999 for discussion); (2) An aliphatic signal was detected in Tertiary *Hymenaea* leaves trapped in amber (Table 2.2), where they are protected from external contamination (Stankiewicz et al. 1998a); (3) The aliphatic signatures in co-occurring plant and insect fossils from the Upper Carboniferous of North America are different, indicating that they could not have been introduced solely from the matrix (Stankiewicz et al. 1998b) and the internal morphology of the cuticle is altered indicating diagenesis; (4) The composition of artificially matured insect tissue is aliphatic (Stankiewicz et al. 2000) showing that endogenous organic matter can generate an aliphatic composition, as observed in fossils; (5) Thermochemolysis (TMAH assisted pyrolysis: Challinor 1989, 1991a, b; de Leeuw and Baas 1993; Martin et al. 1994; Almendros et al. 1998, 1999a; McKinney et al. 1996) of co-occurring insect and plant fossils and the associated organic rich matrix revealed differences in the distribution of the constituent fatty acyl components indicating that the aliphatic component of the fossil is endogenously derived (Gupta et al. 2007b); (6) Logan et al. (1995) showed that leaf lipids in the Miocene *Clarkia* sediments were concentrated on the leaf surfaces without migrating into the surrounding sediment. Introduction from other sources such as sediment is not tenable as an explanation for the highly aliphatic composition of leaf fossils.

In-situ polymerisation of labile aliphatics—In the absence of a diagenetically-stable aliphatic biopolymer in the living relatives, the preservation and aliphatic character of the fossil leaves cannot be explained by selective preservation. Migration from an external source can also be excluded. Thus, the aliphatic composition of the fossil leaves and cuticles (Table 2.2) must have been derived endogenously from other compounds present in the leaf tissues.

Pyrolysates of fossil leaves from the Tertiary of the Ardèche showed the dominance of C₁₆ and C₁₈ fatty acyl moieties (Gupta et al. 2007a). Thermochemolysis released the fatty acyl moieties, ranging in carbon number from C₈ to C₃₂ with a predominance of C₁₆ and C₁₈ homologues, that form part of the geopolymer. C₁₆ and C₁₈ fatty acyl homologues in equivalent modern leaves occur in cutin, phospholipid fatty acids (PLFA) and as triacylglycerides, steryl esters, other complex lipids and free fatty acids (FA). Thus, polymerisation of labile aliphatic components present in the cuticle and internal leaf tissue (cutin, PLFA, FA) during diagenesis is a

potential source of the aliphatic component of the fossil leaf macropolymer. Cutin can become crosslinked (Deshmukh et al. 2003) or intermolecularly ether linked (Schmidt and Schönherr 1982) making it diagenetically stable. As cutin contains C_{16} and C_{18} units these could be the source of the corresponding short chain *n*-alkyl component observed in the fossils. As previously suggested by Collinson et al. (2000) and Finch and Freeman (2001), long chain waxes (Eglinton and Hamilton 1967; Walton 1990) can be incorporated into the fossil geomacromolecule to account for the higher molecular weight long chain *n*-alkanes and *n*-alkenes generated during pyrolysis. Thus, while selective preservation of the biopolymer cutan cannot explain the preservation of fossil leaves, their aliphatic composition may be attributed to *in situ* polymerisation (Briggs 1999; Stankiewicz et al. 2000) of extractable and non-hydrolysable lipid components resulting in an aliphatic geopolymer (not inherited from the biopolymer cutan), a process that may be of widespread importance in the fossilization of organic materials.

The Ecology and Physiology of Plants with Cutan-Containing Leaves

There is no one-to-one correlation between the occurrence of cutan and leaf succulence or thick evergreen leaves with thick cuticles. The leaves of the cutan-containing *Agave* and the stems of the cactus *Cereus* are succulent, but the leaves of *Kalanchoe*, which are also succulent, lack cutan (Finch and Freeman 2001; not based on oxidative isolation, *contra* Boom et al. 2005). The cutan-containing leaves of *Clivia*, *Clusia* and epiphytic orchids are relatively fleshy but much less succulent. Leaves of *Podocarpus* and *Prunus laurocerasus* are evergreen and relatively thick with thick cutan-containing cuticles but leaves that lack cutan, such as *Citrus limon*, are similar in texture. The leaves of *Pinus* are evergreen with thick cuticle but lack cutan; nonetheless they are needle-like with a very low surface area to volume ratio, an adaptation to drought.

Cutan occurs in some CAM plants but it is absent in others, and it is present in plants using the C_3 photosynthetic pathway. *Clusia rosea* and *C. multiflora* both contain cutan (Boom et al. 2005); the former exhibits C_3 or CAM plasticity, and the latter is an obligate C_3 plant (Herzog et al. 1999; Lüttge 1999). Thus, some CAM plants, some succulent plants and some plants with thick cuticles do not contain cutan. A clear correlation cannot be made between any of these attributes and the presence of cutan and, on the basis of the small sample currently available, it is not yet clear that the presence of cutan in cuticles is an adaptation for drought resistance (*contra* Boom et al. 2005).

Most importantly, this study shows that the highly aliphatic signal in fossils is not due to the selective preservation of cutan and we suggest that it derives from *in situ* polymerisation of more labile aliphatic components such as waxes, internal lipids, and cutin. Thus neither the ecology and physiology of plants with cutan-containing leaves nor the presence or absence of cutan in leaves exert any major bias on the preservation of leaves in the fossil record.

References

- Almendros G, González-Vila FJ, Martín F, Sanz J, Álvarez-Ramis C (1998) Appraisal of pyrolytic techniques on different forms of organic matter from a Cretaceous basement in Central Spain. *Org Geochem* 28:613–623
- Almendros G, Dorado J, González-Vila FJ, Martín F, Sanz J, Álvarez-Ramis J,C, Stuchlik L (1999a) Molecular characterization of fossil organic matter in *Glyptostrobus europaeus* remains from the Orawa basin (Poland) Comparison of pyrolytic techniques. *Fuel* 78:745–752
- Almendros G, Dorado J, Sanz J, Alvarez-Ramis C, Fernández-Marrón MT, Archangelsky S (1999b) Compounds released by sequential chemolysis from cuticular remains of the Cretaceous gymnosperm *Squamastrobis tigrensis* (Patagonia, the Argentine). *Org Geochem* 30:623–634
- Ambwani K (1991) Leaf impressions belonging to the Tertiary age of Northeast India. *Phytomorphology* 41:139–146
- Baas M, Briggs DEG, van Heemst JDH, Kear AJ, de Leeuw JW (1995) Selective preservation of chitin during the decay of shrimp. *Geochim Cosmochim Acta* 59:945–951
- Bland HA, van Bergen PF, Carter JF, Evershed RP (1998) Early diagenetic transformations of proteins and polysaccharides in archaeological plant remains. In: Stankiewicz BA, van Bergen PF (eds) Nitrogen-containing macromolecules in the bio- and geosphere, vol 707, ACS symposium series
- Boom A, Sinninghe Damsté JS, de Leeuw JW (2005) Cutan, a common aliphatic biopolymer in cuticles of drought-adapted plants. *Org Geochem* 36:595–601
- Briggs DEG (1999) Molecular taphonomy of animal and plant cuticles: selective preservation and diagenesis. *Philos Trans R Soc Lond B* 354:7–16
- Briggs DEG, Evershed RP, Lockheart MJ (2000) The biomolecular paleontology of continental fossils. In: Erwin DH, Wing SL (eds) Deep time: paleobiology's perspective (supplement to *Paleobiology*, vol 26(4)). Paleontological Society, Lawrence, pp 169–193
- Burnham RJ (1993) Reconstructing richness in the plant fossil record. *Palaios* 8:376–384
- Burnham RJ, Wing SL, Parker GG (1999) The reflection of deciduous forest communities in leaf litter-implications for autochthonous litter assemblages from the fossil record. *Paleobiology* 18:30–49
- Challinor JM (1989) A pyrolysis-derivatization-gas chromatograph technique for the elucidation of some synthetic polymers. *J Anal Appl Pyrolysis* 16:323–333
- Challinor JM (1991a) Structure determination of alkyd resins by simultaneous pyrolysis methylation. *J Anal Appl Pyrolysis* 18:233–244
- Challinor JM (1991b) The scope of pyrolysis methylation reactions. *J Anal Appl Pyrolysis* 20:15–24
- Chefetz B (2003) Sorption of phenanthrene and atrazine by plant cuticular fractions. *Environ Toxicol Chem* 22:2492–2498
- Collinson ME (1992) The early fossil history of Salicaceae: a brief review. *Proc R Soc Edinb* 98B:155–167
- Collinson ME, Hooker JJ (2003) Paleogene vegetation of Eurasia: framework for mammalian faunas. *Deinsea* 10:41–83
- Collinson ME, Boulter MC, Holmes PR (1993) Magnoliophyta (“Angiospermae”). In: Benton MJ (ed) *The fossil record 2*. Chapman & Hall, London, pp 809–841, 864 pp
- Collinson ME, Möslle B, Finch P, Scott AC, Wilson R (1998) The preservation of plant cuticle in the fossil record: a chemical and microscopical investigation. *Anc Biomol* 2:251–265
- Collinson ME, Möslle B, Finch P, Wilson RR, Scott AC (2000) Preservation of plant cuticles. *Acta Palaeobot Suppl* 2:629–632
- Crane PR (1989) Early fossil history and evolution of the Betulaceae. In: Crane PR, Blackmore S (eds) *Evolution, systematics and fossil history of the Hamamelidae, volume 2: 'Higher' Hamamelidae*, vol 40B, Systematics Association special volume. Clarendon Press, Oxford, pp 87–116

- Crepet WL, Nixon KC (1998) Fossil Clusiaceae from the Late Cretaceous (Turonian) of New Jersey and implications regarding the history of bee pollination. *Am J Bot* 85:1122–1133
- Daghlian CP, Crepet WL (1983) Oak catkins, leaves and fruits from the Oligocene Catahoula Formation and their evolutionary significance. *Am J Bot* 70:639–649
- de Leeuw JW, Baas M (1993) The behavior of esters in the presence of tetramethylammonium salts at elevated temperatures; flash pyrolysis or flash chemolysis? *J Anal Appl Pyrolysis* 26:175–184
- de Leeuw JW, Largeau C (1993) A review of macromolecular organic compounds that comprise living organisms and their role in kerogen, coal and petroleum formation. In: Engel MH, Macko SA (eds) *Organic geochemistry: principles and applications*, vol 11, Topics in geobiology. Springer, New York, pp 23–72
- Deshmukh AP, Simpson AJ, Hatcher PG (2003) Evidence for cross-linking in tomato cutin using HR-MAS NMR spectroscopy. *Phytochemistry* 64:1163–1170
- Eglinton G, Hamilton RJ (1967) Leaf epicuticular waxes. *Science* 156:1322–1334
- Ewbank G, Edwards D, Abbott GD (1996) Chemical characterization of Lower Devonian vascular plants. *Org Geochem* 25:461–473
- Finch P, Freeman G (2001) Simulated diagenesis of plant cuticles—implications for organic fossilisation. *J Anal Appl Pyrolysis* 58:229–235
- Fotyranova LI (1997) Lobed-dentate oaks from the Eocene of eastern Asia. *Paleontol J* 31:225–234
- Glasspool IJ, Hilton J, Collinson ME, Wang S-J (2003) Foliar herbivory in Late Palaeozoic Cathaysian giantopterids. *Rev Palaeobot Palynol* 127:125–132
- Glasspool IJ, Hilton J, Collinson ME, Wang S-J, Li C-S (2004) Foliar physiognomy in Cathaysian giantopterids and the potential to track Palaeozoic climates using extinct plant groups. *Palaeogeogr Palaeoclimatol Palaeoecol* 205:69–110
- Gupta NS, Pancost RD (2004) Biomolecular and physical taphonomy of angiosperm leaf in early decay: implications for fossilisation. *Palaios* 19:428–440
- Gupta NS, Briggs DEG, Collinson ME, Evershed RP, Michels R, Jack KS, Pancost RD (2007a) Evidence for the in situ polymerisation of labile aliphatic organic compounds during the preservation of fossil leaves: implications for organic matter preservation. *Org Geochem* 38:499–522
- Gupta NS, Briggs DEG, Collinson ME, Evershed RP, Michels R, Pancost RD (2007b) Molecular preservation of plant and insect cuticles from the Oligocene Enspel formation, Germany: evidence against derivation of aliphatic polymer from sediment. *Org Geochem* 38(3):404–418
- Hably L, Kvaček Z, Manchester SR (2000) Shared taxa of land plants in the Oligocene of Europe and North America in context of Holarctic phytogeography. *Acta Univ Carol Geol* 44:59–74
- Herendeen PS, Crane PR (1995) The fossil history of the monocotyledons. In: Rudall PJ, Cribb PJ, Cutler DF, Humphries CJ (eds) *Monocotyledons: systematics and evolution*. Royal Botanic Gardens, Kew, London, pp 1–21
- Herzog B, Hoffmann S, Hartung W, Lüttge U (1999) Comparison of photosynthetic responses of the sympatric tropical species *Clusia multiflora* H.B.K. and the C3-CAM intermediate species *Clusia minor* L. to irradiance and drought stress in a phytotron. *Plant Biol* 1:460–470
- Hill RS (ed) (1994) *History of the Australian vegetation: Cretaceous to recent*. Cambridge University Press, Cambridge
- Hill RS (2004) Origins of the southeastern Australian vegetation. *Philos Trans R Soc Lond B* 359:1537–1549
- Jacobs BF (2002) Estimation of low latitude palaeoclimates using fossil angiosperm leaves: an example from the Miocene Tugen Hills, Kenya. *Paleobiology* 28:399–421
- Jones TP, Rowe NP (eds) (1999) *Fossil plants and spores modern techniques*. The Geological Society, London, 396 pp
- Kolattukudy PE (1980) Biopolyester membranes of plants: cutin and suberin. *Science* 208:990–1000
- Kowalski EA (2002) Mean annual temperature estimation based on leaf morphology: a test from tropical South America. *Palaeogeogr Palaeoclimatol Palaeoecol* 188:141–165

- Kowalski EA, Dilcher DL (2003) Warmer paleotemperatures for terrestrial ecosystems. *Proc Natl Acad Sci U S A* 100:167–170
- Kvaček Z, Rember WC (2000) Shared Miocene conifers of the *Clarkia* flora and Europe. *Acta Univ Carol Geol* 44:75–85
- Kvaček Z, Walther H (1989) Paleobotanical studies in Fagaceae of the European Tertiary. *Plant Syst Evol* 162:213–229
- Kvaček Z, Walther H (1998) The Oligocene volcanic flora of Kundračice near Litomerice, české Stredohori volcanic complex (Czech Republic)—a review. *Acta Mus Natl Prag Ser B Hist Nat* 54:1–42
- Lee S, Wen J (2001) A phylogenetic analysis of *Prunus* and the Amygdaloideae (Rosaceae) using ITS sequences of nuclear ribosomal DNA. *Am J Bot* 88:150–160
- LePage BA, Williams CJ, Yang H (2005) The geobiology and ecology of *Metasequoia*. Kluwer Academic, Dordrecht
- Liang M-M, Bruch A, Collinson M, Mosbrugger V, Li C-S, Sun Q-G, Hilton J (2003) Testing the climatic estimates from different palaeobotanical methods: an example from the Middle Miocene Shanwang flora of China. *Palaeogeogr Palaeoclimatol Palaeoecol* 198:279–301
- Liu YS, Guo S-X, Ferguson DK (1996) Catalogue of Cenozoic megafossil plants in China. *Palaeontogr B* 238:77–139
- Logan GA, Boon JJ, Eglinton G (1993) Structural biopolymer preservation in Miocene leaf fossils from the *Clarkia* site, Northern Idaho. *Proc Natl Acad Sci U S A* 90:2246–2250
- Logan GA, Smiley CJ, Eglinton G (1995) Preservation of fossil leaf waxes in association with their source tissues, *Clarkia*, northern Idaho, USA. *Geochim Cosmochim Acta* 59:751–763
- Lüttge U (1999) One morphotype, three physiotypes: sympatric species of *Clusia* with obligate C3 photosynthesis, obligate CAM and C3-CAM intermediate behaviour. *Plant Biol* 1:138–148
- Mai DH (1984) Karpologische Untersuchungen der Steinkerne fossiler und rezenter Amygdalaceae (Rosales). *Feddes Repert* 95:299–329
- Mai DH (1995) Tertiäre Vegetationsgeschichte Europas. Gustav Fischer, Jena, 691 pp
- Mai DH, Walther H (1991) Die Oligozänen und untermiozänen Floren NWSachsens und des Bitterfelder Raumes. *Abh Staatl Mus Mineral Geol Dresd* 38:1–230
- Martin F, Gonzalez-Vila FJ, del Río JC, Verdejo T (1994) Pyrolysis derivatization of humic substances 1. Pyrolysis of fulvic acids in the presence of tetramethylammonium hydroxide. *J Appl Anal Pyrolysis* 28:71–80
- McKinney DE, Bortiatynski JM, Carson DM, Clifford DJ, de Leeuw JW, Hatcher PG (1996) Tetramethylammonium hydroxide thermochemolysis of the aliphatic biopolymer cutan: insights into the chemical structure. *Org Geochem* 24:641–650
- Mösle B, Finch P, Collinson ME, Scott AC (1997) Comparison of modern and fossil plant cuticles by selective chemical extraction monitored by flash pyrolysis-gas chromatography-mass spectrometry and electron microscopy. *J Anal Appl Pyrolysis* 40–41:585–597
- Mösle B, Collinson ME, Finch P, Stankiewicz BA, Scott AC, Wilson R (1998) Factors influencing the preservation of plant cuticles: a comparison of morphology and chemical composition of modern and fossil examples. *Org Geochem* 29:1369–1380
- Mösle B, Collinson ME, Scott AC, Finch P (2002) Chemosystematic and microstructural investigations on Carboniferous seed plant cuticles from four North American localities. *Rev Palaeobot Palynol* 120:41–52
- Nip M, Tegelaar EW, de Leeuw JW, Schenk PA (1986a) A new nonsaponifiable highly aliphatic and resistant biopolymer in plant cuticles. *Naturwissenschaften* 73:579–585
- Nip M, Tegelaar EW, Brinkhuis H, de Leeuw JW, Schenk PA, Holloway PJ (1986b) Analysis of modern and fossil plant cuticles by Curie point Py-GC and Curie point Py-GC-MS: Recognition of a new, highly aliphatic and resistant biopolymer. *Org Geochem* 10:769–778
- Palamarev EH, Petkova AS (1987) Les fossiles de Bulgarie VIII. 1. La Macroflore du Sarmatien. Bulgarian Academy of Sciences, Sofia (In Bulgarian, French Summary)
- Poirier N, Derenne S, Rouzaud J-N, Largeau C, Mariotti A, Balesdent J, Maquet J (2000) Chemical structure and sources of the macromolecular, resistant, organic fraction isolated from a forest soil (Lacadée, south-west France). *Org Geochem* 31:813–827

- Prochazka M, Buzek C (1975) Maple leaves from the Tertiary of North Bohemia. *Rozpr Ustred Ustavu Geol* 41:1–86
- Ralph J, Hatfield RD (1991) Pyrolysis-GC-MS characterization of forage materials. *J Agric Food Chem* 39:1426–1437
- Royer DL, Wing SL, Beerling DJ, Jolley DW, Koch PL, Hickey LJ, Berner RA (2001) Palaeobotanical evidence for near present day levels of atmospheric CO₂ during parts of the tertiary. *Science* 292:2310–2313
- Royer DL, Wilf P, Janesko DA, Kowalski EA, Dilcher DL (2005) Correlations of climate and plant ecology to leaf size and shape: potential proxies for the fossil record. *Am J Bot* 92:1141–1151
- Rüffe L (1993) Das Trockenelement in der Flora des Geiseltales und angrenzender Fundstellen des Eozän. In: Pflanzen der geologischen Vergangenheit. Festschrift Herrn Professor Wilfried Krutsch. Museum für Naturkunde der Humboldt-Universität zu Berlin, Berlin, pp 113–127
- Schmidt HW, Schönherr J (1982) Development of plant cuticles: occurrence and role of non-ester bonds in cutin of *Clivia miniata* Reg. leaves. *Planta* 156:380–384
- Schouten S, Moerkerken P, Gelin F, Baas M, de Leeuw JW, Sinninghe Damsté JS (1998) Structural characterization of aliphatic, non-hydrolyzable biopolymers in freshwater algae and a leaf cuticle using ruthenium tetroxide degradation. *Phytochemistry* 49:987–993
- Stankiewicz BA, Mastalerz M, Kruege MA, van Bergen PF, Sadowska A (1997) A comparative study of modern and fossil cone scale and seeds of conifers: a geochemical approach. *New Phytol* 135:375–393
- Stankiewicz BA, Poinar HN, Briggs DEG, Evershed RP, Poinar GO Jr (1998a) Chemical preservation of plants and insects in natural resins. *Proc R Soc Lond B* 265:641–647
- Stankiewicz BA, Scott AC, Collinson ME, Finch P, Möslé B, Briggs DEG, Evershed RP (1998b) Molecular taphonomy of arthropod and plant cuticles from the Carboniferous of North America: implications for the origin of kerogen. *J Geol Soc* 155:453–462
- Stankiewicz BA, Briggs DEG, Michels R, Collinson ME, Evershed RP (2000) Alternative origin of aliphatic polymer in kerogen. *Geology* 28:559–562
- Sun BN, Dilcher DL, Beerling DJ, Zhang CJ, Yan D, Kowalski E (2003) Variation in *Ginkgo biloba* L. leaf characters across a climatic gradient in China. *Proc Natl Acad Sci U S A* 100:7141–7146
- Tanai T (1995) Fagaceous leaves from the Paleogene of Hokkaido, Japan. *Bull Natl Sci Mus Tokyo Ser C* 21:71–101
- Tegelaar EW, de Leeuw JW, Derenne S, Largeau C (1989a) A reappraisal of kerogen formation. *Geochim Cosmochim Acta* 53:3103–3106
- Tegelaar EW, de Leeuw JW, Holloway PJ (1989b) Some mechanisms of flash pyrolysis of naturally occurring higher plant polyesters. *J Anal Appl Pyrolysis* 15:289–295
- Tegelaar EW, de Leeuw JW, Largeau C, Derenne S, Schulten H-R, Muller R, Boon JJ, Nip M, Sprenkels JCM (1989c) Scope and limitations of several pyrolysis methods in the structural elucidation of a macromolecular plant constituent in the leaf cuticle of *Agave americana* L. *J Anal Appl Pyrolysis* 15:29–54
- Tegelaar EW, Kerp H, Visscher H, Schenk PA, de Leeuw JW (1991) Bias of the paleobotanical record as a consequence of variations in the chemical composition of higher vascular plant cuticles. *Paleobiology* 17:133–144
- Tegelaar EW, Wattendorff J, de Leeuw JW (1993) Possible effects of chemical heterogeneity in higher land plant cuticles on the preservation of its ultrastructure upon fossilization. *Rev Palaeobot Palynol* 77:149–170
- van Bergen PF (1999) Pyrolysis and chemolysis of fossil plant remains: applications to palaeobotany. In: Jones TP, Rowe NP (eds) Fossil plants and spores: modern techniques. Geological Society, London, pp 143–148
- van Bergen PF, Scott AC, Barrie PJ, de Leeuw JW, Collinson ME (1994) The chemical composition of upper Carboniferous pteridosperm cuticles. *Org Geochem* 21:107–117
- van Bergen PF, Collinson ME, Briggs DEG, de Leeuw JW, Scott AC, Evershed RP, Finch P (1995) Resistant biomacromolecules in the fossil record. *Acta Bot Neerl* 44:319–342

- van Bergen PF, Flannery MB, Poulton PR, Evershed RP (1998) Organic geochemical studies of soils from Rothamsted Experimental Station: III Nitrogen-containing organic matter in soil from Geescroft Wilderness. In: Stankiewicz BA, van Bergen PF (eds) Nitrogen-containing macromolecules in the bio- and geosphere, vol 707, ACS symposium series. American Chemical Society, Washington, DC, pp 321–338
- Villena JF, Dominguez E, Stewart D, Heredia A (1999) Characterization and biosynthesis of non-degradable polymers in plant cuticles. *Planta* 208:181–187
- Walther H (1999) Die Tertiärflora von Kleinsaubernitz bei Bautzen. *Palaeontogr B* 249:63–174
- Walton TJ (1990) Waxes, cutin and suberin. In: Dey PM, Harborne J (eds) Lipids, membranes and aspects of photobiology, vol 4, Methods in plant biochemistry. Academic Press, London, pp 105–159
- Wiemann MC, Manchester SR, Dilcher DL, Hinojosa LF, Wheeler EA (1998) Estimation of temperature and precipitation from morphological characters of dicotyledon leaves. *Am J Bot* 85:1796–1802
- Wijninga VM (1996) Paleobotany and palynology of Neogene sediments from the high plain of Bogota (Colombia). Chapter 2. Geochemical characterisation of Neogene organic deposits from Colombia. PhD thesis, University of Amsterdam (printed in Wageningen, Published by the author. ISBN 90- 9009414-8)
- Wilde V (1995) Die Makroflora aus dem Mitteleozän des Geiseltalgebietes, kurze Übersicht und Vergleiche. *Hallesch Jahrb Geowiss B* 17:121–138
- Wilf P (1997) When are leaves good thermometers? A new case for Leaf Margin Analysis. *Paleobiology* 23:373–390
- Wilf P, Cuneo NR, Johnson KR, Fhicks J, Wing SL, Obradovich JD (2003) High plant diversity in Eocene South America: evidence from Patagonia. *Science* 300:122–125
- Wing SL, Harrington GJ, Smith FA, Bloch JI, Boyer DM, Freeman KH (2005) Transient floral change and rapid global warming at the Paleocene-Eocene boundary. *Science* 310:993–996
- Wolfe JA (1995) Palaeoclimatic estimates from Tertiary leaf assemblages. *Annu Rev Earth Planet Sci* 23:119–142
- Wolfe JA, Tanai T (1987) Systematics, phylogeny and distribution of *Acer* (maples) in the Cenozoic of western North America. *J Fac Sci Hokkaido Univ* 22:1–246
- Xiao F-M, Goodwin SM, Xiao Y, Sun Z, Baker D, Tang X, Jenks MA, Zhou J-M (2004) *Arabidopsis* CYP86A2 represses *Pseudomonas syringae* type III genes and is required for cuticle development. *EMBO J* 23:2903–2913
- Yang H, Huang Y, Leng Q, LePage BA, Williams CJ (2005) Biomolecular preservation of Tertiary *Metasequoia* fossil *lagerstätten* revealed by comparative pyrolysis analysis. *Rev Palaeobot Palynol* 134:237–256

Chapter 3

Organic Preservation of Biopolymers in Fossil Leaves

Abstract This chapter investigates the morphology and chemical structure of fossil leaves from the Ardèche diatomite (Late Miocene, southeast France) and compares them to their modern equivalents. Chemical analyses of the fossil leaves revealed the presence of a recalcitrant (non-hydrolysable) geopolymer comprised of benzene derivatives, lignin-derived components, pristenes and an aliphatic component; the latter consists partly of fatty acyl subunits ranging in carbon number from C_8 to C_{32} with an abundance of C_{16} and C_{18} units. Chemical degradation of the modern plants failed to reveal the presence of the aliphatic biomacromolecule cutan, thereby precluding selective preservation of this compound as the source for the aliphatic component of the fossil leaves. In contrast, C_{16} and C_{18} fatty acyl units are predominant in the cutin and phospholipid fatty acid (PLFA) fractions of the modern leaves, while C_{10} to C_{32} acid units are characteristic of the free fatty acid (FA) fraction of epicuticular waxes. However, TEM and SEM investigations of the fossils revealed no evidence for cuticle preservation, and while a contribution from cutin cannot be excluded, the aliphatic component of the fossil polymer is possibly derived instead from the *in situ* polymerisation of labile cell membrane lipids and free fatty acids.

Keywords Kerogen • Organic matter preservation • Pyrolysis • n-alkanes, leaves

Introduction

Sedimentary organic matter comprises about 90 % weight of total organic matter on Earth (Berner 1989); kerogen comprises 95 % of this by weight, and the remaining 5 % is attributed to extractable constituents termed bitumen. It is formed by diagenetic alteration of biological material and is converted to petroleum products by thermal catagenesis (Tissot and Welte 1984). Depending on the biological source and final composition kerogen is classified as type I, II or III. Types I and II are hydrogen rich kerogens and often have a high aliphatic contribution in the form of

a non-hydrolysable, organically insoluble macropolymer (Larter and Horsefield 1993) while Type III kerogens are more carbon rich. However, the source of the aliphatic character of kerogens, as well as other sedimentary organic matter such as organic macrofossils, remains a subject of debate.

Kerogen formation has been traditionally attributed either to selective preservation of resistant biomolecules or random polymerisation of labile biomolecules, i.e. neogenesis. According to the neogenesis hypothesis (Tissot and Welte 1984), kerogen is formed by random intermolecular polymerisation and polycondensation of degraded biopolymers (e.g. amino acids, sugars, lipids, lignin, etc). However, it is unclear how such mechanisms could result in the predominantly aliphatic character of many kerogens (e.g. Type I and II) and associated bitumens. The selective preservation model proposes that kerogen is derived predominantly from resistant biopolymers in living organisms that survive decay more readily than other biomolecules (Tegelaar et al. 1989a, b; see de Leeuw and Largeau 1993 for review; Love et al. 1998). As highly aliphatic resistant biopolymers are shown to be present in living counterparts of algae (algaenan) (Gillaizeau et al. 1996; Gelin et al. 1999; Blokker et al. 2000), in plant cuticles (cutan) (Tegelaar et al. 1991; van Bergen et al. 1994), and in suberinised plant tissue (suberan) (Tegelaar et al. 1995), and can be tracked in their fossil counterparts, the aliphatic composition of kerogen was attributed to the selective preservation of these polymers. In addition, natural vulcanisation, which involves the reaction between reduced sulfur and various functional groups in organic compounds, resulting in the formation of a S-rich macromolecule, is also recognised as an important pathway (Kok et al. 2000). The widespread importance of selective preservation is questionable because such resistant biopolymers are not components of many of the living organisms that are present in the fossil record (Mösle et al. 1997, 1998; Collinson et al. 1998; Stankiewicz et al. 1998a, 2000). Such concerns with proposed models for the formation of aliphatic kerogen have prompted dubious, albeit apparently more thermodynamically robust, alternative mechanisms for petroleum *n*-alkane formation, such as the application of mantle-level pressures (Kenney et al. 2002).

An alternative process was invoked recently for fossil organic matter preservation (Briggs 1999; Collinson et al. 1998; Stankiewicz et al. 1998a, 2000). It posits that the aliphatic component of sedimentary organic matter may be formed by the condensation and polymerisation of labile lipids comprised of *n*-alkyl moieties already present in the living counterpart. As this process was recognized within individual organically preserved insect fossils it has been termed *in situ* polymerisation (Briggs et al. 1998; Briggs 1999; Stankiewicz et al. 2000) or 'within cuticle diagenetic stabilisation' in the case of plants (Collinson et al. 1998, 2000). This process has been invoked to explain the aliphatic character of fossil arthropods (Stankiewicz et al. 2000) and fossil leaves (Mösle et al. 1997, 1998; Collinson et al. 1998, by the stabilisation of aliphatic chains, including contributions from entrained and surface waxes). However, previous characterisations of macrofossils were incomplete. Stankiewicz et al. (1997b, 1998a) did not identify explicitly a source of the aliphatic moieties in arthropods and Mösle et al. (1997, 1998) performed only pyrolysis and in some cases FTIR.

To investigate these processes and their relative significance further, we have examined fossil leaves from the Ardèche diatomite and modern representatives of the same genera using chemical and morphological techniques. This approach is useful because direct links between precursor organic materials and their sedimentary products can be established. Previous investigations have applied this approach successfully to both fossil arthropod cuticles and leaves (see Briggs 1999 for review), but we have extended these analyses by employing a combination of pyrolytic, spectroscopic, microscopic and chemical degradation techniques that allowed us to evaluate the composition and structure of the leaves as a consequence of diagenesis and early thermal alteration. From this, we infer the likely source of the aliphatic component of the Ardèche leaves, propose possible processes for its formation and derive implications for organic matter preservation in general.

Samples

Samples were collected by DEGB and NG during August 2002 (and by DEGB in a trip before) from a freshwater lacustrine deposit of Late Miocene age (8–8.5 m.y. old) (St. Bauzile; Ardèche, southeastern France). The Ardèche diatomite represents the largest European deposit of diatomite and is overlain by a Pliocene basalt flow. The Ardèche diatomite was never deeply buried such that, despite the basalt flows, it is largely thermally immature.

At least 81 families of plants, 72 families of insects and 25 families of vertebrates have been reported from the Ardèche diatomite (Riou 1995) making it an important conservation deposit (Konservat-Lagerstätte). The carbon content of the diatomite is low, minimizing the possibility of exogenous organic matter contamination of fossils. For this study all samples were collected from the same horizon; thus presumably they were subjected to the same environmental and diagenetic conditions and are of comparable thermal maturity. Leaves of nine species of angiosperms, *Acer pseudocampestre*, *Castaneavesca*, *Quercus palaeocerris*, *Q. suber*, *Q. hispanica*, *Q. sp.*, *Vitisteutonica*, *Tilia sp.* and *Populus alba*, and one gymnosperm, the conifer *Pinus*, were investigated for chemical analysis. Selected leaves from these were used for microscopic investigation. These are referred to as specimen 1 (sp.1) throughout. Additional samples of *C. vesca*, *Q. hispanica* and *P. alba* were used for ¹³C-NMR microscopic and chemical studies. These are referred to as specimen 2 (sp.2) throughout. Samples of the fossil leaves were removed from the rock by lifting with a dissecting needle or scraping with a scalpel blade. Chemical reagents (HF, etc.) were not used to dissolve the matrix to avoid any chemical alteration of fossil leaves.

Leaves of modern representatives of these genera were collected at the University of Bristol Botanic Garden during November 2002. *Agave americana* and *Cliviaminiata* samples were collected from University of Nancy Botanic gardens. These include *Quercus robur*, *Populus hybrida*, *Castaneasativa*, *Acer campestre*, *Vitisvinifera*, and *Pinussylvestris*.

Chemical analyses were performed by NG and microscopic analyses by MEC.

Microscopic Analyses

Transmission (TEM) and scanning (SEM) electron microscopy were used to identify the leaf components (cuticles, cellular structure, etc.) and to assess the quality of leaf morphological preservation. Leaf pieces were taken from the same samples as those used for chemical analysis. Fossil leaf pieces for electron microscopy were treated with Hydrochloric acid and Hydrofluoric acid to remove minerals, especially diatoms which obscured all surfaces in SEM of untreated material and would also have caused major problems for sectioning work. For SEM leaf pieces were halved and portions mounted with opposite surfaces upwards. From 2 to 5 mm² of surface area were examined for each subsample. Modern samples were studied without use of fixatives and some time (weeks) elapsed between collection and study during which specimens were stored in foil in a refrigerator. For further details of methods see Collinson et al. (1998) and references there cited. Interpretations of structure and organisation were informed by comparison with results previously obtained for other modern and fossil leaves (Collinson et al. 1998).

Organic Geochemical Analyses

Figure 3.1 outlines the analytical strategy in the form of a flowchart. The modern and fossil leaf samples were extracted ultrasonically three times, 30 min each with 2:1- CH₂Cl₂ (DCM): CH₃OH (methanol) to yield the total lipid extract (TLE). The insoluble residues were secured in glass vials, dried in a flow of N₂ and stored in the freezer at -20 °C for analysis. The TLE of the modern plants was saponified in 0.5 M 95 % methanoic NaOH for 1 h at 80 °C. The saponified extract was methylated with borontrifluoride/methanol (14 % w/v) by heating at 70 °C for 1 h, and collected in chloroform. The TLE of the modern plants was further separated into fatty acid (FA), phospholipid fatty acid (PLFA) and neutral fractions using the Bond Elut separation technique. Bonded aminopropyl solid phase cartridges were conditioned first with methanol followed by 2:1 v/v DCM: isopropanol. The neutral fraction was eluted by passing 12 ml 2:1 v/v DCM:isopropanol through the column, followed by 12 ml 2 % acetic acid in diethylether (to elute the FA fraction). Finally, the column was washed with 12 ml methanol to elute the PLFA fraction. The PLFA fraction was saponified in 0.5 M 95 % methanoic NaOH for 1 h at 80 °C. The insoluble residues of the modern plants were saponified in 1 M 95 % methanoic NaOH at 80 °C for 24 h (Mösle et al. 1997) to remove completely the hydrolysable constituents, e.g. cutin. Microscopic analysis of modern *Quercus robur* and *Pinussylvestris* showed that the cuticle was successfully removed. Following this the saponified residues of selected leaves were subjected to acid treatment by heating for 1 h at 80 °C in 1:3, v/v, acetyl bromide-acetic acid to remove the polysaccharide component of the leaf (Mösle et al. 1997).

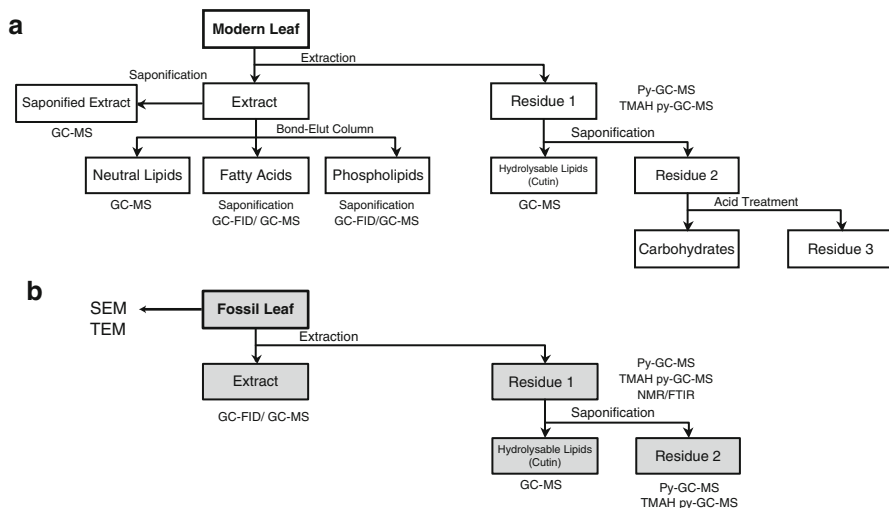


Fig. 3.1 Analytical protocol adopted for analysing the modern (a) and fossil leaves (b)

Insoluble residues of the fossil leaves were saponified in 1 M 95 % methanoic NaOH at 80 °C for 3 h. The saponified extracts were acidified to pH 2 with HCl and collected in hexane. The extract was methylated with borontrifluoride/methanol (14 % w/v) by heating at 70 °C for 1 h and collected in dichloromethane. The methylated extracts were derivatised for GC analysis by treating with BSTFA at 70 °C for 1 h. A C₃₄*n*-alkane was added as an internal standard for quantification.

Flash pyrolysis involves the thermal fragmentation of the chemical constituents of a sample at high temperatures in an inert medium. These fragments are then separated and identified by GC-MS. Thus flash pyrolysis reveals bulk macromolecular information and it has been used extensively in molecular characterisation of both modern and fossil plant material (see van Bergen 1999 for review). Samples were analysed using a Perkin Elmer GC-MS. A CDS (Chemical Data System) AS-2500 Pyroprobe pyrolysis unit was used with both the injector and interface temperature at 290 °C. Between 100 to 150 micrograms of the solvent-extracted modern or fossil leaves were weighed using a microanalytical balance into quartz tubes and pyrolysed at 610 °C. No absolute quantitation was attempted. For instrument parameters see Gupta and Pancost 2004. Compounds were identified from spectra reported in the literature (Ralph and Hatfield 1991; Stankiewicz et al. 1997a; Bland et al. 1998; Stankiewicz and van Bergen 1998; Gupta and Pancost 2004). For TMAH (tetramethylammonium hydroxide) assisted pyrolysis an aliquot of the lipid extracted residue was transferred to a fresh vial and 1 ml TMAH solution added to the sample. The sample was soaked in TMAH solution for 3–4 h prior to analysis to ensure that sufficient TMAH was available during on line pyrolysis.

GC-MS was conducted on a ThermoQuest Trace 2000 gas chromatograph fitted with a CP-Sil 5 fused silica capillary column (60 m, 0.32 mm i.d., 0.1 micron film thickness) coupled to a ThermoQuest single quadrupole mass spectrometer

(scanning a range of m/z 50–650; cycle time 0.6 s; ionisation energy 70 eV). Helium was used as the carrier gas. The oven was programmed from 40 to 200 °C at 10 °C min⁻¹, then to 300 °C at 3 °C min⁻¹ and held at this temperature for 20 min.

FTIR spectra were taken for the mid-IR range (400–6,000 cm⁻¹) using a Nicolet SX800 spectrometer fitted with a Spectratec microscope. A KBr beamsplitter with either DTGS (bench) or MCT (microscope) detector and a glowbar ceramic source were used to acquire 256 scans at a resolution of 4 cm⁻¹. For the microscope, masks were used to generate a beam of 100 micron diameter which was used on selected (thin) areas of the samples. For the pressed pellets (bench) the samples were ground and mixed with 100 g of dried KBr in an approximate ratio of 2:100.

¹³C NMR spectra were collected on a BrukerAvance 400 NMR spectrometer operating at 100.62 MHz with a standard Bruker 4 mm CPMAS probe. The spectra were collected using cross-polarisation (CP), magic-angle-spinning (MAS) at 6.5 KHz and a dipolar decoupling (ca 90 KHz). Typically around 12,000 scans were collected with a cross polarisation time of 0.75 ms and a recycle delay of 3 s. The chemical shifts were referenced with respect to tetramethylsilane (=0 ppm) using solid adamantane as a secondary standard.

Microscopic Investigations

Gross Morphology

All leaf fossils (Fig. 3.2a, b, c, d) show a gross morphology which is distinctive for each taxon. The overall leaf shape and leaf margin morphology is clearly evident. In addition patterns of lighter and darker organic matter define the presence of main veins (darker) and patterns of topography define the positions of lower rank veins (thicker organic matter). Leaf morphology and venation pattern and both very well-preserved.

Internal Organisation

A section through a small portion of the abaxial (lower) part of a modern *Quercus* leaf (Fig. 3.3a) is shown for comparison with fossil angiosperm leaves. The fossils are represented by two different leaves of each of three angiosperm taxa; *Populus alba* (Fig. 3.3b, c), *Castaneavesca* (Fig. 3.3d, e) one partial leaf of *Pinus* (Fig. 3.4) and *Quercushispanica* (Figs. 3.3f, g, and 3.5). In the angiosperms each section (Fig. 3.3b–g) spans the entire leaf thickness but which is the adaxial or abaxial surface is not known. In the *Pinus* (Fig. 3.4) the upper edge is the outside of the leaf which is covered by a thin film of gold coating (thin dark line) as the same fragment was used for SEM and TEM study. Only a portion of the *Pinus* leaf has been

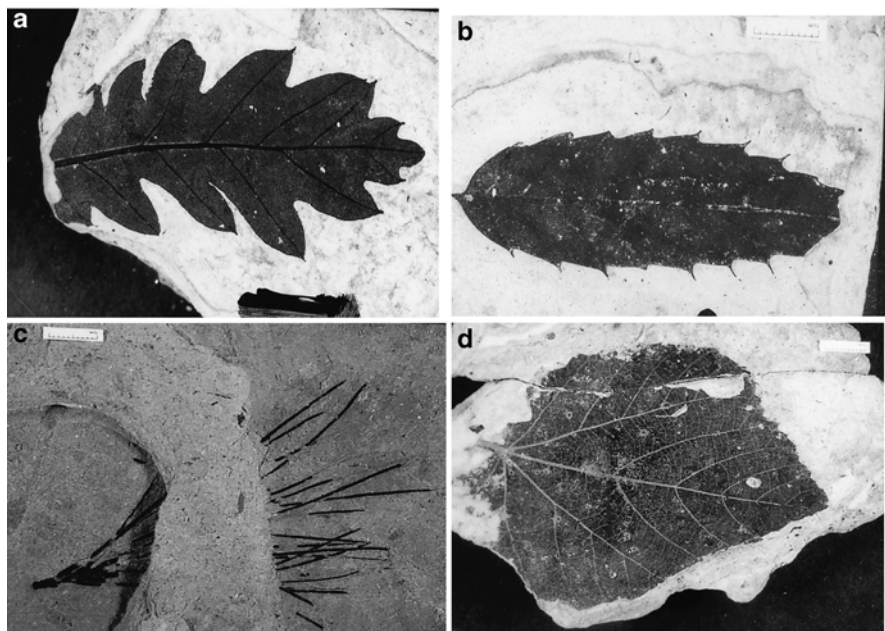


Fig. 3.2 Photographs of fossil leaves from the Ardeche diatomite used for understanding chemical compositions. Note that the gross morphology represents that of a leaf (a) *Quercushispanicasp1* (b) *Castaneavesca* sp1 (c) *Pinus* sp. (d) *Populus alba* sp.1

sectioned as this leaf is much thicker than the angiosperms so the lower edge of the image is an artificial break, not the opposite leaf surface. Specimens of four other genera (*Acer*, *Vitis*, *Tilia* and *Robinia*) and two other *Quercus* species were also studied by SEM and TEM but are not figured.

Figure 3.3 shows very clearly that there is little or no resemblance between the internal organisation of the modern (Fig. 3.3a) and fossil (Fig. 3.3b–g) leaves. The two specimens of *Populus alba* (Fig. 3.3b, c) are quite unrecognisable as being leaf tissue. *P. alba* specimen 1 has an open irregular wavy lamellar structure with a high proportion of space within the organic matter. The uppermost thicker layer somewhat resembles the material of *P. alba* specimen 2 (Fig. 3.3c). Although from a different flowering plant family *Castaneavesca* specimen 1 (Fig. 3.3e) is indistinguishable from *Populus alba* 2. Both have almost no space within the organic matter and both show some discontinuous layering expressed as varying electron lucency (lighter/darker layers). *Castaneavesca* specimen 2 (Fig. 3.3d), in contrast, has an open texture with a large amount of space including circular patches (e.g. upper center of image) with vesiculate structure. *Quercushispanicasp2* (Fig. 3.3g) is very like *C. vesca* 2 though lacking the vesiculate structures and showing some layering similar to *C. vesca* 1. As with the two *Populus* and the two *Castanea*, the two *Quercushispanica* are very different from one another. *Quercushispanica* specimen 1 (Figs. 3.3f, and 3.5b) is exceptional in that parts of the organisation are

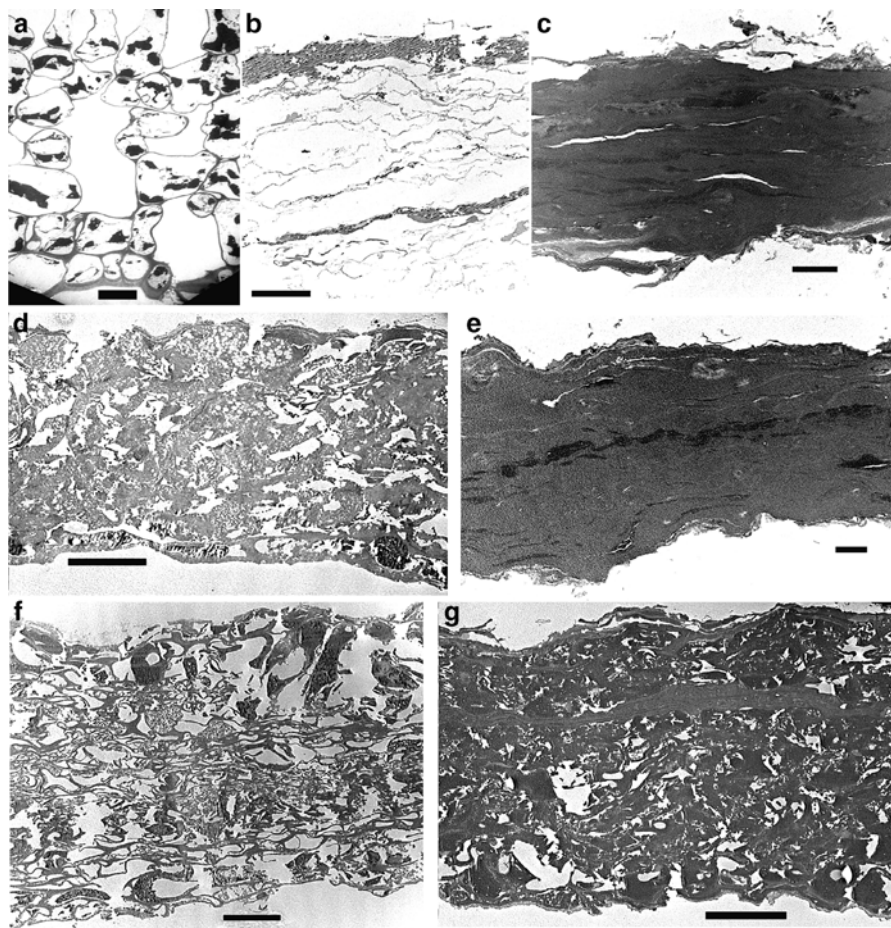


Fig. 3.3 TEM sections of modern (a) and fossils (b–g) angiosperm leaves showing the wide variation of internal organization of the fossils (both within and between taxa) and that with one exception (f) fossils are not recognisable in terms of modern leaf tissues. (a) *Quercus robur*; (b) *Populus alba* specimen 1; (c) *P. alba* 2; (d) *Castanea vesca* specimen 2; (e) *C. vesca* 1; (f) *Quercus hispanica* specimen 1; (g) *Q. hispanica* 2. Scale bars 10 μm in all except b and e where they are 2 μm

recognisable in terms of modern leaves and can be interpreted as partially compressed and distorted cell walls forming a cellular structure. However, in some places these ‘cell walls’ seem to intertwine and anastomose in a manner dissimilar to that seen in modern cells. This we interpret as due to compression and distortion combined with some separation of wall layers. In the light of the preservation seen in *Q. hispanica* 1 the open texture in *Q. hispanica* 2 and *C. vesca* 2 might reflect the original cellular organisation and hints of cell walls might, arguably, be present. The two *Quercus hispanica* leaves both have an open texture, although one is cellular and the other is not both have similar leaf thickness (c. 50 and 43 μm). In contrast, for *Populus* and

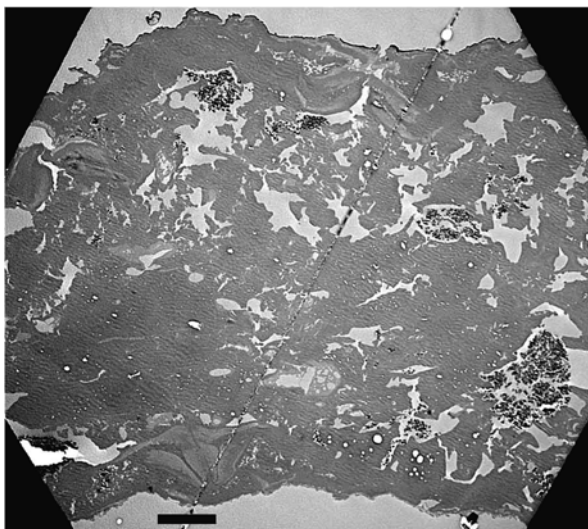


Fig. 3.4 TEM section of portion of leaf of fossil *Pinus*, which, like the angiosperms, is not recognisable in terms of modern leaf tissues. Scale bar 10 μm

Castanea one leaf has open texture and one closed. The closed texture leaf is one quarter of the thickness (c.48 vs. 12 μm , *Populus*) to half the thickness (c. 37 vs. 18 μm , *Castanea*) of the open texture leaf. Therefore the closed versus open texture may be related to differential compaction during fossilisation. Whereas the section of *Populusalba* 1 (Fig. 3.3b) with open layering might be interpreted as merely a decompacted version of *Populus alba* 2 (Fig. 3.3c) such a simple explanation cannot account for the difference in the *Castanea* as the open textured specimen is not layered. The differences between the open and closed textures may therefore reflect different physical or chemical properties of the organic matter, the latter being unlikely as all leaves have been shown to have a similar chemical composition or minor heterogeneities in burial conditions.

Taking the full spectrum of leaf preservation observed in the Ardeche material (13 specimens studied) *Populusalba* 1 and *Quercushispanica* 1 are unique. No other specimen shows the open lamellar structure of the former and no other specimen shows cellular structure like the latter. All other specimens show either open textures like *Q. hispanica* 2 and *C. vesca* 2 or closed textures like *P. alba* 2 and *C. vesca* 1.

The single gymnosperm leaf studied *Pinus* (Fig. 3.4) has an internal organisation combining areas of open and closed texture but lacking any cell-like structure or layering. Electron dense (dark) granular patches are iron pyrites filling spaces in the open texture. Some relatively electron lucent (lighter) organic material is present.

These microscopical observations show that in only one exceptional specimen does the internal organisation of the fossil leaf show any resemblance to modern leaves. In all other cases the organic material is not recognisable as leaf tissue. There is no link between preservation state and leaf taxon but a 'preservational continuum' can be seen from open organisation with cell structure (Fig. 3.3f) through

open but lacking cell structure (Fig. 3.3d, g), mixed open and closed (Fig. 3.4), closed layered (Fig. 3.3c, e) to open layered (Fig. 3.3b) organisations. In the last case it is remarkable that the fossil leaf has survived as an integral structure at all. Only the gross morphology (Fig. 3.2a, b, c, d) of the entire specimens enables recognition of these fossils as leaves. If fragments became dispersed in sediments their origin as higher plant tissue would be obscured, the fragments would be classifiable as amorphous or structured kerogen.

Surface Structures

In modern leaves a cuticle is present on the surface. Depending on the leaf surface (abaxial/adaxial) the cuticle will be a continuous layer sometimes perforated by stomatal apertures. The pattern of the underlying epidermal cells can usually be seen at the surface in SEM study. Figure 3.5a is representative of all of the surfaces (both sides) of all the fossil leaves. There is no continuous surface layer and no pattern of underlying surface cells. The surface structure consists of discontinuous, overlapping and interlocking, multidirectional thread to sheet-like organic matter. There is no resemblance to a leaf cuticle. The origin of this surface organisation is not understood. Possibilities could include (i) major modification (decomposition, dissolution, melting) of the cuticle rendering it unrecognisable, (ii) an usually unseen expression of the microfibrillar layering of the epidermal cell walls or (iii) an externally sourced layer of microbially (bacterial or algal) derived material. In any case, this surface layer represents an extremely small percentage (<1 %) of the fossil leaf organic matter.

In modern leaves, the cuticle surface is sometimes obscured by a covering of surface hairs or waxes. However, the fossil surface structure is quite unlike modern leaf hairs or waxes. The possibility that waxes or hairs are covering and obscuring the surface is also excluded by the fact that all surfaces of all taxa show essentially the same structure whilst hairs and waxes differ in morphology between taxa and occur in different proportions on opposite leaf surfaces. The surface organisation could possibly result from major modifications (dissolution or melting and reprecipitation) of surface waxes but in this scenario a cuticle should still be present beneath the surface and this is not the case as shown by TEM sections.

Much of the surface area of all specimens is covered in impressions of diatoms, recognisable by their shape and also by impressions of the rows of small pores (striae) in their frustules. Their presence confirms that the leaf surface we are studying is the surface into which diatoms were pressed by compaction as sediment built up above the leaves. This shows that we have not removed any surface layers accidentally during collecting or preparation.

The cuticle would be recognised in section as a discrete, single, continuous outer layer usually with a distinct electron density (often lighter than underlying cell walls). Such a layer can be recognised on the lower surface of the modern *Quercus robur* (Fig. 3.3a) in spite of the low magnification of the image. None of the fossil leaves show such a layer. The surfaces are discontinuous in all cases. Although there are layers of differing electron density, electron lucent layers are discontinuous, often

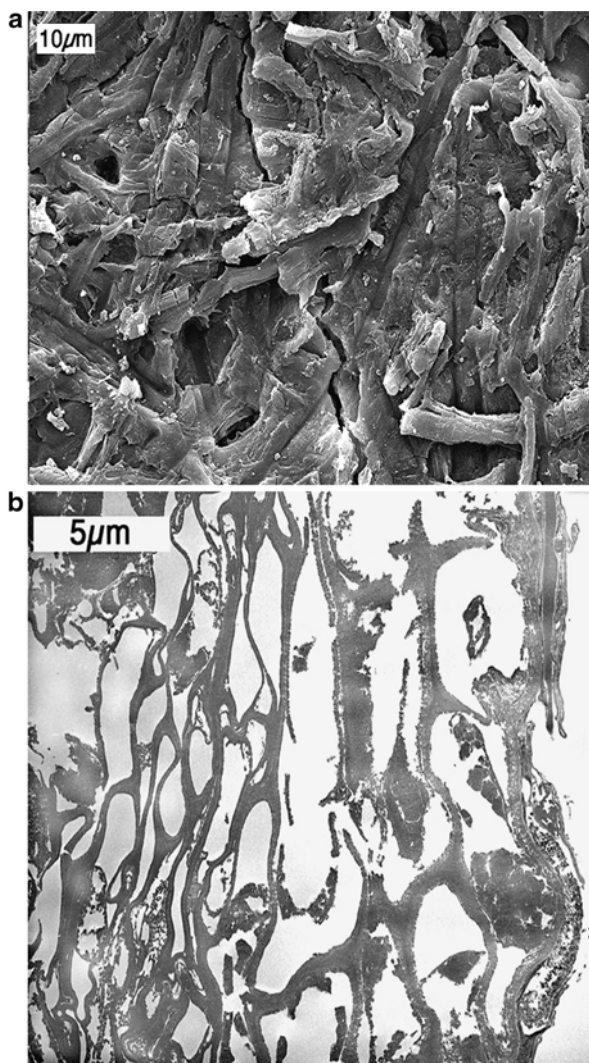


Fig. 3.5 SEM image of surface (a) and detail of portion of TEM section (b) including one surface (at right) of fossil *Quercushispanica* specimen 1. Cuticle is not recognisable in surface or section views in spite of the preservation of recognisable cellular structure in section

multiple, sometimes anastomosing and they occur in various places in the organic matter including some distance away from the surface. These features are particularly obvious in Fig. 3.3c, e and g and upper surface of Fig. 3.3d.

The surfaces of the fossil leaves in SEM (Fig. 3.5a) show none of the features expected in a leaf cuticle. The TEM sections (Fig. 3.3b–g), even in detail on the fossil with the most leaf-like internal organisation (Fig. 3.5b), show no continuous, discrete or distinctive outer layer. These microscopical observations therefore show that the cuticles are not recognisable on any of the fossil leaves.

Chemistry of Modern Leaves

The solvent extract of the modern leaves (total lipid extract) was saponified to give the overall composition of extractable fatty acyl components. The saponified extract consists of *n*-alkanoic acids with chain lengths ranging from C₁₀ to C₃₂ and with an even-over-odd predominance (Fig. 3.6a). The unsaturated C_{18:1} fatty acid (oleic acid) is the most abundant followed by C₁₆ fatty acid, as noted by Padley et al. (1986). The TLE was further separated into neutral, 'free' fatty acid (FA) and phospholipid fatty acid fraction (PLFA) fractions to assess the relative contribution of each of these to the total fatty acid pool. The neutral fractions, as is commonly observed, contain high-molecular-weight *n*-alkanes (*n*-C₂₇ to C₃₃) characterized by an odd-over-even predominance and high molecular weight *n*-alkanols characterised by an even-over-odd predominance (Eglinton et al. 1962; Eglinton and Hamilton 1967), as well as a variety of triterpenoid and steroid alcohols. The PLFAs are comprised primarily of C₁₆ and C₁₈ fatty acids, with C₁₆ being vastly more abundant; longer chain acids are absent. Lesser abundances of C₁₄ fatty acid are also present, while branched components were not detected.

The free fatty acid fraction (from esterified components of lipid extract, analysed as fatty acid methyl esters) contains primarily *n*-alkanoic acids with chain lengths ranging from C₁₂ to C₃₀ and with an even-over-odd predominance as is typical for higher plant functionalised leaf waxes (Eglinton and Hamilton 1967). The C₁₆ followed by the C₁₈ saturated components are the most abundant fatty acids in this fraction as well.

Following extraction, pyrolysis of the modern leaf residues (residue 1, Fig. 3.1) yielded predominantly carbohydrate, lignin, and protein moieties together with C₁₆ and C₁₈ fatty acids (Fig. 3.7a), reflecting the bulk composition of the leaf (see Gupta and Pancost 2004 for detailed discussion). In addition to fatty acids, pyrolysis of extracted modern leaves (residue 1, Fig. 3.1) revealed a series of *n*-alkane/*n*-alk-1-ene homologues. This was reported previously (Tegelaar et al. 1991) and was thought to represent pyrolysis of cutan. Extracted residues were then saponified (hydrolysed under basic conditions) and the extracts, analysed by GC-MS, consist mainly of C₁₆ and C₁₈*n*-alkanoic acids and mono, di and trihydroxy derivatives of these, typical products of cutin hydrolysis (Fig. 3.6b) (Kolattukudy 1980; Nip et al. 1986). Pyrolysis of the post-saponification residues (residue 2, Fig. 3.1) released products solely related to lignin and carbohydrates (Fig. 3.7b), and no aliphatic components (neither fatty acids nor *n*-alkane/*n*-alk-1-ene homologues) were detected, as noted by van Bergen et al. (1998) for leaf litter. This is confirmed clearly by the specific summed mass chromatogram *m/z* 83+85 (Fig. 3.7, inset). The absence of fatty acids (derived from cutin) is consistent with the removal of the cuticle. The successful removal of the cuticle has been monitored and verified by microscopic investigations as well. Vinyl phenol is formed during pyrolysis from the *p*-hydroxyphenol unit in certain types of lignin, but in leaves it is related mainly to *p*-coumaric acid. It is present both as ester and ether linked units in woody tissues (as part of lignin), but also as part of decay resistant cuticle (Tegelaar et al. 1989b). Thus

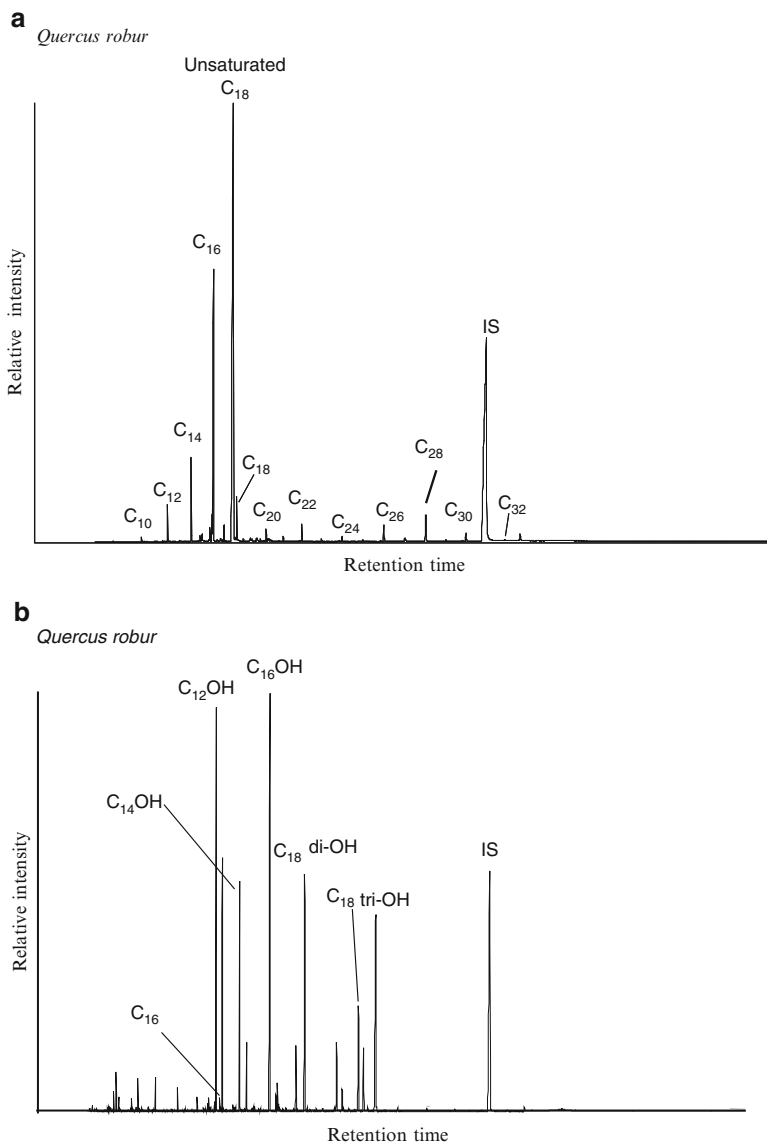


Fig. 3.6 Distribution of fatty acyl moieties in modern *Quercus robur* (a) Distribution of fatty acyl moieties in total lipid extract. (b) Distribution of fatty acyl moieties in saponified extract from residue 1

the absence of vinyl phenol post saponification also attests to the successful removal of the cuticle. Acid hydrolysis post saponification on selected leaves yielded a blackish residue (residue 3, Fig. 3.1) and subsequent analysis revealed the presence of lignin moieties but no aliphatic components.

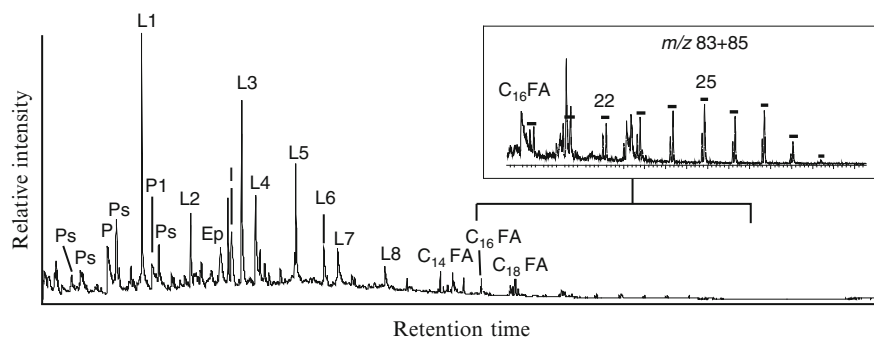
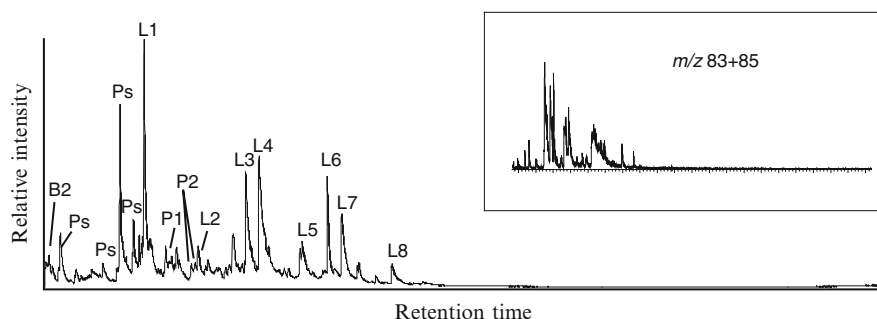
a *Quercus robur*, After extraction**b** *Quercus robur*, After hydrolysis (saponification)

Fig. 3.7 Partial total ion current chromatogram of modern *Quercus robur* after extraction (**a**) and after base hydrolysis (**b**) *Ps*: Polysaccharide products, *B2*: Ethyl benzene, *P*: Phenol, *P1*: Methyl Phenol, *P2*: Dimethyl Phenol, *Ep*: 4-ethenyl phenol, *I*: Indole, *FA*: Fatty acid, *Cn*: carbon chain length. Lignin pyrolysis products: *L1*: 2-methoxyphenol, *L2*: 4-methyl-2-methoxyphenol, *L3*: 4-ethenyl-2-methoxyphenol, *L4*: 2,6-Dimethoxyphenol, *L5*: 3-allyl-6-methoxyphenol, *L6*: 4-ethyl-2,6-dimethoxyphenol, *L7*: 4-ethenyl-2,6-dimethoxyphenol, *L8*: 4-propenyl-2,6-dimethoxy phenol. ■ *n*-alkane/*n*-alk-1-ene homologues series, number indicating carbon chain length. Inset, m/z 85 + 83 mass chromatogram reveals the distribution of the alkane/alkene homologues

Chemistry of the Diatomite

The total organic carbon content of the Ardèche diatomite is low for a lacustrine setting (about 1.84) and it is unlikely that kerogen or other matrix organic matter could have contributed to the fossil leaves. To confirm this, we performed pyrolysis and TMAH-pyrolysis on solvent extracted and non-treated matrix material. However, even samples that had not been extracted failed to generate detectable pyrolysis products during analysis. For detailed discussion on the effect of matrix on fossils, see Chap. 4 for effect of sediment on organic contamination in fossils.

Chemistry of Fossil Leaves

Fossil leaves were extracted and the residues (residue 4, Fig. 3.1) analysed by pyrolysis- and TMAH-pyrolysis-GC-MS. Pyrolysis of fossil leaf residues released a homologous series of *n*-alkanes and *n*-alk-1-enes ranging in carbon number from C₈ to C₃₂ (Fig. 3.8, Table 3.1). Typically, hydrocarbons ranging in carbon number from C₂₆ to C₃₁ are dominant (Figs. 3.8c, 3.9a, b) often maximising at *n*-C₂₉ (Figs. 3.8a, b,, 3.9a, b c, Table 3.1). In addition, the pyrolysates of *A. pseudocampestre*, *Q. hispanica* (Fig. 3.12), *Q. palaeocerris*, *Q. suber*, *V. teutonica*, *C. vesca* (Fig. 3.8a) and *Pinus* (Fig. 3.8b) all contain C₁₆ and, at lower abundances, C₁₈*n*-alkanoic acids. *C. vesca* and *Pinus* reveal the presence of C₁₄*n*-alkanoic acid as well. Other major components released by pyrolysis of fossil leaves are the isoprenoids, prist-1-ene (from all the fossil leaves) and prist-2-ene (from all but *Pinus* and *Vitis*). These isoprenoids most likely are related to the pyrolysis of tocopherol (Goosens et al. 1984; Logan et al. 1993; Hold et al. 2001). In addition to aliphatic components, pyrolysis also released lignin components from all fossil leaves except *Populusalba* 1fossils (Fig. 3.8c, Table 3.1). The internal organisation of *Populusalba* 1 is also unique in having an open layered structure least resembling modern leaf tissues. Specific summed mass chromatograms were used to evaluate the presence of guaiacyl (*m/z* 124 + 138 + 150 + 152 + 164 + 166) and syringyl units (*m/z* 154 + 168 + 180 + 182 + 194 + 196). Guaiacyl-related units include 2-methoxyphenol (guaiacol), 4-methyl-2-methoxyphenol, 4-ethenyl-2-methoxyphenol, 3-allyl-6-methoxyphenol (Figs. 3.8a, b, 3.9a, b). Syringyl-related units, 2,6-dimethoxyphenol and 4-vinyl-2,6-dimethoxyphenol, were detected in *Quercushispanica* (Fig. 3.9a, b), *Q. suber*, *Q. sp.*, *Vitis* and *Pinus* (Fig. 3.8b). Phenol and its alkyl derivatives were observed in all but *Populus* specimen 1, very likely a product of biogeograded lignin (van Bergen et al. 1995; Almendros et al. 1999). Benzene and its alkyl derivatives (revealed by *m/z* 78 + 91 + 92 + 105 + 106 + 119 + 120 + 133 + 134 mass chromatogram) include toluene, ethyl benzene, *m*, *p*, and *o* xylene, trimethyl benzenes and 1,2,3,4-tetramethyl benzene (see Hartgers et al. 1992 for detailed discussion). Napthalene (*m/z* 155 + 170) was detected in all but *Populus* specimen 1. In general, the distribution of lignin components is similar in all analysed fossil leaves; however, the *Pinus* needle (gymnosperm) pyrolysate differs from those of all other leaves in that released aromatic, lignin-derived components are more abundant than aliphatic components (Fig. 3.8b). Additionally, *Pinus* also showed the *n*-alkane/*n*-alk-1-ene homologue maximising at C₃₁ (Fig. 3.8b) unlike any of the other fossil leaves. *Pinus* leaves have a lower surface area to volume ratio than dictyledon leaves and contain a high proportion of thick-walled cells. A higher lignin content would be expected based on living representatives and is not inconsistent with the internal organisation (mixed open and closed texture) of the fossil.

The extracted samples of the fossil leaves were also subjected to TMAH-assisted thermochemolysis (Fig. 3.10, Table 3.1) in order to evaluate further the aliphatic macromolecular composition. This process involves simultaneous pyrolysis and methylation, and assists structural analysis of polar functionalities such as esters,

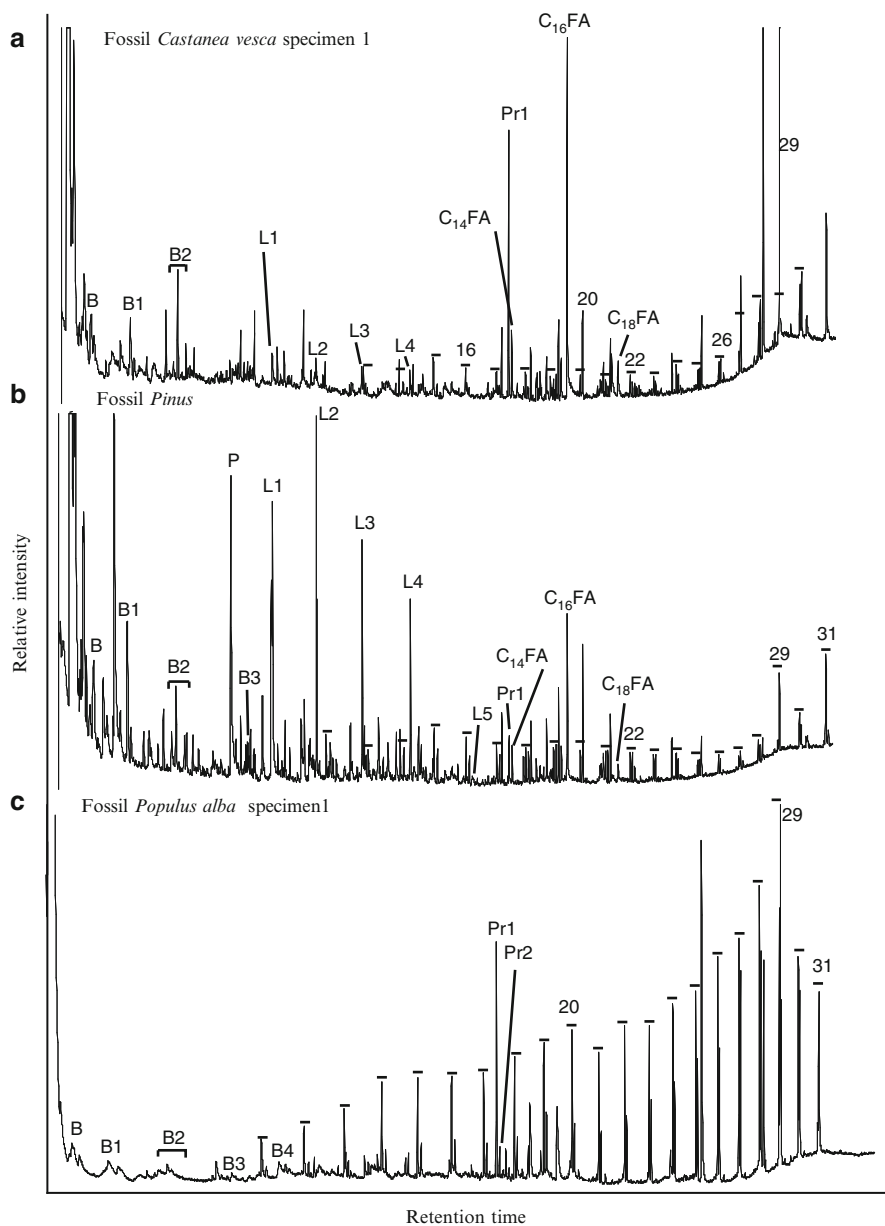


Fig. 3.8 Partial total ion current chromatogram of fossil leaves, shown in Fig. 3.2. (a) *C. vesca* sp1 (b) *Pinus* (c) *Populus alba* sp1 B2: dimethyl benzene, B3: trimethyl benzene, B4: tetramethylbenzene. Lignin units: L1: 2-methoxyphenol, L2: 4-methyl-2-methoxyphenol, L3: 4-ethenyl-2-methoxyphenol, L4: 3-allyl-6-methoxyphenol, L5: 2,6 dimethoxy-4-vinyl phenol. Pr1: Prist-1-ene, Pr2: Prist-2-ene, P: Phenol, FA: Fatty acyl moieties, C_n denotes carbon chain length. ■ *n*-alkane, *n*-alk-1-ene homologues, number indicating the carbon chain length

Table 3.1 Primary constituents of the pyrolysates and TMAH-pyrolysates of fossil leaves from Ardèche diatomite

Fossil leaves sp. 1	Pyrolysis-GC-MS ^a							TMAH-py-GC-MS	
	Benzene + derivatives	Lignin moteties	Pristenes	Tocopherol	<i>n</i> -alkane/alkene doublet range	Most abundant alkane	C ₁₆ FA	FAMES	FAME range ^b
<i>Quercuspalaeocorris</i>	+	+	+	-	10-31	29	+	+	28-32
<i>Quercussuber</i>	+	+	+	-	10-31	29	+	+	N.d.
<i>Quercussp</i>	+	+	+	-	10-31	29	-	+	28-32
<i>Quercushispanica</i>	+	+	+	+	8-31	29, 31	+	+	30
<i>Pinussp</i>	+	+	+	+	10-31	31	+	+	30
<i>Populus alba</i>	+	-	+	+	9-31	29	-	+	28-32
<i>Acer pseudocampestre</i>	+	+	+	-	10-32	29	+	+	N.d.
<i>Vitisstemonica</i>	+	+	+	-	9-31	29	+	+	26-32
<i>Castaneavesca</i>	+	+	+	-	10-30	29	+	+	28-32
<i>Tiliasp</i>	+	+	+	+	10-33	29	-	+	28-34
<i>Matrix</i>	-	-	-	-	-	-	-	-	-

^aPresence or absence of specific pyrolysis products are indicated by a (+) or (-), respectively

^bNote that all TMAH pyrolysates contain a predominance of C₁₆ and C₁₈ FAME along with various other low-molecular-weight components; shown in this column is solely the range of the high-molecular-weight FAMES (all with a strong even-over-odd predominance)

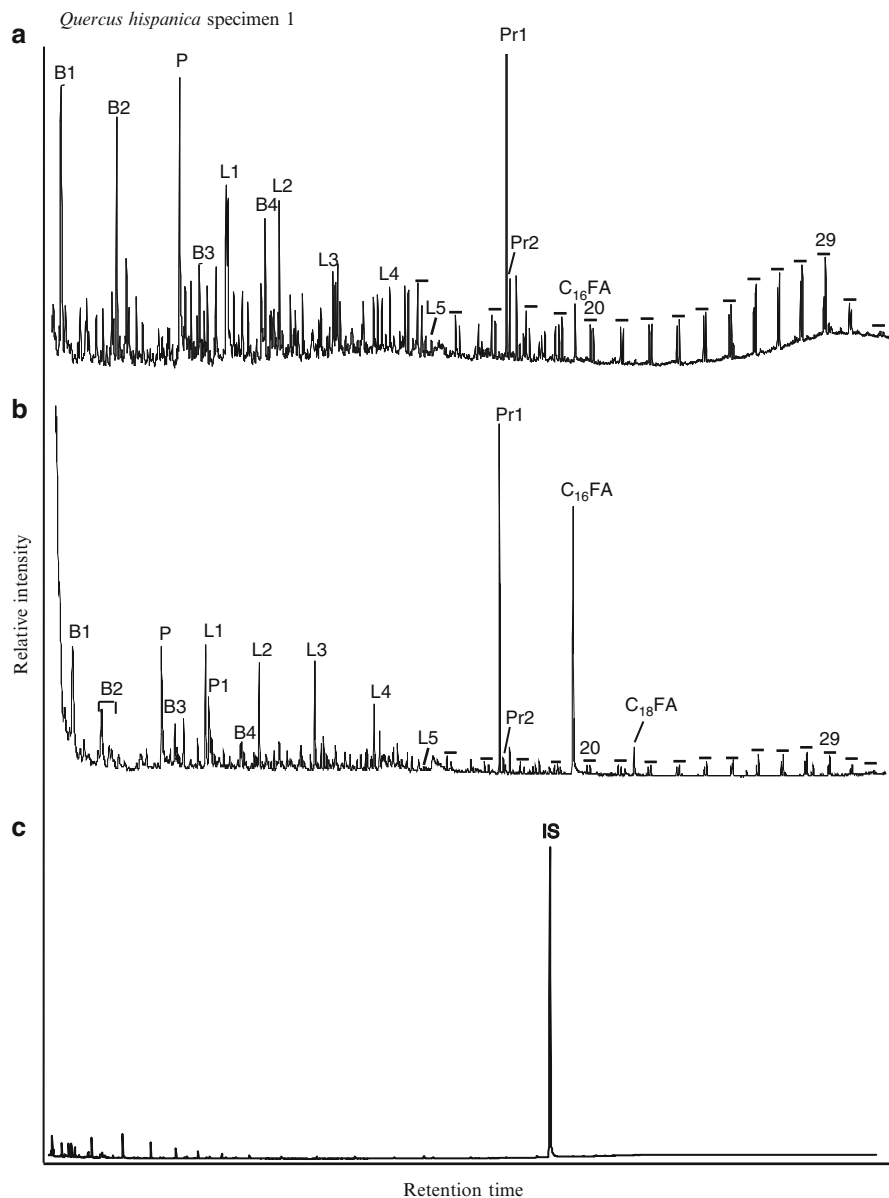


Fig. 3.9 Partial total ion current chromatogram of fossil *Quercus hispanica* sp1 after extraction (a) and after saponification (b). (c) shows the lack of any compounds in the saponified extract. A C₃₄ *n*-alkane was used as the internal standard. Symbols same as those in Fig. 3.8

phenols and acids (Challinor 1989, 1991a, b). It has been used for the structural investigation of biopolymers (Anderson and Winans 1991; de Leeuw and Baas; 1993; Hatcher et al. 1995; Hatcher and Clifford 1994; McKinney et al. 1995; Hatcher and

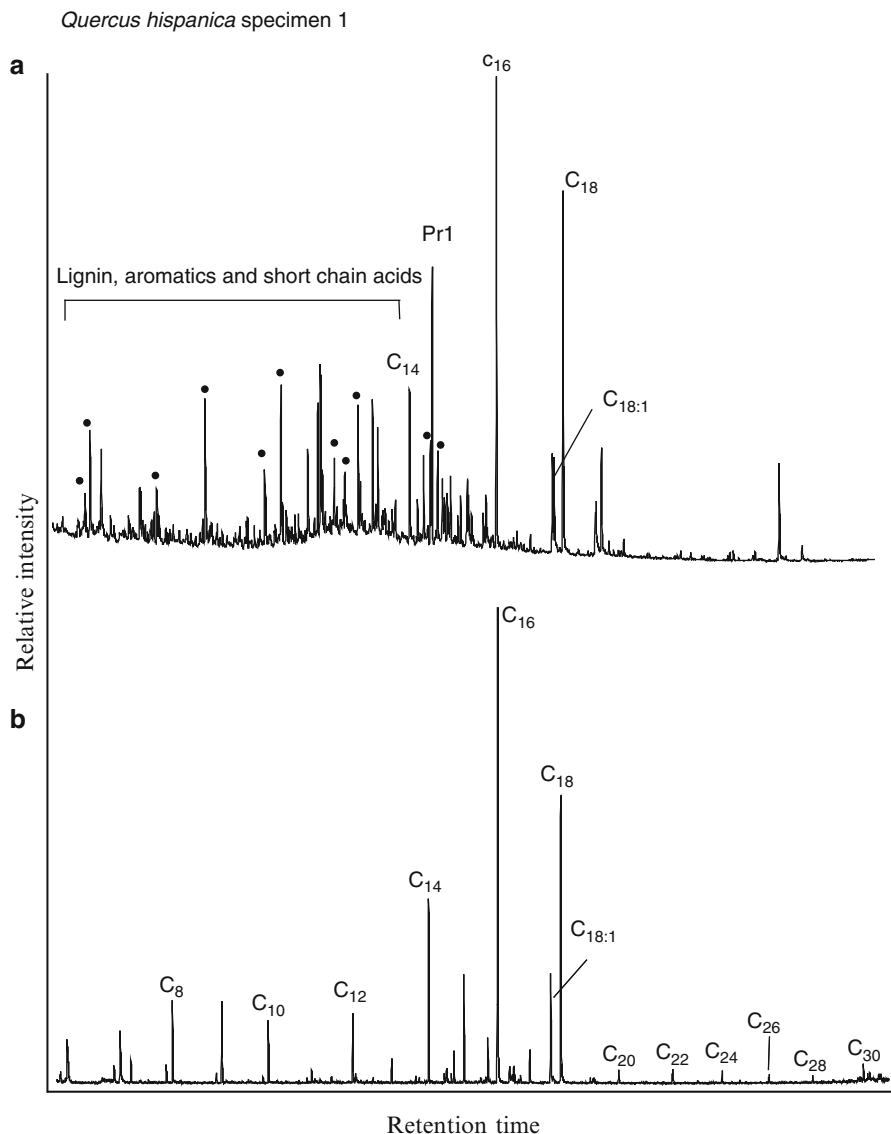


Fig. 3.10 Partial total ion current chromatogram of fossil *Quercus hispanica* sp1 under TMAH conditions (**a**) m/z 74+87 mass chromatogram (**b**) revealing the distribution of fatty acyl moieties (for details on lignin moieties under TMAH conditions see Hatcher and Clifford 1994; Hatcher et al. 1995; Clifford et al. 1995; Almendros et al. 1998, 1999)

Minard 1995); humic material (Saiz-Jimenez 1994; Martin et al. 1994; del Río et al. 1994), coalified wood and kerogen (del Río et al. 1994). This technique has also been applied to plant fossil cuticles (Almendros et al. 1998, 1999). Thermochemolysis reveals that C_{16} and C_{18} fatty acid methyl esters (FAMES) and pristenes are abundant

in the aliphatic component of the pyrolysate (Fig. 3.10a) with comparative reduction in the alkane/alkene homologues seen in normal pyrolysis. Although the C₁₆ and C₁₈ FAMES typically are predominant, other FAMES released during thermochemolysis (Fig. 3.10b) include C₁₄, C₁₅ and C_{18:1}, which are relatively abundant in all analysed samples. Lesser abundances of C₁₀ and C₁₂ FAMES, as well as higher-molecular-weight FAMES ranging in carbon number up to C₃₂, are present (Table 3.1). Methylated derivatives of the lignin components and aromatics observed during routine pyrolysis are also present in the TMAH-pyrolysates, as expected (Fig. 3.10a). Thus, TMAH assisted py-GC-MS, like py-GC-MS, suggests that the fossil leaves consist of aliphatic and aromatic, and lignin derived components. No carbohydrate moieties were detected, confirming their absence.

Spectroscopic Studies

Further compositional information was obtained using ¹³C solid state NMR and global and micro-FTIR of the fossil *Quercushispanica* specimen 1, *Castaneavesca* specimen 1 and *Populusalba* specimen 1 leaves.

Solid state ¹³C NMR has rarely been used for studies of fossil plant cuticles primarily because of the small sample generally obtained from pure fossil cuticles combined with the impure nature of many fossil cuticles. This may account for slightly low signal to noise ratio observed in fossil spectra (Lyons et al. 1992). Notable previous studies making use of this technique in plant fossil cuticles include van Bergen et al. (1994) on Upper Carboniferous pteridosperm cuticles and Lyons et al. (1992) on Carboniferous seed fern cuticles. The NMR spectra of fossil leaves obtained here are in agreement with the pyrolysis data, as also seen in the previous investigations of cuticles. The spectra (Fig. 3.11) show the presence of a number of relatively broad resonances in the range of approximately 0–150 ppm. In the spectra the peak of maximum intensity is centred at ca 30 ppm, ascribed to methylene moieties and the aliphatic component of the leaf. A similar shift was observed in the analysis of *Karinopteriscuticle* (van Bergen et al. 1994). The shoulder at 15 ppm can be ascribed to terminal methyl groups. In addition, the spectra show a relatively narrow resonance at 56 ppm and are likely related to carbon atoms at ether linkages for lignin (aryl alkyl linkages-OCH₃). The peaks from 100 to 150 ppm are due largely to aromatic carbons with varying substituents and may account for the aromatic compounds recognised in the pyrolysate, as noted by van Bergen et al. (1994).

The NMR spectra reveals the predominance of aliphatic moieties relative to aromatic moieties. However, contrary to previous results based on solid state ¹³C NMR spectroscopy and py-GC-MS, which pointed to the highly aliphatic nature of organic matter in forest soils, Poirier et al. (2000) used quantitative methods to show that aliphatic moieties with long alkyl chains are only minor components. Thus, observations via solid state ¹³C NMR spectroscopy and pyrolysis experiments can lead to overestimation of aliphatic moieties in heterogeneous materials when applied without quantitative constraints derived from elemental analysis and/or quantitative pyrolysis.

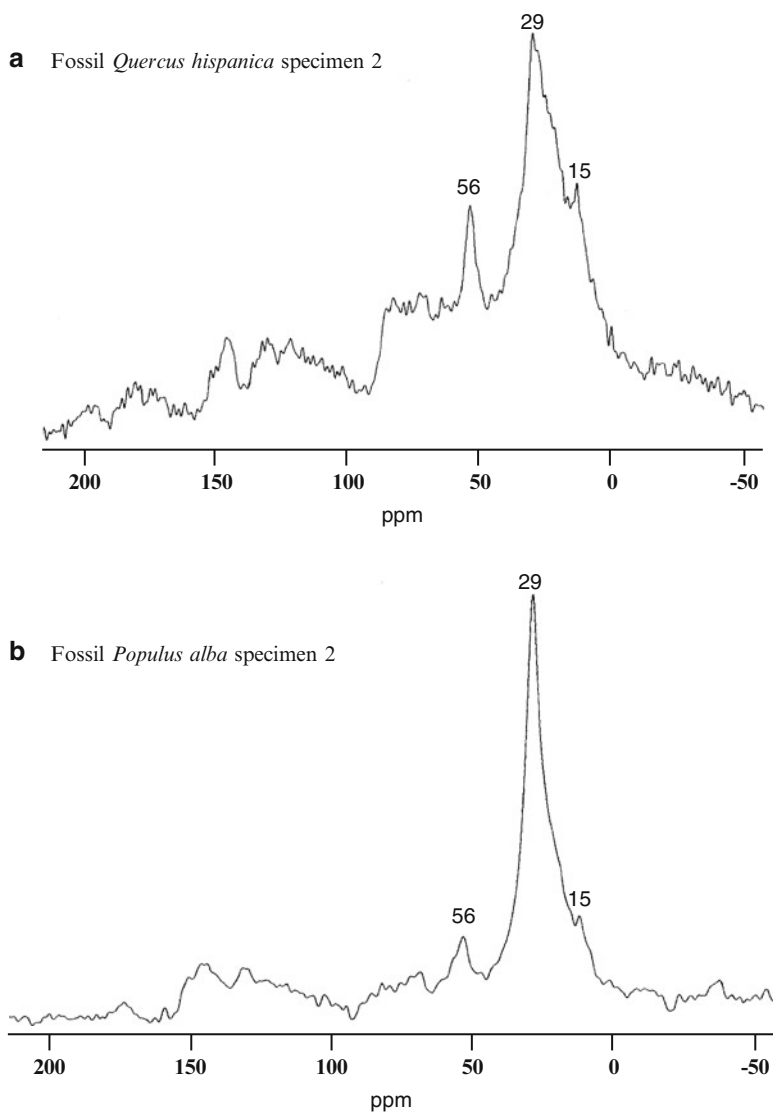


Fig. 3.11 ^{13}C NMR CP-MAS spectra of fossil leaves. (a) *Castaneavesca* specimen 2 (b) *Populus alba* specimen 2

FTIR was used to obtain further structural information. FTIR is particularly effective for the characterisation of oxygen functionalities and has been applied previously to fossil algaenan (Blokker et al. 1998), *Gloeocapsomorphaprisca* microfossils (Derenne et al. 1994), kerogen (Landais et al. 1993) and plant fossil cuticles (Mösle et al. 1998; Collinson et al. 1998). In the traditional global mode analysis (KBr) technique, one of the primary limitations is that the mineral content

of the matrix may interfere with the signal from the sample (Landais et al. 1993). EM shows that all leaves are covered with diatoms and the FTIR spectrum of fossil *Populus* specimen 1 exhibits a strong silicate signal (Fig. 3.12b). Hence, spectra for amorphous silica (diatom) were obtained as a control (Fig. 3.12a). Figure 3.12c shows the micro-FTIR spectrum for fossil *Castaneavesca* specimen 1 which provides much greater information and better resolution than for *Populus*, as analysis under the microscope allows areas with mineral concentrations to be avoided. Table 3.2 provides a list of the absorption bands, their vibration modes and associated functional groups identified in the spectra. The aliphatic nature of the biopolymers is expressed by strong absorption peaks between 2,800 and 3,000 cm^{-1} (those related to both symmetric and asymmetric stretching vibrations: see Table 3.2) and peaks at 1,450 and 1,375 cm^{-1} (related to deformation vibrations). Absorption peaks maximising at 1,600 cm^{-1} indicate the presence of double bonds, and the shoulder around 1,700 cm^{-1} indicates the possible presence of C=O bonds hinting at the presence of carbonyl and carboxyl functionalities. Hydroxyl groups are represented by a broad band related to OH stretching vibrations at 3,100–3,700 cm^{-1} maximising at 3,400. Micro-FTIR also allowed detection of ether bonds (those associated with aromatic, saturated and vinyl linkages, in peaks between 1,020 and 1,280 cm^{-1} , Table 3.2) and aromatic components (750–900 cm^{-1} , Table 3.2), signals that are that are swamped in global analysis by silicate contamination.

Saponification

Extracted residues of leaves of *Quercushispanica* specimen 1 and *Pinus* were hydrolysed under basic conditions in an attempt to remove ester-bound components, in the same way that the modern counterparts were treated. However, after saponification, the released lipid extracts contained no aliphatic components (Fig. 3.9c), demonstrating that the aliphatic material is recalcitrant and that the acyl moieties in the geomacromolecule are resistant to base hydrolysis. Consistent with this, residues (residue 5, Fig. 3.1) after saponification generated pyrolysates containing fatty acids and pristenes, as also observed in the non-saponified fossil leaf pyrolysates (Fig. 3.9b). In fact, the only difference between the pyrolysate of the pre- (Fig. 3.9a) and post saponified (Fig. 3.9b) leaf is the enhanced abundance of fatty acids in the latter. This could be due to more efficient pyrolysis in the absence of diatom fossils that could have been dissolved during base hydrolysis.

Aliphatic Composition of Modern Plants

Previous work (Eglinton et al. 1962; Nip et al. 1986; Tegelaar et al. 1989a, b) indicates that the aliphatic component of leaves is represented by a range of free and macromolecular moieties, characterized by a variety of functionalities. Long-chain *n*-alkyl

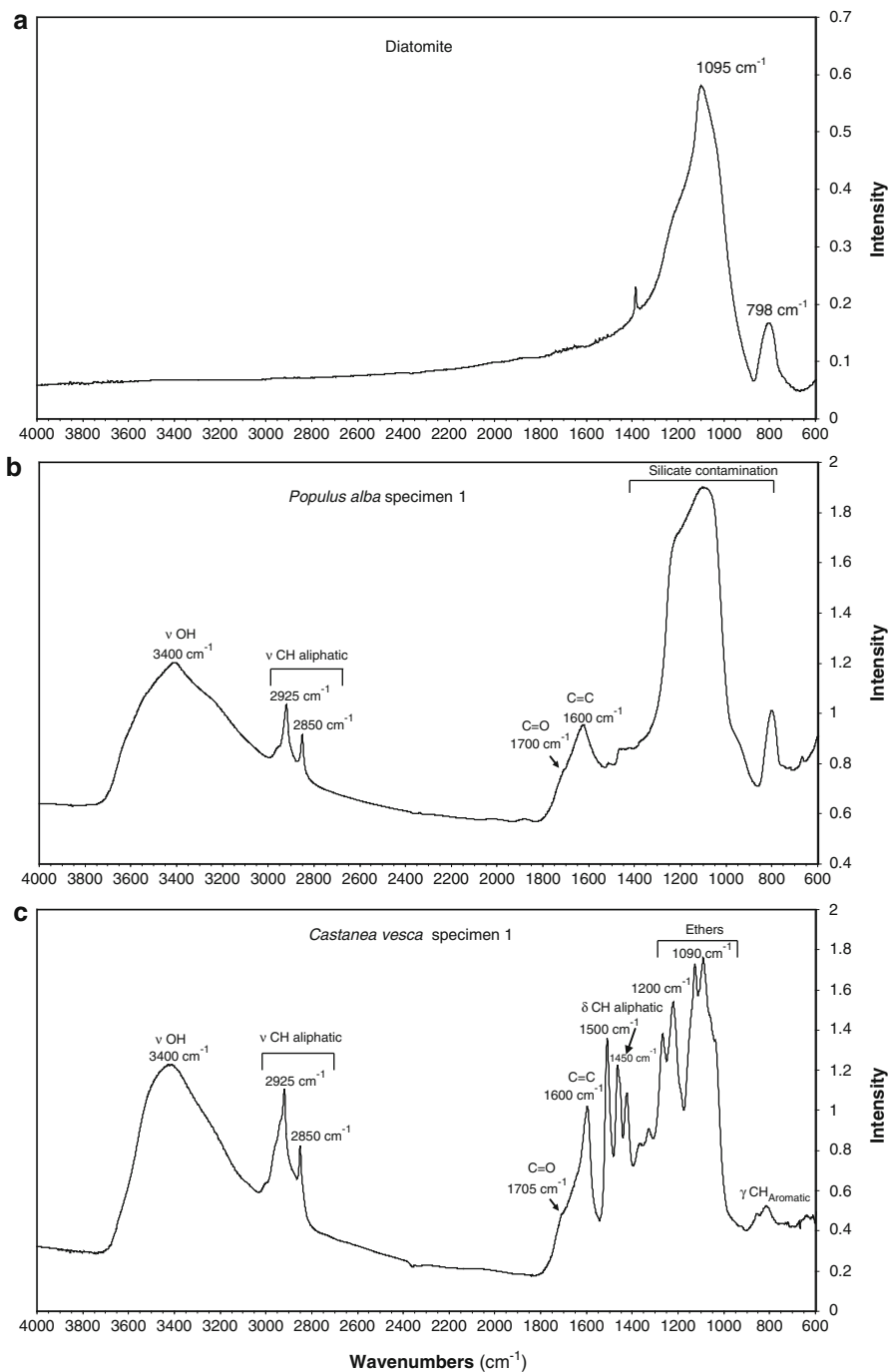


Fig. 3.12 FTIR spectra of fossil leaves and diatomite. (a) Global FTIR Silica (Diatomite), (b) Global FTIR, *Populus alba* sp 1, (c) micro-FTIR, *Castanea vesca* sp 1. For details see Table 3.2

Table 3.2 Absorption bands, their vibration modes and associated functional groups identified in the FTIR spectra of fossil leaves and associated diatomite (Fig. 3.12) from the Ardèche locality

Position (cm ⁻¹)	Group	Type of vibration
3,700–3,100	O—H	
–3,400	OH	Stretching ν
3,000–2,800	C—H Aliphatic	
–2,925	as + sCH ₂ + CH ₃	Stretching ν
–2,850	sCH ₂ + CH ₃	Stretching ν
1,710–1,705	C=O (carboxyls and carbonyl)	
1,600 and 1,495	C=C (double bond)	
1,450	CH ₂ + CH ₃ (aliphatic)	Deformation δ
1,375	CH ₃ (aliphatic)	Deformation δ
900–750	C—H aromatic	
–875	1 H adjacents γ	
–830	2 H adjacents γ	
–750	4 H adjacents γ	
1,200–1,040	C—O—C (saturated ethers)	Stretching ν
1,280–1,200	as=C—O—C (Vinyl ethers)	Stretching ν
1,075–1,020	s=C—O—C (aromatic ethers)	Stretching ν
1,095, 798	Mineral band, SiO ₂	
	s-symmetric	
	as-asymmetric	

compounds are major components of epicuticular waxes (Eglinton et al. 1962; Eglinton and Hamilton 1967) and include *n*-alkanes, *n*-alkanols, *n*-alkanoic acids and wax esters. The *n*-alkanols and *n*-alkanoic acids typically occur in higher plants as C₁₆–C₃₆ homologues with a strong predominance of even-carbon-number homologues over odd-numbered ones, reflecting their biosynthesis from acetyl moieties (Kolattukudy 1981). *n*-Alkanes occur with carbon chain-lengths ranging from C₂₅ to C₃₅ (Kolattukudy 1981; Eglinton et al. 1962; Eglinton and Hamilton 1967) and with an odd-over-even predominance (the most common being C₂₇, C₂₉, C₃₁ and C₃₃), reflecting formation via decarboxylation of carboxylic acids.

In addition to free *n*-alkyl components, a variety of macromolecular components including cutin, suberin and cutan has been described. Of these, cutin appears to be almost ubiquitous and comprises C₁₆ and C₁₈ *n*-alkanoic acids and mono, di and trihydroxy derivatives of these, cross-linked via ester bonds (Kolattukudy 1980). Nip et al. (1986) first described cutan, a highly aliphatic biopolymer comprised of relatively high-molecular-weight *n*-alkyl components immune to hydrolysis, in *Agave americana*. Subsequently, Tegelaar et al. (1991) reported the presence of cutan co-occurring with cutin in the leaves of 14 plant species and, in the case of *Beta vulgaris* (ssp. *maritima*), occurring alone. As comparable fossil leaves showed an aliphatic composition, it was concluded that selective preservation of cutan is responsible for the aliphatic composition of the fossils and has a biasing influence on the fossil record. However, the modern leaves investigated in this study were not subjected to hydrolysis to check rigorously for the presence of cutan.

All the modern leaves that we investigated contain abundant *n*-alkanes, *n*-alkanols and *n*-alkanoic acids and, after saponification, yield characteristic cutin constituents (Fig. 3.6b). However, our combined hydrolysis and py-GC/MS approach revealed no evidence of cutan in any of the modern representatives of our fossil leaves. To test our methodology, we analysed *Agave americana* and *Cliviaminata*, both known to contain cutan (Nip et al. 1986), using methods identical to those that we used for the other leaves. Pyrolysis of lipid-extracted *Agave* and *Clivia* leaves revealed the presence of *n*-alkane/*n*-alk-1-ene homologues ranging from C₈–C₃₄ (including those >C₂₀) similar to those reported by Nip et al. (1986), this signal persisted after saponification. In contrast, in the ten leaves described here, *n*-alkanes and *n*-alkenes were absent after hydrolysis. This might be an effect of preferential cleavage of more labile bonds associated with lignin and cellulose during pyrolysis, swamping the aliphatic signal and inhibiting detection of the aliphatic cutan. Although this seems unlikely, the cutan signal was still detected in *Agave* and in *Clivia* after similar treatment.

We also analysed the extractable fatty acid and fatty acyl component of the modern leaves. These fractions are dominated by the C₁₆ fatty acid, with lower abundances of the C₁₈ homologue. Thus, the aliphatic content of the living leaves comprises C₁₆ and C₁₈ alkyl components present as FAs, PLFAs, di- and tri-glycerides or cutin, with a contribution from long chain free fatty acids up to C₃₂. Critically, aliphatic moieties occur as part of a macromolecule not immune to base attack. Although surprising when compared to the results of Tegelaar et al. (1991), which suggested that cutan is widespread in modern leaves, the absence of cutan in our results is consistent with more recent analyses of the leaves of gymnosperms including *Ginkgo biloba* and 15 genera from 6 families of conifers (Collinson et al. 1998) which involved a more comprehensive procedure.

Composition of the Ardèche Fossil Leaves

All ten of the Ardèche fossil leaves have a chemical composition similar to that of the representative examples discussed in the results section and illustrated in the in spite of the variation in their internal organisation and the general absence (with one exception) of recognisable leaf tissues. Chemical analyses, including ¹³C-NMR, FTIR, py-GC-MS and TMAH-py-GC-MS, indicate an aliphatic composition for each of the leaves. Aromatic components in the form of benzene and lignin derivatives are also present in apparently subordinate abundances. However, as mentioned before, Poirier et al. (2000) have shown that solid state ¹³C NMR can overestimate the contribution of aliphatic moieties in complex refractory material. Similarly, TMAH assisted pyrolysis leads to an increased yield of the aliphatic component when analysing the lipid signature in fossil samples with condensed polymethylene networks (Almendros et al. 1998). Thus, the aromatic component of the Ardèche fossil leaves may be more significant than our results suggest; none the less it is clear that all analysed leaves are comprised of a macromolecule with a strong aliphatic component.

The structure of the aliphatic macromolecule is difficult to elucidate. Py-GC-MS and, in particular, TMAH-py-GC-MS analyses suggest that C_{16} and C_{18} fatty acids are important units of the aliphatic polymer. However, the composition of the macromolecule is clearly more heterogeneous than this. Higher-molecular-weight aliphatic components are revealed by the presence of *n*-alkane/*n*-alk-1-ene doublets extending to *n*- C_{31} in the pyrolysates, and FAMES extending to C_{32} or C_{34} in the TMAH pyrolysates. Pristenes are present in the pyrolysate and apparently bound into a non-hydrolysable structure; their presence in post-saponification residues indicates that they have been incorporated into a resistant geopolymer.

Assessing the relative importance of these components is difficult; quantitative pyrolysis is problematic and has not been attempted rigorously. However, replicate analyses indicate that the increase in the relative abundances of C_{16} and C_{18} components in TMAH thermochemolysis compared to routine pyrolysis is associated with a decrease in the alkane/alkene signal. The methyl esters are likely released from trans-esterification reactions causing the cleavage of polyester domains (McKinney et al. 1996), and the total quantity of alkyl series obtained from fossil cuticles by thermochemolysis is higher than that from routine pyrolysis (Almendros et al. 1999). This may be due to improved elution of FAMES compared to underivatized fatty acids on the GC column. Differences in the analytical results may reflect inherent biases in the techniques. Thermochemolysis produces independent and complementary reactions to conventional pyrolysis, providing additional information depending mainly on the polyalkyl and oxidized character of the fossil sample (Almendros et al. 1998). The technique, which is thought to be direct simultaneous pyrolysis methylation (Kralert et al. 1995), may instead be an effective chemolysis procedure (de Leeuw and Baas 1993; Martin et al. 1994) that does not necessarily require pyrolysis temperatures (Hatcher and Clifford 1994; Clifford et al. 1995) but produces effects additional and/or complementary to those associated with conventional pyrolysis (Almendros et al. 1999). Thus, it is difficult to assess the quantitative contribution to the macromolecule from fatty acyl moieties up to C_{32} with a dominance of C_{16} and C_{18} chain lengths. However, the strong FA signal in both routine and TMAH assisted pyrolysis suggests that such moieties are important component of the fossil leaf macromolecule.

Base hydrolysis of the fossil leaves yielded no hydrolysable components and py-GC-MS analyses of the post saponification residue clearly show the persistence of fatty acids and pristenes. Thus, although fatty acyl moieties are present in the fossil macromolecule they are linked by bonds no longer hydrolysable under basic conditions (in contrast to the modern counterparts). A possible explanation could be that encapsulation of ester linkages in a hydrophobic network of *n*-alkyl chains sterically protects these functional groups from saponification (McKinney et al. 1996). Another possibility is extensive cross linking of the esters in the polymer resulting in a requirement for much harsher saponification conditions (Fujii et al. 1986) to release the monomers. Such cross-linking has been recognised recently in tomato cutin (Deshmukh et al. 2003) using one and two dimensional High resolution-MAS NMR study.

In addition, ^{13}C NMR reveals the importance of alkoxy functional groups (56 ppm) indicating the presence of lignin. Further, Micro-FTIR reveals the presence of ether bonds (those associated with aromatic, saturated and vinyl linkages) in peaks between 1,020 and 1,280 cm^{-1} (Fig. 3.11c, Table 3.2). Thus, the aliphatic macromolecule is likely bonded by a combination of ester and ether linkages.

Possible Origin of the Aliphatic Macromolecule in the Ardèche Fossil Leaves

An unexpected aspect of this study is the absence of cutan in modern representatives of the fossils, precluding it as a source of the aliphatic macromolecule in the fossil leaves. Thus, the aliphatic character of the fossil leaves cannot be explained by selective preservation of cutan (Tegelaar et al. 1989a, b, 1991; de Leeuw and Largeau 1993). The selective preservation process emphasizes the importance of a non hydrolysable polymer to survive diagenesis and eventually enter the fossil record. In the absence of cutan, alternative biogeochemical components must have served as the source of the aliphatic component.

Allochthonous organic matter is also an unlikely source given its paucity in the matrix; although bacteria could have been more abundant in microenvironments within and near the leaves than in the organic-lean diatomite, the lack of diagnostic bacterial compounds (e.g. hopanoids) in any of the analyzed fractions suggests that such organisms did not contribute to the preserved organic matter. Even if some surface material is derived from an external source this would have contributed a minute proportion of the total fossil leaf organic matter (for detailed discussion on the effect on matrix in fossils, see Chap. 4 for effect of sediment on organic contamination in fossils). All leaves show well-preserved gross morphology and venation pattern, one shows internal cellular structure (albeit slightly modified) and the others with open texture have comparable preserved thicknesses. These facts make it unreasonable to argue that the organic matter constituting the leaves was derived from anywhere except the leaves themselves.

Cutin monomers are normally hydrolysable under basic conditions (as observed here in recent leaves); however Schmidt and Schonherr (1982) indicated that intermolecular reactions between epoxy and alcohol groups in the cutin monomers may lead to the formation of ether linkages rendering them resistant to acid and base catalysed reactions and their eventual diagenetic survival (Tegelaar et al. 1991). This would lead normally to hydrocarbon fragments with chain lengths less than the original (typically C_{16} and C_{18}) upon pyrolysis (Hartgers et al. 1995). Hydrocarbon fragments greater than C_{30} may be produced as a result of di/polymerisation of cutin constituents by carbon-carbon bonds with contribution from extra cuticular waxes (Mösle et al. 1998).

The living relatives of the Ardèche leaves contain cutin, phospholipid fatty acids, di and triglycerides, and free fatty acids, all dominated by the C_{16} and C_{18} fatty acid homologues. Cutin is more stable diagenetically than phospholipids and fatty

acids and might be expected to serve as the primary source of C_{16} and C_{18} moieties and the aliphatic component in the fossil leaves. However, microscopic analyses indicate that none of the fossils possess a recognisable cuticle. It could be argued that small fragments of cuticle are preserved in pieces of leaf not subjected to electron microscopy or that cuticle is present but has been modified physically so that it is no longer recognisable. Even in such situations, cuticle likely represents only a small part of the total fossil leaf organic matter given the total leaf thicknesses and the internal organic matter proportions observed in TEM sections of all leaves. The wide variation seen in the preservation of internal leaf organisation shows that the aliphatic macromolecule cannot be linked to preservation of any specific leaf tissue or cell types and suggests that its precursors were probably widespread within the leaves. Alternative sources of the C_{16} and C_{18} moieties of the aliphatic components include membrane lipids may have been preserved by *in situ* polymerisation with contribution from higher molecular weight plant waxes (Walton 1990), and contributed to the formation of an aliphatic macromolecule. Cutin-derived acids could also have been incorporated into the forming macromolecule. Thus, the aliphatic component could be a product of the polymerisation of labile (extractable and hydrolysable) precursors that condense into a recalcitrant non-hydrolysable aliphatic macromolecule. A similar process was suggested by Stankiewicz et al. (1998a, b, 2000) in the case of arthropods, which likewise do not have a resistant aliphatic precursor.

Implications

The results of this investigation demonstrate that C_{16} and C_{18} carboxylic acid together with other fatty acid components ranging from C_8 to C_{32} are important constituents in the aliphatic composition of the Ardèche fossil leaves. Cutan is not the source of this aliphatic material; C_{16} , C_{18} and higher-molecular-weight fatty acyl components could be derived from cutin, free fatty acids (e.g. leaf waxes) or membrane PLFAs. The fossil macromolecule is immune to base hydrolysis, suggesting that the fatty acyl components in the geopolymer could be sterically protected by *n*-alkyl chains. In addition ether bonds are also present. None of the fossil leaves analysed from the Ardèche locality preserves the cuticle; the fossils consist of a substantial thickness of internal tissue, albeit strongly modified. Thus, membrane lipids together with free fatty acids could be the source of components in aliphatic macromolecule. Lipid polymerisation has been observed to contribute significantly to kerogen formation, where the role of selective preservation was limited (Riboulleau et al. 2001), and also in early stages of the formation of coorongite (Gatellier et al. 1993). In such cases the organic matter revealed an amorphous composition to some extent comparable to the loss of recognisable leaf tissues in most fossil leaves here. This reveals that *in situ* polymerisation of labile lipid components could be of widespread importance. All previously reported pyrolysates of 'older' fossil leaves and cuticles, irrespective of age, plant type or enclosing lithology, show the presence of aliphatic components (Nip et al. 1986; Tegelaar et al. 1991; Collinson et al. 1998;

Mösle et al. 1997, 1998). Importantly, aliphatic components are also characteristic of the pyrolysates of most arthropod fossils (Stankiewicz et al. 1997a, b, 1998a, b, 2000; Briggs et al. 1998; Briggs 1999) none of which has a recalcitrant aliphatic precursor. Given the ubiquity of labile aliphatic compounds in organisms, the aliphatic character of sedimentary organic matter, including kerogen, could be attributed to processes similar to those inferred here in fossils. The process of *in-situ* polymerisation could be of widespread importance in addition to selective preservation.

References

- Almendros G, González-Vila FJ, Martín F, Sanz J, Álvarez-Ramis C (1998) Appraisal of pyrolytic techniques on different forms of organic matter from a Cretaceous basement in Central Spain. *Org Geochem* 28:613–623
- Almendros G, José Dorado J, González-Vila FJ, Martín F, Sanz J, Álvarez-Ramis C, Stuchlik L (1999) Molecular characterization of fossil organic matter in *Glyptostrobuseuropaeus* remains from the Orawa basin (Poland). Comparison of pyrolytic techniques. *Fuel* 78:745–752
- Anderson KB, Winans RE (1991) The nature and fate of natural resins in the geosphere. I. Evaluation of pyrolysis-gas chromatography-mass spectrometry for the analysis of natural resins and resinates. *Anal Chem* 63:2901–2908
- Berner RA (1989) Biogeochemical cycles of carbon and sulfur and their effect on atmosphere on phanerozoic time. *Palaeogeogr Palaeoclimatol Palaeoecol* 73:97–122
- Bland HA, van Bergen PF, Carter JF, Evershed RP (1998) Early diagenetic transformations of proteins and polysaccharides in archaeological plant remains. In: Stankiewicz BA, van Bergen PF (eds) Nitrogen-containing macromolecules in the bio- and geosphere, vol 707, ACS symposium series
- Blokker P, Schouten S, van den Ende H, de Leeuw JW, Hatcher PG, Sinninghe-Damsté JSS (1998) Chemical structure of algaenans from the fresh water algae *Tetraedron minimum*, *Scenedesmus communis* and *Pediastrumboryanum*. *Org Geochem* 29:1453–1468
- Blokker P, Schouten S, de Leeuw JW, Sinninghe-Damsté JSS, van den Ende H (2000) A comparative study of fossil and extant algaenans using ruthenium tetroxide degradation. *Geochim Cosmochim Acta* 64:2055–2065
- Briggs DEG (1999) Molecular taphonomy of animal and plant cuticles: selective preservation and diagenesis. *Philos Trans R Soc Lond B Biol Sci* 354:7–16
- Briggs DEG, Stankiewicz BA, Evershed RP (1998) The molecular preservation of fossil arthropod cuticles. *Anc Biomol* 2:135–146
- Challinor JM (1989) A pyrolysis-derivatization-gas chromatograph technique for the elucidation of some synthetic polymers. *J Anal Appl Pyrolysis* 16:323–333
- Challinor JM (1991a) Structure determination of alkyd resins by simultaneous pyrolysis methylation. *J Anal Appl Pyrolysis* 18:233–244
- Challinor JM (1991b) The scope of pyrolysis methylation reactions. *J Anal Appl Pyrolysis* 20:15–24
- Clifford DJ, Carson DM, McKinney DE, Bortiatynski JM, Hatcher PG (1995) A new rapid technique for the characterization of lignin in vascular plants: thermochemolysis with tetramethylammonium hydroxide (TMAH). *Org Geochem* 23:169–175
- Collinson ME, Mösle B, Finch P, Wilson R, Scott AC (1998) The preservation of plant cuticle in the fossil record: a chemical and microscopical investigation. *Anc Biomol* 2:251–265
- Collinson ME, Mösle B, Finch P, Wilson R, Scott AC (2000) Preservation of plant cuticles. *Acta Palaeobot Suppl* 2:629–632
- de Leeuw JW, Largeau C (1993) A review of macromolecular organic compounds that comprise living organisms and their role in kerogen, coal and petroleum formation. In: Engel MH, Macko

- SA (eds) *Organic geochemistry: principles and applications*, vol 11, Topics in geobiology. Springer, New York, pp 23–72
- del Río JC, Gonzalez-Vila FJ, Martin F, Verdejo T (1994) Characterization of humic acids from low-rank coals by ^{13}C NMR and pyrolysis-methylation. In: Formation of benzene carboxylic acid moieties during the coalification process. *Org Geochem* 22:885–891
- deLeeuw JW, Baas J (1993) The behavior of esters in the presence of tetramethylammonium salts at elevated temperatures; flash pyrolysis or flash chemolysis? *J Anal Appl Pyrolysis* 26:175–184
- Derenne S, Largeau C, Landais P, Rochdi A (1994) Spectroscopic features of Gloeocapsomorphaprisca colonies and of interstitial matrix in kukersite as revealed by transmission micro-FT-i.r.: location of phenolic moieties. *Fuel* 73:626–628
- Deshmukh AP, Simpson AJ, Hatcher PG (2003) Evidence for cross-linking in tomato cutin using HR-MAS NMR spectroscopy. *Phytochemistry* 64:1163–1170
- Eglinton G, Hamilton RJ (1967) Leaf epicuticular waxes. *Science* 156:1322–1334
- Eglinton G, Gonzalez AG et al (1962) Hydrocarbon constituents of the wax coatings of plant leaves: a taxonomic survey. *Phytochemistry* 1:89–102
- Fujii M, Hida M, Ono H, Tabata A, Matsumoto M (1986) Improvement of measuring method of saponification value on bees wax, etc. *Nippon Koshohin Kagakkaishi* 10:269–274
- Gatellier J-PLA, de Leeuw JW, Sinninghe Damsté JS, Derenne S, Largeau C, Metzger P (1993) A comparative study of macromolecular substances of a Coorongite and cell walls of the extant alga *Botryococcusbraunii*. *Geochim Cosmochim Acta* 57:2053–2068
- Gelin F, Volkman JK, Largeau C, Derenne S, Sinninghe Damsté JS, de Leeuw JW (1999) Distribution of aliphatic, nonhydrolyzable biopolymers in marine microalgae. *Org Geochem* 30:147–159
- Gillaizeau B, Derenne S, Largeau C, Berkaloff C, Rousseau B (1996) Source organisms and formation pathway of the kerogen of the Göynük Oil Shale (Oligocene, Turkey) as revealed by electron microscopy, spectroscopy and pyrolysis. *Org Geochem* 24:671–679
- Goosens H, de Leeuw JW, Schenck PA, Brassell SC (1984) Tocopherols as likely precursors of pristane in ancient sediments and crude oils. *Nature* 312:440–442
- Gupta NS, Pancost RD (2004) Biomolecular and physical taphonomy of angiosperm leaf during early decay: implications for fossilisation. *Palaios* 19:428–440
- Hartgers WA, Sinninghe Damsté JS, de Leeuw JW (1992) Identification of C₂–C₄ alkylated benzenes in flash pyrolysates of kerogens, coals and asphaltenes. *J Chromatogr A* 606:211–220
- Hartgers WA, Sinninghe Damsté JS, de Leeuw JW (1995) Curie-point pyrolysis of sodium salts of functionalized fatty acids. *J Anal Appl Pyrolysis* 34:191–217
- Hatcher PG, Clifford DJ (1994) Flash pyrolysis and in situ methylation of humic acids from soil. *Org Geochem* 21:1081–1092
- Hatcher PG, Minard RD (1995) Comment on the origin of benzenecarboxylic acids in pyrolysis methylation studies. *Org Geochem* 23:991–994
- Hatcher PG, Nanny MA, Minard RD, Dible SD, Carson DM (1995) Comparison of two thermochemolytic methods for the analysis of lignin in decomposing wood: the CuO oxidation method and the method of thermochemolysis with tetramethylammonium hydroxide (TMAH). *Org Geochem* 23:881–888
- Hold IM, Schouten S, Van der Gaast SJ, Damste JSS (2001) Origin of prist-1-ene and prist-2-ene in kerogen pyrolysates. *Chem Geol* 172:201–212
- Kenney JF, Kutcherov VA, Bendeliani NA, Alekseev VA (2002) The evolution of multicomponent systems at high pressures: VI. The thermodynamic stability of the hydrogen-carbon system: the genesis of hydrocarbons and the origin of petroleum. *Proc Natl Acad Sci U S A* 99:10976–10981
- Kok MD, Schouten S, Damste JSS (2000) Formation of insoluble, nonhydrolyzable, sulfur-rich macromolecules via incorporation of inorganic sulfur species into algal carbohydrates. *Geochim Cosmochim Acta* 64:2689–2699
- Kolattukudy PE (1980) Biopolyester membranes of plants: cutin and suberin. *Science* 208:990–1000
- Kolattukudy PE (1981) Structure, biosynthesis, and biodegradation of cutin and suberin. *Ann Rev Plant Physiol* 32:539

- Kralert PG, Alexander R, Kagi RI (1995) An investigation of polar constituents in kerogen and coal using pyrolysis-gas chromatography-mass spectrometry with in situ methylation. *Org Geochem* 23:627–639
- Landais P, Rochdi A, Largeau C, Derenne S (1993) Chemical characterization of torbanites by transmission micro-FTIR spectroscopy: origin and extent of compositional heterogeneities. *Geochim Cosmochim Acta* 57:2529–2539
- Larter SR, Horsfield B (1993) Determination of structural components of kerogens by the use of analytical pyrolysis methods. *Top Geobiol* 11:271–287
- Logan GA, Boon JJ, Eglinton G (1993) Structural biopolymer preservation in Miocene leaf fossils from the clarkia site, Northern Idaho. *Proc Natl Acad Sci U S A* 90:2246–2250
- Love GD, Snape CE, Fallick AE (1998) Differences in the mode of incorporation and biogenicity of the principal aliphatic constituents of a Type I oil shale. *Org Geochem* 28:797–811
- Lyons PC, Zodrow EL, Orem WH (1992) Coalification of the cuticle and compressed leaf tissue of the Carboniferous seed fern *Macroneuropteris (Neuropteris) scheutzeri*- implications for coalification to the bituminous coal stage. *Geol Soc Am Abstr Progr* A163
- Martin F, Gonzalez-Vila FJ, del Río JC, Verdejo T (1994) Pyrolysis derivatization of humic substances 1. Pyrolysis of fulvic acids in the presence of tetramethylammonium hydroxide. *J Appl Anal Pyrolysis* 28:71–80
- McKinney DE, Carson DM, Clifford DJ, Minard RD, Hatcher PG (1995) Off-line thermochemolysis versus flash pyrolysis for the in situ methylation of lignin: is pyrolysis necessary? *J Appl Anal Pyrolysis* 34:41–46
- McKinney DE, Bortiatynski JM, Carson DM, Clifford DJ, de Leeuw JW, Hatcher PG (1996) Tetramethylammonium hydroxide thermochemolysis of the aliphatic biopolymer cutan: insights into the chemical structure. *Org Geochem* 24:641–650
- Mösle B, Finch P, Collinson ME, Scott AC (1997) Comparison of modern and fossil plant cuticles by selective chemical extraction monitored by flash pyrolysis-gas chromatography-mass spectrometry and electron microscopy. *J Anal Appl Pyrolysis* 4041:585–597
- Mösle B, Collinson ME, Finch P, Stankiewicz BA, Scott AC, Wilson R (1998) Factors influencing the preservation of plant cuticles: a comparison of morphology and chemical comparison of modern and fossil examples. *Org Geochem* 29:1369–1380
- Nip M, Tegelaar EW, Brinkhuis H, de Leeuw JW, Schenk PA, Holloway PJ (1986) Analysis of modern and fossil plant cuticles by Curie point Py-GC and Curie point Py-GC-MS: recognition of a new, highly aliphatic and resistant biopolymer. *Org Geochem* 10:769–778
- Padley FB, Gunstone FD, Harwood JL (1986) Leaf lipids. In: Gunstone FD, Harwood JL, Padley FB (eds) *The lipid handbook*. Chapman & Hall, London, UK
- Poirier N, Derenne S, Rouzaud J-N, Largeau C, Mariotti A, Balesdent J, Maquet J (2000) Chemical structure and sources of the macromolecular, resistant, organic fraction isolated from a forest soil (Lacadée, south-west France). *Org Geochem* 31:813–827
- Ralph J, Hatfield RD (1991) Pyrolysis-GC-MS characterization of forage materials. *J Agric Food Chem* 39:1426–1437
- Riboulleau A, Derenne S, Largeau C, Baudin F (2001) Origin of contrasting features and preservation pathways in kerogens from the Kashpir oil shales (Upper Jurassic, Russian Platform). *Org Geochem* 32:647–665
- Riou B (1995) Les fossils des diatomites du Miocene superieur de la montagne d' Andance (Ardeche, France). *Géol Méditerr* XXII:1–15
- Saiz-Jimenez C (1994) Analytical pyrolysis of humic substances: pitfalls limitations, and possible solutions. *Environ Sci Technol* 28:1773–1780
- Schmidt HW, Schönherr J (1982) Development of plant cuticles: occurrence and role of non-ester bonds in cutin of *Cliviaminiata* Reg. leaves. *Planta* 156:380–384
- Stankiewicz BA, Briggs DEG, Evershed RP, Flannery MB, Wuttke M (1997a) Preservation of chitin in 25-million-year-old fossils. *Science* 276:1541–1543
- Stankiewicz BA, Briggs DEG, Evershed RP (1997b) Chemical composition of Paleozoic and Mesozoic fossil invertebrate cuticles as revealed by pyrolysis-gas chromatography/mass spectrometry. *Energy Fuels* 11:515–521

- Stankiewicz BA, van Bergen PF (1998) Nitrogen and N-containing macromolecules in the bio- and geosphere: an introduction. In: Stankiewicz BA, van Bergen PF (eds) Nitrogen-containing macromolecules in the bio- and geosphere, ACS symposium series 707. Oxford University Press, New York, pp 1–12
- Stankiewicz BA, Möhle B, Finch P, Collinson ME, Scott AC, Briggs DEG (1998a) Molecular taphonomy of arthropod and plant cuticles from the carboniferous of North America: implications for the origin of kerogen. *J Geol Soc* 155:453–462
- Stankiewicz BA, Briggs DEG, Evershed RP, Miller RF, Bierstedt A (1998b) Chapter 12: Fate of chitin in quaternary and tertiary strata. In: van Bergen PF, Stankiewicz BA (eds) Fate of nitrogen containing molecules in the bio- and geosphere, ACS symposium series. Oxford University Press, New York, pp 212–224
- Stankiewicz BA, Briggs DEG, Michels R, Collinson ME, Evershed RP (2000) Alternative origin of aliphatic polymer in kerogen. *Geology* 28:559–562
- Tegelaar EW, de Leeuw JW, Derenne S, Largeau C (1989a) A reappraisal of Kerogen formation. *Geochim Cosmochim Acta* 53:3103–3106
- Tegelaar EW, de Leeuw JW, Holloway PJ (1989b) Some mechanisms of flash pyrolysis of naturally occurring higher plant polyesters. *J Anal Appl Pyrolysis* 15:289–295
- Tegelaar EW, Kerp H, Visscher H, Schenk PA, de Leeuw JW (1991) Bias of the paleobotanical record as a consequence of variations in the chemical composition of higher vascular plant cuticles. *Paleobiology* 17:133–144
- Tegelaar EW, Hollman G, van der Vegt P, de Leeuw JW, Holloway PJ (1995) Chemical characterization of the periderm tissue of some angiosperm species: recognition of an insoluble, non-hydrolyzable, aliphatic biomacromolecule (Suberan). *Org Geochem* 23(1995):239–251
- Tissot B, Welte DH (1984) Petroleum formation and occurrence, 2nd edn. Springer, Berlin-Heidelberg
- van Bergen PF (1999) Pyrolysis and chemolysis of fossil plant remains: applications to palaeobotany. In: Jones TP, Rowe NP (eds) Fossil plants and spores: modern techniques. Geological Society, London, pp 143–148
- van Bergen PF, Scott AC, Barrie PJ, de Leeuw JW, Collinson ME (1994) The chemical composition of Upper Carboniferous pteridosperm cuticles. *Org Geochem* 21:107–112
- van Bergen PF, Collinson ME, Briggs DEG, de Leeuw JW, Scott AC, Evershed RP, Finch P (1995) Resistant biomacromolecules in the fossil record. *Acta Bot Neerl* 44:319–342
- van Bergen PF, Flannery MB, Poulton PR, Evershed RP (1998) Organic geochemical studies from Rothamstead experimental station: III nitrogen-containing organic matter in soil from Geescroft Wilderness. In: Stankiewicz BA, van Bergen PF (eds) Nitrogen-containing macromolecules in the bio- and geosphere, vol 707, ACS symposium series. Oxford University Press, New York
- Walton TJ (1990) Waxes, cutin and suberin. In: Dey PM, Harborne J (eds) Methods in plant biochemistry, lipids, membranes and aspects of photobiology, vol 4. Academic, London, pp 105–159

Chapter 4

Migration of Organic Molecules from Sediment to Fossils

Abstract The 25 mya lacustrine deposit of Enspel, Germany, is important for molecular taphonomy as weevils from this site have yielded the oldest preserved traces of chitin. These weevil cuticles show excellent morphological and ultrastructural preservation. Plant cuticle is also preserved but it is obscured or distorted by diatom impressions. Molecular analysis of dicotyledonous angiosperm leaf from the Enspel deposit revealed the presence of polysaccharide, guaiacyl and syringyl related lignin, and possibly degraded protein moieties in the insoluble macromolecular component. Analysis of fossil conifer leaf showed the same moieties, but syringyl related lignin units were absent. Py-GC/MS revealed C_{9–33} *n*-alkyl components from both types of leaf, with C_{13,14,29} homologues being the most abundant *n*-alkanes. TMAH pyrolysis yielded a fatty acid distribution ranging in carbon number from C_{6–30}, with the C_{16,18,14} components being the most abundant. Analysis of fossil weevil cuticle also revealed the presence of an aliphatic polymer as evidenced by C_{9–33}*n*-alkyl components in the pyrolysate and C_{6–26} FAMES (predominantly even-numbered C_{14–18} components) in the TMAH pyrolysate. Pyrolysates of the sediments contain alkanes with distributions similar to those observed in the fossils; however, TMAH pyrolysates of sediments were distinct from those of the fossils with C_{20–22} components being the most abundant in the conifer-bearing sediment and the even-numbered C_{22–26} components dominating in the weevil-bearing sediment. Thus, the aliphatic polymers in the fossils and sediment are different, apparently comprised of moieties of different chain length. This suggests that the aliphatic polymer in the plant and insect fossils is not derived from migration from the organic-rich host sediment.

Keywords TMAH pyrolysis • Oligocene • Chitin • Aliphatic • Diagenesis • Molecular preservation

Introduction

Weevils from the Oligocene Fossil-Lagerstätte of Enspel preserve the oldest recorded detectable chitin moieties (Stankiewicz et al. 1997a). However, the molecular preservation of associated plants has not been studied. We analysed samples of two major groups of plants (angiosperms and conifers) and applied the same procedures to samples of weevils, using a combination of chemical and microscopical analyses to determine the quality of molecular and morphological preservation.

It has been shown that the Enspel weevils have an aliphatic component (Stankiewicz et al. 1997a) in addition to chitin. Such a chemistry is typical of pre-Tertiary plant and insect fossils, which generally exhibit poor molecular preservation (Briggs et al. 2000), and both are altered drastically to compositions that yield a pyrolysis trace similar to that of type I/II kerogen (see Briggs 1999 for review). Explanations for the widespread occurrence of recalcitrant aliphatics in insect and plant fossils and their enclosing sediment inevitably have included the migration of aliphatics from one to another. Replacement of the original composition by resistant aliphatics derived from plant or other macromolecules was suggested as a possible mechanism for long term preservation of insect fossils (Baas et al. 1995; van Bergen et al. 1995) and graptolites (Briggs et al. 1998). An investigation of co-occurring plant and insect fossils from the Upper Carboniferous of North America (Stankiewicz et al. 1998a) showed that the *n*-alkyl signatures found in the two categories differed indicating that they were not the product of incorporation of biopolymeric material from the sediment. Furthermore, the internal morphology of the cuticle was altered indicating diagenesis. Further evidence that diagenetic alteration rather than the introduction of components from elsewhere was the source of the *n*-alkyl component of the fossils was provided by the composition of cuticles encased in amber (Stankiewicz et al. 1998c), and the transformation of insect material to an aliphatic composition in maturation experiments (Stankiewicz et al. 2000).

A direct way to determine if migration of components is important is to analyse and compare the structure of the *n*-alkyl component in plant/insect fossils and in the associated sediment. With the application of on-line methylation techniques during pyrolysis, greater structural detail can be obtained (Challinor 1989, 1991a, b; deLeeuw and Baas 1993; Martin et al. 1994; Almendros et al. 1998, 1999), enhancing the characterisation of geopolymers that occur in close proximity. The aim of this paper is to understand the degree of molecular preservation of Oligocene plant and insect fossils and to test the hypothesis that the aliphatic composition of cuticles is not a product of the introduction of such components from the sediment or other sources.

Materials and Method

The Enspel lake deposit is located 35 km east of Koblenz at the village of Enspel in the Westerwald, Rhineland-Palatinate, Germany. During the last decade it has attracted numerous paleontological investigations. Mammal remains (Storch et al. 1996)

indicate that the site is 25.8 Mya, a result confirmed by studying the floral assemblage (Köhler 1997). Well preserved fossil insects, fishes, mammals and amphibians have been discovered together with land- derived plants and fruits (Lüniger and Schwark 2002). The oil shale was deposited in a complex maar-like structure in a tectonic graben (Lehmann 1930; Pirrung 1998). A basaltic flow from a nearby volcano terminated the lake sequence by filling the lake basin and preserving the sediments (Schreiber 1995). We have chosen the Enspel Lagerstätte as a study site because of the exceptional molecular preservation of the fossils. The insect cuticles have a partially aliphatic composition (Stankiewicz et al. 1997a), and the high organic matter content would favor contamination of fossil molecular signatures by sediment-derived ones if such a migration occurred.

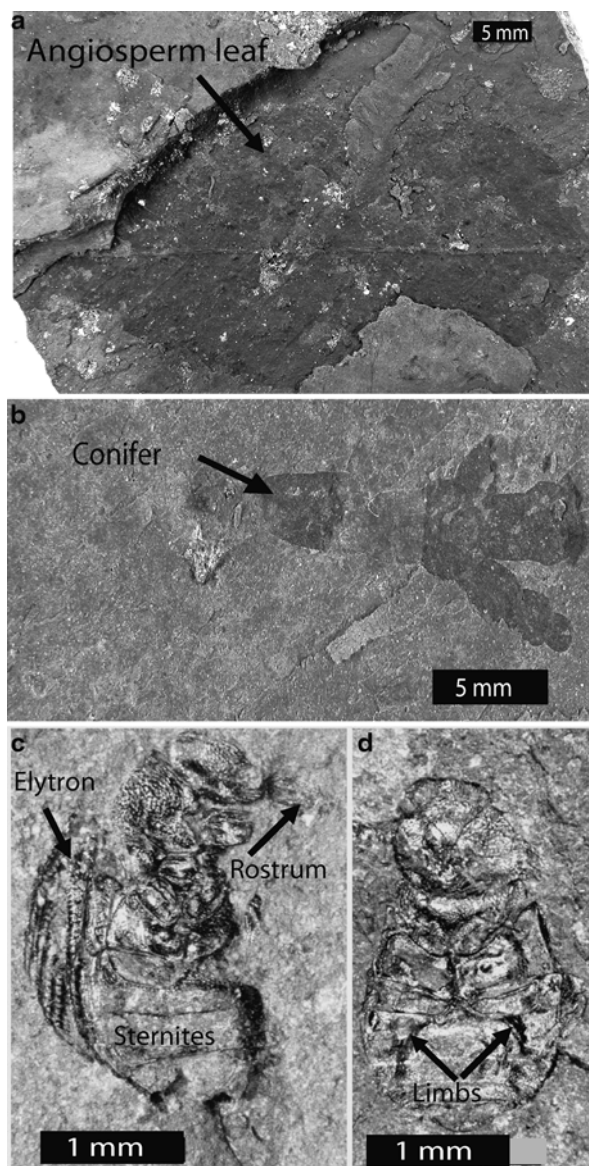
Three fossil samples were analysed: one dicotyledon (angiosperm, Fig. 4.1a), one conifer (gymnosperm, Fig. 4.1b) and one weevil (Fig. 4.1c, d) from Enspel levels 8, 12 and 6 respectively. The dicotyledon leaf was used only to provide data on molecular preservation and not for comparison with the enclosing sediment. The fossil samples were released from the sediment mechanically using a scalpel under a light microscope and any adhering sediment particle was carefully brushed away. After this the samples were agitated in deionised water to facilitate density separation of the fossil and any residual sediment. Reagents were not applied during the cleaning process to avoid chemical alteration. About 5 g of sediment were ground to generate a homogeneous sample.

Portions of the posterior extremity of the abdomen of the weevil (Fig. 4.1c) were removed for electron microscopy prior to fragmentation of the remaining material for chemical analysis. This enabled comparison to be made with similar samples from a modern weevil. In the plants the specimens were fragmented and extracted, and fragments were subsequently retrieved for microscopy. All sub-samples for electron microscopy were cleaned in hydrochloric and hydrofluoric acids to remove mineral matter which would obscure the surfaces and prevent sectioning for microscopic analyses.

For chemical analysis the fossils, and the separated associated matrices, were transferred to glass vials and extracted ultrasonically with 2:1 dichloromethane/methanol for 1 h. Each extracted residue was divided into two fractions for further analysis.

Transmission (TEM) and scanning (SEM) electron microscopy were used to determine the quality of morphological preservation. Pieces of fossils were taken from the same samples as those used for chemical analysis and were demineralised (see above) prior to EM study. In order to maximise the availability of material for chemical analyses, especially from the tiny weevils (Fig. 4.1c), only very small portions of each fossil were studied. Details of methods are given in Collinson et al. (1998) and Stankiewicz et al. (1998a) and references therein. Interpretations of structure and organisation were informed by comparison with results previously obtained for other modern and fossil leaves (Collinson et al. 1998; Gupta et al. 2007) and arthropods (Stankiewicz et al. 1998a, b, c, 2000; Collinson and Briggs unpublished).

Fig. 4.1 Fossils from the Oligocene Enspele Formation, Germany. (a) Dicotyledon leaf, (b) conifer, (c, d) weevils showing strong sclerotization of the cuticle. (c) Specimen in oblique ventral view showing the characteristic rostrum, the right elytron overlying the body, and the abdominal sternites. The posterior extremity of the abdomen was removed for microscopy and the remaining specimen was used for the chemical analyses. (d) Specimen in ventral view showing thoracic limbs



Analytical Protocol

The first fraction of the extracted residue was analysed by normal flash pyrolysis (Py-GC-MS). This involves the thermal fragmentation of the chemical constituents of a sample at high temperatures in an inert medium. These fragments are then separated and identified by GC-MS (Collinson et al. 2000; Kralert et al. 1995;

Nguyen and Harvey 1998; Riou 1995; Schaefer et al. 1987; Tegelaar et al. 1989a, b). Thus, flash pyrolysis reveals bulk macromolecular information and it has been used extensively in molecular characterisation of both modern and fossil plant material (see van Bergen 1999 for review) and insects (Stankiewicz et al. 1997a, 1998a, b). The instrument parameters used in analyses here are listed in Gupta and Pancost (2004). Compounds were identified using spectra reported in the literature (Ralph and Hatfield 1991; Stankiewicz et al. 1997a, b, 1998a, b, 2000; Mösle et al. 1997, 1998; Bland et al. 1998; Gupta and Pancost 2004).

The second fraction of the extracted residue was prepared for thermochemolysis, i.e. TMAH (tetramethylammonium hydroxide) assisted pyrolysis. This aliquot was transferred to a fresh vial and 1 ml TMAH solution was added. The sample was soaked in TMAH solution for 3–4 h prior to analysis to ensure that sufficient TMAH was available during on-line pyrolysis. TMAH-assisted pyrolysis helps to cleave ester domains (McKinney et al. 1996; Almendros et al. 1998, 1999) releasing the constituent acyl moieties in the macromolecule as fatty acid methyl esters (FAME). Instrumental parameters used were identical to those stated for normal pyrolysis.

Analytical Results

Ultrastructural Preservation of Fossils

Only parts of the dicotyledon (dicot) leaf could be seen on the hand specimen (Fig. 4.1a). The apex, base and most of the margin are missing or obscured. A main vein is evident as a topographic high but venation detail is not evident. The fossil conifer specimen is a portion of a branching leafy shoot with attached tiny scale-like leaves (Fig. 4.1b). This fossil thus includes tiny leaves and the stem within. In the case of the broader parts of the specimen the stem may already have been woody if secondary growth had occurred. SEM observation of fractured edges of the cleaned specimens confirms the preservation of a considerable thickness of organic material and reveals probable cellular organisation (Fig. 4.2a).

The plant surfaces are obscured almost entirely by impressions of diatoms (Fig. 4.2a–h). The diatoms are arranged randomly (Fig. 4.2b–d, g, h) and have been deeply impressed into the plant tissues (Fig. 4.2c–d, h). The outlines are those of pennate diatoms in which the raphe (axial groove) and also moulds of the rows of pores aligned normal to the raphe (striae) are clearly evident (Fig. 4.2d, h). The small areas between diatoms, and the nature of the impressions (Fig. 4.2c–d, h), suggests that they were pressed into an originally continuous outer layer, consistent with an original cuticle-covered leaf surface. However, the surface has been modified so strongly that it is not possible to confirm the presence or absence of cuticle from the SEM observations.

In a small area of one surface of the dicotyledon leaf rows of cell outlines are evident, looking rather like rows of bricks in a wall (Fig. 4.2e, f). These probably represent the outer periclinal (parallel to surface) walls of the epidermal cells. Their

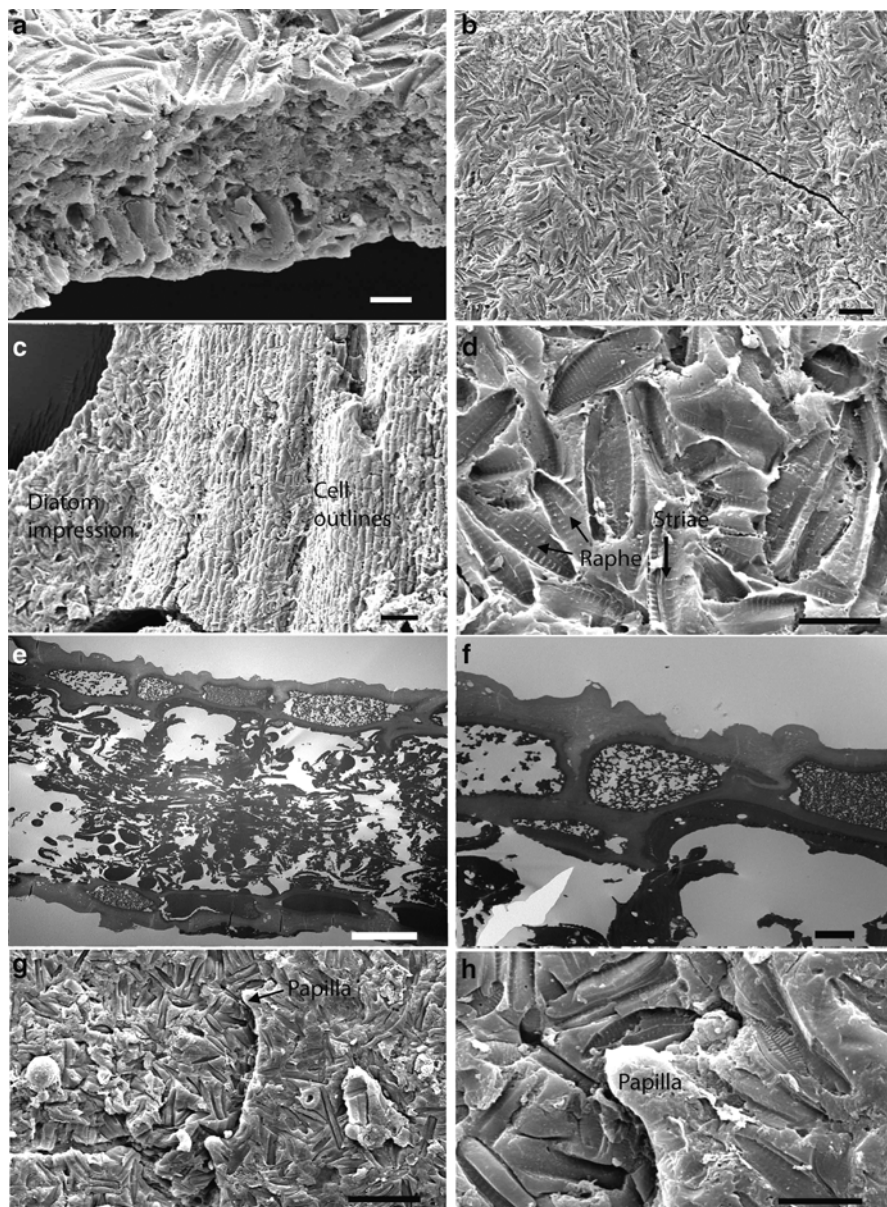


Fig. 4.2 Scanning and transmission electron microscopy of fossil plants from Enspel. **(a–d)** Dicotyledon leaf, **(e–i)** conifer leaf. **(a)** Fractured edge showing thickness of organic matter and possible internal cellular organisation. **(b)** Surface covered in diatom impressions. **(c)** Diatom impressions and probable epidermal cell outlines where diatoms are absent. **(d)** Details of diatom impressions showing their complex, sometimes overlapping arrangement. **(e)** Entire cross-section of fossil conifer showing epidermis and epidermal cells on both surfaces and remnant internal organisation. **(f, g)** Details of the epidermis with cuticle. The cuticle is the thick, outer, more electron lucent (i.e., paler) layer showing details of microlaminated cuticle ultrastructure in **(g)**. **(h, i)** Leaf margin papillae and conifer surface obscured by diatoms. Scale bars: 10 μm in **(a)**, **(d)**, **(e)**, **(i)**; 30 μm in **(b)**, **(c)**, **(h)**; 2 μm in **(f)** and 500 nm in **(g)**

arrangement in rows shows that this area overlies a vein in the leaf. Notably the surface of the adjacent leaf lamina (left of figure) is obscured totally by diatom impressions. Perhaps the vein tissue (which would include thick-walled cells) offered greater resistance or provided a topographic high on which few diatoms came to rest. In places there is a thin film overlying the cell pattern which may be remnants of the cuticle but no diagnostic details are evident.

The only part of the surface of the conifer that shows any original morphology is the slightly curved margin of one of the scale-like leaves that partially enveloped the stem. Two papillae are evident which are clearly original surface features but the surface is too modified (Fig. 4.2g, h) to reveal the original cuticle.

The gross morphology of the weevils is well-preserved. The sclerotized cuticle shows surface sculpture and the characteristic rostrum, elytra, abdominal sternites and thoracic limbs are evident (Fig. 4.1c). Under SEM the outer cuticle surface retains morphological characteristics of modern weevils (Fig. 4.3a) whilst the broken inner surface reveals the microfibrillar organisation typical of modern arthropod cuticle (Fig. 4.3b). Some portions of the weevils show diatom impressions (see plants above) but they do not obscure the entire surface.

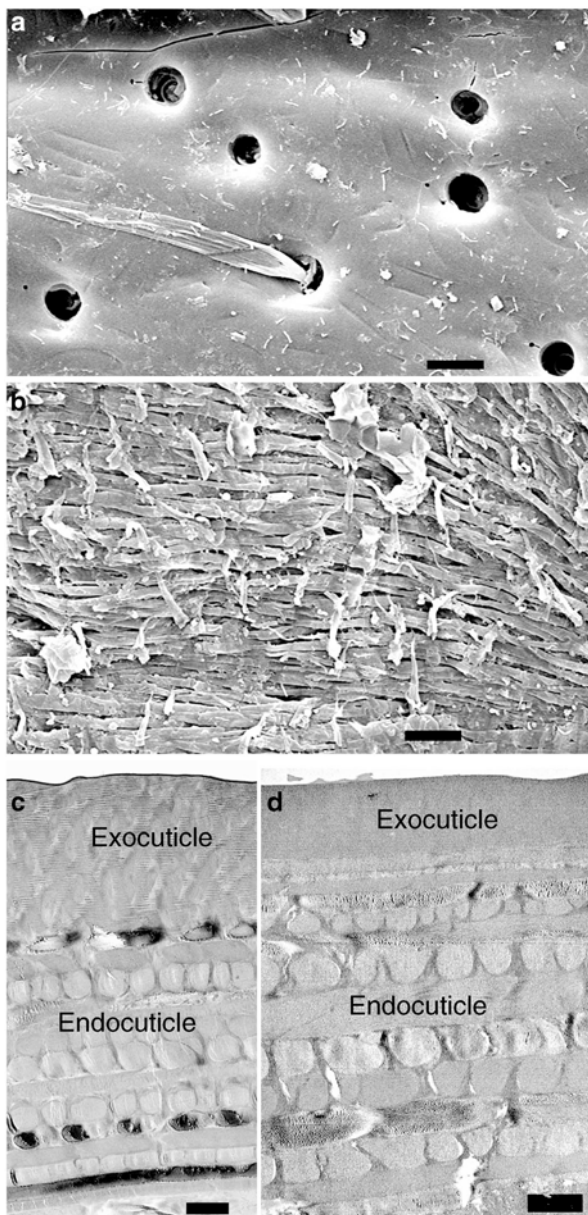
TEM sections show that the fossil weevil cuticle is composed of an outer exocuticle and a thick, inner, multilayered endocuticle (Fig. 4.3d). This organisation is the same as that in a modern weevil (Fig. 4.3c). The preservation of the multilayered endocuticle in the Enspel weevils is unusual. Where the cuticle of fossil scorpions, for example, has been investigated, none have been shown to preserve the endocuticle (Stankiewicz et al. 1998a, 2000).

Molecular Preservation of Fossils and Associated Sediment

The fossil dicot leaf yielded *n*-alkane/*n*-alk-1-ene homologues from chain length C₈ to C₂₈ (Fig. 4.4a; lower-molecular-weight homologues are not apparent in the chromatogram) indicating that it consists partly of an aliphatic macropolymer typical of fossil leaf compressions (Nip et al. 1986; Tegelaar et al. 1991; Logan et al. 1993; van Bergen et al. 1994; Möhle et al. 1997, 1998; Collinson et al. 1998; Stankiewicz et al. 1998a; Gupta et al. 2007). No fatty acyl moieties were detected. Figure 4.4a reveals the presence of guaiacyl lignin markers and the *m/z* 154+168+180+182+194+196 mass chromatogram reveals the presence of syringyl-related units. Phenol and its mono and dialkyl derivatives are present and probably products of biodegraded lignin (van Bergen et al. 1995; Stankiewicz et al. 1997c; Almendros et al. 1999). The isoprenoids prist-1-ene and prist-2-ene are likely derived from tocopherols (Goosens et al. 1984; Logan et al. 1993; Hold et al. 2001). The polysaccharide pyrolysis products detected include 2-methyl-2-cyclopenten-2-one and 2,3-dimethyl cyclopenten-1-one. Methyl indole (*m/z* 130+131) may be derived from aromatic amino acids (e.g., tryptophan) which in turn may indicate the presence of degraded protein products (Stankiewicz et al. 1997a). Benzene and its alkyl derivatives (*m/z* 78+ 91+92+105+106+119+120; Hartgers et al. 1992), together with naphthalene, were also detected.

The fossil conifer leaf (Fig. 4.4b) pyrolysate contains *n*-alkane and *n*-alkene components (Table 4.1) ranging from C₉ to C₃₃. No fatty acyl subunits were detected.

Fig. 4.3 Electron microscopy of cuticles of fossil weevils from Enspel and a modern weevil *Sitophilus zeamais* for comparison. (a, b) SEM, (c, d) TEM. (a, b, d) Fossil weevil; (c) modern weevil; (a) shows outer surface of cuticle and (b) broken inner surface of cuticle. (c, d) shows outer exocuticle and inner multilayered endocuticle; in (c) the exocuticle is thicker and it has also been slightly distorted during sectioning giving an undulating appearance. Scale bars: 10 μm in (a) and (b), 1 μm in (c) and (d)



Lignin preservation is in the form of guaiacyl units but no syringyl-related lignin units were detected. Polysaccharide moieties detected include 2-methyl-2-cyclopenten-2-one, 2,3-dimethyl cyclopenten-1-one and an unknown pyrolysis product characterised by m/z 68,79,93 fragment ions that is very likely derived from polysaccharide (Bland et al. 1998). Methyl indole, benzene and its alkyl derivatives (C_2 to C_4), naphthalene and pristenes were also present in the pyrolysate.

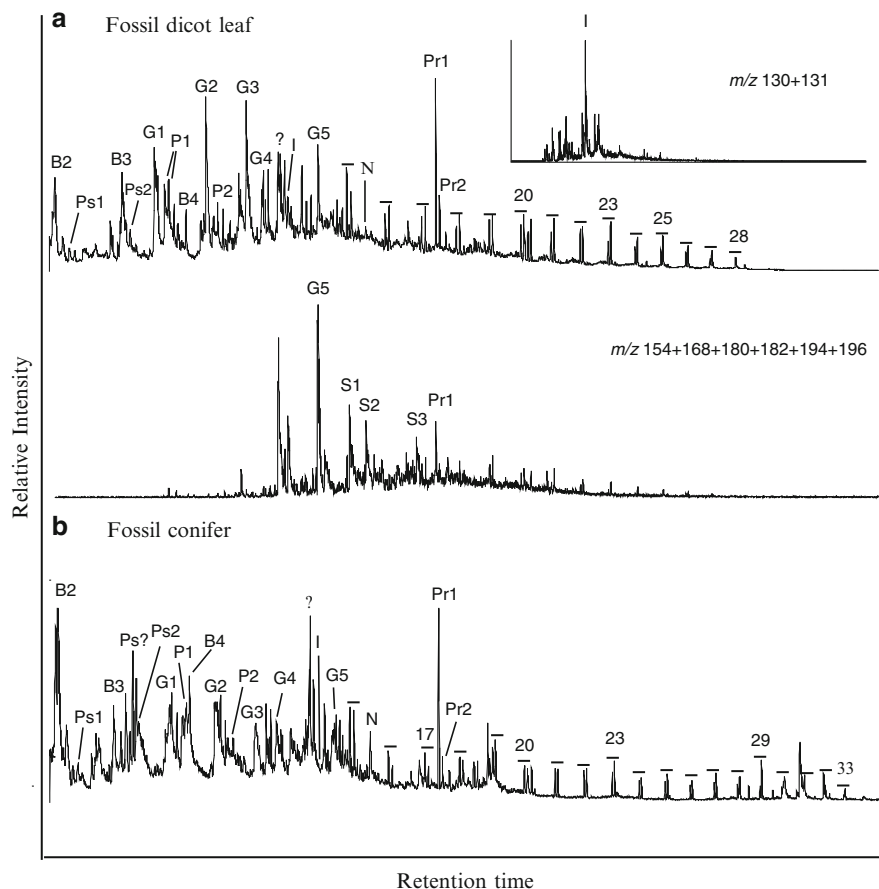


Fig. 4.4 (a) Partial py-GC-MS total ion current chromatogram of fossil dicotyledon leaf indicating the presence of moieties related to benzene derivatives, polysaccharides, phenols, lignin and protein together with n-alkane/n-alk-1-ene homologues, number indicating the carbon chain length. m/z 130+131 reveals the presence of methyl indole. m/z 154+168+180+182+194+196 reveals the distribution of syringyl moieties. (b) Partial py-GC-MS total ion current chromatogram of fossil conifer, showing released moieties related to benzene derivatives, polysaccharides, phenols, lignin and protein, together with n-alkane/n-alk-1-ene homologues. *B2*: dimethylbenzene, *B3*: trimethylbenzene, *B4*: tetramethylbenzene, *N*: naphthalene. Guaiacyl related units. *G1*: 2-methoxyphenol, *G2*: 4-methyl-2-methoxyphenol, *G3*: 4-ethyl-2-methoxyphenol, *G4*: 4-ethenyl-2-methoxyphenol, *G5*: 3-allyl-6-methoxyphenol. Syringyl related units. *S1*: 4-ethyl-2,6-dimethoxyphenol, *S2*: 2,6-dimethoxy-4-vinylphenol, *S3*: 4-allyl-2,6-dimethoxyphenol. *Pr1*: Prist-1-ene. *P1*: methylphenol, *P2*: dimethylphenol. Polysaccharide pyrolysis products: *Ps1*: 2-methyl-2-cyclopenten-2-one, *Ps2*: 2,3-dimethyl cyclopenten-1-one, *Ps??*: unknown moiety

TMAH assisted pyrolysis was conducted on the fossil conifer to characterise further the fossil composition and determine the lipid distribution. The thermochemolysis trace (Fig. 4.5) reveals methylated equivalents of the lignin moieties, aromatics (see Hatcher and Clifford 1994; Hatcher et al. 1995; Clifford et al. 1995; Almendros

Table 4.1 Distribution of pyrolysis and thermochemolysis products between fossil and sediment

Sample	Pyrolysis			Thermochemolysis	
	Alkane/alk-1-ene	Alkanes ^a	Alk-1-enes ^a	FAMES	FAME ^a
Fossil conifer	9–33	13,14,29,15	15,14,13,12	6–30	16,18,14,15
Matrix/ Fossil conifer	9–31	23,21,22,18	13,15,14,11	6–28	22,21,16,20
Fossil weevil	9–33	13,15,21,19	15,13,16,14	6–26	16,14,18,8
Matrix/Fossil Weevil	9–30	15,21,23,16	16,21,22,17	6–28	24,26,22,23

^aMost abundant peaks in descending order

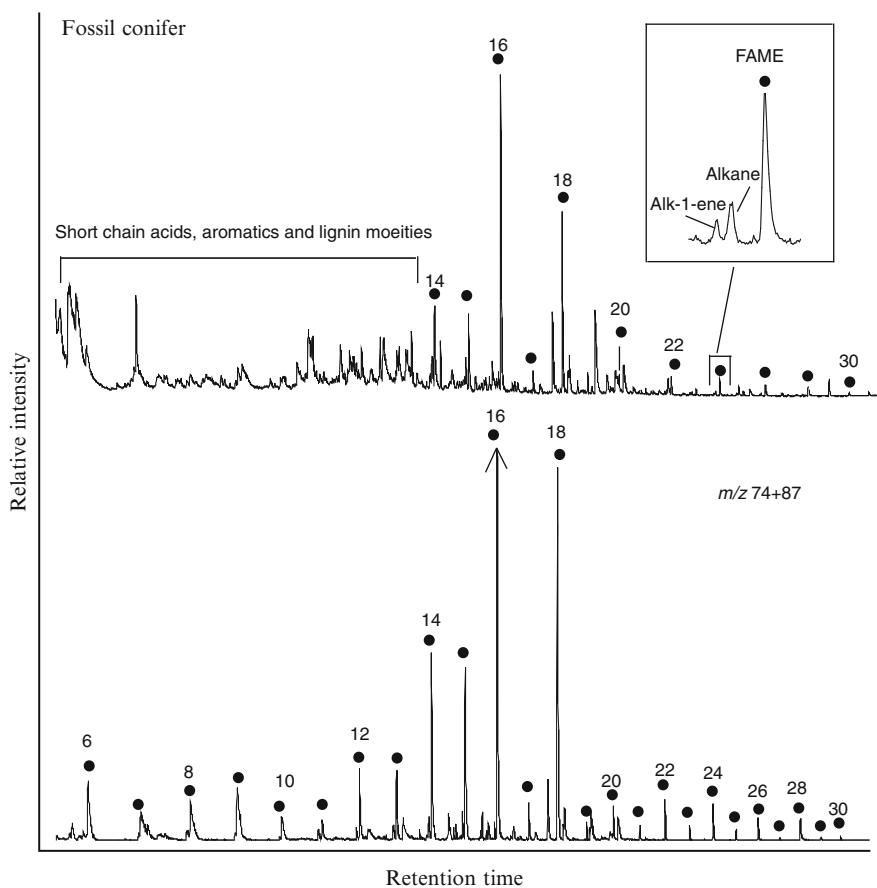


Fig. 4.5 Partial TMAH/Py-GC-MS total ion current chromatogram of fossil conifer showing generated fatty acid methyl esters (FAME), lignin moieties and aromatics. The m/z 74 + 87 mass chromatogram shows the distribution of fatty acid methyl esters, FAME (d), from C6 to C30. C16 is the most abundant followed by C18 and C14. The inset shows that n-alkane/n-alk-1-ene homologues are subordinate in abundance relative to the FAME

et al. 1998, 1999) and FAME ranging from C₆ to C₃₀ (Table 4.1). Most abundant is the C₁₆ FAME followed by the C₁₈ and C₁₄ homologues. The FAME from C₁₂ to C₃₀ show an even over odd predominance. The alkane/alk-1-ene homologues are subordinate in abundance relative to the FAME with an equivalent *n*-alkyl chain. The FAME distribution is very similar to that in the leaves from the Miocene of Ardèche (Gupta et al. 2007) where the sediment is siliceous and TOC contents are ca 1.5, over an order of magnitude lower than those of Enspel. These fatty acyl moieties likely derive from constituent acids in cutin (Kolattukudy 1980), internal lipids (e.g. phospholipid fatty acids) or a combination of both (Gupta et al. 2007). The longer chain acids may be derived from free fatty acids (Gupta et al. 2007).

The total organic content of the sediment associated with the conifer is high (10.6). The most abundant components of the pyrolysates (Fig. 4.6a) are the C₂, C₃ and C₄ alkyl benzenes followed by pristenes. C₁ and C₂ alkyl phenols were detected, very likely derived from biodegraded lignin, along with two unknown compounds with fragment ions *m/z* 131,146 (eluting after C₂ phenol) and *m/z* 173,188 (eluting before naphthalene). No polysaccharide, lignin and protein moieties (as observed in the fossils) were detected in the sediment, consistent with previous results from the same site (Stankiewicz et al. 1997a). Py-GC-MS (Fig. 4.6a) also reveals the presence of *n*-alkane/*n*-alk-1-ene homologues ranging in carbon chain length from C₉ to C₃₃. The most abundant *n*-alkanes have chain lengths *n*-C₂₃, *n*-C₂₁ and *n*-C₂₂, and the most abundant *n*-alk-1-enes are the C₁₃, C₁₅ and C₁₄ homologues (Table 4.1). Thermochemolysis of the sediment (Fig. 4.6b) also shows an abundance of benzene derivatives and pristenes. The fatty acid methylesters released during thermochemolysis range in carbon chain length from C₆ to C₂₈. The most abundant FAME peak is C₂₂ followed by C₂₁, C₁₆ and C₂₀. The FAME in the pyrolysate from C₁₀ to C₂₈ show an even over odd predominance. The *n*-alkane, *n*-alk-1-ene homologues are clearly discernible even in TMAH pyrolysis conditions. These range in carbon number from C₉ to C₃₀. The most abundant *n*-alkanes are C₂₃, C₂₁ and C₂₂ and the most abundant *n*-alk-1-enes are C₂₂, C₁₃ and C₂₁ with relative abundance comparable to the adjoining FAME (except alkane/alk-1-ene homologue C₂₅ which is less abundant compared to FAME *n*-C₂₂).

The pyrolysis trace of the fossil weevil (Fig. 4.7a) reveals a high level of molecular preservation as indicated by the survival of chitin moieties. Preservation of proteinaceous organic matter is indicated by the presence of C₁-pyrrole (derived from tetrapyrroles and possibly the amino acids proline/hydroxyproline) and methyl indole, together with phenol, alkyl phenol and dialkyl phenol (all from tyrosine), and alkyl benzenes derived from phenylalanine. Additionally, the pyrolysate is dominated by *n*-alkane/*n*-alk-1-ene homologues ranging from C₉ to C₃₃ (Table 4.1) as normally encountered in Pre-Tertiary insects (Briggs et al. 2000). The most abundant *n*-alkanes are C₁₃, C₁₅ and C₂₁ and the most abundant *n*-alkenes are C₁₅, C₁₃ and C₂₂. Pyrolysates of weevils from other horizons in the quarry also showed the presence of chitin and protein moieties (abundance in that order; Stankiewicz et al. 1997a).

As with the fossil conifer, TMAH pyrolysis was conducted on the weevil to release fatty acyl moieties. Thermochemolysis (Fig. 4.7b) revealed the presence of *n*-alkane/alkene homologues from C₉ to C₂₉ with both the alkanes and alkenes

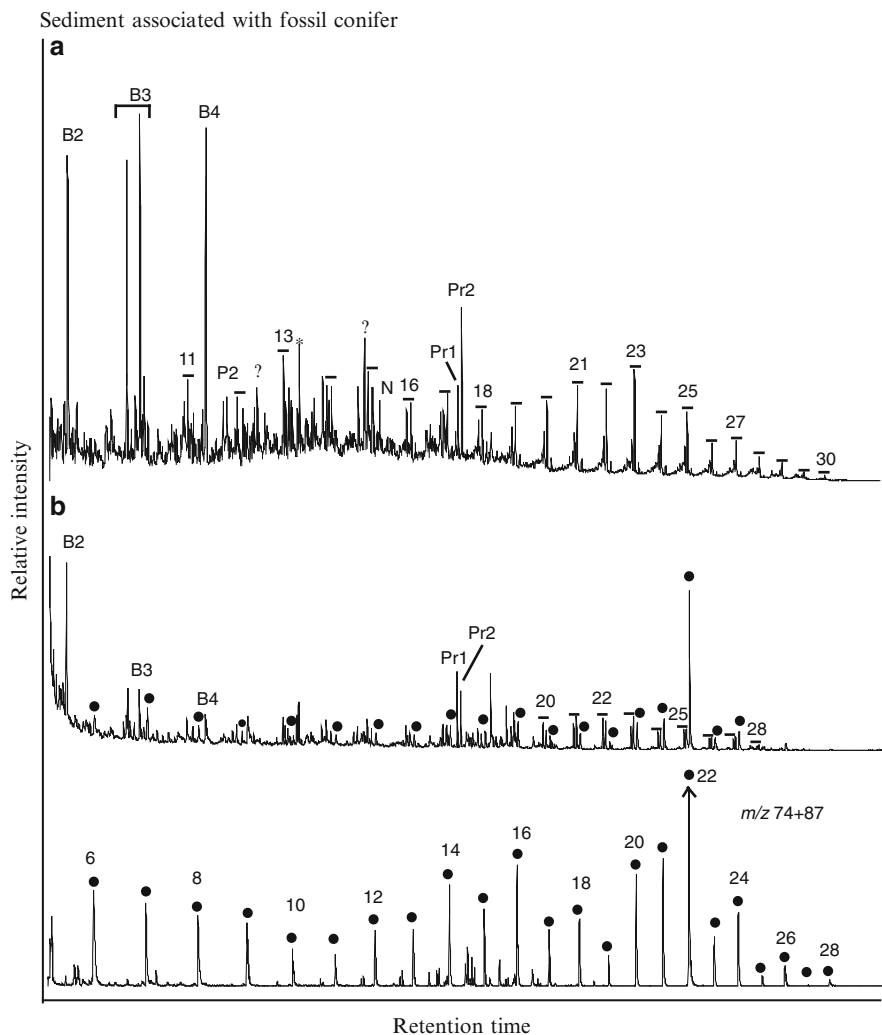


Fig. 4.6 (a) Partial Py-GC-MS total ion current chromatogram of sediment associated with fossil conifer. (b) Partial TMAH/Py-GC-MS total ion current chromatogram of sediment associated with fossil conifer showing the presence of n-alkane/n-alkene homologues, benzene derivatives and pristenes. The m/z 74+87 mass chromatogram reveals the distribution of fatty acid methyl esters, FAME (d); C22 followed by C19 are the most abundant (cf. Fig. 4.5, thermochemolysis of fossil conifer, where the acid distributions are different). Peak labels are the same as in Fig. 4.2. *Contaminant

maximising at C_{13,15} and C₂₃ largely consistent with the py-GC-MS results. FAME ranging from C₆ to C₂₆ and dominated by C₁₆ were the most abundant, followed by C₁₄, C₁₈ and C₈ homologues (Table 4.1). Long-chain acids from C₁₇ to C₂₆ (except for C₁₈ and C₂₂) are the least abundant. Except for C₁₆ FAME, the acids are less abundant than the corresponding alkane/alkene peaks.

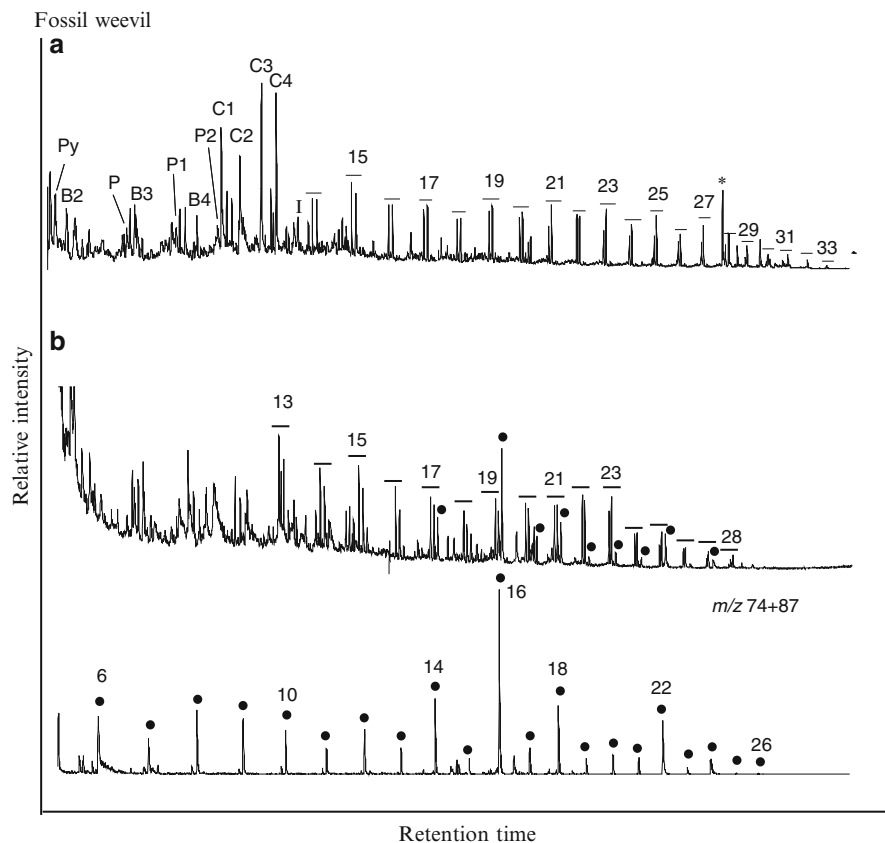


Fig. 4.7 (a) Partial py-GC-MS total ion current chromatogram of fossil weevil showing the presence of *n*-alkane, *n*-alk-1-ene homologues, number indicating the carbon chain length, together with benzene derivatives (peak labels same as in Fig. 4.4). Chitin markers. *C1*: acetylpyridone, *C2*: 3-acetamidofuran, *C3*: 3-acetamido-5-methylfuran, *C4*: 3-acetamido-4-pyone. *I*: methyl indole, *Py*: C1-pyrrole. *Contaminant. (b) Partial TMAH/Py-GC-MS total ion current chromatogram of fossil weevil. *n*-alkane, *n*-alk-1-ene homologues, number indicating the carbon chain length. The m/z 74+87 mass chromatogram reveals the distribution of constituent fatty acid methyl esters, FAME (d); C16 followed by C14 are the most abundant (cf. Fig. 4.8, thermochemolysis of associated sediment, where the acid distributions are different)

The total organic content of the sediment associated with the weevil is exceptionally high (23.6). Pyrolysis (Fig. 4.8a) released *n*-alkane/*n*-alk-1-ene homologues ranging in carbon number from C₉ to C₃₀. The most abundant *n*-alkanes have carbon chain lengths of C₁₅, C₂₁ and C₁₃ (Table 4.1) and the most abundant *n*-alk-1-enes have carbon chain lengths of C₁₆, C₂₁ and C₂₂. Alkyl benzenes from C₂ to C₄ are also abundant in the pyrolysate but no polysaccharide, protein or lignin moieties were released by pyrolysis, consistent with previous results from the same site (Stankiewicz et al. 1997a). Thermochemolysis of the sediment (Fig. 4.8b) generated FAME ranging in carbon number from C₆ to C₂₈. The long-chain FAME,

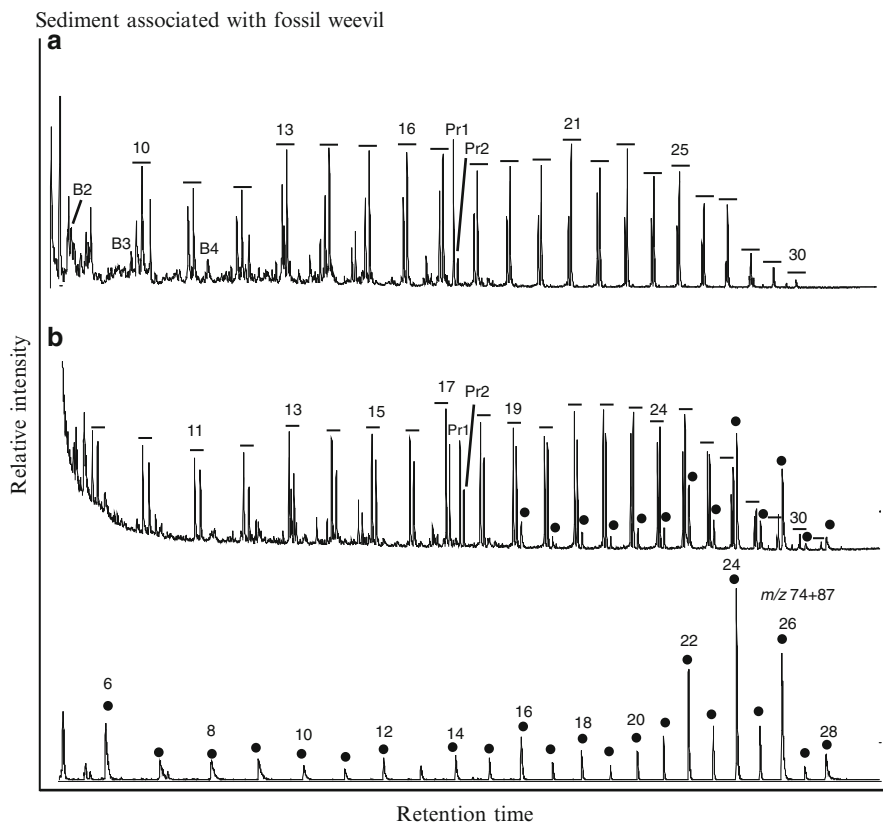


Fig. 4.8 (a) Partial py-GC-MS total ion current chromatogram of sediment associated with fossil weevil. Peak labels are the same as in Fig. 4.4. (b) Partial TMAH/Py-GC-MS total ion current chromatogram of sediment associated with fossil weevil. Peak labels are the same as in Fig. 4.4. The m/z 74+87 mass chromatogram reveals the distribution of fatty acid methyl esters, FAME (•); the C_{24} and C_{26} components are the most abundant (cf. Fig. 4.7 thermochemolysis of fossil weevil where the acid distributions are different)

C_{22} , C_{24} and C_{26} , are the most abundant, and the C_{14} to C_{28} FAME are characterized by an even-over-odd predominance. In the TMAH pyrolysates, the *n*-alkane/*n*-alk-1-ene homologues range from C_9 to C_{30} and are more abundant than adjoining FAME (except the C_{27} and C_{29} -alkane/ *n*-alkene homologues).

Structural and Molecular Preservation

The plant gross morphology is not exceptional for compression fossils, and the plants are incomplete. The plant surfaces are largely obscured by diatom impressions, which also occur on some of the weevils from the site. The diatoms are

pennateraphid and were clearly important in the original depositional environment. Where plant surfaces are evident, epidermal cell wall outlines are preserved and possible cuticle remnants are also present. Cellular organisation is suggested in fractures through specimens. This ultrastructural preservation is inferior to that of leaves from the Miocene of *Clarkia* (Niklas and Brown 1981; Collinson and Rember, unpublished). TEM observation confirms the preservation of internal cellular organisation in plants, although this is somewhat disrupted and discontinuous. A thick cuticle is preserved on the conifer and a thin and partially fragmented cuticle is preserved on the dicotyledon leaf. In contrast, the gross morphology of the fossil weevil is well-preserved; the cuticle is very similar to that of its modern counterpart, and the sclerotized cuticular components are more or less complete. External sculptural details are preserved along with internal microfibrillar organisation. The fossil weevils are remarkable for the preservation of a multilayered endocuticle which is typically lost in arthropods during the early stages of decay.

The high level of molecular preservation for both plant and insect fossils is clearly indicated by the presence of polysaccharide, protein, chitin and lignin moieties, making the Enspel Formation amongst the oldest known sites for such occurrences. However, the polysaccharide and protein moieties may have been chemically altered during diagenesis and reflect the composition of melanoidin compounds. Polysaccharides have been detected in 20 Ka *Hymenea* subfossils (Stankiewicz et al. 1998c) and *Pinusleitzeii* (6 Mya; Stankiewicz et al. 1997c). Polysaccharide markers in the both of these fossils include furaldehyde, furan and pyran markers along with anhydrosugars. However, no polysaccharide-related moieties have been reported previously for older fossil leaves.

Similarly, this site contains the oldest known lignin associated with fossil leaves. The lignin moieties in the Enspel plants include those related to both guaiacyl and syringyl units. Preservation of lignin in 20 Ka *Hymenea* was reflected in both guaiacyl and syringyl moieties; however, such moieties were not detected in the same plant trapped in Dominican amber (25–30 Mya). Lignin markers in fossil 6 Mya *Pinusleitzeii* include the guaiacyl markers guaiacol, guaiacylmethane and vinylguaiacol, but syringyl moieties were not observed. Guaiacyl lignin markers along with C₃ methoxyphenols have also been reported in Miocene *Glyptostrobus* remains, and both guaiacyl and syringyl related markers have been detected in a range of fossil leaves in the 8 My old (upper Miocene) Ardèche diatomite (Gupta et al. 2007) and in *Quercus* and *Magnolia* fossils in the lower Miocene *Clarkia* deposit (Logan et al. 1993).

The preservation of proteinaceous organic matter in the plant is indicated by the presence of tryptophan, and this is possibly the oldest documentation of protein remnants in fossil leaves. The pyrolysis traces of the plants also contain benzene derivatives; in modern leaves these are indicative of phenylalanine (Gupta and Pancost 2004), but in the fossils they are likely products of diagenetic alteration and cannot be used to confirm the presence of proteins. However, these moieties have been used as protein markers in fossil insects (Stankiewicz et al. 1997a). Preservation of proteinaceous organic matter in the insect is indicated by moieties derived from the amino acids proline, hydroxyproline, tryptophan, tyrosine, and phenylalanine.

Although not previously found in ancient fossil leaves, protein moieties have been detected in kerogen samples 140 million years old (Mongenot et al. 2001), reflecting the potential for protein preservation. Encapsulation within a resistant sediment or macromolecule (Knicker et al. 2001; Mongenot et al. 2001; Riboulleau et al. 2001) could protect otherwise labile molecules (including proteins) enhancing their diagenetic survival; thus, it is possible that rapid formation of a resistant aliphatic geomacromolecule (Gupta et al. 2007) from cutin or lipids could facilitate protein preservation. Additionally, tissue type (Opsahl and Benner 1995) and depositional setting (Stankiewicz et al. 1997a; van Bergen et al. 1997, 1998) are important controls on molecular preservation.

Comparison Between Sediment and Fossil

The differences in the aliphatic component of fossil and associated sediment pyrolysates and TMAH-pyrolysates are highlighted in Table 4.1. Py-GC-MS of the fossil conifer generates *n*-alkane/*n*-alk-1-ene homologues ranging from C₉ to C₃₃ with a bimodal distribution of *n*-alkanes (maxima at C₁₃ and C₂₉) and a predominance of relatively short-chain *n*-alkenes. In some respects, pyrolysates of the enclosing sediment are similar, with *n*-alkane/*n*-alk-1-ene homologues ranging from C₉ to C₃₀ and a similar predominance of short-chain *n*-alkenes. However, the *n*-alkane distribution differs considerably, with a broad distribution of abundant *n*-alkanes and a maximum at C_{21–23}.

Thermochemolysis of the conifer generates abundant fatty acid methyl esters, presumably derived from macromolecular fatty acyl moieties, with a broad carbon number range and a clear predominance of even-carbon-number C_{14–18} components and lower abundances of *n*-alkane/*n*-alk-1-ene doublets. This distribution is similar to fossil leaves from the Ardèche diatomite, where the sediment is relatively organic-lean and much less likely to have been a source of fossil leaf organic matter (Gupta et al. 2007). The distribution differs from the TMAH pyrolysate of the associated sediment, which contains relatively higher abundances of *n*-alkane/*n*-alk-1-ene homologues and higher-molecular-weight FAME (>C₂₀). This suggests that the fossil conifer has a different aliphatic composition than the surrounding sediment, both with respect to the distribution of *n*-alkyl chain lengths and the chemical bonds that link the alkyl units together. In particular, it seems that ester linkages are relatively more important in the leaf, reflected by the high FAME to *n*-alkane ratios in the TMAH pyrolysate. Thus, at least part of the fossil leaf aliphatic material, and particularly the fatty acyl component, cannot derive from the associated sediments.

Pyrolysis of the fossil weevil releases *n*-alkanes/*n*-alkenes ranging in carbon number from C₉ to C₃₃. The most abundant *n*-alkanes are the C_{13,15,21} components and the most abundant *n*-alkenes are the C_{15,13, 22} components. This distribution is similar to that of *n*-alkanes and *n*-alkenes generated by pyrolysis of the sediment; *n*-alkyl components range in carbon number from C₉ to C₃₀, and the C_{15,21, 13} and C_{16, 21, 22} homologues are the most abundant *n*-alkanes and *n*-alkenes, respectively.

N-alkanes released by pyrolysis of both the weevil and the enclosing sediment are characterised by a broad distribution of homologues of comparable abundance.

However, thermochemolysis does reveal differences between the fossil and the enclosing sediment. Thermochemolysis of the fossil weevil generates *n*-alkane/*n*-alkene homologues ranging in carbon number from C₉ to C₂₉; both the *n*-alkanes and *n*-alkenes maximise at C_{13,15} and C₂₃. Unlike the plant material, FAME generated by thermochemolysis of the weevil are present in abundances slightly subordinate to those of *n*-alkanes and *n*-alkenes. However, the FAME range in carbon number from C₆ to C₂₆; even-carbon-number components, C_{14,16,18}, are the most abundant, as in the conifer. In contrast, the sediment pyrolysate is dominated by the *n*-alkane/*n*-alkene homologues and FAME with relatively high-molecular-weights and even carbon numbers (C_{22–28}). The similar distributions of *n*-alkanes and *n*-alkenes in the pyrolysate do not limit entirely the possibility that at least part of the aliphatic signal in the fossil weevil is sediment derived; however, as with the leaves, the fatty acyl component of the weevil, comprised of lower-molecular-weight fatty acyl components, does differ from that of the enclosing sediment.

It is possible that some of the described differences in pyrolysates and TMAH-pyrolysates reflect analytical artefacts rather than differences between the fossil and sediment geomacromolecules; such artefacts might be generated by variable analytical reproducibility and the influence of organic-mineral interactions during pyrolysis of sediments. The former is unlikely as comparable pyrolysates and TMAH-pyrolysates were obtained from multiple analyses. A mineral matrix-related effect is also unlikely because the aliphatic compositions of the weevil and plant fossils differ; if the sediment were the source of aliphatic macromolecular material in the fossils, the compositions of the fossils should be similar. Thus, it is unlikely that the sediment serves as the source for the aliphatic component of insoluble fossil organic matter. This is consistent with previous work (Logan et al. 1995), showing that even soluble organic components do not migrate from sediment into leaf fossils.

References

- Almendros G, González-Vila FJ, Martín F, Sanz J, Álvarez-Ramis C (1998) Appraisal of pyrolytic techniques on different forms of organic matter from a Cretaceous basement in Central Spain. *Org Geochem* 28:613–623
- Almendros G, José Dorado J, González-Vila FJ, Martín F, Sanz J, Álvarez-Ramis C, Stuchlik L (1999) Molecular characterization of fossil organic matter in *Glyptostrobuseuropaeus* remains from the Orawa basin (Poland). Comparison of pyrolytic techniques. *Fuel* 78:745–752
- Baas M, Briggs DEG, vanHeemst JDH, Kear AJ, de Leeuw JW (1995) Selective preservation of chitin during the decay of shrimp. *Geochim Cosmochim Acta* 59:945–951
- Bland HA, van Bergen PF, Carter JF, Evershed RP (1998) Early diagenetic transformations of proteins and polysaccharides in archaeological plant remains. In: Stankiewicz BA, van Bergen PF (eds) Nitrogen-containing macromolecules in the bio- and geosphere, vol 707, ACS symposium series
- Briggs DEG (1999) Molecular taphonomy of animal and plant cuticles: selective preservation and diagenesis. *Philos Trans R Soc Lond B Biol Sci* 354:7–16

- Briggs DEG, Stankiewicz BA, Evershed RP (1998) The molecular preservation of fossil arthropod cuticles. *Anc Biomol* 2:135–146
- Briggs DEG, Evershed RP, Lockheart MJ (2000) The biomolecular paleontology of continental fossils. *Palaeobiology* 26(Suppl to no. 4):169–193
- Challinor JM (1989) A pyrolysis-derivatization-gas chromatograph technique for the elucidation of some synthetic polymers. *J Anal Appl Pyrolysis* 16:323–333
- Challinor JM (1991a) Structure determination of alkyd resins by simultaneous pyrolysis methylation. *J Anal Appl Pyrolysis* 18:233–244
- Challinor JM (1991b) The scope of pyrolysis methylation reactions. *J Anal Appl Pyrolysis* 20:15–24
- Clifford DJ, Carson DM, McKinney DE, Bortiatynski JM, Hatcher PG (1995) A new rapid technique for the characterization of lignin in vascular plants: thermochemolysis with tetramethylammonium hydroxide (TMAH). *Org Geochem* 23:169–175
- Collinson ME, Möslle B, Finch P, Wilson R, Scott AC (1998) The preservation of plant cuticle in the fossil record: a chemical and microscopical investigation. *Anc Biomol* 2:251–265
- Collinson ME, Möslle B, Finch P, Wilson R, Scott AC (2000) Preservation of plant cuticles. *Acta Palaeobot* 2(Suppl):629–632
- deLeeuw JW, Baas J (1993) The behavior of esters in the presence of tetramethylammonium salts at elevated temperatures; flash pyrolysis or flash chemolysis? *J Anal Appl Pyrolysis* 26:175–184
- Goosens H, de Leeuw JW, Schenck PA, Brassell SC (1984) Tocopherols as likely precursors of pristane in ancient sediments and crude oils. *Nature* 312:440–442
- Gupta NS, Pancost RD (2004) Biomolecular and physical taphonomy of angiosperm leaf during early decay: implications for fossilisation. *Palaios* 19:428–440
- Gupta NS, Briggs DEG, Collinson ME, Evershed RP, Michels R, Jack KS, Pancost RP (2007) Evidence for the *in situ* polymerisation of labile aliphatic organic compounds during the preservation of fossil leaves: Implications for organic matter preservation. *Org Geochem* 38(3):499–522
- Hartgers WA, Sinninghe Damsté JS, de Leeuw JW (1992) Identification of C2–C4 alkylated benzenes in flash pyrolysates of kerogens, coals and asphaltenes. *J Chromatogr A* 606:211–220
- Hatcher PG, Clifford DJ (1994) Flash pyrolysis and *in situ* methylation of humic acids from soil. *Org Geochem* 21:1081–1092
- Hatcher PG, Nanny MA, Minard RD, Dible SD, Carson DM (1995) Comparison of two thermochemolytic methods for the analysis of lignin in decomposing wood: the CuO oxidation method and the method of thermochemolysis with tetramethylammonium hydroxide (TMAH). *Org Geochem* 23:881–888
- Hold IM, Schouten S, van der Gaast SJ, Sinninghe Damsté JS (2001) Origin of prist-1-ene and prist-2-ene in kerogenpyrolysates. *Chem Geol* 172:201–212
- Knicker H, del Rio JC, Hatcher PG, Minard RD (2001) Identification of protein remnants in insoluble geopolymers using TMAH thermochemolysis/ GC-MS. *Org Geochem* 32:397–409
- Köhler J (1997) Die Fossilagerstätte Enspel. Vegetation, Vegetationsdynamik und Klimaim Oberoligozän, PhD thesis, Eberhard-Karls-Universität Tübingen, 211 p
- Kolattukudy PE (1980) Biopolyester membranes of plants: cutin and suberin. *Science* 208:990–1000
- Kralert PG, Alexander R, Kagi RI (1995) An investigation of polar constituents in kerogen and coal using pyrolysis-gas chromatography-mass spectrometry with *in situ* methylation. *Org Geochem* 23:627–639
- Lehmann E (1930) Der Basalt vom Stöfchel (Westerwald) und seine essentialemisch-theralithischen Differenziate. *Chem Erde* 5:319–375
- Logan GA, Boon JJ, Eglinton G (1993) Structural biopolymer preservation in Miocene leaf fossils from the Clarkia site, Northern Idaho. *Proc Natl Acad Sci U S A* 90:2246–2250
- Logan GA, Smiley CJ, Eglinton G (1995) Preservation of fossil leaf waxes in association with their source tissues, Clarkia, northern Idaho, USA. *Geochim Cosmochim Acta* 59:751–763

- Lüniger G, Schwark L (2002) Characterisation of sedimentary organic matter by bulk and molecular geochemical proxies: an example from Oligocene maar-type Lake Enspel, Germany. *Sediment Geol* 148:275–288
- Martin F, Gonzalez-Vila FJ, del Río JC, Verdejo T (1994) Pyrolysis derivatization of humic substances 1. Pyrolysis of fulvic acids in the presence of tetramethylammonium hydroxide. *J Appl Anal Pyrolysis* 28:71–80
- McKinney DE, Bortiatynski JM, Carson DM, Clifford DJ, de Leeuw JW, Hatcher PG (1996) Tetramethylammonium hydroxide thermochemolysis of the aliphatic biopolymer cutan: insights into the chemical structure. *Org Geochem* 24:641–650
- Mongenot A, Riboulleau A, Garcette-Lepecq A, Derenne S, Pouet Y, Baudin F, Largeau C (2001) Occurrence of proteinaceous moieties in S- and O-rich late Tithonian kerogen (Kashpir oil shales, Russia). *Org Geochem* 32:199–203
- Mösle B, Finch P, Collinson ME, Scott AC (1997) Comparison of modern and fossil plant cuticles by selective chemical extraction monitored by flash pyrolysis-gas chromatography-mass spectrometry and electron microscopy. *J Anal Appl Pyrolysis* 40–41:585–597
- Mösle B, Collinson ME, Finch P, Stankiewicz BA, Scott AC, Wilson R (1998) Factors influencing the preservation of plant cuticles: a comparison of morphology and chemical comparison of modern and fossil examples. *Org Geochem* 29:1369–1380
- Nguyen RT, Harvey HR (1998) Protein preservation during early diagenesis in marine waters and sediments. In: Stankiewicz BA, van Bergen PF (eds) Nitrogen containing macromolecules in the bio- and geosphere, vol 707, ACS symposium series. American Chemical Society, Washington, DC
- Niklas KJ, Brown RM Jr (1981) Ultrastructural and palaeobiochemical correlations among fossil leaf tissues from the St. Maries River (Clarkia) area, northern Idaho, USA. *Am J Bot* 68:332–341
- Nip M, Tegelaar EW, Brinkhuis H, de Leeuw JW, Schenk PA, Holloway PJ (1986) Analysis of modern and fossil plant cuticles by Curie point Py-GC and Curie point Py-GC-MS: recognition of a new, highly aliphatic and resistant biopolymer. *Org Geochem* 10:769–778
- Opsahl S, Benner R (1995) Early diagenesis of vascular plant tissues: lignin and cutin decomposition and biogeochemical implications. *Geochim Cosmochim Acta* 59:4889–4904
- Pirrung BM (1998) Zur Entstehung isolierter alttertiärer Seesedimente in Zentraleuropäischen Vulkanfeldern. *Mainz Naturwiss Arch Beih* 20:118 p
- Ralph J, Hatfield RD (1991) Pyrolysis-GC-MS characterization of forage materials. *J Agric Food Chem* 39:1426–1437
- Riboulleau A, Derenne S, Largeau C, Baudin F (2001) Origin of contrasting features and preservation pathways in kerogens from the Kashpir oil shales (Upper Jurassic, Russian Platform). *Org Geochem* 32:647–665
- Riou B (1995) Les fossils des diatomites du Miocene superieur de la montagne d' Andance (Ardeche, France). *Géol Méditerr XXII*:1–15
- Schaefer J, Kramer KJ, Garbow JR, Jacob GS, Stejskal EO, Hopkins TL, Speirs RD (1987) Aromatic cross-links in insect cuticle: detection by solid-state ¹³C and ¹⁵N NMR. *Science* 235:1200–1204
- Schreiber U (1995) Die magmatotektonische Entwicklung der tertiären Westerwald-Vulkanprovinz. Symposium "Fossilagerstätte Enspel", Bad Marienberg, Abstract Volume, Landesamt für Denkmalpflege Rheinland-Pfalz, Mainz
- Stankiewicz BA, Briggs DEG, Evershed RP, Flannery MB, Wuttke M (1997a) Preservation of chitin in 25-million-year-old fossils. *Science* 276:1541–1543
- Stankiewicz BA, Briggs DEG, Evershed RP (1997b) Chemical composition of Paleozoic and Mesozoic fossil invertebrate cuticles as revealed by pyrolysis-gas chromatography/mass spectrometry. *Energy Fuels* 11:515–521
- Stankiewicz BA, Mastalerz M, Kruege MA, van Bergen PF, Sadowska A (1997c) A comparative study of modern and fossil cone scale and seeds of conifers: a geochemical approach. *New Phytol* 135:375–393

- Stankiewicz BA, Möslle B, Finch P, Collinson ME, Scott AC, Briggs DEG (1998a) Molecular taphonomy of arthropod and plant cuticles from the carboniferous of North America: implications for the origin of kerogen. *J Geol Soc* 155:453–462
- Stankiewicz BA, Briggs DEG, Evershed RP, Miller RF, Bierstedt A (1998b) Fate of Chitin in Quaternary and Tertiary strata (chapter 12). In: van Bergen PF, Stankiewicz BA (eds) Fate of nitrogen containing molecules in the bio- and geosphere. American Chemical Society, Washington, DC, pp 212–224
- Stankiewicz BA, Poinar HN, Briggs DEG, Evershed RP, Poinar GO Jr (1998c) Chemical preservation of plants and insects in natural resins. *Proc R Soc Lond B* 265:641–647
- Stankiewicz BA, Briggs DEG, Michels R, Collinson ME, Evershed RP (2000) Alternative origin of aliphatic polymer in kerogen. *Geology* 28:559–562
- Storch G, Engesser B, Wuttke M (1996) Oldest fossil record of gliding in rodents. *Nature* 379:439–441
- Tegelaar EW, de Leeuw JW, Holloway PJ (1989a) Some mechanisms of flash pyrolysis of naturally occurring higher plant polyesters. *J Anal Appl Pyrolysis* 15:289–295
- Tegelaar EW, de Leeuw JW, Derenne S, Largeau C (1989b) A reappraisal of kerogen formation. *Geochim Cosmochim Acta* 53:3103–3106
- Tegelaar EW, Kerp H, Visscher H, Schenk PA, de Leeuw JW (1991) Bias of the paleobotanical record as a consequence of variations in the chemical composition of higher vascular plant cuticles. *Paleobiology* 17:133–144
- van Bergen PF (1999) Pyrolysis and chemolysis of fossil plant remains: applications to palaeobotany. In: Jones TP, Rowe NP (eds) Fossil plants and spores: modern techniques. Geological Society, London, pp 143–148
- van Bergen PF, Scott AC, Barrie PJ, de Leeuw JW, Collinson ME (1994) The chemical composition of Upper Carboniferous pteridosperm cuticles. *Org Geochem* 21:107–112
- van Bergen PF, Collinson ME, Briggs DEG, de Leeuw JW, Scott AC, Evershed RP, Finch P (1995) Resistant biomacromolecules in the fossil record. *Acta Bot Neerl* 44:319–342
- van Bergen PF, Bull ID, Poulton PR, Evershed RP (1997) Organic geochemical studies of soils from the Rothamsted Classical Experiments—I. Total lipid extracts, solvent insoluble residues and humic acids from Broadbalk Wilderness. *Org Geochem* 26:117–135
- van Bergen PF, Flannery MB, Poulton PR, Evershed RP (1998) Organic geochemical studies from Rothamsted Experimental Station: III nitrogen-containing organic matter in soil from Geescroft Wilderness. In: Stankiewicz BA, van Bergen PF (eds) Nitrogen-containing macromolecules in the bio- and geosphere, vol 707, ACS symposium series. American Chemical Society, Washington, DC

Chapter 5

Molecular Transformation of Plant Biopolymers in High P-T Conditions

Abstract Experimental heating of plant tissues (350 °C, 700 bars) generated a resistant non-hydrolysable aliphatic macromolecule similar to that comprising organic matter in ancient sediments and fossil leaves. Comparison of the products derived from such heating of different pre-treated plant tissues clearly demonstrates that solvent-extractable and hydrolysable lipids are precursors of the generated macromolecular material. Thus, these experiments indicate that labile alkyl compounds can be a source of the insoluble aliphatic component of fossil organic matter in the absence of a resistant aliphatic precursor (e.g. cutan) in the living organism.

Keywords Maturation • Aliphatic macromolecule • Fossil organic matter • Kerogen • Pyrolysis

Introduction

Ancient sedimentary organic matter is formed by diagenetic and catagenetic alteration of biological material, typically yielding a non-hydrolysable, organic solvent insoluble macropolymer called kerogen (Tissot and Welte 1984). The composition and type of kerogen is heavily dependent on the nature of the biological input, the environment of deposition and the diagenetic pathway (de Leeuw and Largeau 1993) but many kerogens are highly aliphatic (especially Type I/II) and serve as a source of petroleum products during thermal maturation. Thus, the pathways and mechanism of kerogen formation and preservation are critical to the formation of fossil fuel deposits, have important implications for the global carbon cycle and are essential processes in the preservation of macroscopic and morphologically intact organic materials in the fossil record.

Kerogen formation is generally attributed to neogenesis (Tissot and Welte 1984) in which sedimentary organic matter is preserved by random intermolecular polymerisation and polycondensation of biological residues, natural vulcanisation which involves the reaction between reduced sulfur and various functional groups in organic

compounds, resulting in the formation of a S-rich macromolecule, (Kok et al. 2000), oxidative reticulation (Riboulleau et al. 2001) where lipids may be crosslinked with oxygen and selective preservation of highly aliphatic and resistant biopolymers (e.g. algaenan or cutan; Tegelaar et al. 1989a; de Leeuw and Largeau 1993). However, recent analysis of a wide variety of gymnosperms and angiosperms failed to detect cutan in plants previously thought to contain it (following chemical degradation techniques different from that used in this investigation, Möhle et al. 1998; Collinson et al. 1998; Gupta et al. 2006a, 2007), and it has been suggested that cutan may have limited occurrence in modern plants (Boom et al. 2005; Gupta et al. 2006a). This has renewed interest in understanding the origin of aliphatic components in fossil organic matter (Briggs 1999; Stankiewicz et al. 2000; Gupta et al. 2006b) and particularly fossil leaves (Gupta et al. 2007). Here we report the results of experimental heating (350 °C, 700 bars) of various plant tissues attempted for the first time with plants and examine the role of different biological components in the formation of chemically-resistant macromolecules.

Materials and Methods

Extant leaves and plant tissues were crushed in liquid N₂ and powdered and matured in sealed gold cells at 350 °C, under a confinement pressure of 700 bars (see description below, Monthieux et al. 1985; Landais et al. 1989; Michels et al. 1995) for a duration of 24 h in the absence of water. This temperature was chosen because during a previous investigation of scorpion cuticle and arthropods (Stankiewicz et al. 2000; Gupta et al. 2006b) that was the temperature at which the most dramatic change in chemical composition was observed. Whole leaves of extant *Castanea*, *Acer*, *Pinus*, *Quercus* and *Ginkgo* (see Gupta et al. 2006a for further information on plant species investigated) were matured to investigate the products formed from various constituents: lignin, polysaccharides, cutin, cuticular lipids and internal lipids. All of these plants have a well-documented fossil record and in each case the composition of the fossil leaves includes a strong aliphatic component (Logan et al. 1993; Möhle et al. 1998; Gupta et al. 2007). The leaf tissues were also matured after (1) lipid extraction in dichloromethane:methanol (2:1 v:v, 3×30 min in an ultrasonicator) to remove internal+cuticular lipids and (2) extraction followed by saponification (by refluxing in 1 M methanolic NaOH for 24 h at 70 °C) to remove cutin (Kolattukudy 1980) as well as lipids. The following materials were also matured to evaluate the fate of specific structural biopolymers: (3) tomato cuticle representative of cutin (which lacks cutan) prepared by mechanical isolation followed by lipid extraction and acid hydrolysis (Möhle et al. 1998); (4) commercially prepared lignin and cellulose; (5) fleshy tomato mesocarp (i.e., the succulent fleshy edible layer in fruits); and (6) the mechanically isolated cuticle of *Agave americana* and associated epidermal tissue, which contains cutan (Nip et al. 1986). Samples obtained after maturation were either extracted as described above or subjected to thermodesorption of weakly bound or non-covalently bound components (at 310 °C,

Stankiewicz et al. 2000) and, thus, they represent the macromolecular component. Pyrolysis after either solvent extraction or thermodesorption lead to very similar results. Thermodesorption was used in all samples for thermal extraction of compounds not bound to macromolecule (e.g. encapsulated lipids generated during the heating protocol), furthermore this technique had been previously used in a similar heating protocol successfully (Stankiewicz et al. 2000; Gupta et al. 2006b). Solvent extraction was used for select samples (e.g. saponified residue of post matured leaf) but both methods lead to very similar results.

Preparing the Gold Cell

A 50 cm gold tube of 10 mm diameter was cut into 10 pieces and heated at 700 °C for 3 h in a furnace to make it permanently malleable. Subsequently, one side of each cell was sealed with a clamp and welded at 1,400 °C with a graphite rod. The cell was weighed in a balance, the experimental sample was inserted, and the cell and sample were weighed.

The cells was then sealed in an argon chamber to eliminate oxygen. The cell was cooled with a blast of liquid nitrogen to ensure that welding did not affect the sample. Following this the gold cell + sample was weighed again.

Autoclave Experiment

Gold cells were inserted into the body of a stainless steel reactor (Fig. 5.1) and the cylinder was filled with water. A high-pressure sealing head was screwed to the reactor and the entire set-up was installed into the heater. The reactor head

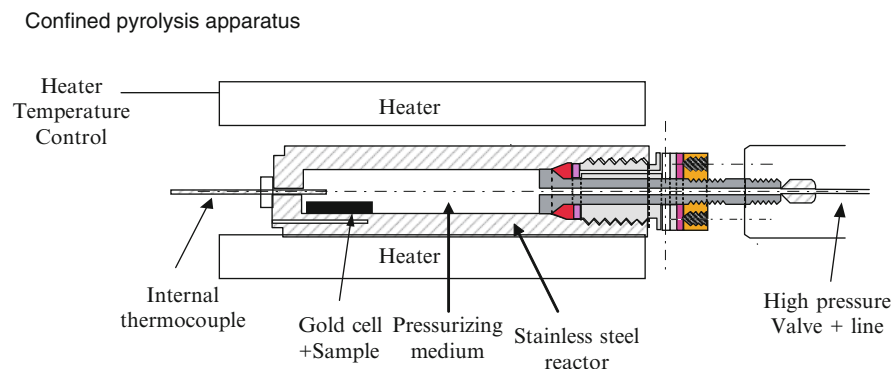


Fig. 5.1 Confined pyrolysis autoclave setup

was bolted to a main pressure line while the internal a thermocouple was attached to a temperature reader. The autoclave was heated to 350 °C and the hydraulic pressure adjusted to 700 Bars. After 24 h, the reactor was removed, cooled to room temperature within 5 min by a heat exchanger. The gold cells were removed and then weighed to record any difference in weight before and after the experiment.

Following this they were analysed by pyrolysis-gas chromatography-mass spectrometry (py-GC/MS) at 610 °C (for experimental parameters see Gupta and Pancost 2004). No absolute quantification was attempted. Selected experimental samples were subjected to base hydrolysis (for 3 h) after solvent extraction to evaluate further the nature of the maturation products (Table 5.1).

Implications

Pyrolysis-GC/MS of extracted but otherwise untreated leaves (Fig. 5.2a) other than *A. americana* yielded chromatograms dominated by carbohydrate, lignin (guaiaacyl and syringyl related components) and protein moieties, together with C₁₆ and C₁₈ fatty acids, reflecting the bulk composition of the leaf (Ralph and Hatfield 1991; Van Bergen et al. 1998; Gupta and Pancost 2004). The fatty acyl moieties are derived from internal lipids and from the biopolyester cutin. With the exception of *Agave*, none of the examined leaves contain cutan (Gupta et al. 2006a). Except for *Agave*, all the other leaves investigated gave similar results and therefore the discussion focusses on *Castanea*.

Leaves matured without any chemical pre-treatment (Fig. 5.2b) yielded chromatograms dominated by *n*-alkane/*n*-alk-1-ene homologues, indicating the presence of an *n*-alkyl component in the post-maturation leaf. The *n*-alkanes ranged from C₉ to C₃₁ and the *n*-alkenes from C₉ to C₂₉. The most abundant *n*-alkanes were the C₁₅, C₁₇, C₂₇, C₂₉ and C₃₁ homologues. Of the fatty acids generated during pyrolysis, the C₁₆ and C₁₈ straight-chain homologues were the most abundant, with straight chain C₁₂, C₁₃, C₁₄, and C₁₅ components also detected. Apart from the aliphatics, other important pyrolysis products included phenol and its alkyl derivatives, benzene and its alkyl derivatives, and indoles (possibly derived from proteins). The guaiaacyl and syringyl related lignin moieties evident in the unmaturation leaf tissue were not observed in detectable amounts in the matured leaves, presumably due to decomposition of lignin during the experiment.

Matured leaves were solvent-extracted and saponified, with subsequent analysis of the non-hydrolysable residue revealing that the polymeric components yielding alkane/alkene homologues (up to C₁₈) persisted (Fig. 5.3, Table 5.1). The C₁₃, C₁₅ and C₁₇ *n*-alkanes and the C₁₀, C₁₂, C₁₃ and C₁₄ *n*-alkenes were the most abundant components in their respective classes. This indicates that a significant portion of the aliphatic polymer is resistant to base hydrolysis and confirms that it is not an artefact of pyrolysis. Thus, the macromolecule in matured leaf tissue is resistant to degradation and at least partly aliphatic. However, non-hydrolysable and aliphatic

Table 5.1 The presence or absence of aliphatic macromolecular components in matured plant tissues and model compounds

		Tomato						Agave						Model compounds							
		Leaf		Leaf		Leaf		Cuticle		Fleshy mesocarp		Cuticle		Cuticle		Cuticle		Lignin		Cellulose	
		Untreated	Extracted ^b	Untreated	Extracted	Untreated	Extracted	Untreated	Extracted	Untreated	Extracted	Untreated	Extracted	Untreated	Extracted	Untreated	Extracted	Untreated	Extracted	Untreated	Extracted
		saponified		saponified		saponified		saponified		saponified		saponified		saponified		saponified		saponified		saponified	
Treatment before maturation	Products	+	+	+	+	+	+	+	+	+	+	+	+	+	+	+	+	+	+	+	+
Treatment after maturation	LMW ^c	+	+	+	+	+	+	+	+	+	+	+	+	+	+	+	+	+	+	+	+
	HMW ^d	+	+	+	+	+	+	+	+	+	+	+	+	+	+	+	+	+	+	+	+
	Fatty acyl ^e	+	+	+	+	+	+	+	+	+	+	+	+	+	+	+	+	+	+	+	+

Composition (before maturation) of *Castanea* leaf : polysaccharides, lignin, fatty acids, cutin; *Agave* cuticle: cutin, cutan, polysaccharides, phenols; Tomato peel: cutin; Tomato mesocarp: polysaccharides, fatty acids, phenols

^a“+” Denotes presence and “-” absence of components

^bFigure 5.1 shows the results for *Castanea*; other leaves yielded similar results

^cSamples were analysed after solvent extraction or thermal desorption: both extraction methods gave equivalent results

^dLMW: Low molecular weight aliphatic compounds (<C₂₀)

^eHMW: High molecular weight aliphatic compounds (>C₃₀)

^fFatty acyl: fatty acyl moieties

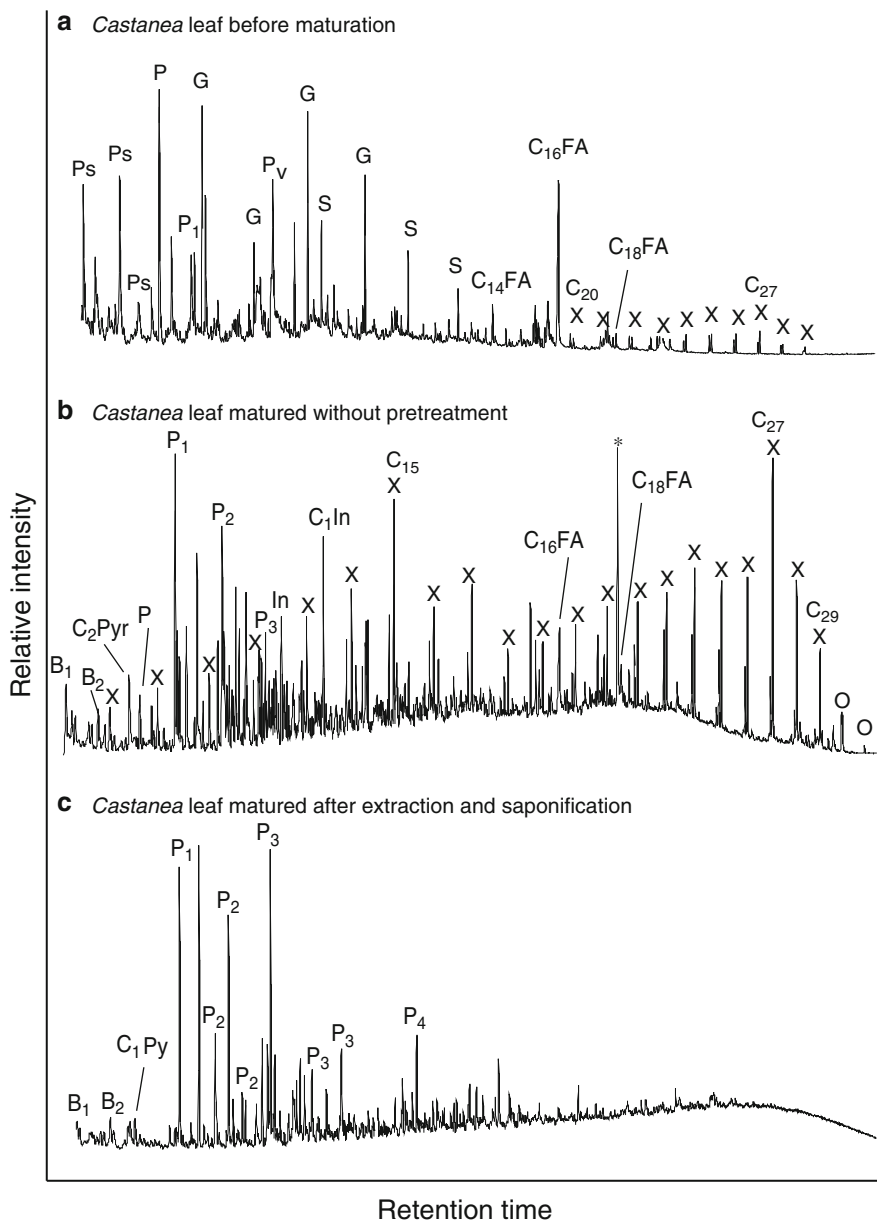


Fig. 5.2 Partial ion chromatograms showing the pyrolysis-GC/MS analysis of modern *Castanea* leaf; (a) without maturation, (b) matured at 350 °C, 700 Bars for 24 h without any chemical pretreatment, and (c) matured after extraction followed by saponification. Note the presence of *n*-alkane/alkene homologues in high relative abundance in (b) ranging from C₉ to C₃₁, including long chain homologues suggesting the presence of a strong *n*-alkyl component similar to that encountered in leaf fossils, and the lack of these in (c). B_n: Benzene derivative, C_nFA: Fatty acyl moieties, P: Phenol, P_n: phenol derivatives (where _n refers to the carbon chain length of the alkyl component) C₂Pyr C₂: pyrrole derivative, In: indole, C₁In: methyl indole, C₁Py: methyl pyridine, Ps: polysaccharide pyrolysis products, G: guaiacyl units, S: syringyl units and C₁₆: fatty acid (C₁₆ FA), * contaminant. X *n*-alkane/alkene homologues and O *n*-alkanes, C_n referring to the carbon chain length

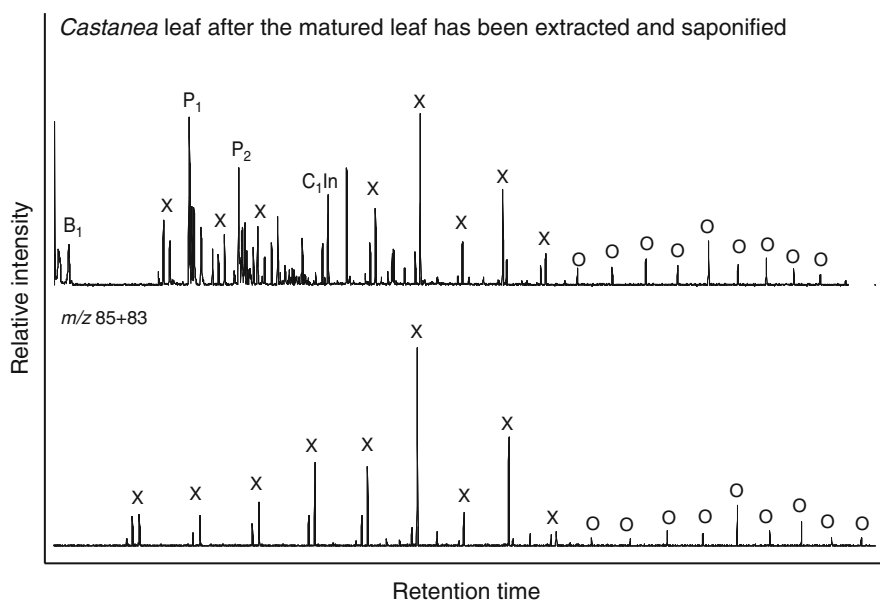


Fig. 5.3 Partial ion chromatograms showing the pyrolysis-GC/MS analysis of modern *Castanea* leaf after the matured product has been extracted and saponified. This reveals the recalcitrant nature of the aliphatic polymer formed after maturation. For key to symbols see Fig. 5.2. M/z 85+83 mass chromatogram focuses on the distribution of *n*-alkane/alkene homologues

biomolecules (e.g. cutan) are not present in the original leaf tissue, and the observed aliphatic signal must derive from the generated macromolecular component(s). Critically, the pyrolysis characteristics of this material are similar to those derived from naturally occurring recalcitrant leaf fossils (Stankiewicz et al. 1998; Gupta et al. 2007).

The pyrolysates of leaves matured after lipid extraction lacked detectable *n*-alkane/alkene homologues above C_{18} (see discussion on cutin below) and pyrolysates of those matured after extraction and saponification (Fig. 5.2c; Table 5.1) lacked any detectable *n*-alkyl components, including *n*-alkane/alkene homologues and *n*-alkanoic acids. The pyrolysates did contain the other compounds present in leaves matured without any pre-treatment. Thus, the long-chain *n*-alkanes and *n*-alkenes in the pyrolysate of leaf matured without chemical pre-treatment are derived from organic solvent extractable lipids; indeed, long-chain *n*-alkyl compounds are major components of epicuticular waxes (Eglinton and Hamilton 1967) and include *n*-alkanes, *n*-alkanols, *n*-alkanoic acids and wax esters.

The source of the *n*-alkyl components in leaves matured after extraction (but not base hydrolysis) must derive from insoluble but hydrolysable precursors. One posited source is cutin and to test this we analysed tomato cuticle pre-treated with solvent extraction and acid hydrolysis. Upon maturation, this treated cuticle yielded

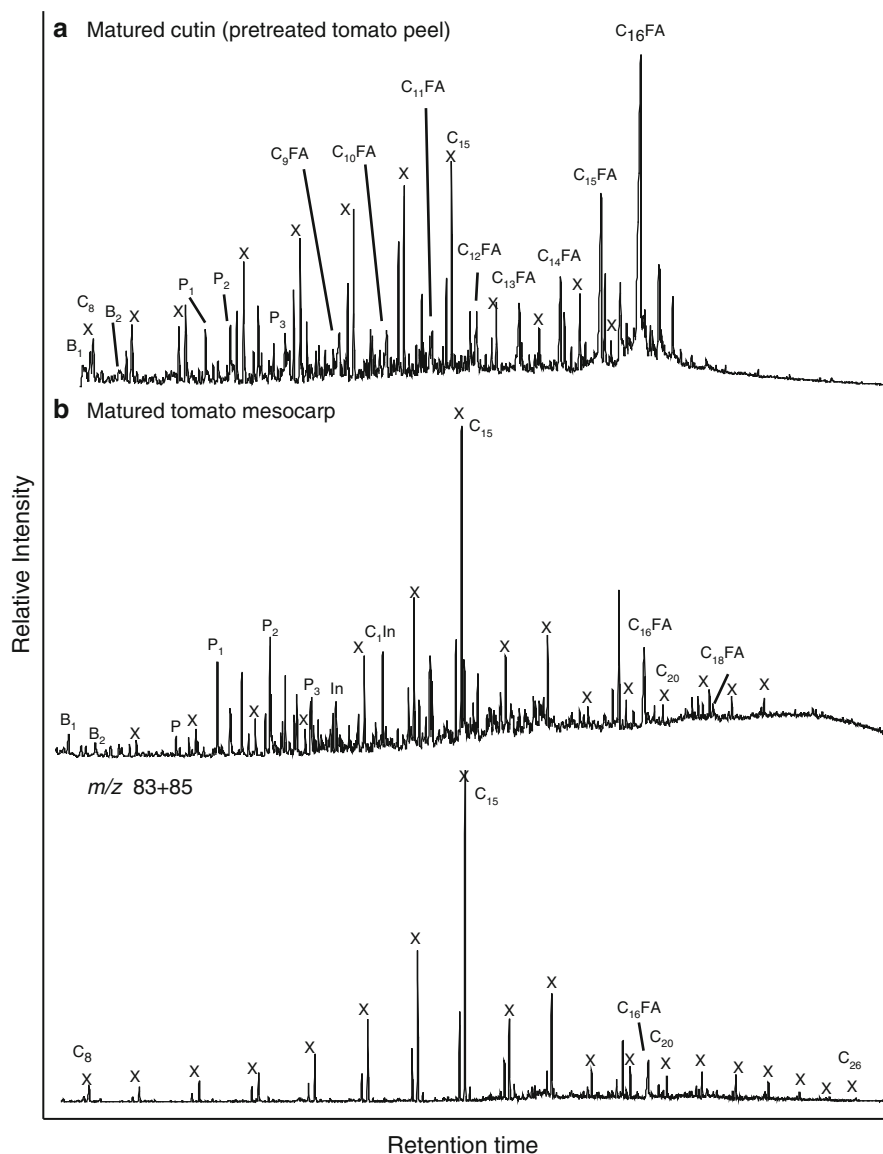


Fig. 5.4 Partial ion chromatograms showing the pyrolysis-GC/MS analysis of (a) modern Tomato peel/Cutin and (b) tomato mesocarp, m/z 85 + 83 mass chromatogram focuses on the distribution of alkane/alkene homologues. For key to symbols see Fig. 5.2. M/z 85 + 83 mass chromatogram focuses on the distribution of *n*-alkane/alkene homologues

an aliphatic component consisting of fatty acyl moieties from *n*-C₈ to *n*-C₁₆ (C₁₆ FA the most abundant) and *n*-alkane/alk-1-ene homologues ranging from *n*-C₉ to *n*-C₁₈ (Fig. 5.4a). Only trace abundances of the longer chain homologues were detected. Thus, cutin contributes to the low-molecular-weight aliphatic pyrolysis products.

This composition differs from that of unmaturred cutin which yielded vinyl phenol and C₁₆ (di) unsaturated and hydroxy fatty acids as the main moieties without any alkane/alkene homologues (Tegelaar et al. 1989b).

An alternative or additional source for the low molecular weight *n*-alkyl components are labile lipids, including membrane lipids and di- and triacylglycerides. To test this, we matured and analysed tomato mesocarp (cutin-free) tissue. This also yielded a distinct aliphatic component comprising *n*-alkane/alkene homologues ranging from *n*-C₈ to *n*-C₂₆ and *n*-alkanoic acids ranging from *n*-C₉ to *n*-C₁₆ (Fig. 5.4b); the unmaturred mesocarp consisted of polysaccharides, phenolic compounds and fatty acyl moieties.

We also matured and analysed pure lignin and cellulose and the cuticle of *Agave*, the last of which is comprised largely of cutan and provides a control (Table 5.1). Matured lignin and cellulose yielded aromatic and phenolic moieties, but neither fatty acids nor *n*-alkanes were detected. Pyrolysates of *Agave* matured without any pre-treatment contained *n*-alkane/alk-1-ene homologues ranging from *n*-C₈ to *n*-C₃₅ (Fig. 5.5a). Benzene derivatives, phenols and fatty acyl moieties were also observed as in the other plant tissues. The *n*-alkane/alk-1-ene homologues (including those with carbon number >*n*-C₂₀) were also present in *Agave* that had been pre-extracted (Fig. 5.5b), or pre-extracted and saponified (Fig. 5.5c), prior to maturation, in contrast to all other pre-treated leaf tissues. Thus, cutan survives exposure to these elevated temperatures and pressures.

The high pressure and temperature conditions used in the experiments have been used before to understand the origin of the aliphatic component in kerogen using modern scorpion cuticle (Stankiewicz et al. 2000). It is critical to acknowledge that these conditions do not simulate organic diagenesis and represent only an indirect simulation (due to compressed timescales) of catagenesis. Consequently, while we could speculate that a range of reaction pathways, particularly free radical reactions, are likely important during our experiment, it remains unclear how important such reactions are during natural kerogen formation. Nonetheless, the experiment does provide a direct test of the possible role of different plant molecular constituents in contributing to the formation of an aliphatic polymer.

All previously reported pyrolysates of pre-Tertiary fossil leaves and cuticles (Briggs et al. 2000), irrespective of age, plant type or enclosing lithology, contain aliphatic components (Nip et al. 1986; Tegelaar et al. 1991; Möslle et al. 1998; Collinson et al. 1998; Gupta et al. 2007). The experiments described here provide a closed system that precludes the incorporation of compounds from an external source. They indicate that, in the absence of cutan, other components, including cutin, higher plant waxes and internal lipids, have served as the sources for high- and low-molecular-weight aliphatic components of a generated macromolecule(s). As such, the incorporation of lipids into macromolecules or even the formation of macromolecules from lipids could play a major role in the fossilisation of plant constituents and the formation of aliphatic moieties commonly observed in kerogen (especially those of terrestrial origin) and sedimentary organic matter (Gillaizeau et al. 1996).

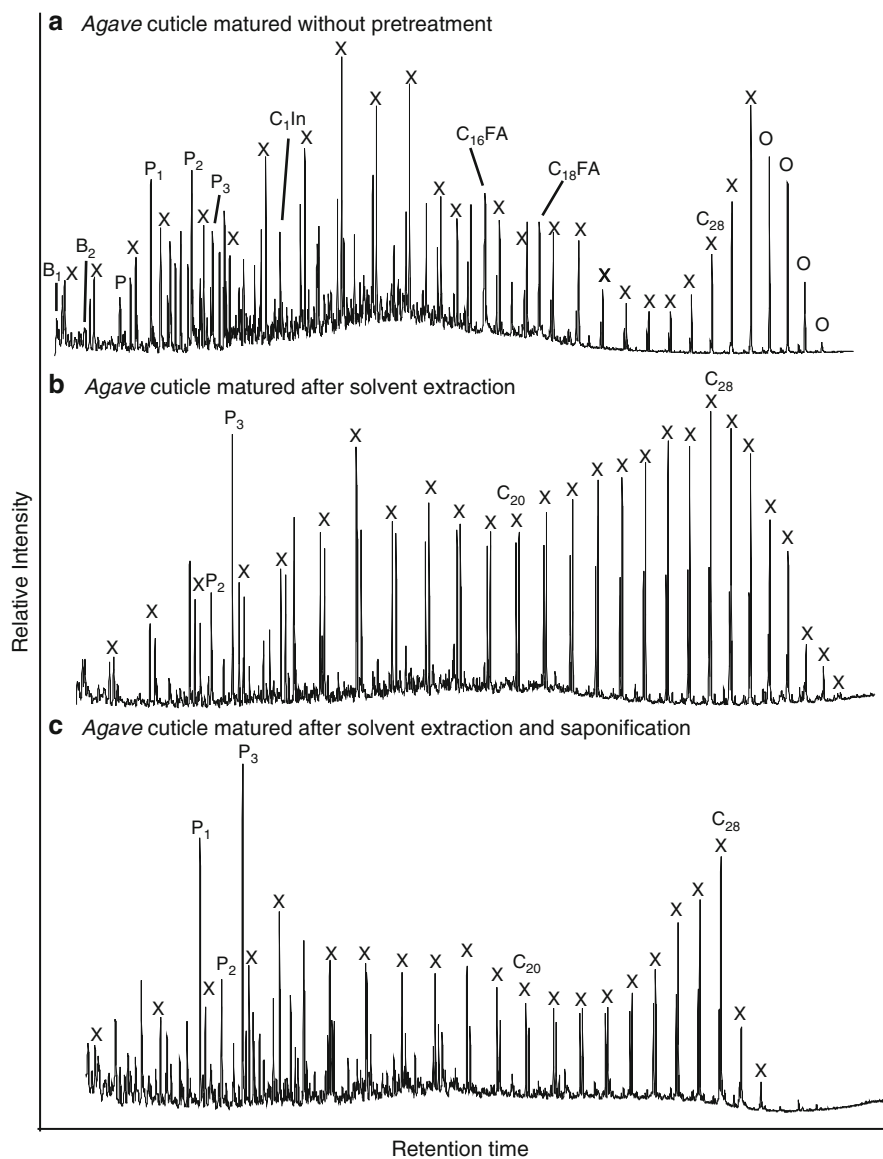


Fig. 5.5 Partial ion chromatograms showing the pyrolysis-GC/MS analysis of *Agave* matured (a) without chemical treatment, (b) after solvent extraction and (c) after extraction and saponification. For key to symbols see Fig. 5.2

References

- Boom A, Sinninghe Damsté JS, de Leeuw JW (2005) Cutan, a common aliphatic biopolymer in cuticles of drought-adapted plants. *Org Geochem* 36:595–601
- Briggs DEG (1999) Molecular taphonomy of animal and plant cuticles: selective preservation and diagenesis. *Philos Trans R Soc Lond* 354:7–16
- Briggs DEG, Evershed RP, Lockheart MJ (2000) The biomolecular paleontology of continental fossils. *Paleobiology* 26(Suppl to no. 4):169–193
- Collinson ME, Möslle B, Finch P, Scott AC, Wilson R (1998) The preservation of plant cuticle in the fossil record: a chemical and microscopical investigation. *Anc Biomol* 2:251–265
- de Leeuw JW, Largeau C (1993) A review of macromolecular organic compounds that comprise living organisms and their role in kerogen, coal and petroleum formation. In: Engel MH, Macko SA (eds) *Organic geochemistry: principles and applications*, vol 11, *Topics in geobiology*. Springer, New York, pp 23–72
- Eglinton G, Hamilton RJ (1967) Leaf epicuticular waxes. *Science* 156:1322–1334
- Gillaizeau B, Derenne S, Largeau C, Berkaloff C, Rousseau B (1996) Source organisms and formation pathway of the kerogen of the Göynük Oil Shale (Oligocene, Turkey) as revealed by electron microscopy, spectroscopy and pyrolysis. *Org Geochem* 24:671–679
- Gupta NS, Pancost RD (2004) Biomolecular and physical taphonomy of angiosperm leaf during early decay: implications for fossilisation. *Palaios* 19:428–440
- Gupta NS, Briggs DEG, Collinson ME, Evershed RP, Pancost RD (2006a) Re-investigation of the occurrence of cutan in plants: implications for the leaf fossil record. *Paleobiology* 32(3):432–449
- Gupta NS, Briggs DEG, Collinson ME, Evershed RP, Michels R, Pancost RD (2006b) Organic preservation of fossil arthropods: an experimental study. *Proc R Soc Lond B* 273(1602):2777–2783
- Gupta NS, Briggs DEG, Collinson ME, Evershed RP, Michels R, Jack KS, Pancost RD (2007) Evidence for the in situ polymerisation of labile aliphatic organic compounds during the preservation of fossil leaves: implications for organic matter preservation. *Org Geochem* 38(3):499–522
- Kok MD, Schouten S, Sinninghe Damsté JS (2000) Formation of insoluble, nonhydrolyzable, sulfur-rich macromolecules via incorporation of inorganic sulfur species into algal carbohydrates. *Geochim Cosmochim Acta* 64:2689–2699
- Kolattukudy PE (1980) Biopolyester membranes of plants: cutin and suberin. *Science* 208:990–1000
- Landais P, Michels R, Poty B (1989) Pyrolysis of organic matter in cold-seal autoclaves. *J Anal Appl Pyrolysis* 16:103–115
- Logan GA, Boon JJ, Eglinton G (1993) Structural biopolymer preservation in Miocene leaf fossils from the Clarkia site, Northern Idaho. *Proc Natl Acad Sci U S A* 90:2246–2250
- Michels R, Landais P, Torkelson BE, Philp RP (1995) Effects of confinement and water pressure on oil generation during confined pyrolysis, hydrous pyrolysis and high pressure hydrous pyrolysis. *Geochim Cosmochim Acta* 59:1589–1604
- Monthioux M, Landais P, Monin J-C (1985) Comparison between natural and artificial maturation series of humic coals from the Mahakam delta, Indonesia. *Org Geochem* 8:275–292
- Möslle B, Collinson ME, Finch P, Stankiewicz BA, Scott AC, Wilson R (1998) Factors influencing the preservation of plant cuticles: a comparison of morphology and chemical composition of modern and fossil examples. *Org Geochem* 29:1369–1380
- Nip M, Tegelaar EW, Brinkhuis H, de Leeuw JW, Schenk PA, Holloway PJ (1986) Analysis of modern and fossil plant cuticles by Curie point Py-GC and Curie point Py-GC-MS: recognition of a new, highly aliphatic and resistant biopolymer. *Org Geochem* 10:769–778
- Ralph J, Hatfield RD (1991) Pyrolysis-GC-MS characterization of forage materials. *J Agric Food Chem* 39:1426–1437

- Riboulleau A, Derenne S, Largeau C, Baudin F (2001) Origin of contrasting features and preservation pathways in kerogens from the Kashpir oil shales (Upper Jurassic, Russian Platform). *Org Geochem* 32:647–665
- Stankiewicz BA, Poinar HN, Briggs DEG, Evershed RP, Poinar GO Jr (1998) Chemical preservation of plants and insects in natural resins. *Proc R Soc Lond B* 265:641–647
- Stankiewicz BA, Briggs DEG, Michels R, Collinson ME, Evershed RP (2000) Alternative origin of aliphatic polymer in kerogen. *Geology* 28:559–562
- Tegelaar EW, de Leeuw JW, Derenne S, Largeau C (1989a) A reappraisal of kerogen formation. *Geochim Cosmochim Acta* 53:3103–3106
- Tegelaar EW, de Leeuw JW, Holloway PJ (1989b) Some mechanisms of flash pyrolysis of naturally occurring higher plant polyesters. *J Anal Appl Pyrolysis* 15:289–295
- Tegelaar EW, Kerp H, Visscher H, Schenk PA, de Leeuw JW (1991) Bias of the paleobotanical record as a consequence of variations in the chemical composition of higher vascular plant cuticles. *Paleobiology* 17:133–144
- Tissot B, Welte DH (1984) *Petroleum formation and occurrence*. Springer, Berlin, p 538
- van Bergen PF, Flannery MB, Poulton PR, Evershed RP (1998) Organic geochemical studies from Rothamstead Experimental Station: III nitrogen-containing organic matter in soil from Geescroft Wilderness. In: Stankiewicz BA, van Bergen PF (eds) *Nitrogen-containing macromolecules in the bio- and geosphere*, vol 707, ACS symposium series. American Chemical Society, Washington, DC

Chapter 6

Lipid Incorporation During Experimental Decay of Arthropods

Abstract Laboratory decay experiments were carried out on shrimps, scorpions and cockroaches to monitor changes in the chitin-protein of the arthropod cuticle and associated lipids. The cockroach and scorpion exoskeleton remained largely unaltered morphologically, but the shrimp experienced rapid decomposition within a month that progressed through the 44 week duration of the experiment as revealed by electron microscopy. Mass spectrometry and ^{13}C NMR spectroscopy revealed the association of an *n*-alkyl component with labile lipids, such as fatty acids with up to 24 carbon atoms, which were incorporated into the decaying macromolecule. The scorpion and cockroach cuticle did not reveal the incorporation of additional lipids indicating that decay is important in initiating *in situ* lipid association. This experiment provides evidence that lipids can become associated with carbohydrate and proteinaceous macromolecules during the very early stages of decay representing the first stage of the transformation process that contributes to the aliphatic rich composition ubiquitous in organic fossils and in kerogens.

Keywords Taphonomy • Kerogen • Fossil • Pyrolysis • Spectroscopy • Gas chromatograph-mass spectrometry • Chitin • Lipids • Melanoidin

Introduction

Research on the organically preserved cuticles of fossil arthropods has shown that only younger examples retain traces of the chitin-protein complex that is the primary component of the cuticle of living arthropods (Stankiewicz et al. 1997; Gupta et al. 2007a; de Leeuw 2007). Cuticles of plant and animal origin are transformed during diagenesis to geopolymers with a significant long chain aliphatic component (Briggs 1999; Stankiewicz et al. 2000). Such a transformation is common to a range of other organic remains (de Leeuw et al. 2006) with different starting compositions, including graptolites (Briggs et al. 1995; Gupta et al. 2006a) and leaves (Mösle et al. 1998; Gupta et al. 2006b, 2007b), and the analysis of such fossils is

fundamental to understanding the formation of hydrogen-rich kerogens (e.g. type II kerogen; Briggs 1999). Analysis of successively older fossil examples revealed that the transformation to a recalcitrant aliphatic composition is gradual and time dependent but it has been assumed to require many millions of years. The source of the aliphatic components is not external (Gupta et al. 2007c); they are generated by polymerization of molecules present within the original organism. Analysis of cuticles showed that these molecules are incorporated lipids (Versteegh et al. 2004; Gupta et al. 2006c, 2007a, c) often fatty acyl moieties with a dominance of chain lengths C_{16} and C_{18} . However, the constituent chitin and protein biopolymers and lipid molecules are prone to degradation during decay and presumably undergo transformation prior to and during diagenesis. Thus, we set up a series of experiments to determine the fate of the lipid components and other constituent biopolymers in a decaying arthropod.

Some earlier experimental investigations of the molecular taphonomy of arthropods focused on the cuticle components of crustaceans (Baas et al. 1995; Stankiewicz et al. 1998a) and were run for 8 weeks. They revealed the loss of protein within the first 2 weeks, while chitin remained largely intact for the duration of the experiments, attesting to its greater preservation potential (Stankiewicz et al. 1998a). For the present investigation we used laboratory incubation techniques to determine the fate of the constituent biopolymers over a much longer period (44 weeks), and compared the chemical changes in shrimps, cockroaches and scorpions.

Materials and Methods

Specimens of the penaeid shrimp *Litopenaeus setiferus* (Linnaeus) (~10 cm long), the scorpion *Heterometrus spinifer* (~11 cm long), and the cockroach *Eublabeus posticus* (~6 cm long) were killed by asphyxiation in air (shrimp) or drowning in deionised water (scorpion and cockroach – the latter was wrapped in aluminium foil to make it sink). Six specimens of each arthropod were placed in individual 400 ml beakers (i.e., 18 in all) with 200 ml of natural sea water obtained from Long Island Sound at West Haven. An inoculum was prepared in advance by decaying a small piece of scorpion cuticle and associated tissue for a week in a quantity of the same sea water with anoxic sediment for a week. This resulted in the development of a biofilm. A sample of fresh scorpion cuticle and tissue was reinoculated two more times successively with a sample of seawater and biofilm obtained from immediately adjacent to the tissue in the previous sample in an attempt to concentrate those microbes colonizing the carcass. Five milliliters of this inoculum was added to the sea water in each beaker which was then covered with aluminum foil and placed in an environmental chamber maintained at 30 °C and 80 % relative humidity. A specimen of each arthropod was removed from the incubator and processed after 1, 2, 4, 8, 12, and 24 weeks. Material remaining from the second week sample was returned to the incubator to monitor chemical changes after 44 weeks decay.

Electron microscopy was performed on the original, 4 week- and 44 week- decayed shrimp, cockroach and scorpion cuticles without any chemical treatment and using a Philips XL 30 environmental scanning electron microscope.

Specimens were photographed before incubation and on recovery from the experiment to record the state of decay. Samples of tissue and cuticle were transferred to glass vials and frozen at $-60\text{ }^{\circ}\text{C}$ for subsequent analysis. Three posterior segments in the cockroach, segments 5–7 of the pre-abdomen in the scorpion and two posterior segments in the shrimp were targeted for chemical analysis, but in the last stage of decay in the shrimp available cuticle was sampled. For each analysis the cuticle of a single segment was cleaned of any adhering exogenous matter and internal soft tissue with tweezers and scalpel and then subjected to ultrasonication in deionised water for 30 min. The isolated cuticle was then extracted in 2:1 dichloromethane:methanol, for 30 min three times, to remove solvent-soluble, organic components.

Chemical Analysis

The insoluble residue remaining at each sample stage was analysed using a CDS 5150 Pyroprobe by heating at $650\text{ }^{\circ}\text{C}$ for 20s (py-GC-MS: mass spectral identifications were based on model compounds—see Gupta et al. 2008a). Compound detection and identification were performed with on-line GC-MS in full scan mode using a Hewlett Packard HP6890 gas chromatograph interfaced to a Micromass AutoSpec Ultima magnetic sector mass spectrometer. GC was performed with a J&W Scientific DB-1MS capillary column ($60\text{ m}\times 0.25\text{ mm ID}$, $0.25\text{ }\mu\text{m}$ film thickness) using He as carrier gas. The oven was programmed from $50\text{ }^{\circ}\text{C}$ (held 1 min) to $300\text{ }^{\circ}\text{C}$ (held 28 min) at $8\text{ }^{\circ}\text{C min}^{-1}$. The source was operated at $250\text{ }^{\circ}\text{C}$ and 70 eV ionization energy in the electron ionization (EI) mode. The AutoSpec full scan rate was 0.80 s-decade over a mass range of 50–700 Da and a delay of 0.20 s. The original, 1 month and 44 week decayed shrimp cuticle samples were also subjected to thermodesorption at $310\text{ }^{\circ}\text{C}$ prior to pyrolysis at $650\text{ }^{\circ}\text{C}$, to compare the macromolecular moieties obtained after pyrolysis of the solvent extracted residue with those obtained after thermodesorption.

¹³C NMR Analysis

Solid state ¹³C nuclear magnetic resonance spectroscopy (¹³C-NMR) was conducted on the fresh and 44 week decayed shrimp and scorpion, after crushing the solvent extracted residue in liquid nitrogen followed by freeze drying to remove excess water. All ¹³C solid state NMR experiments were performed on a Varian-Chemagnetics Infinity spectrometer located at the W. M. Keck Solid State NMR Facility at the Geophysical Laboratory. The static field of this instrument is 7.05 T;

the corresponding Larmor frequencies of ^1H and ^{13}C are ~ 300 and 75 MHz, respectively. All experiments were performed using a 5 mm double resonance probe with zirconia rotors. ^1H - ^{13}C cross polarization was employed utilizing a RF ramp protocol on the ^{13}C channel. The ^1H 90° pulse width was $4 \mu\text{s}$ and high power decoupling ($w/2\pi = 75$ kHz) was employed during signal acquisition. The Magic Angle spinning frequency ($w_r/2\pi$) was 11.6 kHz. The contact time was determined from a standard of chitin to optimum at 6 ms. A recycle delay of 2 s was chosen to minimize longitudinal interference during signal averaging. Typically $36,000$ acquisitions were obtained per sample.

Changes in Gross Morphology During Decay

The shrimp and cockroach showed a sequence of morphological decay stages similar to that recorded in previous experiments (Briggs and Kear 1994; Duncan et al. 2003). The shrimp cephalothorax separated from the abdomen within 2 weeks and the cuticle was easy to remove. The muscle tissue in the abdomen, however, remained relatively solid. The scorpion and cockroach remained intact, but the abdomen of the latter was visibly bloated and the soft tissue inside both had largely liquified. Within 4 weeks the shrimp disarticulated completely on removal from the vessel; the cuticle had become very thin and brittle but some soft tissue remained in the posterior abdomen. The scorpion skeleton was still intact and remarkably robust although the soft tissue had largely decayed away. The cockroach skeleton largely disarticulated when the specimen was removed from the vessel; some tissue remained inside but was not intact structurally. Within 24 weeks the scorpion skeleton remained intact, the cockroach cuticle showed some thinning on the ventral side and very little cuticle could be recovered from the shrimp. At 44 weeks there was little further change, but one scorpion appendage separated from the rest of the exoskeleton

Changes in Ultrastructure During Decay

Figure 6.1 documents the key changes observed during decay of shrimp and scorpion cuticle as observed by SEM. Figure 6.1a shows the cross section of the undecayed shrimp cuticle and Fig. 6.1b that after 44 weeks decay revealing loss of exocuticle and reduction in thickness. Figure 6.1d shows the surface of the undecayed shrimp cuticle and Fig. 6.1e that after 44 weeks of decay showing extensive loss of the exocuticle exposing the endocuticle underneath. The loss of exocuticle commenced within 4 weeks of decay in the shrimp cuticle. In contrast, the scorpion and cockroach cuticle showed little change in the ultrastructural features after decay. Figure 6.1c shows the cross section of the scorpion cuticle after 44 weeks decay and Fig. 6.1f the surface after 44 weeks decay where no obvious change was observed from the undecayed samples.

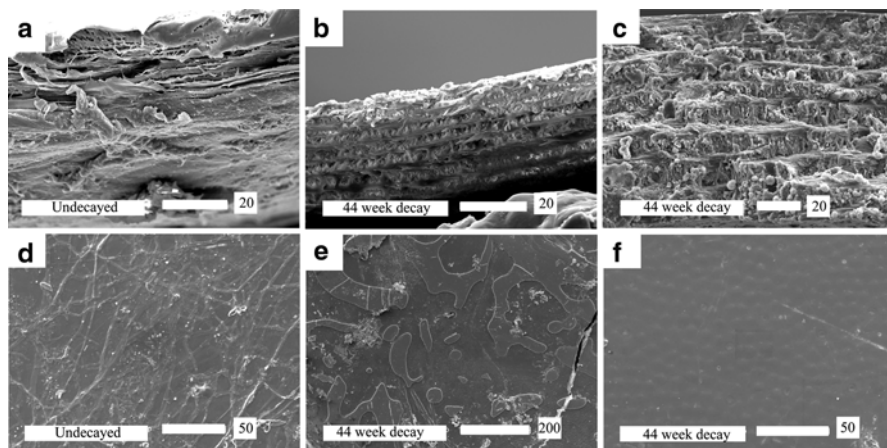


Fig. 6.1 Scanning electron microscopy of cross section of undecayed and decayed shrimp cuticle (a, b) and 44 week decayed scorpion cuticle (c). (d) and (e) show surface of shrimp cuticle, undecayed and after 44 weeks decay respectively. (e) and (f) reveal SEM of the cross section and surface of scorpion cuticle. Note loss of exocuticle in shrimp cuticle after 44 week decay and reduction in thickness. In contrast, SEM of undecayed and decayed scorpion cuticles showed no obvious change in thickness and surface features after 44 weeks decay. The scales are in microns

Changes in Macromolecular Chemistry During Decay

Analysis of undecayed shrimp, scorpion and cockroach cuticle using py-GC-MS revealed the presence of diagnostic chitin markers: 3-acetamidofuran, 3-methyl-5-acetamidofuran, oxazoline structures, acetylpyridone and 3-acetamido-4-pyrone together with protein-amino acid derived markers such as phenols, indoles, benzenes and diketopiperazine structures (Figs. 6.2a, 6.3a, 6.4a). Following 4 weeks decay (Fig. 6.2b) the shrimp carcass showed chitin-protein moieties, but in addition it revealed the presence of *n*-alkane/alkene homologues extending up to C₂₄ derived from a macromolecular *n*-alkyl (aliphatic) component. Such an *n*-alkyl component was also observed in the pyrolyzate after thermodesorption at 310 °C without any prior chemical treatment, indicating that the *n*-alkyl component is not an artifact of analysis. This aliphatic component was detected in all the samples that were allowed to decay for more than 4 weeks; the final sample (Fig. 6.2c), at 44 weeks, also revealed a general reduction in the relative abundance of protein derived moieties compared to chitin. In contrast, the scorpion and cockroach showed little chemical change (Fig. 6.3b); the chitin-protein moieties were retained in relative abundances similar to those in the fresh sample (Fig. 6.3a) and there was no evidence of the presence of *n*-alkane/alkene peaks (i.e., a macromolecular aliphatic component) in any of the decayed samples, including the one that decayed for 44 weeks (Fig. 6.4b).

Figure 6.4a shows an expanded view of the ¹³C NMR spectra of model compound chitin, providing a basis for identifying chitin peaks in the undecayed scorpion and shrimp sample (Fig. 6.4b) and those in shrimp and scorpion cuticle decayed for

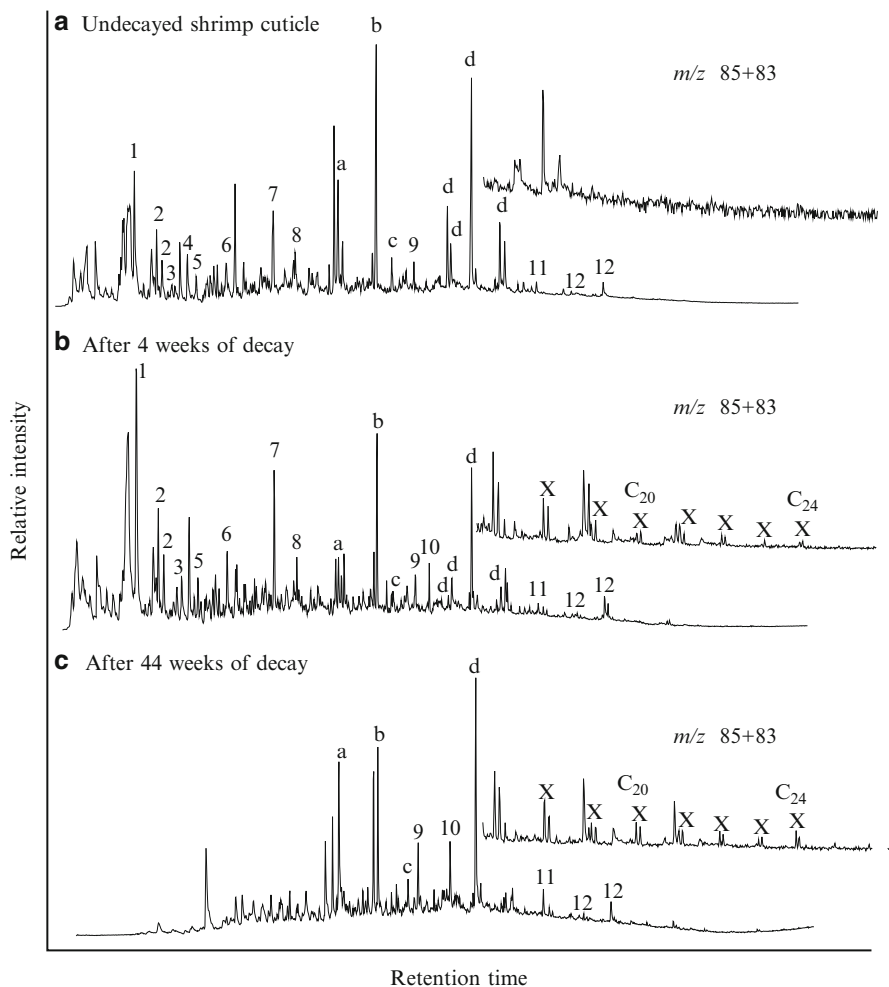


Fig. 6.2 Analysis of undecayed shrimp cuticle (**a**), shrimp decayed for 4 weeks (**b**), and 44 weeks (**c**) revealing presence of diagnostic chitin-protein moieties using py-GC-MS. Note the presence of the *n*-alkyl component (alkane/alkene peaks, denoted by X) up to C₂₄ in the 4 week and 44 week decayed sample, and noted decrease in relative abundance of proteinaceous moieties after 44 weeks of decay. Numbers annotated on peaks refer to protein derived pyrolysis moieties and letters to those related to chitin. 1: toluene, 2: C₁ pyrrole, 3: C₂ benzene, 4: styrene, 5: C₂-pyrrole, 6: phenol, 7: C₁-phenol, 8: ethylcyanobenzene, 9: propylcyanobenzene, 10: C₁-indole, 11: diketodipyrrole, 12: 2,5 diketopiperazine structure (base peak at 70 Da, M⁺ is 168 Da for proline-alanine and 194 Da for Pro-Pro), a: 3-acetamidofuran, b: 3-acetamido-5-methylfuran, c: 3-acetamido-4-pyrone, d: oxazoline structure (base peak at 84 Da). In C_n 'n' refers to the number of carbon atoms in the alkyl component

44 weeks (Fig. 6.4c). There is minimal difference between the fresh and degraded (44 week) scorpion cuticle. However, there is considerable enrichment in aliphatic carbon (at ~30 ppm) in the 44 week decayed shrimp cuticle compared to undecayed shrimp, and compared to the 44 week decayed scorpion cuticle, confirming the

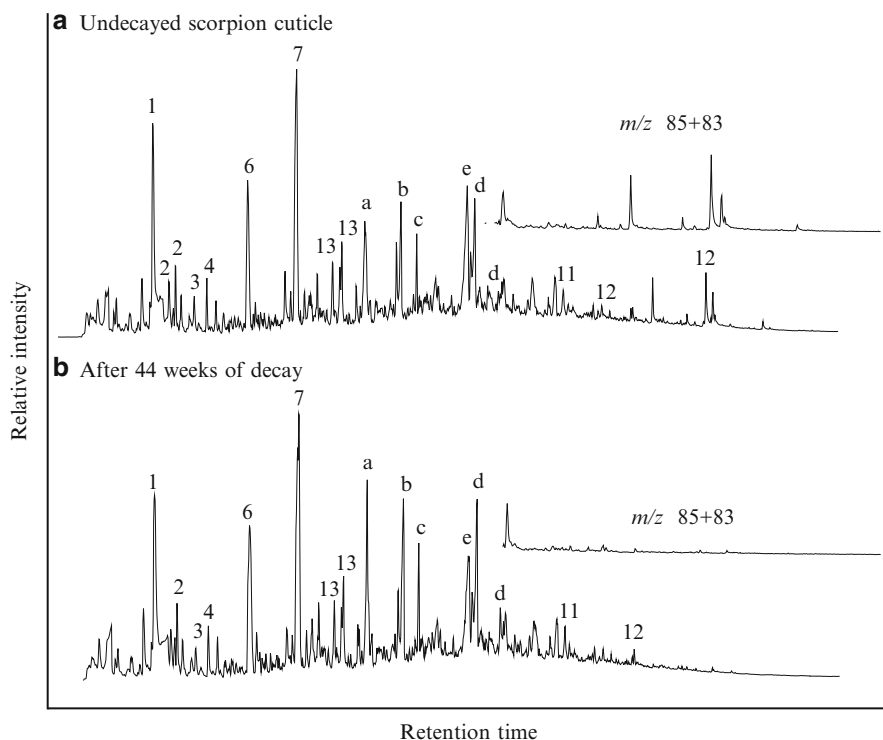
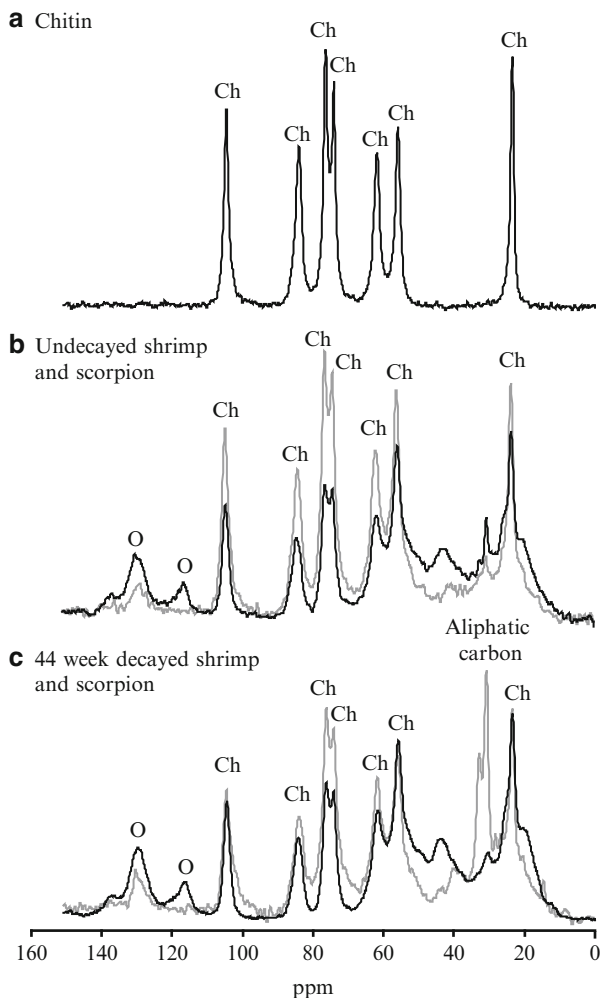


Fig. 6.3 Analysis of an undecayed scorpion cuticle (a) and scorpion cuticle decayed for 44 weeks (b), revealing the presence of diagnostic chitin-protein moieties using py-GC-MS. Both samples reveal a similar relative abundance of chitin-protein derived pyrolysis products indicating very little chemical change in the cuticle over the 44 week decay period. No macromolecular aliphatic component is detected (cf. Fig. 6.4). Key to annotated symbols on peaks as in Fig. 6.4 with the addition of 13: C₂ phenol and *e*: isobutylpyrimidine

results obtained using mass spectrometry. As all samples were solvent extracted, the aliphatic carbon peak derived from lipids (in Fig. 6.4c) is a component of the macromolecule. The spectrum is normalized to the total intensity, and it is evident that gains in aliphatic carbon are paralleled by a concomitant loss of chitin as a consequence of decay.

The importance of lipids in generating an aliphatic composition during diagenesis was demonstrated previously by subjecting arthropods (Stankiewicz et al. 2000; Gupta et al. 2006c), leaves (Gupta et al. 2007c) and their lipids and other constituent biopolymers to artificial maturation in a gold tube hydrothermal apparatus. The cuticle of the emperor scorpion, following degradation for 8.5 months in a bacterial inoculum, generated abundant phenol at 260 °C (Stankiewicz et al. 2000). Markers directly related to chitin and protein were absent, showing that thermal maturation alone can transform chitin, but C₅ to C₂₀ *n*-alk-1-enes and *n*-alkanes were present, indicating the presence of an *n*-alkyl component. Thermal maturation at 350 °C resulted in extensive alteration of the arthropod cuticle. Alkenes and alkanes with

Fig. 6.4 An expanded view of the ^{13}C NMR spectra of (a) model compound chitin, (b) fresh shrimp and scorpion cuticle and (c) shrimp and scorpion cuticle decayed for 44 weeks. Grey line corresponds to shrimp cuticle and black line to scorpion cuticle. *Ch* denotes peaks related to chitin. The open circle (O) highlights the presence of olefinic carbon. The protein component is evident at ~40 and 115–140 ppm (Note the significant aliphatic carbon peak (30 ppm) in shrimp cuticle after 44 weeks decay as compared to fresh shrimp, and fresh and decayed scorpion cuticle)



aliphatic carbon chain numbers up to $n\text{-C}_{30}$ were the dominant pyrolysis products, and phenols were barely detected (Stankiewicz et al. 2000). Subsequent experiments (Gupta et al. 2006c) involving maturation of a mixture of pure C_{16} and C_{18} fatty acids (similar to those obtained from extraction and hydrolysis of the lipid component of the cuticle) produced a distribution of n -alkane/alkene homologues similar to that in the matured untreated cuticles. In striking contrast, maturation of cuticle that had first been extracted and saponified (i.e., was devoid of labile aliphatic compounds) yielded no aliphatic component but only moieties related to matured chitin and protein. These results provided the initial experimental evidence that lipids present in the extractable and hydrolysable fraction of the arthropod cuticle are critical for the formation of the aliphatic component. Similar experiments

demonstrated that lipids are also necessary for the diagenetic alteration of leaf components to an aliphatic composition in fossil leaves (Gupta et al. 2007d). Similarly, Versteegh et al. (2004) conducted heating experiments with vegetable oil demonstrating that lipids were capable of forming aliphatic polymer abiologically.

The living arthropods investigated here do not contain any resistant non-hydrolysable aliphatic biopolymer such as the algaenan or cutan found in some green algae and plants. Hence, the aliphatic component has been incorporated during decay and decomposition of the shrimp cuticle. However, such an aliphatic component was not observed in the incubated scorpion and cockroach cuticle. Thermodesorption of the decayed shrimp cuticle also revealed the aliphatic component indicating that it is not an artifact of chemical pre-treatment but an actual component of the macromolecule.

Scanning electron and general morphological analysis reveal extensive decay of the shrimp cuticle from the early stages of the experiment, while the cockroach and scorpion remained relatively unaltered. Decomposition of chitin and proteins in the shrimp cuticle likely yielded sugars and amino acids. Thus the more rapid decay of this shrimp cuticle could have generated an intermediate component that was prone to bind lipids thereby promoting a progressive transformation to an aliphatic composition.

The chain length of the aliphatic component of the decayed shrimp cuticle extends up to C_{24} (Fig. 6.2b, c). The samples were pyrolysed after lipid extraction without hydrolysis while the solvent extraction ensures that the residue we analyzed is macromolecular (as noted in Gupta et al. 2006c). The distribution of fatty acids in modern shrimp ranges from C_{12} to C_{24} (Krzeczkowski 1970), including saturated and unsaturated fatty acids (occurring as free fatty acids or bound in membrane), consistent with the upper chain length that was found within the neoformed macromolecule. Thus, it is likely that lipids that are originally functionalized (e.g. unsaturated and saturated fatty acids in this experiment) are a component of the macromolecule. Further, the chain length of the aliphatic component in fossil shrimp does not exceed C_{24} (Baas et al. 1995; Gupta et al. 2008b), presumably reflecting the maximum chain length of the lipid available for incorporation from the organism. Analysis of 191 Da mass chromatograms did not reveal any bacterially derived hopanoids and the *n*-alkyl chain length remained at C_{24} during the course of the experiment without any change in distribution, likely reflecting the maximum chain length of the fatty acid incorporated from the decaying carcass. Despite these observations, a minor bacterial contribution to the *n*-alkyl component cannot be ruled out completely. The lack of lipid incorporation into the scorpion and cockroach cuticles (both of which are much thicker and more robust than the shrimp cuticle) during the course of the experiment presumably reflects their resistance to decay as clearly demonstrated using electron microscopy. Indeed, analysis of fossils from the Oligocene at Enspel, Germany revealed that beetles retain a chitin-protein signature but flies, which have a thinner more decay-prone cuticle, are transformed to an aliphatic composition (Stankiewicz et al. 1997). Shrimp cuticle does not have the waxy epicuticle that is present in the cockroach and scorpion; waxes offer additional protection from microbial attack.

Ancient sedimentary organic matter is formed by diagenetic alteration of precursor biological material yielding a non-hydrolysable, organic solvent-insoluble macromolecule called kerogen (Tissot and Welte 1984). Kerogen formation is fundamental to the formation of fossil fuels and to the preservation of organic fossils. The formation of kerogen depends on the nature of the biological input, the environment of deposition and the diagenetic pathway (de Leeuw 2007; de Leeuw et al. 2006). Kerogens that serve as a source of petroleum products following catagenesis have a high hydrogen content because of significant aliphatic components in the macromolecule (e.g., Type I/II). Recent research revealed that labile components such as lipids become incorporated *in situ* to generate an aliphatic component, a process demonstrated in a range of fossils of diverse starting compositions including chitin, protein, lignin, polysaccharides, cutin and cutan (for review see Gupta et al. 2007e; de Leeuw 2007). Oxidative crosslinking may play an important role during early diagenesis where molecular oxygen reacts with unsaturated lipids to form a macromolecular *n*-alkyl component as demonstrated in fossil algae (Versteegh et al. 2004) and invertebrates (Gupta et al. 2008a).

The focus on seeking the oldest examples of original chemical constituents such as chitin and protein in fossils (e.g., Stankiewicz et al. 1997; Gupta et al. 2007c), has meant that less attention has been devoted to determining the rate at which the transformation to an aliphatic composition takes place. Future studies should focus on archaeological and late Cenozoic remains, investigating progressively older material in order to detect the onset of lipid incorporation and presence of an aliphatic component in the geopolymer. Aliphatics are present in *Hymenaea* leaves from ~20,000 year old fossil resin from Kenya, for example, although they are absent from insect remains from the same source (Stankiewicz et al. 1998b). The evidence presented here demonstrates that the formation an aliphatic macromolecule through the incorporation of lipids into decaying tissues does not require elevated temperatures and pressures. This result lends important experimental confirmation of the concept of *in situ* lipid incorporation and geopolymer formation as a mechanism for generating the significant aliphatic content ubiquitous in fossil organic matter. Furthermore it shows that this process can start at a very early stage, during the decay of the organism.

References

- Baas M, Briggs DEG, van Heemst JDH, Kear AJ, de Leeuw JW (1995) Selective preservation of chitin during the decay of shrimp. *Geochim Cosmochim Acta* 59:945–951
- Briggs DEG (1999) Molecular taphonomy of animal and plant cuticles: selective preservation and diagenesis. *Philos Trans R Soc Lond B Biol Sci* 354:7–16
- Briggs DEG, Kear AJ (1994) Decay and mineralization of shrimps. *Palaios* 9:431–456
- Briggs DEG, Kear AJ, Baas M, de Leeuw JW, Rigby S (1995) Decay and composition of the hemichordate Rhabdopleura: implications for the taphonomy of graptolites. *Lethaia* 28:15–23
- de Leeuw JW (2007) On the origin of sedimentary aliphatic macromolecules: a comment on recent publications by Gupta et al. *Org Geochem* 38:1585–1587

- de Leeuw JW, Versteegh GJM, Van Bergen PF (2006) Biomacromolecules of plants and algae and their fossil analogues. *Plant Ecol* 189:209–233
- Duncan IJ, Titchener F, Briggs DEG (2003) Decay and disarticulation of the cockroach: implications for the preservation of the blattoids of Writhlington (Upper Carboniferous), UK. *Palaios* 18:256–265
- Gupta NS, Collinson ME, Briggs DEG, Evershed RP, Pancost RD (2006a) Reinvestigation of the occurrence of cutan in plants: implications for the leaf fossil record. *Paleobiology* 32:432–449
- Gupta NS, Briggs DEG, Pancost RD (2006b) Molecular taphonomy of graptolites. *J Geol Soc Lond* 163:897–900
- Gupta NS, Michels R, Briggs DEG, Evershed RP, Pancost RD (2006c) The organic preservation of fossil arthropods: an experimental study. *Proc R Soc Lond B* 273:2777–2783
- Gupta NS, Tetlie OE, Briggs DEG, Pancost RD (2007a) Fossilization of eurypterids: a product of molecular transformation. *Palaios* 22:399–407
- Gupta NS, Briggs DEG, Collinson ME, Evershed RP, Michels R, Jack KS, Pancost RP (2007b) Evidence for the in situ polymerisation of labile aliphatic organic compounds during the preservation of fossil leaves: implications for organic matter preservation. *Org Geochem* 38:499–522
- Gupta NS, Briggs DEG, Collinson ME, Evershed RP, Michels R, Pancost RD (2007c) Molecular preservation of plant and insect cuticles from the Oligocene Enspel Formation, Germany: evidence against derivation of aliphatic polymer from sediment. *Org Geochem* 38:404–418
- Gupta NS, Michels R, Briggs DEG, Collinson ME, Evershed RP, Pancost RD (2007d) Experimental evidence for the formation of geomacromolecules from plant leaf lipids. *Org Geochem* 38:28–36
- Gupta NS, Briggs DEG, Collinson ME, Michels R, Evershed RP, Pancost RD (2007e) De Leeuw comment “On the origin of sedimentary aliphatic macromolecules”. *Org Geochem* 38:1588–1591
- Gupta NS, Briggs DEG, Landman NH, Tanabe K, Summons RE (2008a) Molecular structure of organic components in cephalopods: evidence for oxidative cross linking in fossil marine invertebrates. *Org Geochem* 39:1405–1414
- Gupta NS, Cambra-Moo O, Briggs DEG, Love GL, Fregenal-Martinez MA, Summons RE (2008b) Molecular taphonomy of macrofossils from the Cretaceous Las Hoyas Formation, Spain. *Cretac Res* 29:1–8
- Krzczkowski RA (1970) Fatty acids in raw and processed Alaska pink shrimp. *J Am Oil Chem Soc* 47:451–452
- Mösle B, Collinson ME, Finch P, Stankiewicz BA, Scott AC, Wilson R (1998) Factors influencing the preservation of plant cuticles: a comparison of morphology and chemical comparison of modern and fossil examples. *Org Geochem* 29:1369–1380
- Stankiewicz BA, Briggs DEG, Evershed RP, Flannery MB, Wuttke M (1997) Preservation of chitin in 25-million year-old fossils. *Science* 276:1541–1543
- Stankiewicz BA, Mastalerz M, Hof CHJ, Bierstedt A, Briggs DEG, Evershed RP (1998a) Biodegradation of chitin protein complex in crustacean cuticle. *Org Geochem* 28:67–76
- Stankiewicz BA, Poinar HN, Briggs DEG, Evershed RP, Poinar GO Jr (1998b) Chemical preservation of plants and insects in natural resins. *Proc R Soc Lond B* 265:641–647
- Stankiewicz BA, Briggs DEG, Michels R, Collinson ME, Evershed RP (2000) Alternative origin of aliphatic polymer in kerogen. *Geology* 28:559–562
- Tissot B, Welte DH (1984) *Petroleum formation and occurrence*, 2nd edn. Springer, Berlin
- Versteegh GMJ, Blokker P, Wood GD, Collinson ME, Sinninghe Damsté JS, de Leeuw JW (2004) An example of oxidative polymerization of unsaturated fatty acids as a preservation pathway for dinoflagellate organic matter. *Org Geochem* 35:1129–1139

Chapter 7

Molecular Preservation of Eurypterids

Abstract The fossil remains of eurypterid cuticles, yield long-chain (<C₉ to C₂₂) aliphatic components during Pyrolysis-Gas chromatography-mass spectrometry, similar to type II kerogen in contrast to chitin and protein that constitutes the bulk of modern analogs. Structural analysis (thermochemolysis) of the eurypterid cuticle revealed fatty acyl moieties (derived from lipids) of chain lengths C₇ to C₁₈, with C₁₆ and C₁₈ being the most abundant. The residue was immune to base hydrolysis, indicating a highly recalcitrant nature and suggesting that if ester linkages are present in the macromolecule, they are sterically protected. Some samples yielded phenols and polyaromatic compounds indicating a greater degree of aromatisation, which correlates with higher thermal maturity as demonstrated by Raman spectroscopy. Analysis (including thermochemolysis) of the cuticle of modern scorpion and horseshoe crab, living relatives of the eurypterids, showed that C₁₆ and C₁₈ fatty acyl moieties likewise dominate. Assuming that the original composition of the eurypterid cuticle was similar to that in living chelicerates, fossilization likely involved the incorporation of such lipids into an aliphatic polymer.

Keywords Marine • Sea scorpion • Aliphatic • Fatty acid • Raman spectroscopy

Introduction

In this chapter the chemistry of eurypterid cuticles from a range of localities (Table 7.1) is analyzed and compared to the composition of the cuticle of their modern relatives—scorpions and horseshoe crabs—in order to interpret their molecular preservation. Eurypterids, known also as sea scorpions, are extinct aquatic arthropods belonging to the Chelicerata. They first appeared in the Middle Ordovician, peaked in diversity in the Late Silurian, and became extinct towards the end of the Permian (Plotnick 1999). The large number of mainly Silurian species makes the eurypterids the most diverse Paleozoic chelicerate group. About 30 % of eurypterid genera include representatives over 80 cm long (Briggs 1985).

Table 7.1 Cuticles analysed in this study

Sample and taxon	Locality and stratigraphy	Lithology (total organic content)	Composition
<i>Pandanus imperator</i> ^a , <i>Limulus polyphemus</i> ^b	Recent		Chitin, protein, lipids (including C ₁₆ and C ₁₈ fatty acids)
<i>Adelophthalmus</i> sp. ^{a,c}	Joggins, Nova Scotia, Canada Bashkirian	Greenish-grey shale	Aliphatic (C ₆ -C ₃₀), benzene, phenol and naphthalene derivatives
Scorpion ^{a,c}	Joggins, Nova Scotia, Canada Bashkirian	Greenish-grey shale	Aliphatic (C ₆ -C ₃₀), benzene, phenol derivatives
Scorpion ^{a,c}	Lone Star Lake, Kansas, USA, Kazimovian/Gzelian	Grey shale	Aliphatic (C ₆ -C ₃₀), benzene, phenol derivatives, polyaromatic hydrocarbons
<i>Eurypterus dekeyi</i> ^{b,c} YPM 209619 (paddle)	Ridgemount Quarry, Ontario, Canada, Williamsville Fm., Pridolian	Dolomite (0.81)	Aliphatic (<C ₉ -C ₂₀)
<i>E. lacustris</i> ^{b,c} YPM 209615 (coxa)	Ridgemount Quarry, Ontario, Canada, Williamsville Fm.	Dolomite (0.81)	Aliphatic (<C ₉ -C ₂₂)
<i>E. lacustris</i> ^{b,c} YPM 209616 (pretelson)	Ridgemount Quarry, Ontario, Canada, Williamsville Fm.	Dolomite (0.81)	Aliphatic (<C ₉ -C ₂₁)
<i>E. lacustris</i> ^{b,c} YPM 209618 (carapace)	Ridgemount Quarry, Ontario, Canada, Williamsville Fm.	Dolomite (0.81)	Aliphatic (<C ₉ -C ₂₂)
<i>E. lacustris</i> ^{b,c} YPM 209620 (paddle)	Fort Erie Rail cut, Ontario, Canada, Williamsville Fm.	Dolomite (1.14)	Aliphatic (<C ₉ -C ₂₂); fatty acyl moieties (C ₇ -C ₁₈)
<i>Pterygotus startei</i> ^{b,c} YPM 174611 (telson)	Spring house, Pittsford, New York, USA, Vernon Fm., Ludlovian	Shales and calcareous mudstones	Aliphatic (<C ₉ -C ₃₀); fatty acyl moieties (C ₇ -C ₁₈)
<i>P. venricosus</i> ^{b,c} YPM 209622 (telson)	Kokomo, Indiana, USA, Wabash Fm., Ludlovian	Laminated, argillaceous limestone (0.22)	Aliphatic (<C ₉ -C ₂₂)

^aSubjected to py-GC-MS^bSubjected to thermochemolysis and py-GC-MS^cSubjected to Raman spectroscopy

They were the dominant predators in certain nearshore and peritidal settings (Kluessendorf 1994). Eurypterids are considered to be the sister group of Arachnida (Weygoldt and Paulus 1979).

The organic nature of eurypterid cuticles has long been known, and early studies of the detailed morphology of these arthropods were based on material from the Silurian of Oesel (Saaremaa), Estonia, prepared by dissolving the enclosing matrix (Holm 1898; Wills 1965; Selden 1981). The fossil record of eurypterids is primarily the result of organic preservation of the cuticle, mainly representing molts (Selden 1984), although the Ordovician Soom Shale of South Africa preserves evidence of such internal structures as muscle tissue, as a result of very early authigenic mineralization (Braddy et al. 1995, 1999).

Most work on eurypterid cuticle has dealt with its ultrastructure (e.g., Dalingwater 1973). An early analysis of the chemistry of cuticle from Saaremaa tested its resistance to weak acids and bases, and suggested that it is composed of chitin (Rosenheim 1905), although other long-chain polymers are also resistant to such treatment. A preliminary study of the composition of the cuticle of a Carboniferous eurypterid, *Adelophthalmus* sp., showed that it lacked traces of chitin and the cuticle had been altered to an aliphatic geopolymer (Stankiewicz et al. 1998a). The original composition of eurypterid cuticle was presumably similar to that of *Limulus* and scorpions, as inferred from the extant phylogenetic bracket (Witmer 1995).

Material

A number of settings preserve eurypterid cuticles in a manner that allows them to be peeled or scraped off the rock surface. Fossil cuticles were analysed from six different localities and five different horizons in Ontario and Nova Scotia (Canada), Kansas, Indiana and New York (USA); three of the horizons are Silurian, whereas two are Carboniferous in age (Table 7.1). The oldest is the Kokomo Member of the Wabash Formation of Indiana, interpreted as Ludlow (ca 420 MA) based on conodonts (Kleffner and Rexroad 1999). The Kokomo Member is a finely laminated, argillaceous limestone with alternating dark and light bands. The other Silurian horizons sampled are in New York and Ontario, Canada, and their stratigraphic relationships are well known. The Pittsford Member of the Vernon Formation in New York is Late Ludlow, and slightly younger (ca 419 MA) than Kokomo, and is composed of dark grey to black shales and olive calcareous mudstones. The youngest Silurian horizon is the Williamsville A Member (ca 417 MA), represented by the fossils from Ridgemount Quarry and Fort Erie town, both in Ontario, Canada. The Williamsville A Member of the Williamsville Formation is a dolomite with high magnesium content. The Carboniferous sequence at Joggins, Nova Scotia, is Bashkirian in age (ca 312–313 MA) and consists of alluvial and lacustrine deposits in the Cumberland Group; the sample analyzed here came from a greenish grey shale horizon from within a red mudrock and sandstone sequence close to the

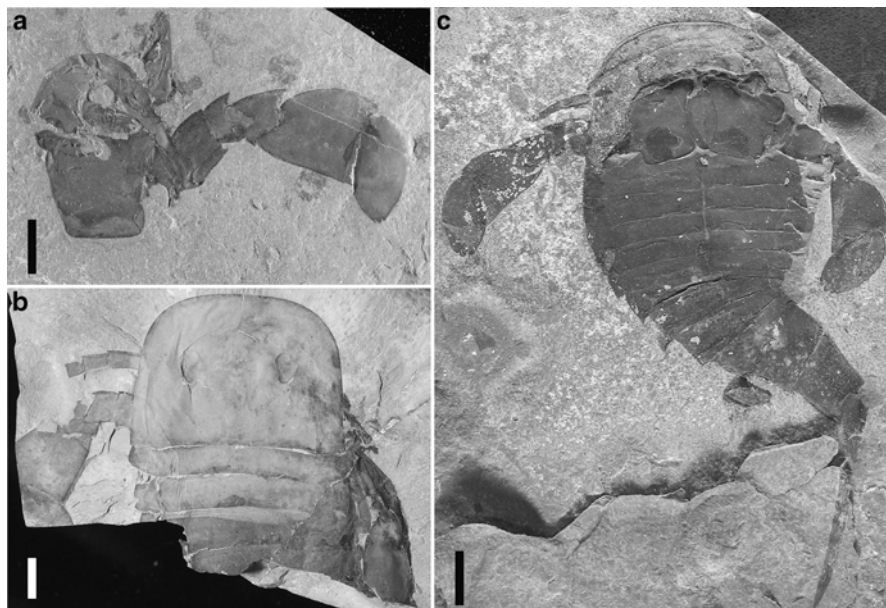


Fig. 7.1 Some of the specimens with preserved cuticle that were analysed (for correlation, see Table 7.1). Scale bars 10 mm. (a) *Eurypterus lacustris* from Ridgemount Quarry, Canada (YPM 209615). (b) *E. lacustris* from Fort Erie railroad cut, Canada (YPM 209620). (c) *E. dekayi* from Ridgemount Quarry, Canada (YPM 209619)

base of the Joggins Formation (Stankiewicz et al. 1998a). The slightly younger horizon at Lone Star Lake, Kansas, which yields scorpion material used for comparison, is Kasimovian or Gzelian age (ca 303 MA). The samples came from bed 13 of Archer and West (1991), a grey shale. The new cuticle samples analyzed are held in the Yale Peabody Museum (YPM) under the repository numbers given in Table 7.1.

The eurypterid cuticles analysed represent five different taxa belonging to three different clades, or superfamilies, of eurypterids. They were almost exclusively carbonaceous and no mineralization (e.g., phosphatisation) was observed. The superfamily Eurypteroidea is represented by *Eurypterus lacustris* (Fig. 7.1a–b) and *E. dekayi* (Fig. 7.1c), both from the Williamsville Formation. The superfamily Adelophthalmoidea is represented by *Adelophthalmus* sp. from the Joggins Formation, while the Pterygotoidea is represented by *Pterygotus ventricosus* from the Wabash Formation and *P. sarlei* from the Vernon Formation. The cuticle of two modern chelicerates, the emperor scorpion *Pandinus imperator* and the North American horseshoe crab *Limulus polyphemus*, were used for comparative analysis. Horseshoe crabs are widely accepted as a sister group to (eurypterids + arachnids); the position of scorpions is more equivocal, but they are usually considered close to eurypterids (e.g., Dunlop and Braddy 2001).

Methods

Fossil samples were carefully removed from host rock, crushed with a mortar and pestle, and transferred to glass vials. They were then ultrasonicated in deionised water for 10 min for three times to remove adhering rock. Following this, the samples were baked at 70 °C for 1 h to remove any residual water. Samples of eurypterid cuticle were then extracted ultrasonically three times, 15 min each with 2:1- CH₂Cl₂ (DCM): CH₃OH (methanol) to yield an insoluble residue. Thus, care was taken to ensure that samples analysed were pure and without contamination that might otherwise be adsorbed or absorbed to the organic matter (e.g. see Brocks et al. 2003). Residue was analysed by *in situ* Raman imagery to determine the nature of the carbonaceous material and by Pyrolysis-Gas chromatography-mass spectrometry (Py-GC-MS) to reveal the molecular distribution of compounds. Selected samples were analysed by thermochemolysis (pyrolysis in the presence of tetramethyl ammonium hydroxide (TMAH); de Leeuw and Baas 1993) to permit structural analysis of the macromolecule and particularly ester moieties. Other samples were hydrolysed in 1 M 95 % methanoic NaOH (saponification) for 1 h at 70 °C to test the resistance of the macromolecule to base hydrolysis and then subjected to thermochemolysis to determine the structure of the recalcitrant residue. Table 7.1 outlines the samples investigated and the specific techniques applied to them.

Cuticle was physically removed from modern specimens of *Pandinus imperator* and boiled in deionised water for 1 h to eliminate any residual epidermal tissue. Cuticle was analysed from a molt of *Limulus polyphemus*. The modern samples were analysed without solvent extraction in order to evaluate the entire molecular distribution including the lipid moieties, which would be removed by solvent extraction. For discussion on lipid composition of arthropods see Howard and Blomquist (2005), Stankiewicz et al. (2000). In contrast, the fossils were solvent extracted prior to analysis to reveal the composition of the macromolecular organic matter by removing soluble impurities. Raman imagery, pyrolysis, and thermochemolysis were applied to samples of *Eurypteruslacustris*, *Pterygotusventricosus* and *P. sarlei* (Table 7.1), and Raman imagery and pyrolysis were applied to *Eurypterusdekayi*. Raman imagery was performed on an adelophthalmid and a scorpion from Joggins, and a scorpion from the Lone Star Formation, a sample suite which had been subjected to pyrolysis previously (Stankiewicz et al. 1998a). The host sediment was extracted in organic solvent (as described) and analysed with Py-GC-MS in order to compare it with the composition of the eurypterids.

Flash pyrolysis involves the thermal fragmentation of the chemical constituents of a sample at high temperatures in an inert medium. These fragments are then separated and identified by GC-MS. Thus, flash pyrolysis (Py-GC-MS) reveals bulk macromolecular information, and the method has been used extensively in the molecular characterisation of insoluble fossil organic matter (Larter and Horsfield 1993; Logan et al. 1993; van Bergen et al. 1995; Stankiewicz et al. 1996). Samples were analysed with a Perkin Elmer GC-MS. A CDS (Chemical Data System) AS-2500 Pyroprobe pyrolysis unit was used with both the injector and interface temperature at 290 °C. One hundred to 150 micrograms of

solvent-extracted scorpion or eurypterid cuticle were weighed into quartz tubes using a microanalytical balance and pyrolysed at 610 °C. No absolute quantitation was attempted. Separation of pyrolysis products was achieved using a DB-1 fused silica capillary column (30 m, 0.25 mm i.d., 0.1 µm film thickness). The GC oven was programmed from 40–50 °C (held at 4 min) to 320 °C at 5 °C min⁻¹ and held at that temperature for 15 min. A thermal hold of 3–5 min was applied. Helium was the carrier gas. The MS was operated at 70 eV scanning over the range m/z 45–600 at 1 scan/s with an emission current of 300 micro-amperes (full scan mode). Compounds were identified using the NIST mass spectral library and spectra reported in the literature (Stankiewicz et al. 1996). Modern *Limulus* cuticle was pyrolysed using a CDS 5150 Pyroprobe by heating at 650 °C for 20 s to fragment macromolecular organic components. Compound detection and identification was performed by on-line GC-MS in full-scan mode on a Hewlett Packard HP6890 gas chromatograph interfaced to a MicromassAutoSpecUltima magnetic sector mass spectrometer. GC separation was performed on a J&W Scientific DB-1MS capillary column (60 m length, 0.25 mm internal diameter, 0.25 µm film thickness) using He as the carrier gas. Samples were injected in splitless mode at 300 °C. The oven was programmed from 60 (held for 2 min) to 150 °C at 10 °C min⁻¹, then at 3 °C min⁻¹ to 315 °C and held isothermal for 24 min. The source was operated in electron ionization (EI) mode at 70 eV ionization energy at 250 °C. The AutoSpec full-scan rate was 0.80 s/decade over a mass range of 50–600 Da and a delay of 0.20 s/decade.

For TMAH (tetramethylammonium hydroxide) assisted pyrolysis, an aliquot of the lipid-extracted residue was transferred to a fresh vial and 1 ml TMAH solution (25 wt %) was added to the sample. The sample was soaked in TMAH solution for 3–4 h prior to analysis to ensure that sufficient TMAH was available during on-line pyrolysis, also conducted at 610 °C. Blanks with and without TMAH were run before analysis of all samples as a control to ensure that there was no contamination.

Raman scattering provides a nondestructive, noninvasive method for microscale characterization of carbonaceous material. It can be applied to samples ranging from megascopic to as small as 1 µm (Kudryavtsev et al. 2001), which is especially useful when the amount of cuticle is minimal and not amenable to other techniques. *In situ* Raman microspectroscopy was carried out with a LABRAM spectrometer (JobinYvon) with a Nd-YAG 532 nm laser source and a Peltier-cooled CCD detector. Cuticle samples were mounted on standard glass slides. The laser was focused on the sample with a 500 nm confocal hole using the 50x objective under reflected light. The spot on the sample was ~1.5 µm in diameter and had a power ~1 mW at the sample surface. Jobin Yvon's LabSpec program was used for data acquisition and estimation of Raman peaks. A minimum of 10 independent spots was analyzed and data were collected for 10–20 s per spot depending upon the Raman intensity. The spot was measured over a spectral window of 1,000–2,000 cm⁻¹. The spectra were deconvoluted into bands (Rahl et al. 2005), pertaining to ordered and disordered carbonaceous matter. Carbonaceous material is best characterized by first-order Raman peaks or bands, which occur with

wavenumber offsets between 1,000 and 1,800 cm^{-1} (Kudryavtsev et al. 2001). The LabSpec program was used to estimate the dimensional parameters of the bands (Rahl et al. 2005).

Results

Py-GC-MS of the cuticle of the modern scorpion *Pandinus imperator* (Fig. 7.2a, Table 7.2) and the horseshoe crab *Limulus polyphemus* (Fig. 7.2b) reflect the known composition of living arthropod cuticles, which consist of chitin fibres embedded in a protein matrix interlinked by catechol moieties (Schaefer et al. 1987, Fig. 7.2b; See Stankiewicz et al. (1996) for details on identification and structure of fragment ions). Thermochemolysis of *Limulus* cuticle reflects the distribution of fatty acyl moieties; C_{16} and C_{18} fatty acids were the most dominant (Fig. 7.2c). Such acyl moieties are not detected during pyrolysis of model chitin or protein compounds (Stankiewicz et al. 1996); hence, the C_{16} and C_{18} fatty acyl moieties in the pyrolysate of *Limulus* and modern scorpion likely derive from lipids associated with the cuticle.

No chitin or protein was detected in the eurypterid cuticles. Py-GC/MS analyses of samples in this study revealed the breakdown products of an aliphatic polymer with detected chain lengths typically extending from $<\text{C}_9$ to C_{22} (Fig. 7.3). Those $<\text{C}_9$ were not detected as they probably eluted during the thermal hold time of the MS. All the samples showed a very similar distribution, with the C_9 to C_{15} alkane and alkene homologues being the most abundant, irrespective of body part, species and lithology (Table 7.1). Benzene derivatives were also detected, but phenols and polyaromatic hydrocarbons (naphthalene, anthracene) were absent. Pyrolysis of the surrounding sediment resulted in no yield, due to its organic lean nature.

Thermochemolysis of the eurypterid cuticle yielded fatty acids ranging from C_7 to C_{18} with an even over odd predominance (Fig. 7.4). The most abundant fatty acyl moieties were those with chain lengths of C_{16} and C_{18} . Hydrolysis of the cuticle in basic conditions followed by thermochemolysis yielded a similar distribution of fatty acyl moieties. No sulfur-bearing compounds were detected in the pyrolysate.

Raman scattering of areas of cuticle (Fig. 7.5) revealed vibrational bands characteristic of carbonaceous materials at 1,350 and 1,580 cm^{-1} , which are commonly designated D(disordered) and G(ordered or graphitic), respectively. The ratio between the two bands is temperature sensitive: with increased thermal maturity, the ordered band Gband becomes more prominent (Beysac et al. 2002). Samples of *Eurypterusdekayi*, *E. lacustris*, *Pterygotussarlei* and *P. ventricosus* showed a similar band distribution—a typical spectrum of *E. lacustris* (Fig. 7.5), attesting to the similar maturity of all the samples independent of body part and lithology. In contrast, the Raman spectra of the adelophthalmid eurypterid and scorpion from Joggins previously analysed by Stankiewicz et al. (1998a) revealed band parameters, such as a more pronounced peak height of the G band than that of the D band (Fig. 7.5), indicating greater thermal maturity (Rahl et al. 2005). Raman spectra of the scorpion from LoneStarLake indicate a thermal maturity intermediate between the other two sample sets.

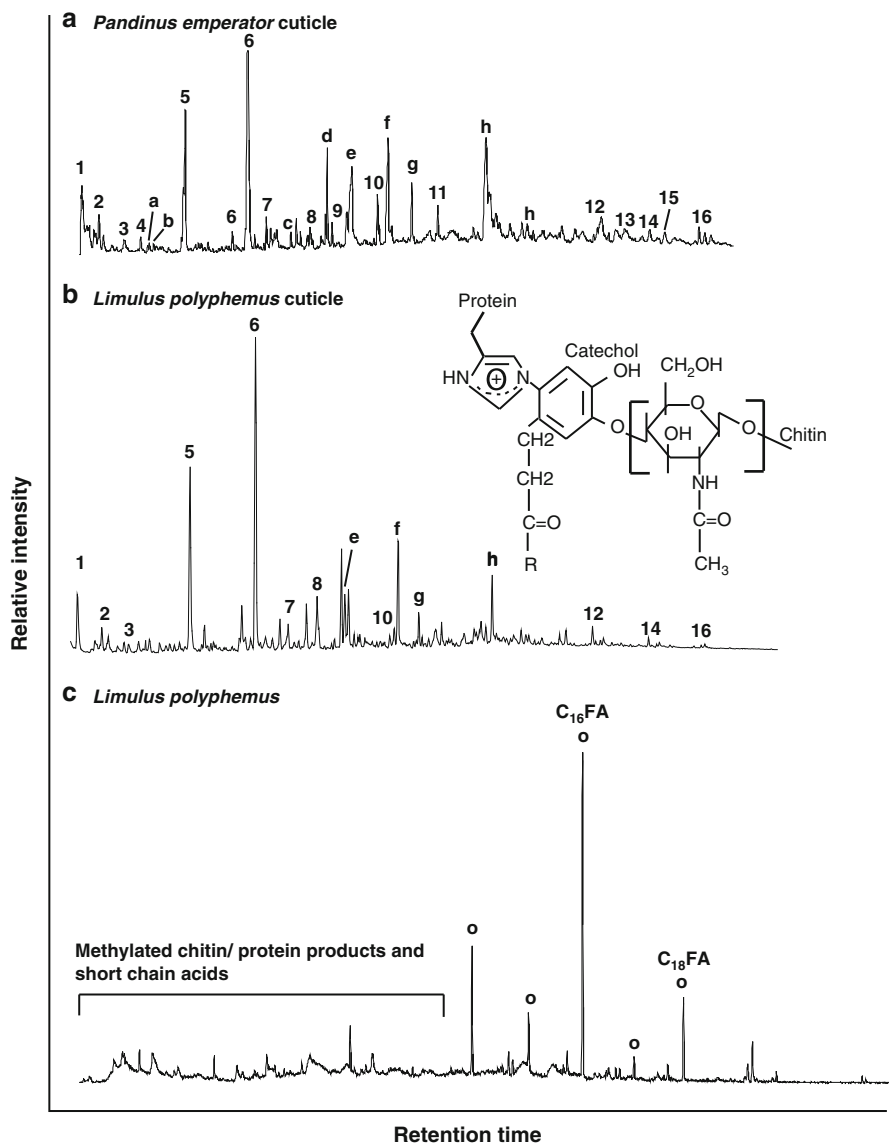


Fig. 7.2 Py-GC-MS analysis of modern scorpion and *Limulus* cuticles. (a) Partial Py-GC-MS chromatogram of modern *Pandinus imperator* cuticle revealing the presence of chitin or protein and cuticular lipids. (b) Partial Py-GC-MS chromatogram of *Limulus* cuticle revealing the same, with the inset showing the chemical structure of arthropod cuticle (adapted from Stankiewicz et al. 1996). (c) Partial TMAH pyrolysis (thermochemolysis)-GC/MS chromatogram of *Limulus* cuticle revealing the distribution of fatty acyl moieties (o). Note difference in retention time of the acids during thermochemolysis (Fig. 7.2c) compared to that from pyrolysis (Fig. 7.2a) due to methylation reactions. Retention time in Fig. 7.2a b and are different because of different GC programs used. For key to annotations see Table 7.2

Table 7.2 List of major products in the pyrolyzates of *Pandinus imperator* and *Limulus polyphemus*

Peak	MS characteristics (m/z)	Compound name	Origin
1	92 , 91, 65	Toluene	Phenylalanine
2	81 , 80 , 52	C ₁ -Pyrroles	Proline, Hydroxyproline
3	104 , 78, 51	Styrene	Phenylalanine
4	95 , 94 , 80	C ₂ -Pyrrole	Hydroxyproline?
a	107 , 79 , 51, 78	2-Pyridinecarboxaldehyde	Chitin
b	109 , 67 , 107	Acetylpyrrole	Chitin
5	94 , 66	Phenol	Tyrosine
6	108 , 107, 77	C ₁ -Phenol	Tyrosine
7	117 , 90, 116	Ethylcyanobenzene	Phenylalanine
c	123 , 80 , 81, 52	Acetyldihydropyridine	Chitin
8	122 , 107	C ₂ -Phenol	Tyrosine
d	137 , 109 , 95, 81, 68, 53	Acetylpyridone	Chitin
9	131 , 91 , 65	Propylcyanobenzene	Phenylalanine
e	125 , 83 , 54, 42, 53	3-Acetamidofuran	Chitin
10	117 , 90, 89	Indole	Tryptophan
f	139 , 97 , 69, 42, 53	3-Acetamido-5-methylfuran	Chitin
g	153 , 111 , 82, 42, 83	3-Acetamido-4-pyrone	Chitin
11	131 , 130 , 77	C ₁ -Indole	Tryptophan
h	185 , 84 , 55, 83, 42	Oxazoline structure	Chitin
12	168 , 70 , 97, 125, 165	2,5-Diketopiperazine derivatives	Proline-Alanine
13	154 , 83 , 111, 70, 98	Pyrrolidinopiperazine derivatives	Proline-Glycine, Proline-Lysine
14	70 , 154, 72, 55, 125	2,5-Diketopiperazine derivative	Proline-Valine, Proline-Arginine
15	70 , 154, 125, 40, 54	2,5-Diketopiperazine derivative	Proline-Valine, Proline-Arginine
16	194 , 70 , 154, 54, 86	2,5-Diketopiperazine derivative	Proline-Proline

Notes:

Letters=compounds characteristic of chitin and numbers refer to pyrolysis products of proteins. *m/z* values in **bold** indicate base peak and masses underlined indicate molecular ions (M⁺). Ions after the base peak are in descending order of their relative abundances
C₁ refers to methyl, C₂ refers to dimethyl or ethyl etc.

Discussion

The fossilization of eurypterids was attributed to the decay resistant properties of their cuticle (e.g., Clarke and Ruedemann 1912). Indeed, the composition of the cuticle of the most closely related living chelicerates as scorpions and horseshoe crabs indicates that it is more decay resistant than other parts of the body. Nonetheless, chitin is prone to degradation by chitinophosphatic bacteria (Stankiewicz et al. 1998b), as well as by oxidation and hydrolysis. The results of this study confirm that the cuticle of eurypterids is composed of a nonhydrolyzable macromolecule with a long-chain aliphatic component similar to Type II kerogen, and such a nonhydrolyzable aliphatic component is absent in the cuticle of their

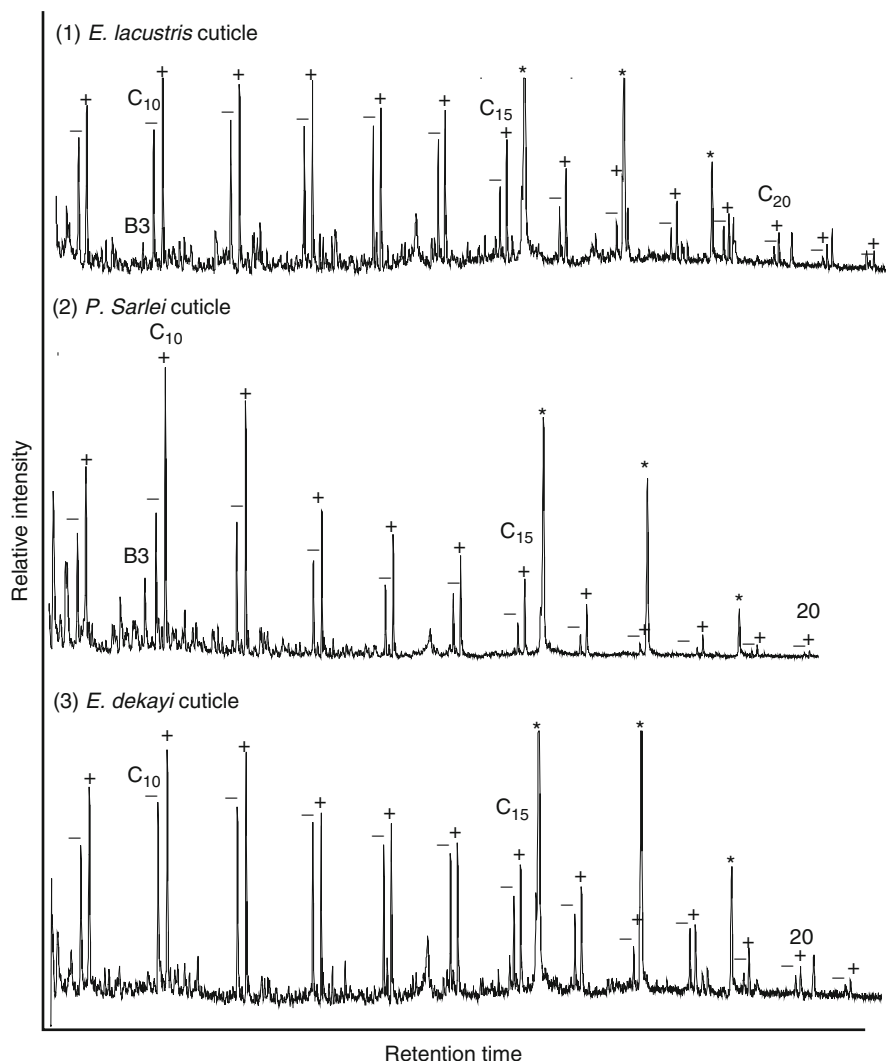


Fig. 7.3 Py-GC-MS analysis of eurypterids. Partial Py-GC-MS chromatogram of (a) *Eurypterus lacustris*, (b) *Pterygotussarlei* and (c) *E. dekeyi* cuticles revealing the presence of dominant aliphatic component as indicated by the homologues series of *n*-alkanes (+) and *n*-alkenes (-). B3: trimethyl benzene, methyl ethyl benzene. C_n indicates alkane and alkene homologue with *n* denoting the carbon chain length. * contaminant from GC septum

living relatives. Aliphatic components may be overestimated by pyrolysis and NMR studies (Poirier et al. 2000) and other such structures as condensed aromatics that may be structurally important in the fossil polymer may not be amenable to pyrolysis. It is difficult to obtain a sufficient sample of fossil arthropod cuticle for ¹³C solid-state NMR studies so pyrolysis has been the preferred mode of analysis.

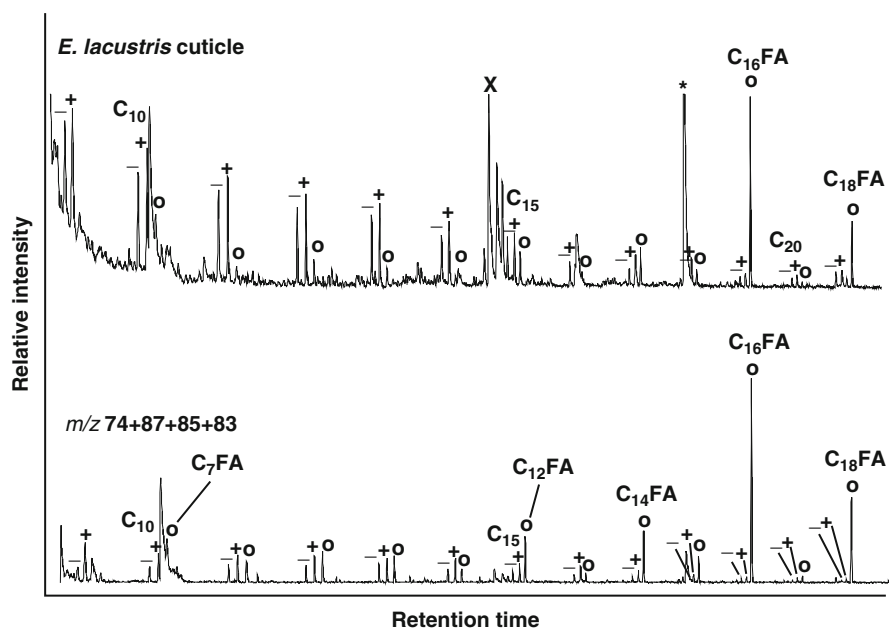


Fig. 7.4 Partial TMAH Py-GC-MS chromatogram of *Eurypterus lacustris* cuticle and m/z 74+87+85+83 mass chromatogram revealing the presence of constituent fatty acyl moieties (o) with respect to the alkane/alkene homologues (+). C_n indicates alkane/alkene or fatty acyl homologue with n denoting the carbon chain length. X is an unknown compound with mass fragment ions 164 and 193

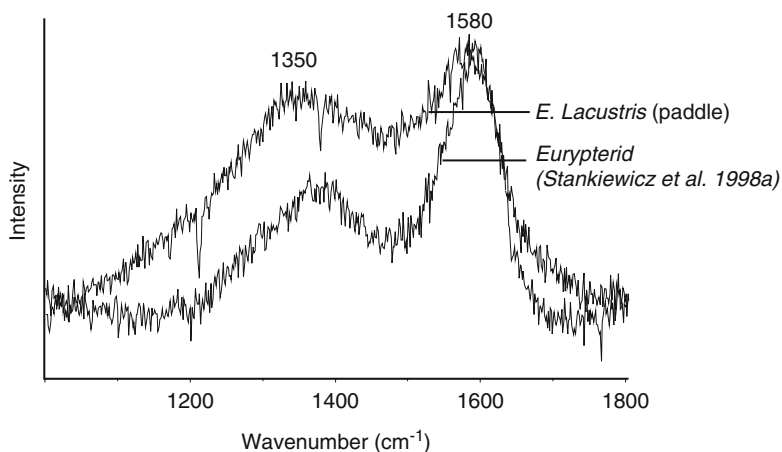


Fig. 7.5 *In situ* Raman imagery of samples of cuticles of *Eurypterus lacustris*, Fort Erie Rail cut, Ontario, Canada, and *Adelophthalmus* sp. from the Joggins Formation, Nova Scotia, Canada, revealing spectral characteristics of carbonaceous material and, particularly, peaks associated with the presence of disordered (D; $\sim 1,350$ cm^{-1}) and ordered (G; $\sim 1,580$ cm^{-1}) carbon

Solid-state ^{13}C NMR analysis (Gupta et al. 2007a), however, revealed a significant aliphatic content in an analogous investigation of fossil leaves (Gupta et al. 2007b).

Given the widespread occurrence of aliphatic components in sediments, insect, and plant fossils, the occurrence of aliphatic components in organic fossils might be attributed to migration (Baas et al. 1995; van Bergen et al. 1995). This possibility, however, has been countered by a number of considerations: (1) Aliphatic polymers are characteristically insoluble, and therefore relatively immobile (for discussion see Briggs 1999); (2) An aliphatic signal was detected in Tertiary *Hymenaea* leaves and beetles trapped in amber (Table 7.2), where they are protected from external contamination (Stankiewicz et al. 1998c); (3) The aliphatic signatures in co-occurring plant and insect fossils from the Late Carboniferous of North America are different, indicating that they could not have been introduced solely from the original sediment (Stankiewicz et al. 1998a), and the internal morphology of the cuticle is altered indicating diagenesis; (4) The composition of artificially matured arthropod tissue is aliphatic (Stankiewicz et al. 2000; Gupta et al. 2006a) showing that endogenous organic matter can generate an aliphatic composition, as observed in fossils; (5) Thermochemolysis, providing distribution of fatty acids in fossils (de Leeuw and Baas 1993) of co-occurring insect and plant fossils and the associated organic-rich matrix revealed differences in the distribution of the constituent fatty acyl components, indicating that the aliphatic component of the fossil differ structurally from that in rock where the TOC is very high (ca. 20). The TOC of rock that yielded the eurypterids is ca 0.81 % and provided no yield during pyrolysis, such that migration is even more unlikely (Gupta et al. 2006a); (6) Logan et al. (1995) showed that leaf lipids in the Miocene *Clarkia* strata were concentrated on the leaf surfaces without migrating into the surrounding sediment. These lines of evidence show that introduction from other such sources as the host rock is not tenable as an explanation for the highly aliphatic composition of macrofossils.

Thermochemolysis of the eurypterid cuticles yielded fatty acyl moieties from C_7 to C_{18} (Fig. 7.4) dominated by C_{16} and C_{18} components. The presence of a very similar distribution in the cuticle of modern *Limulus*, presumably similar in composition to that of living eurypterids, suggests that lipids from the cuticle of the once-living eurypterid were incorporated into the fossil macromolecule. Py-GC-MS of *Pandinus* cuticle by thermochemolysis also yielded C_{16} and C_{18} fatty acyl moieties similar to the distribution observed in *Limulus*. Additionally, GC-MS and high temperature GC-MS analysis of the extractable lipid fraction of the modern scorpion cuticle showed that the fatty acyl moieties are dominated by long-chain saturated moieties ranging from C_{16} to C_{28} , and unsaturated moieties from C_{18} to C_{30} (Stankiewicz et al. 1998a, 2000). After base hydrolysis cleaves ester-bound lipids from the cuticular matrix, the cuticular fatty acyl moieties consist of C_{15} to C_{36} saturated and C_{16} to C_{28} mono-unsaturated components (Stankiewicz et al. 2000), which may also contribute to the formation of the aliphatic component.

The presence of fatty acid moieties in the pyrolysates suggests that ester linkages are important components of the fossils; however, if present, they are immune to base hydrolysis. This could be the result of steric protection of ester functional groups by the cross linking of aliphatic chains. Gupta et al. (2007b) posited a similar

explanation for the similar distribution of acids in leaf fossils before and after hydrolysis. Crosslinking via other such functional groups as vulcanisation via sulfur incorporation (Kok et al. 2000) or crosslinking through ether functional groups and oxidation could be important in kerogen (Gatellier et al. 1993; Riboulleau et al. 2001) and algae (Versteegh et al. 2004; de Leeuw et al. 2006). A lack of sulfur-bearing compounds, however, suggests that sulfur may not have been important in crosslinking the polymer in eurypterid cuticles, and data suggest that crosslinking is related instead to a combination of ether and sterically hindered ester bonds.

Such incorporation of lipids via *in situ* polymerization appears to be a major factor in the preservation of eurypterids. Such a process has been proposed to explain the preservation of fossil leaves (Gupta et al. 2006b, 2007b), graptolites (Gupta et al. 2006c) and the experimental maturation of modern arthropod cuticles (Gupta et al. 2006a). We have not detected characteristic such bacterial markers as hopanes in the extractable and hydrolysable fraction of organic fossils (Gupta et al. 2007b); thus evidence for incorporation of bacterial lipids is weak.

The aliphatic component in the Carboniferous cuticles from Joggins, Nova Scotia, Canada, and Lone Star Lake, Kansas, ranged to longer chain compounds (from C₆ to C₃₀, Stankiewicz et al. 1998a) than the samples analysed here, which did not exceed C₂₂. The Joggins and LoneStarLake samples also yielded phenols and polyaromatic compounds, indicating a greater degree of aromatisation (Table 7.1). This is consistent with the Raman spectra (Fig. 7.5). Increasing thermal maturity results in progressively more ordered carbonaceous matter (Beysac et al. 2002; Rahl et al. 2005). The Gpeak is more prominent relative to the D peak in the analysis of the adelophthalmid from Joggins than in the eurypterids from the Midcontinent, indicating greater thermal maturity, which is in turn reflected in greater aromatisation (Miknis et al. 1993). The disordered band is more prominent in *E. lacustris* from Ontario indicating that the thermal maturity of these eurypterid cuticles is lower than that of the adelophthalmid (Stankiewicz et al. 1998a), corresponding to their lower aromatic content. The Raman spectrum for the LoneStarLake scorpion indicates a thermal maturity intermediate between these two. These contrasts are echoed in other data on the thermal maturity of the rocks that yielded the cuticles. While thermal maturity varies within the Cumberland Group, which includes the Joggins Formation, a vitrinite reflectance value of 0.66 % R_o was obtained for the coal nearest the samples analysed here, indicating a burial temperature of >100°, and the majority of the deposits lie within the oil window (Mukhopadhyay et al. 2003). The vitrinite reflectance value of the Williamsburg Coal, source of the Lone Star Lake scorpion, is 0.51 % R_o, and the rank of the coal is high-volatile B bituminous (Brady and Hatch 1997), indicating a burial temperature of around 100 °C. The burial temperature of Silurian strata in southern Ontario, however, from which most of the eurypterids were collected, is only 60–80 °C, based on the Conodont Alteration Index (Legall and Barnes 1980). Raman imagery clearly holds promise for nondestructive, rapid, and inexpensive microscale characterisation of organic matter. Relative thermal maturity can also be assessed when vitrinite reflectance and measurement of such traditional biomarkers as hopane or sterane stereochemical ratios and other approaches are difficult due to small sample sizes.

References

- Archer A, West R (1991) Lone Star Spillway, Upper Lawrence Shale. In: Upper Pennsylvanian (Virgillian and Missourian) cyclothems in the Lawrence, Kansas Area, Kansas Geological Survey open-file report, vol 91–22, pp 89–94
- Baas M, Briggs DEG, van Heemst JDH, Kear AJ, de Leeuw JW (1995) Selective preservation of chitin during the decay of shrimp. *Geochim Cosmochim Acta* 59:945–951
- Beysac O, Geoffé B, Chopin C, Rouzaud JN (2002) Raman spectra of carbonaceous material in metasediments; a new geothermometer. *J Metamorph Geol* 20:859–871
- Braddy SJ, Aldridge RJ, Theron JN (1995) A new eurypterid from the Late Ordovician Table Mountain Group, South Africa. *Palaeontology* 38:563–581
- Braddy SJ, Aldridge RJ, Gabbott SE, Theron JN (1999) Lamellate book-gills in a late Ordovician eurypterid from the SoomShale, South Africa: support for a eurypterid-scorpion clade. *Lethaia* 32:72–74
- Brady LL, Hatch JR (1997) Chemical analyses of Middle and Upper Pennsylvanian Coals from south eastern Kansas. *Kans Geol Surv Bull* 240(4):43–65
- Briggs DEG (1985) Gigantism in Palaeozoic arthropods. *Spec Pap Palaeontol* 33:157
- Briggs DEG (1999) Molecular taphonomy of animal and plant cuticles: selective preservation and diagenesis. *Philos Trans R Soc Lond B* 354:7–16
- Brocks JJ, Love GD, Snape CE, Logan GA, Summons RE, Buick R (2003) Release of bound aromatic hydrocarbons from late Archean and Mesoproterozoic kerogens via hydroxyprolysis. *Geochim Cosmochim Acta* 67:1521–1530
- Clarke JM, Ruedemann R (1912) The eurypterida of New York, vol 14. New York State Museum Memoir, Albany, 439p
- Dalingwater JE (1973) The cuticle of a eurypterid. *Lethaia* 6:179–186
- de Leeuw JW, Baas M (1993) The behavior of esters in the presence of tetramethylammonium salts at elevated temperatures; flash pyrolysis or flash chemolysis? *J Anal Appl Pyrolysis* 26:175–184
- de Leeuw JW, Versteegh GJM, van Bergen PF (2006) Biomacromolecules of algae and plants and their fossil analogues. *Plant Ecol* 182:209–233
- Dunlop JA, Braddy SJ (2001) Scorpions and their sister-group relationships. In: Selden PA, Fet V (eds) *Scorpions 2001: in memoriam Gary A. Polis*. British Arachnological Society, Burnham Beeches, pp 1–24
- Gatellier J-PLA, de Leeuw JW, Sinninghe-Damsté JS, Derenne S, Largeau C, Metzger P (1993) A comparative study of macromolecular substances of a coorongite and cell walls of the extant alga *Botryococcus braunii*. *Geochim Cosmochim Acta* 57:2053–2068
- Gupta NS, Michels R, Briggs DEG, Evershed RP, Pancost RD (2006a) The organic preservation of fossil arthropods: an experimental study. *Proc R Soc Lond B* 273(1602):2777–2783
- Gupta NS, Collinson ME, Briggs DEG, Evershed RP, Pancost RD (2006b) Re-investigation of the occurrence of cutan in plants: implications for the leaf fossil record. *Paleobiology* 32:432–449
- Gupta NS, Briggs DEG, Pancost RD (2006c) Molecular taphonomy of graptolites. *J Geol Soc Lond* 163(6):897–900
- Gupta NS, Briggs DEG, Collinson ME, Evershed RP, Michels R, Pancost RD (2007a) Molecular preservation of plant and insect cuticles from the Oligocene Enspel Formation, Germany: evidence against derivation of aliphatic polymer from sediment. *Org Geochem* 38(3):404–418
- Gupta NS, Briggs DEG, Collinson ME, Evershed RP, Michels R, Jack KS, Pancost RD (2007b) Evidence for the *in situ* polymerisation of labile aliphatic organic compounds during the preservation of fossil leaves: implications for organic matter preservation. *Org Geochem* 38(3):499–522
- Holm G (1898) Über die Organisation des *Eurypterus fischeri* Eichw. *Mém Acad Imp Sci St Petersburg* 8:1–57
- Howard RW, Blomquist GJ (2005) Ecological, behavioral and biochemical aspects of insect hydrocarbons. *Annu Rev Entomol* 50:371–393

- Kleffner MA, Rexroad CB (1999) Preliminary conodont biostratigraphy of the Salina Group (Silurian) of the northern Indiana and recognition of the Wenlock/Ludlow boundary: American Association of Petroleum Geologists, Eastern Section 28th annual meeting, program with abstracts, pp 33–34
- Kluessendorf J (1994) Predictability of Silurian Fossil-Konservat-Lagerstätten in North America. *Lethaia* 27:337–344
- Kok MD, Schouten S, Sinningh-Damsté JS (2000) Formation of insoluble, nonhydrolyzable, sulfur-rich macromolecules via incorporation of inorganic sulfur species into algal carbohydrates. *Geochim Cosmochim Acta* 64:2689–2699
- Kudryavtsev AB, Schopf JW, Agresti DG, Wdowiak TJ (2001) *In situ* laser-Raman imagery of Precambrian microscopic fossils. *Proc Natl Acad Sci U S A* 98:823–826
- Larter SR, Horsfield B (1993) Determination of structural components of kerogens by the use of analytical pyrolysis methods. *Top Geobiol* 11:271–287
- Legall FD, Barnes CR (1980) Organic metamorphism and thermal maturity of Paleozoic strata of southern Ontario based on studies of conodont and acritarch alteration. *Abh Geol Bundesanst* 35:203
- Logan GA, Boon JJ, Eglinton G (1993) Structural biopolymer preservation in Miocene leaf fossils from the Clarkia site, Northern Idaho. *Proc Natl Acad Sci U S A* 90:2246–2250
- Logan GA, Smiley CJ, Eglinton G (1995) Preservation of fossil leaf waxes in association with their source tissues, Clarkia, northern Idaho, USA. *Geochim Cosmochim Acta* 59:751–763
- Miknis FP, Jiao ZS, MacGowan DB, Surdam RC (1993) Solid-state NMR characterization of Mowry shale from the Powder River Basin. *Org Geochem* 20:339–347
- Mukhopadhyay PK, Harvey PJ, MacDonald DJ (2003) Petroleum systems of selected basins from onshore Nova Scotia and feasibility of carbon dioxide sequestration. *Geol Soc Am Northeast Sect 38th Annu Meet Abstr Progr* 35(3):81
- Plotnick RE (1999) Habitat of Llandoveryan-Lochkovian eurypterids. In: Boucot AJ, Lawson J (eds) *Paleocommunities: a case study from the Silurian and Lower Devonian*. Cambridge University Press, Cambridge, pp 106–131
- Poirier N, Derenne S, Rouzaud J-N, Largeau C, Mariotti A, Balesdent J, Maquet J (2000) Chemical structure and sources of the macromolecular, resistant, organic fraction isolated from a forest soil (Lacadée, south-west France). *Org Geochem* 31:813–827
- Rahl JM, Anderson KM, Brandon MT, Fassoulas C (2005) Raman spectroscopic carbonaceous material thermometry of low-grade metamorphic rocks: calibration and application to tectonic exhumation in Crete, Greece. *Earth Planet Sci Lett* 240:339–354
- Riboulleau A, Derenne S, Largeau C, Baudin F (2001) Origin of contrasting features and preservation pathways in kerogens from the Kashpir oil shales (Upper Jurassic, Russian Platform). *Org Geochem* 32:647–665
- Rosenheim O (1905) Chitin in the carapace of *Pterygotus siliensis*, from the Silurian rocks of Oesel. *Proc R Soc Lond B* 76:398–400
- Schaefer J, Kramer KJ, Garbow JR, Jacob GS, Stejskal EO, Hopkins TL, Speirs RD (1987) Aromatic cross-links in insect cuticle: detection by solid-state ^{13}C and ^{15}N NMR. *Science* 235:1200–1204
- Selden PA (1981) Functional morphology of the prosoma of *Baltoerypterustetragonophthalmus* (Fischer) (Chelicerata: Eurypterida). *Trans R Soc Edinb Earth Sci* 72:9–48
- Selden PA (1984) Autecology of Silurian eurypterids. In: Bassett MG, Lawson JD (eds) *Autecology of Silurian organisms*, vol 32, Special papers in palaeontology. Palaeontological Association, London, pp 39–54
- Stankiewicz BA, Van Bergen PF, Duncan IJ, Carter JF, Briggs DEG, Evershed RP (1996) Recognition of chitin and proteins in invertebrate cuticles using analytical pyrolysis-gas chromatography and pyrolysis-gas chromatography/mass spectrometry. *Rapid Commun Mass Spectrom* 10:1747–1757
- Stankiewicz BA, Scott AC, Collinson ME, Finch P, Möslé B, Briggs DEG, Evershed RP (1998a) Molecular taphonomy of arthropod and plant cuticles from the Carboniferous of North America: implications for the origin of kerogen. *J Geol Soc Lond* 155:453–462

- Stankiewicz BA, Poinar HN, Briggs DEG, Evershed RP, Poinar GO (1998b) Chemical preservation of plants and insects in natural resins. *Proc R Soc Lond B* 265:641–647
- Stankiewicz BA, Masterlerz M, Hof CHJ, Bierstedt A, Flannery MB, Briggs DEG, Evershed RP (1998c) Biodegradation of the chitin-protein complex in crustacean cuticle. *Org Geochem* 28:67–76
- Stankiewicz BA, Briggs DEG, Michels R, Collinson ME, Evershed RP (2000) Alternative origin of aliphatic polymer in kerogen. *Geology* 28:559–562
- van Bergen PF, Collinson ME, Briggs DEG, de Leeuw JW, Scott AC, Evershed RP, Finch P (1995) Resistant biomacromolecules in the fossil record. *Acta Bot Neerl* 44:319–342
- Versteegh GMJ, Blokker P, Wood GD, Collinson ME, Damsté JSS, de Leeuw JW (2004) An example of oxidative polymerization of unsaturated fatty acids as a preservation pathway for dinoflagellate organic matter. *Org Geochem* 35:1129–1139
- Weygoldt P, Paulus HF (1979) Untersuchungen zur Morphologie, Taxonomie und Phylogenie der Chelicerata. II. Cladogramme und die Entfaltung der Chelicerata. *Z Zool Syst Evolutionsforsch* 17:177–200
- Wills LJ (1965) A supplement to Gerhard Holm's "Über die Organisation des *Eurypterus Fischeri* Eichw." with special reference to the organs of sight, respiration and reproduction. *Ark Zool* 2:93–145
- Witmer LM (1995) The extant phylogenetic bracket and the importance of reconstructing soft tissues in fossils. In: Thomason JJ (ed) *Functional morphology in vertebrate paleontology*. Cambridge University Press, Cambridge, pp 19–33

Chapter 8

Transformation of Arthropod Biopolymers in High P-T Conditions

Abstract Modern arthropod cuticles consist of chitin fibres in a protein matrix, but fossil arthropods, particularly those earlier than Tertiary, yield an aliphatic composition. This apparent contradiction is addressed in this chapter. Modern cockroach, scorpion and shrimp cuticle were subjected to artificial heating (maturation) techniques (350 °C/700 Bars/24 h) following various chemical treatments, and analysing them with pyrolysis-gas chromatography-mass spectrometry. Artificially matured untreated cuticle yielded moieties related to phenols and alkylated substituents, pyridines, pyrroles and possibly indenes (derived from chitin). Amides, C₁₆ and C₁₈ fatty acids and alkane/alk-1-ene homologues ranging from C₁₀ to C₁₉ were also present, the last indicating the presence of an aliphatic polymer, as often encountered in fossil arthropods. Cuticles matured after lipid extraction and hydrolysis did not show the presence of these alkane/alk-1-ene homologues providing direct experimental evidence that lipids incorporated from the cuticle were the source of the aliphatic polymer.

Keywords Arthropod • Lipids • Experimental maturation • Confined pyrolysis • Taphonomy • Fossilisation

Introduction

Arthropod cuticles consist of chitin fibres embedded in a protein matrix, cross-linked by catechol, aspartate and histidyl moieties (Schaefer et al. 1987). Calcification, in the form of calcium carbonate, further strengthens the cuticle of many crustaceans, and that of the extinct trilobites; such biomineralised skeletons dominate the marine fossil record of arthropods. The fossil record of many arthropods, however, particularly in non-marine settings, relies on organic matter preservation, because they lack a biomineralized exoskeleton. Fossil eurypterids, scorpions and insects, for example, are abundant as cuticular remains (see Briggs 1999 for review).

Decay of crustacean cuticle in previous experiments resulted in extensive loss of the protein component within the first 2 weeks, while chitin remained largely intact for the first 8 weeks, attesting to its greater survival potential (Stankiewicz et al. 1998a). Traces of chitin are present in Pleistocene beetles (Stankiewicz et al. 1997a) and in weevils as old as 25 million years (Stankiewicz et al. 1997b; Gupta et al. 2007a). However, the cuticles of fossil arthropods older than the Tertiary show no trace of chitin or protein (Briggs et al. 2000), but have a dominant aliphatic component similar to type I/II kerogen (Briggs 1999) at times partially interlinked by fatty acyl moieties (Gupta et al. 2007a). Selective preservation of resistant aliphatics is not a plausible explanation as they do not occur in the exoskeletons of modern arthropods. Initially, the aliphatic composition was interpreted as the result of diagenetic replacement by aliphatic organic matter from an external source (Baas et al. 1995). However, recent research makes this argument untenable (see discussion in Briggs 1999; Gupta et al. 2007a). Arthropod cuticles have surface waxes composed of hydrocarbons and fatty acids (Howard and Blomquist 2005) that are labile, i.e., extractable/hydrolysable. Thus, it has been suggested that the aliphatic composition of the fossils was generated by *in situ polymerisation* of constituent cuticular waxes (Briggs et al. 1998; Stankiewicz et al. 2000).

Taphonomic experiments have been used to investigate the various parameters that control the preservation of arthropod cuticles in the fossil record (modern shrimp: Briggs and Kear 1993, 1994; Baas et al. 1995; Hof and Briggs 1997; Sagemann et al. 1999; cockroach: Duncan et al. 2003). The emphasis of these studies was on controlled necrolysis and/or the effect of transportation on disarticulation. Few experiments have addressed changes in the chemistry of modern arthropod cuticles to explain their composition in the fossil record. Stankiewicz et al. (2000) used artificial maturation techniques in a preliminary study of the transformation of the cuticle of the emperor scorpion *Pandinus imperator*. An aliphatic composition was generated but the investigation did not determine the source of the aliphatic components. Similar experiments have been used successfully to investigate the origin of aliphatic constituents in fossil plants (Gupta et al. 2005, 2007b). Here we describe an experimental investigation, using similar artificial maturation techniques, to determine the source of the aliphatic component that accounts for the long term organic preservation of fossil arthropods.

Material and Methods

The living arthropods *Pandinus imperator* (emperor scorpion), *Crangoncrangon* (shrimp) and *Gromphadorhina portentosa* (Madagascan hissing cockroach) were investigated as they all belong to groups with a well-documented fossil record that have been the subject of taphonomic experiments (Briggs and Kear 1993, 1994; Sagemann et al. 1999; Stankiewicz et al. 1998a; Duncan et al. 2003). The large size

and abundant cuticle of these organisms provide additional advantages for handling and experimentation. Specimens were obtained live from Bristol Zoo and killed by freezing at $-20\text{ }^{\circ}\text{C}$ for 24 h. They were dissected with a scalpel to remove the internal tissues and the cuticle was recovered. The cuticle was frozen in liquid nitrogen and crushed with a mortar and pestle. It was then boiled in double distilled water at $100\text{ }^{\circ}\text{C}$, 3 times for 1 h each, to remove any remaining internal tissue, and then washed thoroughly with double distilled water. The recovered cuticles were subjected to two different preparations prior to artificial maturation. Cuticle from scorpion and cockroach was: (1) untreated; or (2) solvent extracted in 2:1 dichloromethane/methanol (*v/v*, 5 times, sonication for 30 min each) to remove extractable lipids, and then saponified (i.e., subjected to base hydrolysis) in 95 % 1 M methanolic NaOH for 24 h to remove hydrolysable lipids. Shrimp cuticle was also untreated prior to maturation. Commercially prepared pure chitin (derived from crab, Sigma Aldrich) was solvent extracted in the same way as the scorpion and cockroach cuticle to remove soluble impurities.

The cuticles and commercial chitin (0.1–0.15 g) were artificially matured at $350\text{ }^{\circ}\text{C}$, 700 Bars for 24 h in gold cell reactors (Monthieux et al. 1985; Landais et al. 1989; Stankiewicz et al. 2000). A successful experiment was indicated by no weight loss; i.e. no change before and after the experiment. No other quantitation was attempted. The volatiles and condensates that were generated were not characterized. The shrimp cuticle was also matured in two separate experiments in the presence of commercial powder CaCO_3 (1:1 *w/w*) and kaolinite (1:1 *w/w*) to explore the effect of different inorganic matrix materials on cuticle transformation. The shrimp cuticle was not subjected to any further extraction/saponification prior to maturation. Pure C_{16} and C_{18} fatty acids (Sigma Aldrich, 1:1 *w/w*) were matured to investigate the transformation of pure lipids reaction products (as detected in the extractable and hydrolysable fractions). Fresh unmatured samples were analysed without extraction to reveal the entire range of chemical constituents. The matured samples were analysed using thermal desorption-GC/MS (TD-GC/MS) at $300\text{ }^{\circ}\text{C}$ followed by (Py-GC-MS) at $610\text{ }^{\circ}\text{C}$ to reveal composition of experimentally heated biopolymers after thermodesorption (see Gupta and Pancost 2004 for instrument parameters). Thermal desorption was used to remove volatile compounds (i.e., thermal extraction: Hartgers et al. 1995) in order to purify material prior to pyrolysis (i.e., to thermally extract compounds volatile at $300\text{ }^{\circ}\text{C}$). It also provided a basis for direct comparison with the results of Stankiewicz et al. (2000). Aliquots of the artificially matured samples were subjected additionally to base hydrolysis by heating in 1 M methanolic NaOH for 1 h at $70\text{ }^{\circ}\text{C}$ to assess the degree of recalcitrance.

Composition of Samples Used in Experiments

Py-GC/MS of solvent extracted commercial chitin (Fig. 8.1a) yielded 3-acetamido-4-pyrone, 3-acetamido-5-methylfuran, acetylpyridone, and 3-acetamidofuran as the major products. However, protein and fatty acyl moieties were not observed.

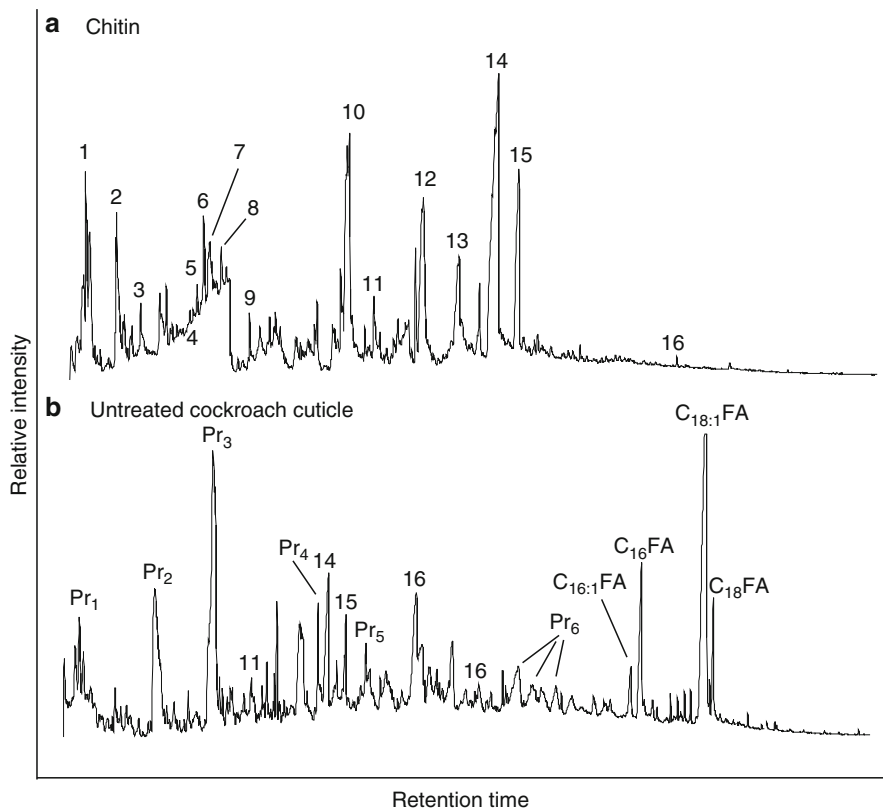


Fig. 8.1 Partial pyrolysis-GC/MS chromatograms of (a) pure chitin and (b) cockroach cuticle. 1: pyridine; 2: methyl pyridine; 3: acetamide; 4: 3-hydroxy-2-pyridone; 5: 2-pyridine carboxaldehyde; 6: acetylpyrrole; 7: acetylpyrroline; 8: amine derivative; 9: levoglucosenone; 10: unknown; 11: acetyldihydropyridine; 12: acetylpyridone; 13: 3-acetamidofuran; 14: 3-acetamido-5-methylfuran; 15: 3-acetamido-4-pyrone; 16: oxazoline structures; Pr₁: methyl pyrrole, Pr₂: phenol, Pr₃: unknown, Pr₄: indole, Pr₅: methylindole, Pr₆: diketopiperazines, C_nFA: fatty acyl moieties, where n refers to the carbon chain length and n:1 denotes mono-unsaturation in the alkyl chain. No n-alkanes/alkenes were detected. The analysis time was 55 min

The pyrolysates of the untreated cockroach cuticle (Fig. 8.1b) contain these chitin markers but also protein pyrolysis products (see Stankiewicz et al. 1997a for identification and mass spectral characteristics). The straight chain fatty acids *n*-C₁₆ and *n*-C₁₈ (both saturated and unsaturated components) were also observed in the cuticle pyrolysates (and were also detected in modern stingless bee cuticle: Stankiewicz et al. 1998b). No alkane/alkene homologues were detected. The modern scorpion and shrimp cuticle pyrolysates were similar to that of the cockroach cuticle (traces not shown).

Composition of the Cuticle and Lipid Compounds Matured Without Chemical Treatment

The pyrolysate of matured commercial chitin, analysed after thermodesorption at 300 °C (Fig. 8.2a), contained pyridine and its alkyl derivatives, and phenol and its mono, di, tri and tetra alkyl derivatives. The phenol derivatives are amongst the most abundant in the pyrolysate. Other important compounds tentatively identified include indene and its alkyl derivatives. Furans, pyrones, pyridones, pyrroles and oxazoline structures, which are the most important pyrolysis products of unmaturred chitin, were not detected thereby confirming that the chitin has undergone chemical change. No *n*-alkane/alk-1-ene homologues were detected. Benzene derivatives also were not detected but, along with alkylated phenols, were the primary thermally desorbed components.

The chitin-derived compounds are clearly evident in the pyrolysates of artificially matured scorpion, cockroach and shrimp cuticle (the latter two shown in Fig. 8.2b, c). The fatty acids *n*-C₁₆ and *n*-C₁₈ are abundant, as they were in the fresh cuticles. The relative abundance of fatty acids in the artificially matured shrimp cuticle (Fig. 8.2c) is less than in the cockroach (Fig. 8.2b) and scorpion (not shown), and *n*-C₁₈ fatty acid was released only in trace abundances. The thermally desorbed products of all the matured cuticles consisted primarily of alkylated phenols, benzene derivatives and *n*-alkanes (primarily C₉ to C₂₀).

The matured cuticles also yielded a range of compounds upon Py-GC/MS that were not detected in either the matured commercial chitin (Fig. 8.2a) or the non-matured cuticles (Fig. 8.1b). These include *n*-alkyl amides, with C₁₆ and C₁₈ homologues being the most abundant (Fig. 8.2b, c). Although not readily apparent in the partial ion current chromatogram, the *m/z* 83+85 mass chromatogram reveals the presence of *n*-alkane/alk-1-ene homologues ranging at least from C₉ to C₁₉ with the C₁₄ to C₁₇ components being dominant. Such *n*-alkane/alk-1-ene homologues (*n*-C₈ to *n*-C₁₉; Fig. 8.3a) were also generated during pyrolysis of matured pure C₁₆ and C₁₈ fatty acid mixture. However, base hydrolysis of the matured cuticle yielded no recoverable residue.

Shrimp cuticle matured in the presence of clay and calcium carbonate (Fig. 8.3b) yielded pyrolysates similar to those of shrimp cuticle matured in the absence of any minerals.

Composition of Cuticle Matured After Chemical Treatment

Cockroach cuticle matured following lipid extraction and base hydrolysis (Fig. 8.4) yielded pyrolysis products related to chitin and protein similar to those observed in the cuticle matured without chemical treatment. However, *n*-alkyl components, including *n*-alkanoic acids, *n*-alkyl amides and *n*-alkanes/alkenes, were not detected in the pyrolysate (inset, Fig. 8.4). Thermodesorbed products were similar to those released from matured chitin; in particular, no alkanes were detected.

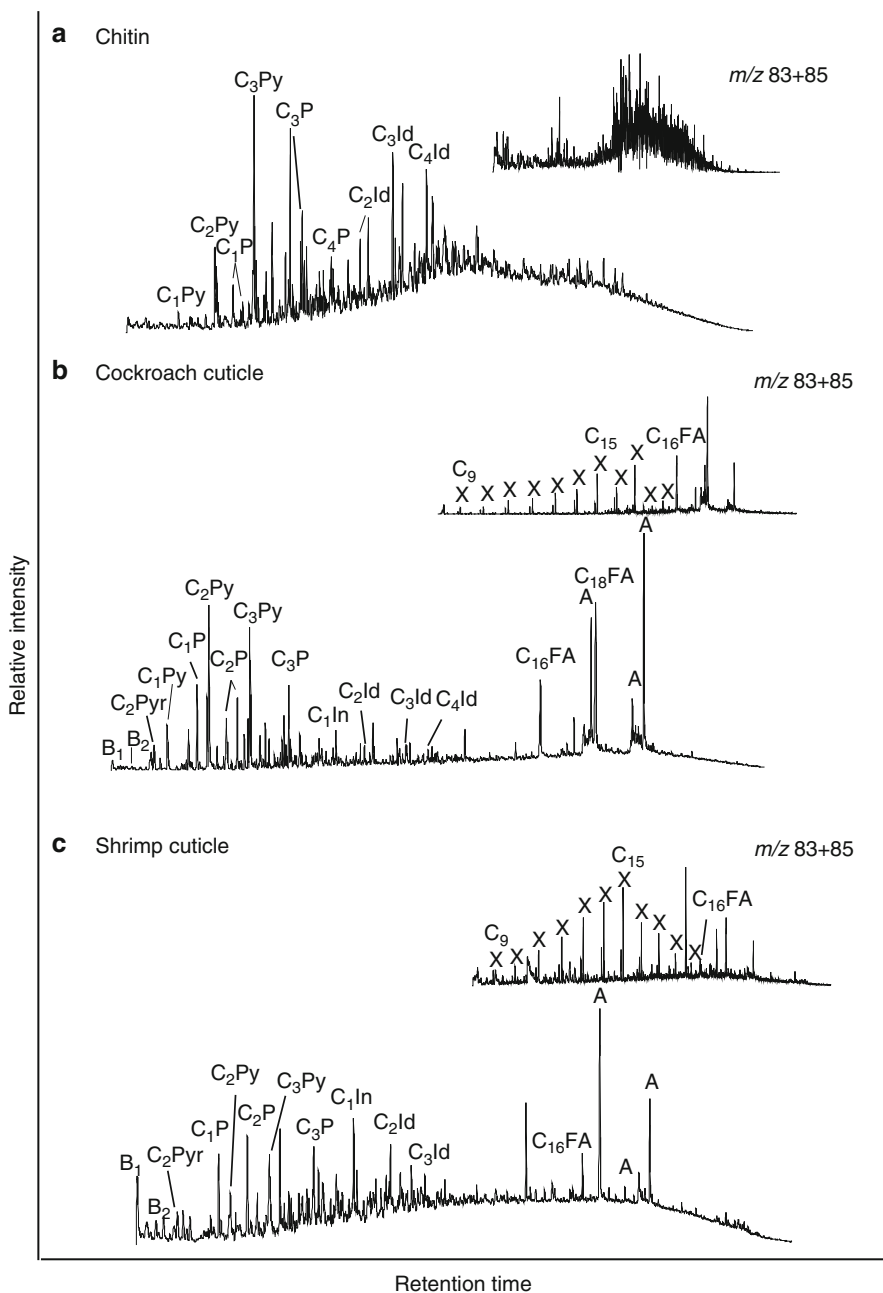


Fig. 8.2 Partial pyrolysis-GC/MS chromatograms of (a) matured chitin, (b) matured cockroach cuticle and (c) matured shrimp cuticle. *B_n*: benzene derivatives (*n* refers to the number of carbon atoms in the alkyl component), *C_nIn*: methyl indole; *A*: amide derivative (primarily *C*₁₆ and *C*₁₈ derivatives); *C_nPy*: pyridine pyrolysis products, where *n* is the number of carbon atoms in the alkyl substituent; *P*: phenol derivative; *Id*: alkyl indenenes. (Inset mass chromatograms m/z 83+85 reveal the presence of *n*-alkane/alkenes.) The analysis time was 55 min

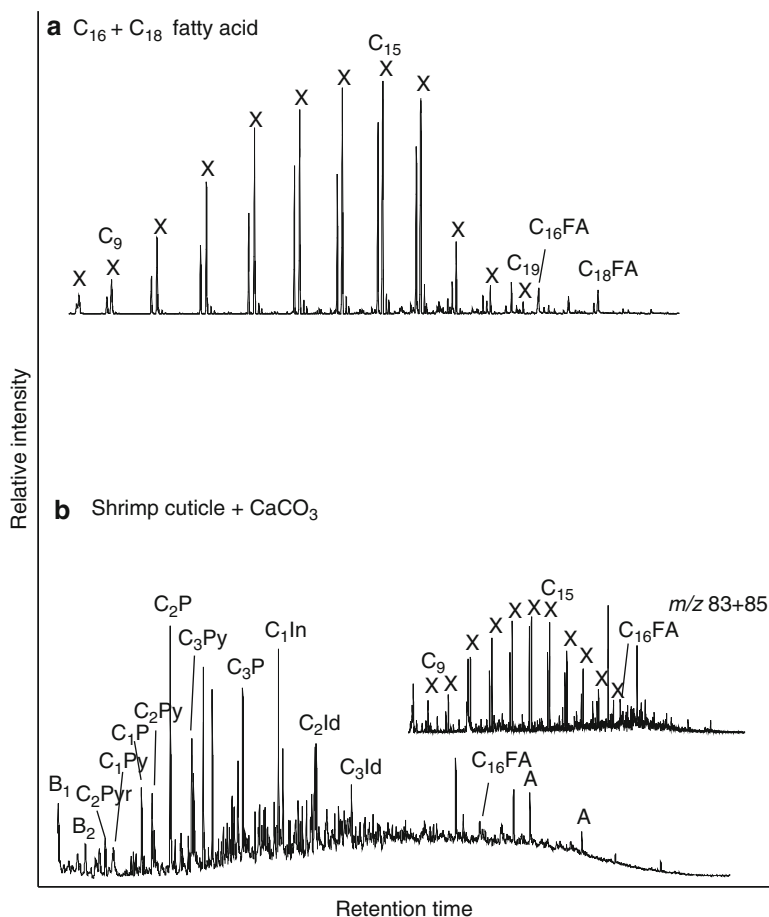


Fig. 8.3 Partial pyrolysis-GC/MS chromatograms of (a) matured mixture of C₁₆ and C₁₈ fatty acids with kaolinite and (b) shrimp cuticle matured in the presence of calcium carbonate. Annotations as in Fig. 8.2. The analysis time was 55 min

Discussion

The results of these artificial maturation experiments reveal the source of the aliphatic component in fossil arthropod cuticles (Table 8.1). Previous experiments (Stankiewicz et al. 2000) involved maturation of cuticle of the emperor scorpion, which had been solvent-extracted (but not saponified) and then degraded experimentally for 8.5 months in a bacterial inoculum. The sample matured at 260 °C generated abundant phenol during Py-GC/MS but markers directly related to chitin and protein were absent showing that thermal maturation alone can degrade chitin. C₅ to C₂₀*n*-alk-1-enes and *n*-alkanes were present, indicating the presence of an *n*-alkyl component. Thermal maturation at 350 °C resulted in more extensive

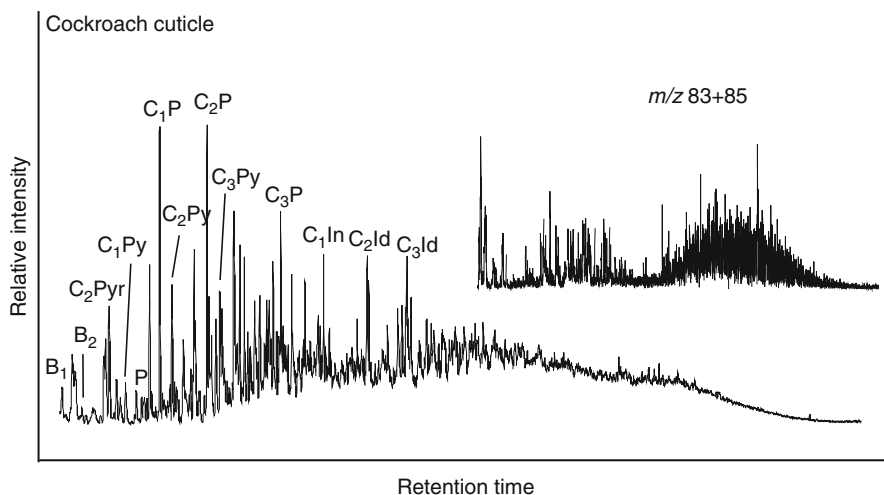


Fig. 8.4 Partial pyrolysis-GC-MS chromatograms of cockroach cuticle matured after lipid extraction followed by saponification. Annotations as in Fig. 8.2. The analysis time was 55 min

Table 8.1 The products of maturation of different arthropod cuticle biochemical components

Starting material	Composition	Chemical treatment	Products of maturation
Commercial chitin	Pure chitin	Extraction	Matured chitin products and no aliphatics
Fresh scorpion, shrimp and cockroach cuticle	Chitin + protein + lipids	None	Matured chitin products + acids + amides + aliphatics ^a
Fresh scorpion and cockroach cuticle	Chitin + protein	Extraction + saponification	Matured chitin products and no aliphatics

^a Shrimp cuticle matured with CaCO₃ or clay and without any chemical pre-treatment also yielded these moieties

alteration of the cuticle. Alkenes and alkanes with aliphatic carbon chain numbers up to n -C₃₀, significantly higher than those observed here, were the dominant pyrolysis products, and phenols were barely detected. Indenes and amides, which occur in our experiments, were not reported. These differences probably reflect alteration of the chitin-protein complex through decay prior to the maturation process; the cuticles used in the present experiments were not decayed.

In the present experiments artificial maturation of untreated arthropod cuticle at 350 °C resulted in significant changes in the macromolecular composition (Table 8.1). Thermally induced changes to the chitin-protein complex (deacetylation of chitin and formation of aromatic products of both chitin and protein) resulted in the presence of phenol and alkyl substituted phenols in the pyrolysate. The presence of n -alk-1-enes and n -alkanes indicate that an aliphatic component

was generated during maturation. These homologues are often encountered in the pyrolysates of fossil arthropods, including scorpions and eurypterids (Stankiewicz et al. 1998c) and shrimp (Stankiewicz et al. 1998a). Matured cuticle also revealed an abundance of *n*-alkyl amides along with compounds detected as alkylated indenenes. While long-chain amides (e.g., ceramides) do occur naturally, the observed components are most likely formed by nucleophilic substitution reactions between N-bearing components in the chitin/protein complex and the fatty acyl components. They appear to be a product of accelerated maturation, since they have not been detected in fossil arthropod cuticles. Interestingly, such amides did not form in the experiment of Stankiewicz et al. (2000) where the loss of more reactive nitrogen-containing compounds during decay may have prevented their formation thereby leading to relative enhancement of the *n*-alkyl component. Shrimp cuticle matured in the presence of clay and calcium carbonate also yielded *n*-alk-1-enes and *n*-alkanes, demonstrating that lithological components do not inhibit the reaction.

Similarly, maturation of a mixture of pure C₁₆ and C₁₈ fatty acids (similar to those obtained after extraction and saponification of the lipid component from the cuticle) produced a distribution of *n*-alkane/alkene homologues similar to that observed in the matured untreated cuticles (for a discussion of the behaviour of unmaturing C₁₆ and C₁₈ fatty acids during analytical pyrolysis see Hartgers et al. 2005). In striking contrast, maturation of cuticle that had first been extracted and saponified (i.e., was devoid of labile aliphatic compounds) yielded no aliphatic component but only moieties related to chitin and protein. These results provide direct experimental evidence that lipids present in the extractable and hydrolysable fraction of the cuticle are necessary for the formation of the aliphatic component. It is possible that aliphatic compounds from the cuticle become chemically bound to a macromolecular structure formed from chitin and proteins (as suggested by the presence of alkyl-amides). Indeed, fatty acyl moieties have been detected in the cuticle of fossil weevils (Gupta et al. 2007a).

When the matured cuticle was subjected to base hydrolysis no residue remained, indicating that the polymer formed in the experiments is hydrolysable even though fossil cuticles are resistant to such hydrolysis. The recalcitrant nature of fossil material must be the result of further cross linking and steric protection of functional groups that occurs over geological time. Formation of such a recalcitrant aliphatic macromolecule from the labile components of plant leaves was achieved using identical conditions to those reported here (Gupta et al. 2005, 2007b). Comparison of the products derived from maturation of different pre-treated plant tissues demonstrated that soluble lipids are constituents of the macromolecular material generated, indicating that labile organic compounds are a potential source of the aliphatic component of fossil organic matter and kerogen where decay resistant aliphatic material (e.g. cutan) is not present in the living organism.

In the absence of a recalcitrant aliphatic polymer in living arthropods, its presence in fossils has been interpreted as a product of the polymerisation of cuticular lipids (Briggs et al. 1998; Stankiewicz et al. 2000). The experiment described here provides the first test of this hypothesis. It shows that artificial maturation of arthropod cuticle in a closed system (eliminating contamination from an external source) can yield an

aliphatic component generated from constituents within the cuticle itself. Lipids from the internal tissue of the organism could also contribute to the aliphatic component (this occurs in plants: Gupta et al. 2005, 2007b). This demonstrates that the aliphatic component encountered in fossil insect tissues is not necessarily the result of migration from an external source (Baas et al. 1995) but rather a product of incorporation of lipids present in the organism itself. The major proportion of the fossil record of terrestrial arthropods, and of marine arthropods without a biomineralized exoskeleton, may be the result of this process of in situ polymerization.

This project was funded in part through a research grant awarded to RDP, DEGB and RM by the Petroleum Research Fund, American Chemical Society. I. Bull and R. Berstan are thanked for analytical support. The mass spectrometry facilities used in this study at the Bristol Biogeochemistry Research Centre were supported in part by a grant from the UK Joint Higher Education Research Investment Fund, and the University of Bristol. We are grateful to M. E. Collinson for advice and discussion.

References

- Baas M, Briggs DEG, van Heemst JDH, Kear AJ, de Leeuw JW (1995) Selective preservation of chitin during the decay of shrimp. *Geochim Cosmochim Acta* 59:945–951
- Briggs DEG (1999) Molecular taphonomy of animal and plant cuticles: selective preservation and diagenesis. *Philos Trans R Soc Lond B354*:7–16
- Briggs DEG, Kear AJ (1993) Fossilization of soft-tissue in the laboratory. *Science* 259:1439–1442
- Briggs DEG, Kear AJ (1994) Decay and mineralization of shrimps. *Palaios* 9:431–456
- Briggs DEG, Stankiewicz BA, Evershed RP (1998) The molecular preservation of fossil arthropod cuticles. *Anc Biomol* 2:135–146
- Briggs DEG, Evershed RP, Lockheart MJ (2000) The biomolecular paleontology of continental fossils. *Paleobiology* 26(Suppl to no. 4):169–193
- Duncan IJ, Titchener F, Briggs DEG (2003) Decay and disarticulation of the cockroach: implications for the preservation of the blattoids of Writhlington (Upper Carboniferous), UK. *Palaios* 18:256–265
- Gupta NS, Pancost RD (2004) Biomolecular and physical taphonomy of angiosperm leaf during early decay: implications for fossilisation. *Palaios* 19:428–440
- Gupta NS, Michels R, Briggs DEG, Collinson ME, Evershed RP, Pancost RD (2005) Experimental simulation of organic fossilisation. *Geochim Cosmochim Acta* 69:A343
- Gupta NS, Briggs DEG, Collinson ME, Evershed RP, Michels R, Pancost RD (2007a) Insoluble aliphatics do not migrate from matrix to fossils: evidence from molecular preservation of leaves and insects in the Oligocene of Enspel, Germany. *Org Geochem*
- Gupta NS, Michels R, Briggs DEG, Collinson ME, Evershed RP, Pancost RD (2007b) Experimental evidence for the formation of geomacromolecules from plant leaf lipids. *Org Geochem* 38(1):28–36
- Hartgers WA, Sinninghe-Damsté JSS, de Leeuw JW (1995) Curie-point pyrolysis of sodium salts of functionalized fatty acids. *J Anal Appl Pyrolysis* 34:191–217
- Hof CHJ, Briggs DEG (1997) Decay and mineralization of mantis shrimps (Stomatopoda: Crustacea)—a key to their fossil record. *Palaios* 12:420–438
- Howard RW, Blomquist GJ (2005) Ecological, behavioral and biochemical aspects of insect hydrocarbons. *Annu Rev Entomol* 50:371–393

- Landais P, Michels R, Poty B (1989) Pyrolysis of organic matter in cold-seal autoclaves. Experimental approach and application. *J Anal Appl Pyrolysis* 16:103–115
- Monthioux M, Landais P, Monin JC (1985) Comparison between natural and artificial maturation series of humic coals from the Mahakam delta, Indonesia. *Org Geochem* 8:275–292
- Sagemann J, Bale SJ, Briggs DEG, Parkes RJ (1999) Controls on the formation of authigenic minerals in association with decaying organic matter: an experimental approach. *Geochim Cosmochim Acta* 63:1083–1095
- Schaefer J, Kramer KJ, Garbow JR, Jacob GS, Stejskal EO, Hopkins TL, Speirs RD (1987) Aromatic cross-links in insect cuticle: detection by solid-state ^{13}C and ^{15}N NMR. *Science* 235:1200–1204
- Stankiewicz BA, Briggs DEG, Evershed RP, Duncan IJ (1997a) Chemical preservation of insect cuticles from the Pleistocene asphalt deposits of California, USA. *Geochim Cosmochim Acta* 61:2247–2252
- Stankiewicz BA, Briggs DEG, Evershed RP, Flannery MB, Wuttke M (1997b) Preservation of chitin in 25-million-year-old fossils. *Science* 276:1541–1543
- Stankiewicz BA, Mastalerz M, Hof CHJ, Bierstedt A, Briggs DEG, Evershed RP (1998a) Biodegradation of chitin protein complex in crustacean cuticle. *Org Geochem* 28:67–76
- Stankiewicz BA, Poinar HN, Briggs DEG, Evershed RP, Poinar GO Jr (1998b) Chemical preservation of plants and insects in natural resins. *Proc R Soc Lond B* 265:641–647
- Stankiewicz BA, Möslle B, Finch P, Collinson ME, Scott AC, Briggs DEG, Evershed RP (1998c) Molecular taphonomy of arthropod and plant cuticles from the Carboniferous of North America: implications for the origin of kerogen. *J Geol Soc* 155:453–462
- Stankiewicz BA, Briggs DEG, Michels R, Collinson ME, Evershed RP (2000) Alternative origin of aliphatic polymer in kerogen. *Geology* 28:559–562

Chapter 9

Molecular Preservation in Graptolites

Abstract Graptolites are important fossils in the Lower Palaeozoic. Preserved graptolite periderm consists dominantly of an aliphatic polymer, immune to base hydrolysis. It contains no protein even though its structure, and chemical analyses of the periderm of the living relative *Rhabdopleura*, indicate that it was originally collagen. This anomaly was previously interpreted as the result of replacement by macromolecular material from the surrounding sediment. New analyses suggest that the aliphatic composition of graptolite periderm reflects direct incorporation of lipids from the organism itself by *in situ* polymerization.

Keywords Graptolite • Protein • Kerogen • Aliphatic • *In situ* polymerization

Graptolites are the dominant component within many Lower Palaeozoic fossil planktic assemblages, and may be enormously abundant within organic-rich hemipelagic mudstone facies. This, combined with their widespread distribution and rapid evolution, accounts for their importance in biostratigraphy. Graptolites lacked a biomineralized skeleton. Similarities to the periderm of closely related living pterobranchs such as *Rhabdopleura* (Briggs et al. 1995 and references therein) and *Cephalodiscus* indicate that the periderm of graptolites was composed originally of collagen. This confirms interpretations of its composition based on the structure of the periderm as revealed by transmission electron microscopy (Towe and Urbanek 1972; Crowther and Rickards 1977; Crowther 1981).

The skeleton of graptolites often provided a locus for the precipitation of authigenic minerals such as clays, which may be altered to chlorite (Underwood 1992). Pyrite may preserve the 3-dimensional morphology by growing as an infill (Underwood and Bottrell 1994). In many cases, however, the graptolite periderm is preserved as organic material (Bustin et al. 1989; Briggs et al. 1995), and graptolites can be released from carbonates by dissolving the matrix. Carbonaceous traces of the stolon of graptoloid graptolites have been reported (Loydell et al. 2004) but evidence of the morphology of the zooids rarely survives and relies on authigenic mineralization (Rickards et al. 1991).

Table 9.1 Molecular composition of graptolites

Sample (Yale Peabody Museum number)	Age; locality	Composition
<i>Rhabdopleura</i>	Modern	Protein/lipids (e.g. C ₁₆ and C ₁₈ fatty acyl moieties)
<i>Palaeodictyota anastomotica</i> (YPM 205210)	Middle Silurian; Lockport, New York, USA	<i>n</i> -alkyl chains (C ₉ to C ₂₁)/fatty acyl moieties (C ₁₆ and C ₁₈ components most dominant).
<i>Dictyonema peltatum</i> (YPM 202222)	Silurian; Wisby; Sweden	Phenols, naphthalene and benzene derivatives (in relative abundance minor to aliphatics)
<i>Diplograptus</i> sp. (YPM 205225)	Ordovician; Gotska, Sweden	
<i>Monograptus instrenuus</i> ^a	Silurian; Arctic archipelago, Canada	Benzene derivatives and <i>n</i> -alkyl chains
<i>Monograptus</i> ^b	Silurian; Arctic archipelago, Canada	Aromatic with <i>n</i> -alkyl chains
<i>Amphigraptus</i> ^a	Ordovician; Oklahoma, USA	<i>n</i> -alkyl chains, benzene derivatives and sulfur bearing compounds

^aAfter Briggs et al. (1995)^bAfter Bustin et al. (1989)

Analysis of *Monograptus* from the Wenlock Cape Phillips Formation of Cornwallis Island revealed an aromatic structure with aliphatic Group (Bustin et al. 1989). Briggs et al. (1995) analysed *Monograptus instrenuus* from the same locality, and *Amphigraptus* sp. from the Caradoc Viola Limestone Formation of Oklahoma (Table 9.1), and concluded that the aliphatic material that they discovered in the periderm could not have been derived from an original proteinaceous material like collagen. They argued that the material in the fossils must have been introduced from an external source that included a decay resistant macromolecule. The aliphatic material might have been derived by diagenetic replacement from algal cell walls, for example, which were a component of the surrounding matrix (Briggs et al. 1995). This was proposed in the light of the prevailing paradigm of organic matter preservation in sediments as a result of the selective preservation of decay resistant components (Tegelaar et al. 1989; de Leeuw and Largeau 1993; Bass et al. 1995).

Recent research has shown that selective preservation is not an adequate explanation for the preservation of a number of fossil materials, including leaves (Gupta et al. 2006a, 2007a, b) and arthropod cuticle (Briggs 1999; Stankiewicz et al. 2000; Gupta et al. 2006b). Nor can the preservation of fossil arthropod cuticle be explained by the introduction of material from external sources: thermochemolysis of co-occurring insect and plant fossils, and the associated organic-rich matrix, from the Oligocene Enspel Formation, Germany, revealed differences in the distribution of the constituent fatty acyl components, indicating that the aliphatic component of the fossil is at least partly derived endogenously (Gupta et al. 2007b).

Here we test the hypothesis that the organic preservation of graptolite periderm, like that of the cuticle of arthropods and leaves (Gupta et al. 2006a), is a result of *in situ* polymerization of the lipid and other labile constituents rather than selective preservation of decay resistant components or the introduction of material from an

external source such as the matrix. This study also provides a further test of the model of *in situ* polymerization, as the original composition of graptolite periderm differs from that of arthropod cuticles and leaves but fossils of all three are composed of dominantly aliphatic macromolecular material.

Methods

The graptolites investigated were selected from the Yale Peabody Museum collections to provide stratigraphic coverage from the Early Ordovician to the Silurian and a variety of genera from different localities (Table 9.1). They were either on the rock (e.g., *Paleodictyota anastomotica*), in which case samples were scraped from the surface, or they had been released from the matrix by acid digestion and stored in glass vials in glycerin (e.g., *Dictyonema peltatum*). Samples were extracted ultrasonically three times, 15 min each with 2:1- CH₂Cl₂ (dichloromethane):CH₃OH (methanol), to yield an insoluble residue. This residue was analysed by Pyrolysis-Gas Chromatography/Mass Spectrometry (Py-GC/MS) to reveal the molecular distribution of compounds. Samples of selected graptolites were subjected to thermochemolysis (de Leeuw and Baas 1993) to permit further structural analysis of the macromolecule. Graptolites were hydrolysed in 1 M 95 % methanoic NaOH (saponification) for 1 h at 70 °C to yield a non-hydrolysable residue in order to test the resistance of the macromolecule to base hydrolysis. Py-GC/MS was carried out on the periderm of modern *Rhabdopleura* before and after solvent extraction to evaluate the molecular distribution in the presence and absence of lipids. Further structural analysis of *Rhabdopleura* was carried out by subjecting samples to thermochemolysis without solvent extraction to reveal the complete molecular distribution including lipids.

Solvent-extracted graptolite and *Rhabdopleura* periderm were analysed using py-GC/MS for analysis of macromolecular composition, (see Gupta and Pancost 2004 for parameters), and compounds were identified using spectra reported in the literature (Reeves and Francis 1998; Stankiewicz et al. 1997a). For thermochemolysis, the extracted residues were transferred to a fresh vial and 1 ml TMAH (tetramethylammonium hydroxide) solution was added. They were soaked in TMAH solution for 3–4 h prior to analysis to ensure that sufficient TMAH was available during on-line pyrolysis. Thermochemolysis cleaves ester bonds to release constituent fatty acyl moieties (Challinor 1991a, b; de Leeuw and Baas 1993). For a discussion of the behaviour of protein compounds under TMAH conditions see Zhang et al. (2001).

Results

The major pyrolysis products of *Rhabdopleura* periderm (without lipid/solvent extraction) included phenols, indoles, pyrimidine, diketodipyrrole and diketopiperazine derivatives (Fig. 9.1a, Table 9.1). The abundance of diketodipyrrole, a marker

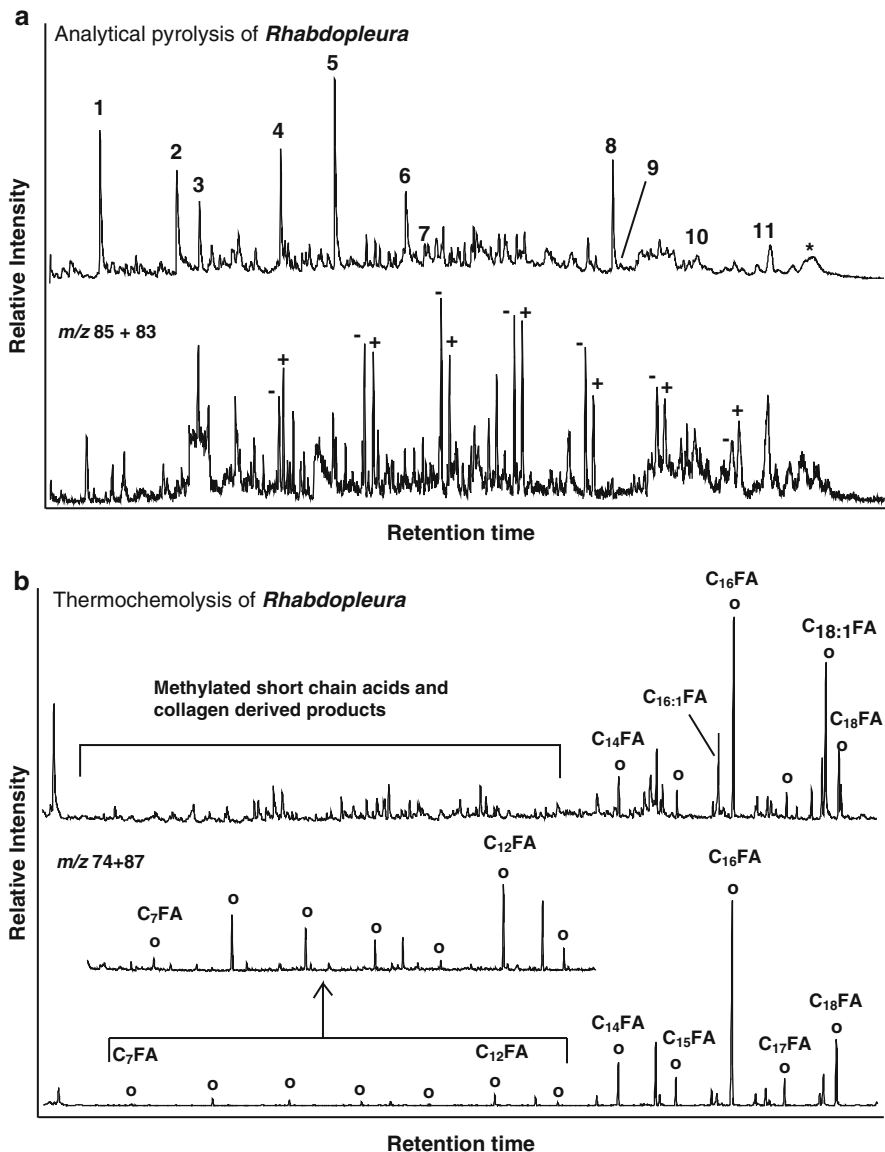


Fig. 9.1 Partial ion chromatogram showing (a) the pyrolysis-GC/MS analysis and (b) TMAH pyrolysis/thermochemolysis of *Rhabdopleura*. The mass chromatogram m/z 85 + 83 reveals the distribution of *n*-alkanes (+) and *n*-alkenes (–), and m/z 74 + 87 that of fatty acyl moieties (C_nFA/o). C_n where *n* indicates the carbon chain length. 1: phenol; 2: methylphenol; 3: ethylcyanobenzene; 4: 2,5-diketopiperazine; 5: indole; 6: methylindole; 7: trimethylpyrimidine; 8: diketodipyrrole; 9: 2,5-diketopiperazine; 10: pyrrolidinopiperazine derivative; 11: propylcyanobenzene; * contaminant

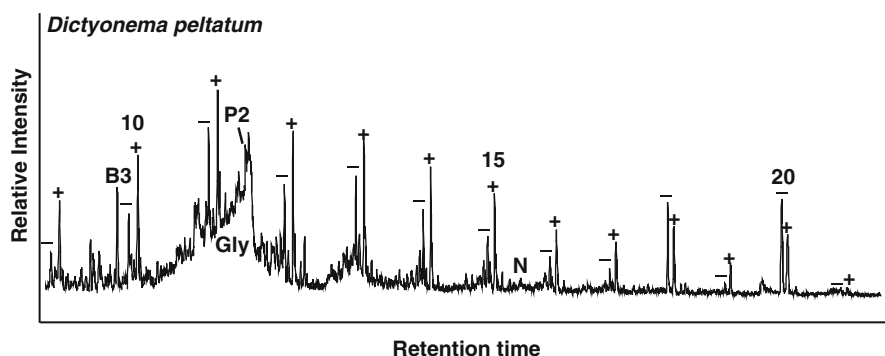


Fig. 9.2 Partial ion chromatogram showing the pyrolysis-GC/MS analysis of *Dictyonema peltatum* revealing the absence of any protein moieties and the presence of a dominant aliphatic component. +: *n*-alkanes; -: *n*-alkenes; B3: trimethyl benzene; P2: dimethyl phenol/ethyl phenol; Gly: glycerin; N: naphthalene

for hydroxyproline, is characteristic of collagen (Stankiewicz et al. 1997a). Pyrimidine is also derived from collagen, although it cannot be ascribed to any particular amino acid. The m/z 85+83 (Fig. 9.1a) mass chromatogram revealed a series of *n*-alkanes and *n*-alkenes. However, analysis of *Rhabdopleura* periderm after lipid extraction did not reveal the presence of these *n*-alkanes and *n*-alkenes (figure not shown), indicating that they were derived from a soluble, probably lipid, component.

Thermochemolysis of *Rhabdopleura* (Fig. 9.1b) revealed a distribution of fatty acyl moieties ranging in carbon number from C₇ to C₁₈. C₁₆ and C₁₈ saturated and unsaturated components were the most abundant (see Fig. 9.1b: m/z 74+87). Homologues greater than C₁₀ showed an even over odd predominance.

Samples of the graptolites *Paleodictyota anastomtica*, *Dictyonema peltatum* and *Diplograptus* sp. were analysed after solvent extraction. No moieties diagnostic of collagen were detected (Fig. 9.2). The graptolites comprised a largely aliphatic polymer with *n*-alkyl components in the pyrolysate extending at least from C₉ to C₂₁; C₁₀ to C₁₅ alkane/alkene homologues were the most abundant (Fig. 9.2, Table 9.1). A very similar distribution of chain lengths was observed in *Monograptus* and *Amphigraptus* (Briggs et al. 1995, Table 9.1). The aromatic component detected in all these consisted of benzene derivatives, phenols and naphthalene. Some glycerin was detected in the analysis of *Dictyonema peltatum* (Fig. 9.2), presumably as a result of contamination from the storage medium which could not be completely removed during extraction (no glycerin was detected in the samples obtained directly from rock).

Fatty acyl moieties released by thermochemolysis of the same graptolite samples (Fig. 9.3) ranged from C₇ to C₁₈ with an even-over-odd predominance (especially for those >C₁₀). The most abundant of these were C₁₆ and C₁₈ fatty acyl moieties, both saturated and unsaturated. These fatty acyl moieties were dominant when compared to the alkane/alkene homologues (see mass chromatogram m/z 74+87+85+83).

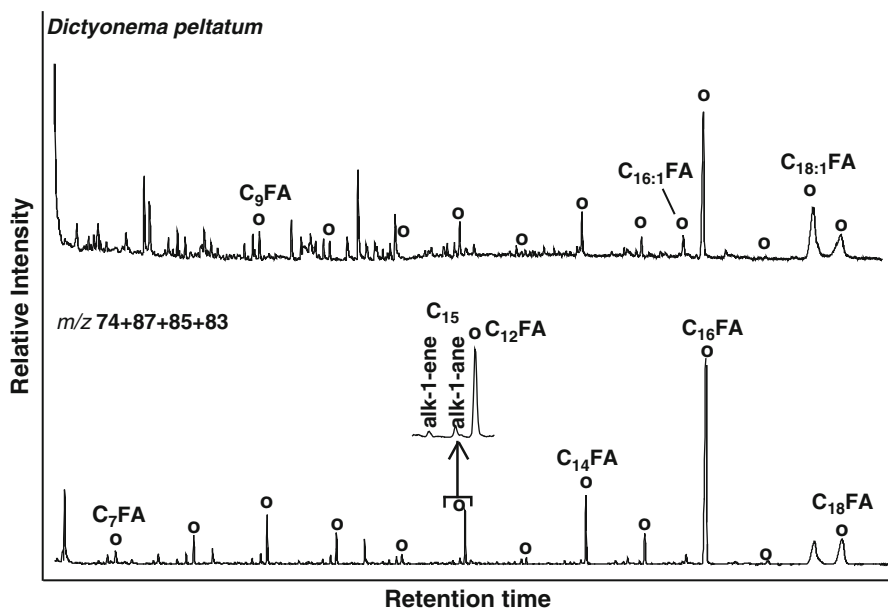


Fig. 9.3 Partial ion chromatogram showing the TMAH/pyrolysis-GC/MS analysis of *Dictyonema peltatum* revealing the distribution of fatty acyl moieties in relation to the alkane/alkene homologues highlighted by the mass chromatogram m/z 74 + 87 + 85 + 83. Note the similarity in distribution of the fatty acyl moieties in the fossils and *Rhabdopleura*. For key to symbols see Fig. 9.1

The predominance of fatty acyl moieties emphasizes the importance of ester functional groups in crosslinking the aliphatic polymer in these fossils (Versteegh et al. 2004; Gupta et al. 2007b). To determine the nature of these bonds the fossils were hydrolysed in basic conditions and a residue was recovered. The weight of residue after hydrolysis was similar to that after extraction and thermochemolysis of this residue yielded fatty acids in distribution similar to that after extraction. Thus, the aliphatic polymer in the fossils is non-extractable and largely non-hydrolysable attesting to its recalcitrant nature. Pyrolysis failed to detect any ketones (Fig. 9.2) suggesting low amounts of ether linkages in the graptolite periderm. The primary oxygen-containing functional group in the graptolites may be as esters. The *n*-alkyl chains may protect the ester functional group in 3-dimensions by steric hindrance, accounting for their immunity to base hydrolysis (McKinney et al. 1996; Gupta et al. 2007a, b).

Discussion

The ultrastructure of graptolite periderm suggests that its original composition was collagen (Towe and Urbanek 1972; Crowther and Rickards 1977). Collagen, like other proteins, (Tegelaar et al. 1989; de Leeuw and Largeau 1993; but see Nguyen

and Harvey 1998) is decay-prone, except where it has undergone substantial cross-linking, as in the jaws of polychaetes (Briggs and Kear 1993). Protein and polysaccharide remnants have been shown to survive in archaeological plant remains 1,400 years old (Bland et al. 1998), in weevil samples as old as 24.7 m.y. (Stankiewicz et al. 1997b; Gupta et al. 2007a) and even in kerogen 140 million years old (Mongenot et al. 2001) where preservation of labile moieties was facilitated by encapsulation within a resistant aliphatic matrix. The presence of diketodipyrrole and pyrimidine in the periderm of *Rhabdopleura* is diagnostic of collagen (Stankiewicz et al. 1997a), but these moieties are absent in the periderm of graptolites. Thus, the ultrastructure may reflect the original composition even though the molecular components have been transformed to an aliphatic polymer.

The phenols in the graptolite periderm are likely the product of diagenesis of aromatic structures in the fossil, and not derived from original amino acids. Although encapsulation may promote protein preservation by steric protection of labile compounds (Knicker et al. 2001; Mongenot et al. 2001; Riboulleau et al. 2002), no nitrogen-bearing compounds were detected in the pyrolysates. Thus proteins, including collagen, appear not to have been preserved within the resistant aliphatic matrix that makes up graptolites, and it is likely that protein moieties do not survive in Early Palaeozoic fossils.

Analysis of the periderm of *Rhabdopleura* confirmed that it is proteinaceous in composition and contains no resistant aliphatic components (Briggs et al. 1995). The graptolites reveal a composition with a dominant aliphatic component similar to Type II kerogen [Bustin et al. (1989) noted that the hydrogen and oxygen indices of graptolite periderm (as determined by Rock-Eval pyrolysis) were similar to Type II kerogen]. Although sulphur-bearing compounds were not detected during pyrolysis, such components were detected in the pyrolysate of *Monograptus* and *Amphigraptus* in a previous study (Briggs et al. 1995) due to diagenetic incorporation of inorganic sulphur species under anoxic conditions in their samples; such conditions were likely absent in our samples. This facilitates further cross-linking of the macromolecule, as is often observed in natural vulcanization of kerogen (e.g. Kok et al. 2000).

In the absence of a diagenetically-stable aliphatic biopolymer in the living relative, the preservation and aliphatic character of the graptolites cannot be explained by selective preservation. The organic content of the sediment differs from that of the fossils, so migration from an external source can be excluded. Thus, the aliphatic component probably has been derived from compounds present in the organism itself. This is supported by the molecular structure. Thermochemolysis of modern *Rhabdopleura* and the graptolites investigated revealed a very similar saturated fatty acyl distribution ranging from C₇ to C₁₈ with a maximum abundance of C₁₆ and C₁₈ moieties (Table 9.1). The unsaturated fatty acyl components (e.g., C_{16:1} and C_{18:1}), on the other hand, are more abundant in *Rhabdopleura* than in the fossils, suggesting there was loss of unsaturated compounds during diagenesis (Wakeham et al. 1984, 1997).

Preservation of graptolites involves transformation of labile aliphatic components (such as fatty acids) into a recalcitrant crosslinked polymer with a dominant

aliphatic component via *in situ* polymerization. Organic fossils younger than the Tertiary tend to reveal preservation of intact biomolecules (e.g. Gupta et al. 2006b). However, older fossils reveal a dominant aliphatic composition with poor molecular preservation, irrespective of depositional environment and enclosing lithology (for discussion see Briggs et al. 2000). Evidence for a similar process of lipid incorporation has been reported in fossil leaves (Gupta et al. 2007a, b), dinoclasts (Versteegh et al. 2004), and arthropods (Briggs 1999; Gupta et al. 2006b, 2007a) suggesting that preservation by lipid incorporation is important in preservation of organic fossils.

References

- Bass M, Briggs DEG, Van Heemst JDH, Kear AJ, De Leeuw JW (1995) Selective preservation of chitin during the decay of shrimp. *Geochim Cosmochim Acta* 59:945–951
- Bland HA, van Bergen PF, Carter JF, Evershed RP (1998) Early diagenetic transformations of proteins and polysaccharides in archaeological plant remains. In: Stankiewicz BA, van Bergen PF (eds) Nitrogen-containing macromolecules in the bio- and geosphere, vol 707, ACS symposium series
- Briggs DEG (1999) Molecular taphonomy of animal and plant cuticles: selective preservation and diagenesis. *Philos Trans R Soc Lond B* 354:7–16
- Briggs DEG, Kear AJ (1993) Decay and preservation of polychaetes: taphonomic thresholds in soft-bodied organisms. *Paleobiology* 19:107–135
- Briggs DEG, Kear AJ, Baas M, De Leeuw JW, Rigby S (1995) Decay and composition of the hemichordate *Rhabdopleura*: implications for the taphonomy of graptolites. *Lethaia* 28:15–23
- Briggs DEG, Evershed RP, Lockheart MJ (2000) The biomolecular paleontology of continental fossils. *Paleobiology* 26(Suppl to no. 4):169–193
- Bustin RM, Link C, Goodarzi F (1989) Optical properties and chemistry of graptolite periderm following laboratory simulated maturation. *Org Geochem* 14:355–364
- Challinor JM (1991a) Structure determination of alkyd resins by simultaneous pyrolysis methylation. *J Anal Appl Pyrolysis* 18:233–244
- Challinor JM (1991b) The scope of pyrolysis methylation reactions. *J Anal Appl Pyrolysis* 20:15–24
- Crowther PR (1981) The fine structure of graptolite periderm. *Spec Pap Palaeontol* 26:119 pp
- Crowther PR, Rickards RB (1977) Cortical bandages and the graptolite zooid. *Geol Palaeontol* 11:9–46
- De Leeuw JW, Baas M (1993) The behavior of esters in the presence of tetramethylammonium salts at elevated temperatures; flash pyrolysis or flash chemolysis? *J Anal Appl Pyrolysis* 26:175–184
- de Leeuw JW, Largeau C (1993) A review of macromolecular organic compounds that comprise living organisms and their role in kerogen, coal and petroleum formation. In: Engel MH, Macko SA (eds) *Organic geochemistry: principles and applications*, vol 11, Topics in geobiology. Springer, New York, pp 23–72
- Gupta NS, Pancost RD (2004) Biomolecular and physical taphonomy of angiosperm leaf during early decay: implications for fossilisation. *Palaios* 19:428–440
- Gupta NS, Briggs DEG, Collinson ME, Evershed RP, Pancost RD (2006a) Re-investigation of the occurrence of cutan in plants: implications for the leaf fossil record. *Paleobiology* 32(3):432–449

- Gupta NS, Briggs DEG, Collinson ME, Evershed RP, Michels R, Pancost RD (2006b) Organic preservation of fossil arthropods: an experimental study. *Proc R Soc Lond B* 273(1602):2777–2783
- Gupta NS, Briggs DEG, Collinson ME, Evershed RP, Michels R, Pancost RD (2007a) Molecular preservation of plant and insect cuticles from the Oligocene Enspel Formation, Germany: evidence against derivation of aliphatic polymer from sediment. *Org Geochem* 38(3):404–418
- Gupta NS, Briggs DEG, Collinson ME, Evershed RP, Michels R, Jack KS, Pancost RD (2007b) Evidence for the in situ polymerisation of labile aliphatic organic compounds during the preservation of fossil leaves: implications for organic matter preservation. *Org Geochem* 38(3):499–522
- Knicker H, del Rio JC, Hatcher PG, Minard RD (2001) Identification of protein remnants in insoluble geopolymers using TMAH thermochemolysis/GC-MS. *Org Geochem* 32:397–409
- Kok MD, Schouten S, Damsté JSS (2000) Formation of insoluble, nonhydrolyzable, sulfur-rich macromolecules via incorporation of inorganic sulfur species into algal carbohydrates. *Geochim Cosmochim Acta* 64:2689–2699
- Loydell DK, Orr PJ, Kearns S (2004) Preservation of soft tissues in Silurian graptolites from Latvia. *Palaeontology* 47:503–513
- Mckinney DE, Bortiatynski JM, Carson DM, Clifford DJ, De Leeuw JW, Hatcher PG (1996) Tetramethylammonium hydroxide thermochemolysis of the aliphatic biopolymer cutan: insights into the chemical structure. *Org Geochem* 24:641–650
- Mongenot A, Riboulleau A, Garcette-Lepecq A, Derenne S, Pouet Y, Baudin F, Largeau C (2001) Occurrence of proteinaceous moieties in S- and O-rich late Tithonian kerogen (Kashpir oil shales, Russia). *Org Geochem* 32:199–203
- Nguyen RT, Harvey HR (1998) Protein preservation during early diagenesis in marine waters and sediments. In: Stankiewicz BA, van Bergen PF (eds) Nitrogen-containing macromolecules in the bio- and geosphere, vol 707, American chemical society symposium series. American Chemical Society, Washington, DC, pp 88–112
- Reeves JB III, Francis BA (1998) Pyrolysis-gas chromatography for the analysis of proteins: with emphasis on forages. In: Stankiewicz BA, van Bergen PF (eds) Nitrogen-278 containing macromolecules in the bio- and geosphere, vol 707, American chemical society symposium series. American Chemical Society, Washington, DC, pp 47–62
- Riboulleau A, Mongenot T, Baudin F, Derenne S (2002) Factors controlling the survival of proteinaceous material in Late Tithonian kerogens (Kashpir oil shales, Russia). *Org Geochem* 33:1127–1130
- Rickards RB, Partridge PL, Banks MR (1991) *Psigraptus jacksoni* Rickards & Stait—systematics, reconstruction, distribution and preservation. *Alcheringa* 15:243–254
- Stankiewicz BA, Hutchins JC, Thomson R, Briggs DEG, Evershed RP (1997a) Assessment of bog-body tissue preservation by pyrolysis-gas chromatography/mass spectrometry. *Rapid Commun Mass Spectrom* 11:1884–1890
- Stankiewicz BA, Briggs DEG, Evershed RP, Flannery MB, Wuttke M (1997b) Preservation of chitin in 25-million-year-old fossils. *Science* 276:1541–1543
- Stankiewicz BA, Briggs DEG, Michels R, Collinson ME, Evershed RP (2000) Alternative origin of aliphatic polymer in kerogen. *Geology* 28:559–562
- Tegelaar EW, De Leeuw JW, Derenne S, Largeau C (1989) A reappraisal of kerogen formation. *Geochim Cosmochim Acta* 53:3103–3106
- Towe KM, Urbanek A (1972) Collagen-like structures in Ordovician graptolite periderm. *Nature* 237:443–445
- Underwood CJ (1992) Graptolite preservation and deformation. *Palaios* 7:178–186
- Underwood CJ, Bottrell SH (1994) Diagenetic controls on multiphase pyritization of graptolites. *Geol Mag* 131:315–327
- Versteegh GMJ, Blokker P, Wood GD, Collinson ME, Damsté JSS, De Leeuw JW (2004) An example of oxidative polymerization of unsaturated fatty acids as a preservation pathway for dinoflagellate organic matter. *Org Geochem* 35:1129–1139

- Wakeham SG, Gagosian RB, Farrington JW, Canuel EA (1984) Sterenes in suspended matter in the eastern tropical North Pacific. *Nature* 308:840–843
- Wakeham SG, Lee C, Hedges JI, Hernes PJ, Peterson ML (1997) Molecular indicators of diagenetic status in marine organic matter. *Geochim Cosmochim Acta* 61:5363–5369
- Zhang X, Brown JC, Van Heemst JDH, Palumbo A, Hatcher PG (2001) Characterization of amino acids and proteinaceous materials using online tetramethylammonium hydroxide (TMAH) thermochemolysis and gas chromatography-mass spectrometry technique. *J Anal Appl Pyrolysis* 61:181–193

Chapter 10

Molecular Transformation of Bacteria at High P-T Conditions

Abstract Analysis of the solvent insoluble residue of a cyanobacterium (*Oscillatoria* sp.) subjected to simulated diagenesis under hydrothermal conditions (350 and 260 °C and hydrostatic pressure of 700 atmospheres) affords a macromolecule with significant aliphatic content that is similar to that found in hydrogen rich kerogen. The aliphatic component is primarily derived from incorporation of the original fatty acids into a solvent insoluble polymer, as demonstrated by performing similar experiments with model lipid compounds. Bacterial biomass can, therefore, contribute significantly to the insoluble organic inventory in ancient sediments.

Keywords Confined pyrolysis • *Oscillatoria* • Algaenan • Precambrian

Introduction

The importance of bacteria in cycling of carbon in all environments is central to the fate of organic carbon preservation in sediments, the formation of fossil fuels (Ourisson et al. 1984) and for paleoenvironmental reconstruction (Head et al. 1995; Parkes et al. 1993, 1994). It has been stated that up to 80 % of photosynthetically fixed carbon may be converted to bacterial biomass (Torréton et al. 1989) and indeed Parks et al. (1994) have demonstrated that bacterial populations are present in sediments up to 500 m depth thereby attesting to its importance in the deep biosphere as well. However, over the last two decades the importance of bacteria in contributing to fossilized biomass has been debated and it has been suggested that bacterial biomass may ‘commonly represent only a minor component of C_{org} in carbonaceous rocks’ (Hartgers et al. 1994) even though molecular extracts of most sediments through time contain an abundance of bacterially derived molecules, e.g., hopanoids, aromatic carotenoids (Ourisson and Albrecht 1992; Summons and Powell 1986). The primary argument against bacterial contribution is based on the fact that characteristic carotenoid markers from photosynthetic green sulphur bacteria present in some ancient sediments are isotopically

distinct from the isotopic signal from the bulk organic biomass in those sediments and therefore represent a different carbon pool (Damsté and Schouten 1997). Further, it has been demonstrated that bacteria do not contain any form of refractory macromolecular carbon, as is present in some algae and plant cuticles (de Leeuw et al. 2006) thus rendering bacterial biomass particularly labile (Allard et al. 1997; Damsté and Schouten 1997). However, in other locations (Moers et al. 1993) bulk organic carbon and bacterial markers have similar isotope signatures making the claim of Hartgers et al. (1994), debatable. In this study we experimentally ‘fossilised’ pure cultures of *Oscillatoria* sp. (a cyanobacterium) as this bacterium has a geologically significant contribution (Westall and Folk 2003). Experiments were conducted in the laboratory by placing biomass in sealed gold tubes, and heating the cultures at 350 and at 260 °C independently at a hydrostatic pressure of 700 atmospheres for one day to simulate organic metamorphism in natural sediments (Stankiewicz et al. 2000; Gupta et al. 2006, 2007) to understand the organic fossilization of bacteria, and to understand if bacterial biomass can contribute to the recalcitrant part of sedimentary organic matter (Harvey and Macko 1997; Head et al. 1995).

Materials and Methods

Pure cultures of *Oscillatoria* grown in aseptic conditions at the Geobiology lab at Carnegie were heated in sealed gold cells at 350 and 260 °C under a hydrostatic pressure of 700 bar (Michels et al. 1995) for 24 h in the absence of water. These conditions were chosen because, during a previous investigation of arthropods (Stankiewicz et al. 2000; Gupta et al. 2006) and modern leaves (Gupta et al. 2007, 2009), these revealed the most dramatic change in chemical composition to a macromolecule with significant aliphatic content. Pure C₁₆ and C₁₈ fatty acid mixture (Sigma-Aldrich) was hydrothermally treated to investigate the transformation of pure lipids as detected in the extractable and hydrolysable fraction of the bacteria. Bacterial residue obtained after heating were extracted ultrasonically in dichloromethane-methanol (2:1 v/v) and then subjected to thermodesorption of weakly bound or non-covalently bound components at 310 °C (Stankiewicz et al. 2000; Gupta et al. 2006, 2009) and to pyrolyse the macromolecular component. Pyrolysis after either solvent extraction or thermodesorption yields similar results and thermodesorption was used in all samples for thermal extraction of non-macromolecular components after solvent extraction. The heated lipid molecules were pyrolysed at 615 °C after thermodesorption as these were soluble in dichloromethane-methanol, unlike the heated bacterium that was insoluble. This paper deals with the analysis of the macromolecular component.

Hydrothermal experiments conducted at 700 bars and temperatures of 260 and 350 °C, were performed in sealed 4.5-mm OD gold cells. Prior to use, the gold cells were annealed at 900 °C and then refluxed in 6 N hydrochloric acid for

approximately 1 h. Reactant materials (50 mg) were sealed into the gold capsule, after welding both end of the cell by utilizing a tungsten inert-gas arc welder (Lampert PUK3) with high precision welding capabilities (0.3 mm) that minimize heat generation along the weld. The capsules are hosted in small volume (~30 ml) pressure vessels to minimize the duration of quenching to ambient conditions during experiment termination (Cody et al. 2001). After quenching, the gold tube reactors were removed from the high-pressure apparatus and rinsed with methanol and then dried.

Modern and heated *Oscillatoria* samples were pyrolysed at Carnegie using a CDS 1000 Pyroprobe by heating at 615 °C for 10 s. Compound detection and identification were performed using on line GC-MS in full scan mode with a Hewlett Packard HP6890 gas chromatograph interfaced to a HP 6890 mass selective detector. GC was performed with a Supelco MD-5S column (30 m, 0.25 mm I.D., 0.25 ml film thickness) using He as the carrier gas. The oven was programmed from 50 (held 1 min) to 300 °C (held 28 min) at 5 °C min⁻¹. The source was operated in the electron ionization (EI) mode with 70 eV ionization energy at 250 C. The mass selective detector scan rate was 0.80 s/decade over a mass range of 50–500 Da with an inter-scan delay of 0.20 s.

Results and Discussion

A solvent-insoluble residue was recovered after the hydrothermal experiment on bacteria that was subsequently subjected to thermal extraction at 310 °C to further remove any volatile components and then analysed by pyrolysis-gas chromatography-mass spectrometry, at 615 °C, to evaluate the macromolecular composition. Py-GC-MS is commonly used to characterise solvent insoluble sedimentary organic carbon, that is, kerogen (Larter and Horsfield 1993; de Leeuw et al. 2006; de Leeuw 2007). The unheated precursor bacterium was also similarly extracted and then analyzed by Py-GC-MS revealing the biopolymer and lipid distribution. The unheated bacterial pyrolysate consists predominantly of small molecules derived unambiguously from protein (alkyl benzenes, alkyl phenols, indoles, cyanobenzenes), polysaccharides (furans and levoglucosan) and lipids. Of these compound classes, the lipids consist predominantly of fatty acids with up to 18 carbon atoms (Fig. 10.1), consistent with distributions of these molecules from the soluble extracts of *Oscillatoria* sp. (Oren et al. 1985). Analysis of the heated material reveals that the biopolymeric composition has drastically changed and most biopolymers detected in the modern bacteria are chemically transformed to a different macromolecular composition. Py-GC-MS after solvent and thermal extraction reveals a macromolecule with significant aliphatic carbon, represented by the alkane, alkene homologues in the gas chromatogram analysis distinct up to C₁₈. Alkane-alkene doublets such as these are ubiquitous in pyrolysates derived from ancient sediments and reflect the aliphatic nature of ancient refractory organic carbon (Larter and Horsfield

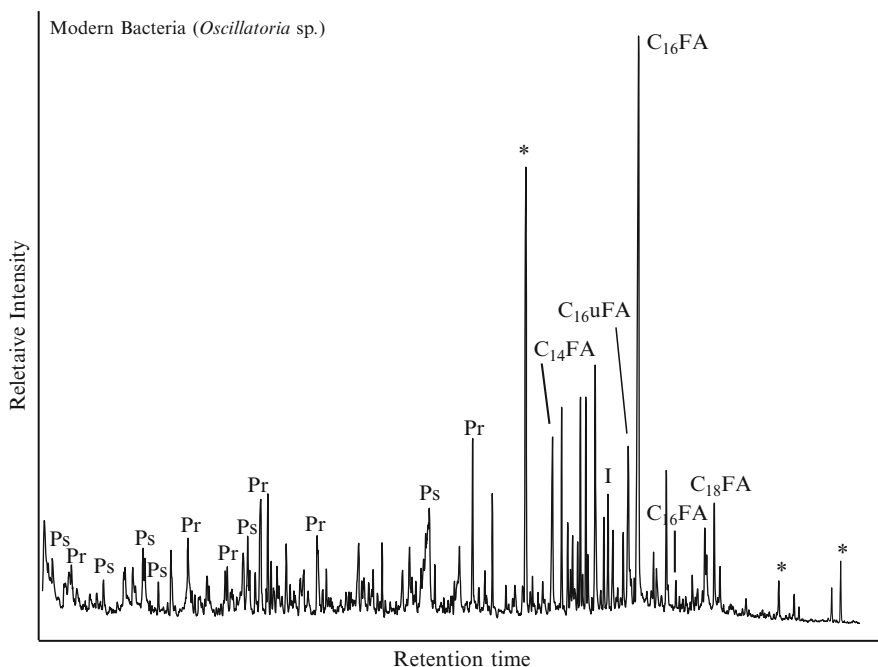


Fig. 10.1 Gas chromatographic analysis of modern *Oscillatoria* after solvent extraction, thermodesorption and pyrolysis. *Pr*: Proteins, *Ps*: Polysaccharides, *C₁₆FA*: *C₁₆* Fatty acid, *C₁₆uFA*: *C₁₆* unsaturated fatty acid, *C₁₈FA*: *C₁₈* fatty acid, *C₁₄FA*: *C₁₄* fatty acid, *B*: benzene derivative, *P*: Phenol derivative, *I*: Isoprenoid, *: phthalate contaminant

1993). Alkanes are abundant in the solvent extracted fraction from sediments and bacteria but homologous alkane-alkene doublets, as seen here after pyrolysis, represent macromolecularly-bound aliphatic compounds and do not represent presence of compounds from the soluble fraction (Larter and Horsfield 1993). As modern bacteria lack any resistant biopolymers, including resistant aliphatic biopolymers (Allard et al. 1997), the aliphatic residue-containing macromolecule we observe is a product of simulated thermal metamorphism. Interestingly, fatty acid molecules up to *C₁₈* are observed along with alkyl amides, the latter formed by the reaction of fatty acids with nitrogen containing molecules such as proteins (Gupta et al. 2006). Alkane and alkenes are highly soluble in solvent used in this study and also volatile, thus their abundance in the pyrolysate of the insoluble residue indicate the presence of covalently bound functionalized lipids into the thermally generated macromolecule. Experiments at 260 °C resulted in a similar macromolecular composition as was obtained at 350 °C (Fig. 10.2). Analysis of the heated mixture of *C₁₆* and *C₁₈* fatty acid after thermodesorption yielded alkane-alkene peaks up to *C₁₈* along with *C₁₆* and *C₁₈* fatty acids (Fig. 10.3), indicating that the lipids were a source of the

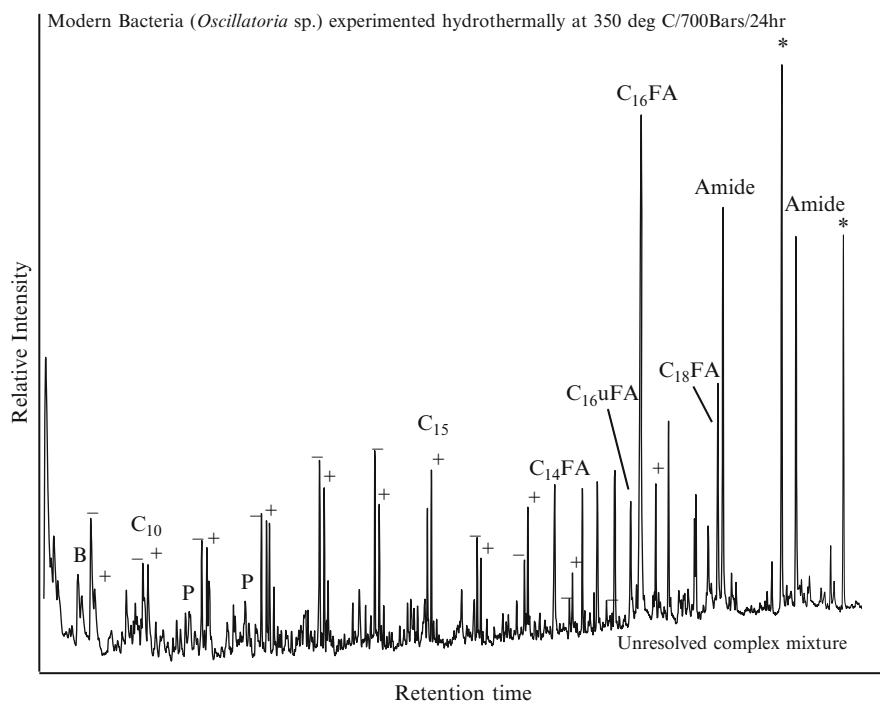


Fig. 10.2 Gas chromatographic analysis of experimentally heated *Oscillatoria* after solvent extraction, thermodesorption and pyrolysis. Symbols same as in Fig. 10.1. Additionally, +: *n*-alkane, -: *n*-alkene. Note presence of alkane alkene peaks after the experiment signifying presence of macromolecularly bound aliphatic moieties

aliphatic component in the heated bacterium. This experiment demonstrates that although bacteria consist of degradable biopolymers, diagenesis of bacterial biomass can lead to the formation of a lipid-rich aliphatic geomacromolecule, as has now been demonstrated for leaves (Gupta et al. 2007), arthropods (Gupta et al. 2006) and algae (Versteegh et al. 2004; de Leeuw et al. 2006; Kodner et al. 2009). The experiment further demonstrates that lipids need a biopolymeric substrate to form an insoluble geopolymer, as evidenced by formation of a solvent soluble polymer when only the fatty acid mixture was hydrothermally heated. Notwithstanding the simulated fossilization employed here (Stankiewicz et al. 2000), this experiment does produce a solvent insoluble, high molecular weight material that is similar in composition to immature kerogen in ancient sediments. Thus, bacteria, along with higher plants and algae all have the capacity to contribute refractory organic carbon to sediments, a point that is especially important in the context of the early part of Earth history when life was largely microbial.

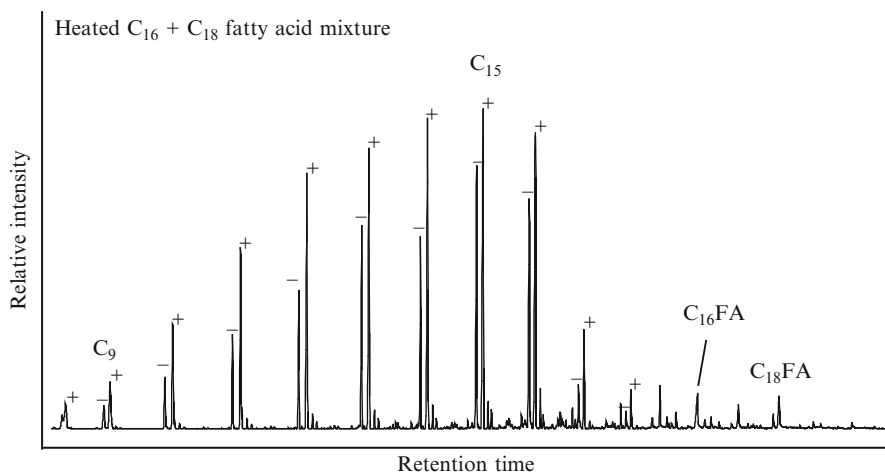


Fig. 10.3 Gas chromatographic analysis of experimentally heated C_{16} and C_{18} fatty acid after thermodesorption and pyrolysis. Symbols same as in Figs. 10.1 and 10.2. Note presence of alkane alkene peaks up to C_{18} demonstrating that these acids are responsible for the aliphatic component in the heated bacteria as well

References

- Allard B, Templier J, Largeau C (1997) Artfactual origin of mycobacterial bacteran. Formation of melanoid-like artifactual macromolecular material during the usual isolation process. *Org Geochem* 26:691–703
- Cody GD, Boctor NZ, Hazen RM, Brandes JA, Morowitz HJ, Yoder HS (2001) Geochemical roots of autotrophic carbon fixation: hydrothermal experiments in the system citric acid, H_2O -(FeS)-(NiS). *Geochim Cosmochim Acta* 65:3557–3576
- Damsté JSS, Schouten S (1997) Is there evidence for a substantial contribution of prokaryotic biomass to organic carbon in Phanerozoic carbonaceous sediments? *Org Geochem* 26:517–530
- de Leeuw JW (2007) On the origin of sedimentary aliphatic macromolecules: a comment on recent publications by Gupta et al. *Org Geochem* 38:1585–1587
- de Leeuw JW, Versteegh GJM, van Bergen PF (2006) Biomacromolecules of algae and plants and their fossil analogues. *Plant Ecol* 182:209–233
- Gupta NS, Michels R, Briggs DEG, Evershed RP, Pancost RD (2006) The organic preservation of fossil arthropods: an experimental study. *Proc R Soc Lond B* 273:2777–2783
- Gupta NS, Michels R, Briggs DEG, Collinson ME, Evershed RP, Pancost RD (2007) Experimental evidence for the formation of geomacromolecules from plant leaf lipids. *Org Geochem* 38:28–36
- Gupta NS, Yang H, Leng Q, Briggs DEG, Cody GD, Summons RE (2009) Diagenesis of plant biopolymers: decay and macromolecular preservation of *Metasequoia*. *Org Geochem* 40:802–809
- Hartgers WA, Sinninghe Damste JS, Requejo AG, Allan J, Hayes JM, de Leeuw JW (1994) Evidence for a small bacterial contribution to sedimentary organic carbon. *Nature* 369:224–227
- Harvey HR, Macko SA (1997) Catalysts or contributors? Tracking bacterial mediation of early diagenesis in the marine water column. *Org Geochem* 26:531–544
- Head I, Farrimond P, Larter S (1995) Organic carbon in sediments. *Nature* 373:293

- Kodner RB, Summons RE, Knoll AH (2009) Phylogenetic investigation of the aliphatic, non-hydrolyzable biopolymer algaenan, with a focus on green algae. *Org Geochem* 40:854–862
- Larter SR, Horsfield B (1993) Determination of structural components of kerogens by the use of analytical pyrolysis methods. *Top Geobiol* 11:271–287
- Michels R, Landais P, Torkelson BE, Philp RP (1995) Effects of confinement and water pressure on oil generation during confined pyrolysis, hydrous pyrolysis and high pressure hydrous pyrolysis. *Geochim Cosmochim Acta* 59:1589–1604
- Moers MEC, Jones DM, Eakin PA, Fallick AE, Griffiths H, Larter SR (1993) Carbohydrate diagenesis in hypersaline environments: application of GC-IRMS to the stable isotope analysis of derivatized saccharides from surficial and buried sediments. *Org Geochem* 20:927–933
- Oren A, Fattom A, Padan E, Tietz A (1985) Unsaturated fatty acid composition and biosynthesis in *Oscillatoria limnetica* and other cyanobacteria. *Arch Microbiol* 141:138–142
- Ourisson G, Albrecht P (1992) Hopanoids. 1. Geohopanoids: the most abundant natural products on earth? *Acc Chem Res* 25:398–402
- Ourisson G, Albrecht P, Rohmer M (1984) The microbial origin of fossil fuels. *Sci Am* 251:44–51
- Parkes RJ, Cragg BA, Getliff JM, Harvey SM, Fry JC, Lewis CA, Rowland SJ (1993) A quantitative study of microbial decomposition of biopolymers in recent sediments from the Peru Margin. *Mar Geol* 113:55–66
- Parkes RJ, Cragg BA, Bale SJ, Getliff JM, Goodman K, Rochelle PA, Fry JC, Weightman AJ, Harvey SM (1994) Deep bacterial biosphere in Pacific Ocean sediments. *Nature* 371:410–412
- Stankiewicz BA, Briggs DEG, Michels R, Collinson ME, Evershed RP (2000) Alternative origin of aliphatic polymer in kerogen. *Geology* 28:559–562
- Summons RE, Powell TG (1986) Chlorobiaceae in Palaeozoic seas revealed by biological markers, isotopes and geology. *Nature* 319:763–765
- Torréon J-P, Guiral D, Arfi R (1989) Bacterioplankton biomass and production during destratification in a monomictic eutrophic bay of a tropical lagoon. *Mar Ecol Prog Ser* 57(53):67
- Versteegh GJM, Blokker P, Wood GD, Collinson ME, Damsté JS, de Leeuw JW (2004) An example of oxidative polymerization of unsaturated fatty acids as a preservation pathway for dinoflagellate organic matter. *Org Geochem* 35:1129–1139
- Westall F, Folk RL (2003) Exogenous carbonaceous microstructures in early Archean cherts and BIFs from the greenstone belt: implications for the search for life in ancient rocks. *Precambrian Res* 126:313–330

Chapter 11

Preservation of Organic Fossils at the Las Hoyas Formation, Spain

Abstract Molecular analysis of fossil fish scales from the Cretaceous Las Hoyas Formation revealed a dominant aliphatic composition (C_8 to C_{22}) whereas modern fish scale is proteinaceous (largely collagenous). Analysis of the aliphatic polymer using thermochemolysis revealed the importance of ester linkages; saturated fatty acids C_{14} to C_{18} (particularly C_{16}) are the most abundant. These acid components and their unsaturated counterparts are evident in the lipid composition of modern fish scale. Thus, the aliphatic composition of the fossil scales is likely a result of the incorporation of lipids (including a C_{19} aromatic hydrocarbon) from the original indicating preservation by *in situ* polymerization of labile aliphatic components. Fossil arthropods and plants from the same deposit also show a dominant aliphatic macromolecular component, likely derived predominantly by crosslinking of free lipid precursors. Differences in the relative distribution of molecular components indicate likely chemosystematic differences between different fossil groups.

Keywords Fish • Pyrolysis • Lipid • Kerogen • Aliphatic • Konservat-Lagerstätte

Introduction

The Cretaceous lacustrine limestones of Las Hoyas have yielded a well preserved and diverse biota of plants, crustaceans, insects, fishes, tetrapods (including the dinosaur *Pelecanimimus*) and birds (see Fregenal Martínez 1998 for review). Here, as in the majority of other pre-Tertiary deposits, arthropod and plant fossils are altered to a macromolecule with a dominant aliphatic component, similar in composition to type I and/or II kerogens (Briggs 1999; Briggs et al. 2000). The aliphatic composition of such fossils was attributed previously to selective preservation of resistant aliphatic biopolymers such as cutan (de Leeuw and Largeau 1993). However, resistant aliphatic biopolymers are absent in arthropods and in most plants and preservation of these fossils cannot be attributed simply to selective preservation.

An alternative explanation for organic matter preservation is the incorporation of labile lipids into a resistant aliphatic macromolecule via *in situ polymerization* (see Briggs 1999 for review). This is based on evidence obtained from analyses of organically preserved macrofossils of plants, arthropods (Briggs 1999), graptolites and on simple thermal maturation experiments (confined pyrolysis in gold tubes). Although plant and insect cuticles have been studied extensively, little is known about the organic preservation of fossil fish. This investigation considers the molecular preservation of fossils from the Las Hoyas Formation (Cretaceous, Barremian, c. 126 Ma) of Spain with emphasis on the organic preservation of fish in relation to their modern counterparts.

Geological Setting and Fossil Material

The fossils of the Konservat-Lagerstätte of Las Hoyas (La Huérguina Limestones Formation, Upper Barremian, Serranía de Cuenca, Spain) are preserved in finely laminated limestones composed almost entirely of calcium carbonate with a small fraction of clays and organic matter. These limestones were produced in the context of a continental (freshwater) subtropical, seasonal summer wet, carbonate wetland that overlay a low-relief karstic terrain. The wetland was drained by carbonate-rich freshwater and comprised a typical environmental mosaic of swampy plains, ponds, lakes, ephemeral channels and sloughs. Fossiliferous laminated sediments formed in a pond covered by thick microbial mats (Fig. 11.1) that experienced strong cyclical oscillations of water level. During seasonal flooding and prolonged wet periods lacustrine sedimentation dominated including chemical and bioinduced precipitation of calcium carbonate and accumulation of thin microbial mats. Microbial mats and

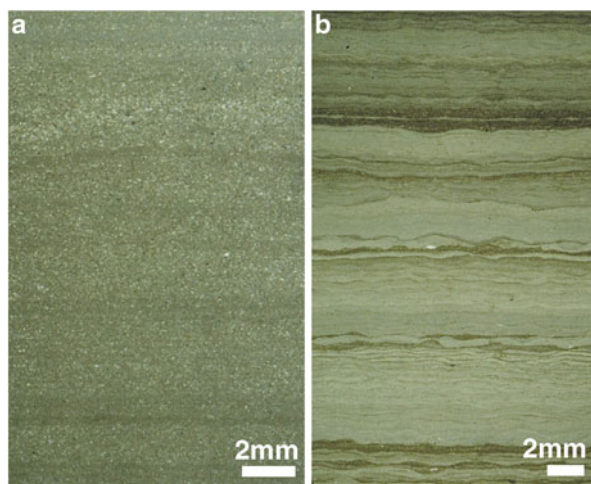


Fig. 11.1 Wet (a) and dry (b) microfacies from Las Hoyas laminated limestones (La Huérguina Formation, Upper Barremian, Serranía de Cuenca, Spain) (After Fregenal-Martínez 1998). Scale bar in millimeters

laminae of very fine detrital carbonate sediments with plant and other organic debris transported during occasional floods characterized sedimentation during dry periods when the water column was reduced drastically to probably just a few centimeters. The warm environment, prolonged periods of stagnation, and the high rate of accumulation of organic debris carried by floods maintained anoxic to dysaerobic conditions in sediments and bottom waters and prevented bioturbation.

Sediments of wet periods record the maximum productivity of Las Hoyas, although the sediments of dry periods contain the best preserved and most abundant fossils (about 7× the number in sediments of wet periods). This difference reflects greater environmental stress, mainly due to dehydration, and the greater prevalence of microbial mats. The microbial mats facilitated rapid burial and the establishment of conditions favourable for preservation as revealed by this and previous studies.

The Konservat-Lagerstätte of Las Hoyas is a product of the interaction of geological and biological conditions widespread at the margin of Tethys in the Northern Hemisphere during the Lower Cretaceous (Buscalioni and Fregenal-Martínez 2006)

Fish, decapods and plants are the most abundant fossils at Las Hoyas. The sample LH-50.082 corresponds to *Montsechiavidali*, an aquatic freshwater small wedge plant. LH-50.083 is a small decapod attributed to the *Austrapotamobius* (Family Astacidae). Fish remains include an isolated 2 cm scale of an actinopterigianamii form (LH-50.081) and two juveniles (LH-50.085 and LH-50.087) of primitive teleosts of uncertain phylogenetic relationship that were formerly considered to be “leptolepid-like” fishes.

Analytical Protocol

The structure and mineralogy of fossil samples were analysed using a Philips XL 30 environmental scanning electron microscope with energy dispersive x-ray analysis (Princeton Gamma-Tech).

Fossil samples and modern equivalents were pyrolysed using a CDS 5150 Pyroprobe by heating at 650 °C for 20s to fragment macromolecular organic components. Compound detection and identification was performed by on-line gas chromatography–mass spectrometry (GC-MS) in full-scan mode on a Hewlett Packard HP6890 gas chromatograph interfaced to a MicromassAutoSpecUltima magnetic sector mass spectrometer. GC separation was performed on a J&W Scientific DB-1MS capillary column (60 m length, 0.25 mm internal diameter, 0.25 µm film thickness) using He as the carrier gas. Samples were injected in splitless mode at 300 °C. The oven was programmed from 60 (held for 2 min) to 150 °C at 10 °C min⁻¹, then at 3 °C min⁻¹ to 315 °C and held isothermal for 24 min. The source was operated in electron ionization (EI) mode at 70 eV ionization energy at 250 °C. The AutoSpec full-scan rate was 0.80 s/decade over a mass range of 50–600 Da and an interscan delay of 0.20 s.

For thermochemolysis samples were soaked in tetramethylammonium hydroxide solution (TMAH) for an hour prior to pyrolysis. Samples were solvent extracted in 2:1—dichloromethane:methanol solution prior to analysis as necessary.

Results

The major pyrolysis products of modern fish scale (without lipid/solvent extraction) (Fig. 11.2a) included phenols, benzenes, indoles, pyrimidine, diketodipyrrole and diketopiperazine derivatives (Table 11.1). The abundance of diketodipyrrole, a marker for hydroxyproline, is characteristic of collagen. Thermochemolysis of modern fish scale (Fig. 11.2b) revealed a distribution of fatty acyl moieties ranging up to C₂₄ with an even over odd predominance; the shorter chain moieties, methylated protein products and short chain acids, were difficult to detect. C₁₆ and C₁₈ saturated and unsaturated components were the most abundant (see mass chromatogram *m/z* 74 + 87).

EDX analysis of the fish scale (LH-50.081) showed that it is composed mainly of Ca, P and O, indicating a preponderance of apatite. The composition of fish bone (LH-50.085 and LH-50.087) is essentially the same. The surface of the fossil fish scale displays linear ridges ~30–150 μm across. The surface is granular and shows no evidence of finer scale structure (not figured). The surface of the bone in specimen LH-50.087 (Fig. 11.3a, b) similarly lacked structure but the bones of another specimen (LH-50.085) (Fig. 11.3d, e) showed negative impressions of coccoid, rod shaped and some more elongate bacteria.

The eyes of fish may be preserved as an organic material (in which case this is the only part of the fish preserved in this way) or as an authigenic mineral. EDX analysis of the organic preservation (LH-50.087) showed that it consists mainly of C, O and S, with some Ca. The eye is dark in colour with a blocky fragmented appearance (Fig. 11.3a). It is preserved as a microbial film dominated by coccoids but with rare rod shaped forms (Fig. 11.3c). The mineralized preservation (LH-50.085) lacks C, and is composed of Ca, O and Fe, indicating a diagenetic mineral, perhaps an iron carbonate. It is pale orange in colour with a sugary texture under SEM (Fig. 11.3f).

Samples of the fossil fish scale (Fig. 11.4) were analysed by Py-GC-MS after solvent extraction. No moieties diagnostic of protein (e.g., collagen) were detected (Fig. 11.4a). The fossil revealed largely an aliphatic polymer extending at least from C₈ to C₂₁ with benzene and phenol derivatives, confirmed by repeated analysis (Fig. 11.4a). Analysis revealed an unresolved complex mixture around alkane/alkene homologue C₂₀, possibly due to unresolved compounds; however, this was not evident in repetitions of the analysis. Additionally, an unknown compound was detected, not observed in any other fossil (Fig. 11.5). Fatty acyl moieties released by thermochemolysis of the same fossil range up to C₂₂ with an even over odd predominance (Fig. 11.4b). The most abundant of these were C₁₆ and C₁₈ fatty acyl saturated moieties as also seen in the modern fish scale (Fig. 11.2b). Analysis of an isolated

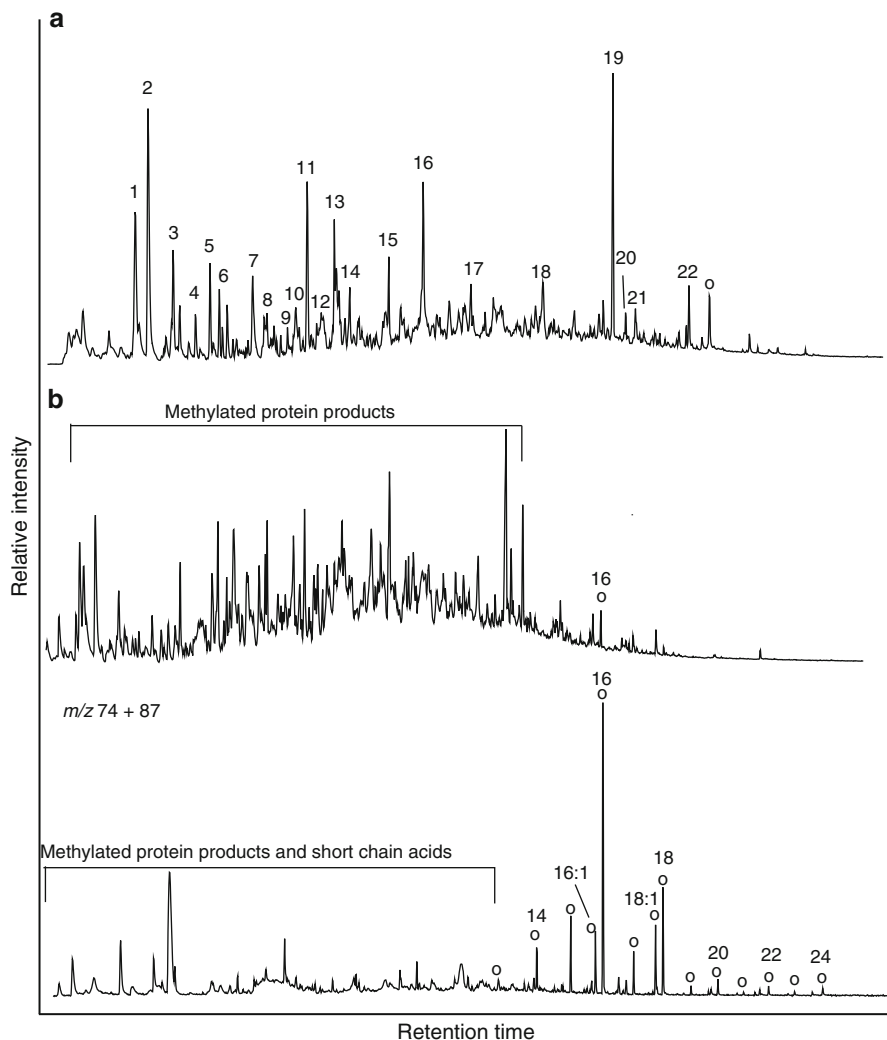


Fig. 11.2 Analysis of modern fish scale. (a) Partial ion chromatogram of Pyrolysis-GC/MS analysis revealing a proteinaceous composition (see Table 11.1 for peak identification). (b) Partial ion chromatogram of TMAH-Pyrolysis-GC/MS analysis showing methylated derivatives of protein compounds and distribution of fatty acyl moieties (as revealed by m/z 74+87)

fish bone revealed the presence of a similar aliphatic component (C_8 to C_{30} , data not shown). The eye was not analysed.

EDX analysis of the decapod revealed a composition dominated by Ca and P with some O, indicating apatite. No fine surface structure was evident. Py-GC-MS revealed an aliphatic composition (C_8 to C_{21}) with benzene and phenol derived compounds and no original chitin/protein (Fig. 11.6b).

Table 11.1 Peak identifications of protein compounds from modern fish scale as analysed in Fig. 11.1

Peak	Characteristic ions (m/z)	Compound name	Origin
1	67,52,41,40	Pyrrole	Proline
2	92,91,65,51	Toluene	Phenylalanine
3	81,80,53,40	C ₁ pyrrole	Proline, Hydroxyproline
4	106,91	Ethylbenzene	Phenylalanine
5	104,78,51	Styrene	Phenylalanine
6	95,94,80,67	C ₂ pyrrole	Diketopiperazine
7	94,66,65,40	Phenol	Tyrosine
8	94,67	Pyridinamine	?
9	107,106,67	p-aminotoluene	?
10	111,83,68,48	?	Proline-Asparagine
11	108,107,66,79	Methylphenol	Tyrosine
12	99,56,40	Succimide	Asparagine
13	117,116,90,89	Ethylcyanobenzene	Phenylalanine
14	125,68,54,43	?	Proline-Leucine
15	131,91,78,66,51	Propylcyanobenzene	Phenylalanine
16	117,90,89,63	Indole	Tryptophan
17	131,130,103	Methylindole	Tryptophan
18	136,107,80,53,40	?	?
19	186,130,93,66	Diketodipyrrole	Hydroxyproline
20	172,171,143,65	5-Hydroxy-4-phenyl pyrimidine	?
21	176,94,66	?	Proline-Arginine
22	194,138,96,70	2,5-Diketopiperazine	Proline-Proline

? signifies not certain/unknown

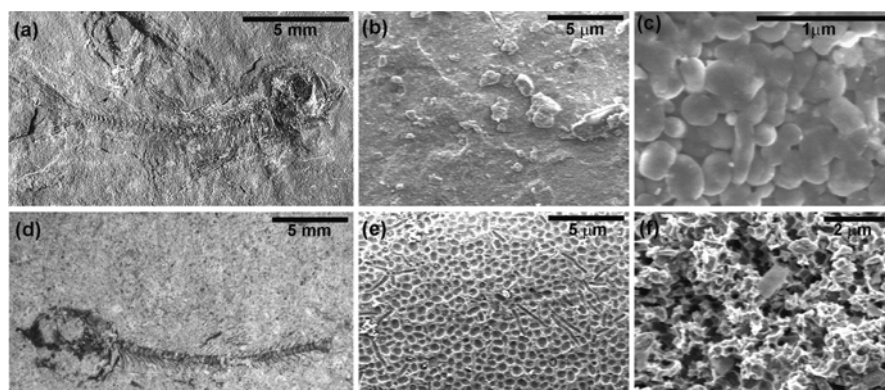


Fig. 11.3 Fishes from Las Hoyas, Spain. (a) Specimen LH-50.087. (b) Scanning electron micrograph (SEM) of the surface of bone. (c) SEM of the eye showing carbon preserved bacteria. (d) Specimen LH-50.085. (e) SEM of the surface of bone showing impressions of coccoid and filamentous bacteria in negative relief. (f) SEM of the eye showing iron carbonate authigenic mineral

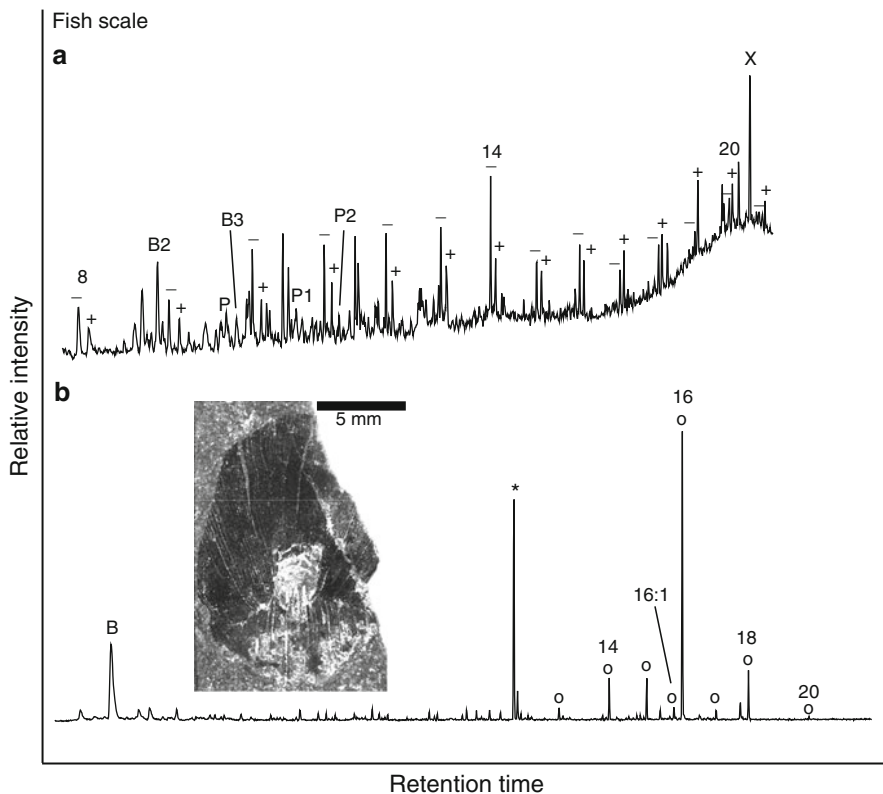


Fig. 11.4 Analysis of fossil fish scale from Las Hoyas, Spain (specimen LH-50.081). **(a)** Partial ion chromatogram of Pyrolysis-GC-MS analysis of fish scale revealing the dominance of an aliphatic polymer (+: *n*-alkanes, -: *n*-alkenes) similar to Type I/II kerogen. **(b)** Partial ion chromatogram of TMAH-Pyrolysis-GC-MS analysis of fish scale revealing the distribution of fatty acyl moieties (o). *Bn*: benzene derivative, *Pn*: Phenol derivative where *n* represents number of carbon atoms in alkyl group. Number on top of peaks denote carbon chain length of the alkane/alkene homologues or fatty acyl moieties. *X*: unknown C_{19} hydrocarbon

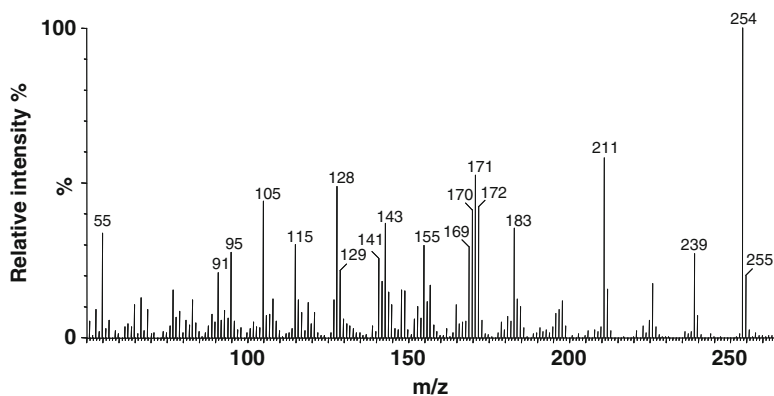


Fig. 11.5 Mass spectra of unknown compound present in the fish scale pyrolysate. Analysis of the ion series and isotopic abundances suggest a polyunsaturated hydrocarbon with an elemental composition $C_{19}H_{26}$

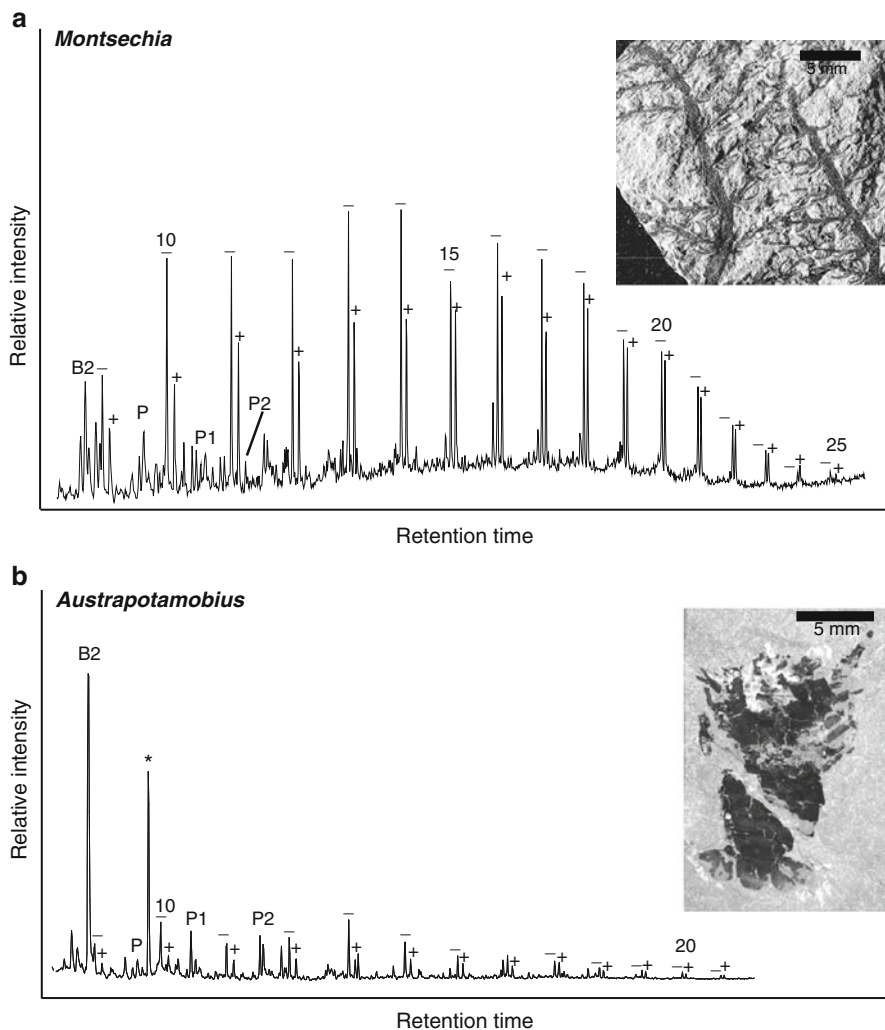


Fig. 11.6 Partial ion chromatogram of pyrolysis-GC-MS analysis of (a) fossil plant *Montsechiavidali* and (b) fossil decapod *Austrapotamobius*. Figure symbols same as in Fig. 11.4

EDX analysis of the plant *Montsechia* (LH-50.082, Fig. 11.6a) showed that it consists mainly of C, O and S, with some Ca, a similar composition to the organically preserved fish eye (LH-50.087). The surface is granular with associated filamentous structures and sediment grains. Py-GC-MS of the fossil plant also showed an aliphatic composition (Fig. 11.6a, C₉ to C₂₅) as commonly observed in fossil plants with no preservation of original lignin, polysaccharides or the structural polyester cutin. Analysis of fossil decapod (Fig. 11.6b) revealed an aliphatic component from C₉ to C₂₁ with benzene and phenol derivatives.

Discussion and Conclusion

The soft tissues of organisms at Las Hoyas may be preserved either as organic remains or as a result of authigenic mineralization (Briggs et al. 1997) and both may occur in association. The preservation of the eyes of fish as a carbonaceous bacterial film is reported here for the first time although a similar phenomenon (where bacteria likewise are not mineralized) occurs in the Jurassic ichthyosaurs from Holzmaden.

The aliphatic component of the organic remains must have been derived from compounds present in the organism itself. Migration from an external source can be excluded (Briggs 1999). This is supported by the results of thermochemolysis. Both modern and fossil fish scale revealed a very similar saturated fatty acyl distribution with a maximum abundance of C₁₆ and C₁₈ moieties. The predominance of fatty acyl moieties emphasizes the importance of ester functional groups in crosslinking the aliphatic polymer in these fossils. Alkanones, which are generally indicative of ether linkages, are absent. Thus the primary oxygen-containing intermolecular bonds in the fossil scale macromolecular organic matter may be esters, although carbon-carbon bonds are also likely to serve as important cross-linkages. The *n*-alkyl chains may protect the ester functional group in three dimensions by steric hindrance, assisting crosslinking.

Evidence for lipid incorporation has also been reported in fossil leaves dinoclasts, graptolites, eurypterids, shrimp beetles (Briggs 1999) and in kerogens. Thus the evidence indicates that polymerization and incorporation of labile aliphatic components present in the organism are responsible for generating the aliphatic macromolecular component in the fossils during diagenesis.

The molecular components in the various fossils show differences in relative abundance. Aliphatics in the Las Hoyas fish range to C_{21/22}. The decapod shows alkyl benzene and phenols as major components, the aliphatics ranging to C₂₁. Py-GC-MS of beetles from the site, on the other hand, revealed only aliphatics, ranging from C₈ up to C₃₁ (Boulton 2003). This may reflect the presence of long chain waxes (greater than C₃₀) in insect cuticle which may contribute to the long chain *n*-alkyl component in the fossil. The *Montsechia* plant shows a predominantly aliphatic composition (C₉ to C₂₅) with very little aromatic content. Differences between the fossil taxa may indicate inherent contrasts in the original labile aliphatic components and their thermal alteration products derived from the living organism.

The diagenetic history of organic components varies with starting composition, but also with environmental setting and time (Briggs 1999; Briggs et al. 2000). Degree of aromaticity may reflect thermal maturity. Thus chemosystematic differences are not consistent from locality to locality. Differences between plants and arthropods have been reported in cuticles from the Carboniferous of North America, for example, but here the contrasts are mainly in the distribution of alkenes/alkanes rather than in the total chain length or the proportion of aromatics. To investigate fossil chemosystematics further, a comprehensive analysis of comparable material from different ages and environments is required.

References

- Boulton H (2003) Taphonomy of non-biomineralised tissues in fossils from lacustrine Konservat-Lagerstätten. Unpublished PhD thesis, University of Bristol, 274 pp
- Briggs DEG (1999) Molecular taphonomy of animal and plant cuticles: selective preservation and diagenesis. *Philos Trans R Soc Lond B Biol Sci* 354:7–16
- Briggs DEG, Wilby PR, Pérez-Moreno BP, Sanz JL, Fregenal-Martínez M (1997) The mineralization of dinosaur soft-tissue in the Lower Cretaceous of Las Hoyas, Spain. *J Geol Soc Lond* 154:587–588
- Briggs DEG, Evershed RP, Lockheart MJ (2000) The biomolecular paleontology of continental fossils. *Paleobiology* 26(supplement to no. 4):169–193
- Buscalioni AD, Fregenal-Martínez M (2006) Archosaurian size bias in Jurassic and Cretaceous freshwater ecosystems. *Mesozoic Terrestrial Ecosystems 2006*, Manchester. In: Barrett PM, Evans S (eds) 9th Mesozoic terrestrial ecosystems and biota, Manchester. Natural History Museum, London, pp 9–12
- de Leeuw JW, Largeau C (1993) A review of macromolecular organic compounds that comprise living organisms and their role in kerogen, coal and petroleum formation. In: Engel MH, Macko SA (eds) *Organic geochemistry: principles and applications*, vol 11, Topics in geobiology. Springer, New York, pp 23–72
- Fregenal Martínez MA (1998) Análisis de la cubeta sedimentaria de Las Hoyas y su entorno paleogeográfico (Cretácico inferior, Serranía de Cuenca): sedimentología y aspectos tafonómicos del yacimiento de Las Hoyas. PhD thesis, Universidad Complutense de Madrid